Progress in Materials Science 102 (2019) 222–295

Contents lists available at ScienceDirect

Progress in Materials Science

journal homepage: www.elsevier.com/locate/pmatsci

Substantial breakthroughs on function-led design of advanced materials used in mixed matrix membranes (MMMs): A new horizon for efficient CO_2 separation

Abtin Ebadi Amooghin[a,*], Samaneh Mashhadikhan[a], Hamidreza Sanaeepur[a], Abdolreza Moghadassi[a], Takeshi Matsuura[b], Seeram Ramakrishna[c]

[a] Department of Chemical Engineering, Faculty of Engineering, Arak University, Arak 38156-8-8349, Iran
[b] Department of Chemical and Biological Engineering, University of Ottawa, 161 Louis Pasteur Street, Ontario K1N 6N5, Canada
[c] Department of Mechanical Engineering, National University of Singapore, 9 Engineering Drive 1, Singapore 117576, Singapore

Abbreviations: [C_3NH_2bim][Tf_2N], N-aminopropyil-3-butyl imidazolium bis(trifluoromethyl-sulfonyl)imide; SIFSIX-3-Cu, [$Cu(SiF_6)(pyz)_2]_n$; AlFFIVE-1-Ni, [$Ni(AlF_5)(pyz)_2]_n$; NbOFFIVE-1-Ni, [$Ni(NbOF_5)(pyz)_2]_n$; BTC, 1,3,5-benzenetricarbonyl trichloride; DAM, 1,3-phenylenediamine; BDO, 1,4-butanediol; naph, 1,4-naphthalenedicarboxylate; [bmim][Ac], 1-butyl-3-methylimidazolium acetate; [bmim][Tf_2N], 1-butyl-3-methylimidazolium bis (trifluoromethylsulfonyl) imide; [bmim][BF_4], 1-butyl-3-methylimidazolium tetrafluoroborate; [bmim][BF_4], 1-butyl-3-methylimidazolium tetrafluoroborate; [Emim][BF_4], 1-ethyl-3-methyl imidazolium tetrafluoroborate; [emim][Ac], 1-ethyl-3-methylimidazolium acetate; [C_2mim][Tf_2N], 1-ethyl-3-methylimidazolium bis (trifluoromethanesulphonyl) imide; [emim][$B(CN)_4$], 1-ethyl-3-methylimidazolium tetracyanoborate; HFDS, 1H,1H,2H,2H-perflourodecyltriethoxy silane; [smim][Tf_2N], 1-styrenemethyl-3-methylimidazolium bis(trifluoromethylsulfonyl) imide; [vbim][NTf_2], 1-vinyl-3-benzyl imidazolium-bis(trifluoromethane-sulphonyl)imidate; 6FAHP, 2,2-bis(3-amino-4-hydroxyphenyl) hexafluoropropane; THDT, 2,4,6-trihydazino-1,3,5-triazine; TMPDA, 2,4,6-trimethyl-1,3-phenylenediamine; DAM, 2,4-diamino mesitylene; DAP, 2,4-diaminophenol; MPD, 2-methyl-1,3-propanediol; HAB, 3,3′-Dihydroxybenzidine; HAB, 3,3′-dihydroxy-4,4′-diamino-biphenyl; DABA, 3,5-diaminobenzoic acid; APTMS, 3-aminopropyltrimethoxy silane; BPDA, 4,4′-(4,4′-isopropylidenediphenoxy)bis(phthalic anhydride); 6FDA, 4,4′-hexafluoroisopropylidene diphthalic anhydride; OBC, 4,4′-oxybis (benzoicacid chloride); ODA, 4,4′-oxydianiline; ODPA, 4,4′-Oxydiphthalic anhydride; DAR, 4,6-diaminoresorcinol; FDH-xy, 6FDA-$(DAM)_x$-$(HAB)_y$; APDEMS, amino-propyl-diethoxymethyl silane; APTES, aminopropyltriethoxy silane; AAO, anodic aluminum oxide; ATP, attapulgite; BDCA, benzene 1,4-dicarboxylic acid; BILPs, benzimidazole linked polymers; β-CD, beta-cyclodextrins; COBD, canola oil based diol; CMS, carbon molecular sieve; CNTs, carbon nanotubes; CNTs, carbon nanotubes; CA, cellulose acetate; Cs, chitosan; C15A, cloisite15A; CoBBP, cobalt ion (Co^{2+}) 6-bis(2-benzimidazolyl)pyridine; COE, cost of electricity; COFs, covalent organic frameworks; COFs, covalent organic frameworks; XLPEG, cross-linked polyethylene glycol; XLPEO, cross-linked polyethylene oxide; CD, cyclodextrine; DMS, disordered meso-porous silica; EDS, Energy dispersive X-ray spectroscopy; EDA, ethylenediamine; fcu, face-centered cubic; FTMs, facilitated transport membrane; FFV, fractional free volume; fum, fumarate; γ-CD, gamma-cyclodextrins; GS, gas separation; GO, graphene oxide; HA, hexylamine; HPNs, hollow polyamide nanoparticles; HD5, hydroxyl polyimide-co-polyimide; HCP, hyper cross-linked polymer; ImGO, imidazole functionalized graphene oxide; IPCC, intergovernmental panel on climate change; IL, ionic liquid; LDH, layered double hydroxide; LMW, low molecular weight; MOFs, metal organic frameworks; MOP, metal organic polyhedral; [P_{122i4}][PF_6], methyl(diethyl)isobutylphosphonium hexafluorophosphate; MDEA, methyl-di-ethanolamine; MOPs, Microporous organic polymers; MMMs, mixed matrix membranes; MEA, mono ethanol amine; MMT, montmorillonite; MWCNTs, multi walled carbon nanotubes; MFSs, multi-functional sites; [C_3NH_2bim][Tf_2N], N-aminopropyil-3-butyl imidazolium bis (trifluoromethyl-sulfonyl) imide; NPs, nanoparticles; NETL, national energy technology laboratory; NIPAM, N-isopropylacrylamide; [C_2mpyr][BF_4], N-methyl-N-ethylpyrrolidinium tetrafluoroborate; OIPCs, organic ionic plastic crystals; PTMSP, poly(1-trimethylsilyl-1-propyne; PBI, poly benzimidazoles; PBZ, poly benzothiazoles; PBO, poly benzoxazole; PD, poly dopamine; Pebax, poly ether-b-amide; PEBA, poly ether-block-amide; PEG, poly ethylene glycol; PEG, poly ethylene glycol; PEI, poly ethylene imine; PPG, poly propylene glycol; PPL, poly pyrrolone; PVDF, poly vinylidene fluoride; Pebax 1657, poly(ether-b-amide-6); PEGDMA, poly(ethylene glycol) dimethacrylate; PEGMA, poly(ethylene glycol) methacrylate; HPI, poly(hydroxyimide)s; PVC-g-POEM, poly(vinyl chloride)-graft-poly(oxyethylene methacrylate); PAN, polyacrylonitrile; PDMS, polydimethylsiloxane; PES, polyethersulfone; POSS, polyhedral oligomeric silsesquioxane; PI, polyimide; PILs, polymeric ionic liquids; PIMs, polymers of intrinsic microporosity; POZ, polyoxazoline; PSf, polysulfone; PUs, polyurethanes; PVA, polyvinyl alcohol; PVAm, poly-vinylamine; PAFs, porous aromatic framework; POP, porous organic polymer; RE, rare-earth; RTILs, room temperature ionic liquids; SIB, Ship-in-a-bottle; Sm, silane modified; SWCNTs, single walled carbon nanotubes; SPEEK, sulfonated poly ether ether ketone; sPPSU, sulfonated polyphenylene sulfone; TSILs, task specific ionic liquids; TR-PBOI, thermally rearranged polybenzoxazole-co-imide; TR-PBOI, thermally rearranged polybenzoxazole-co-imide; TR-PBOI, thermally rearranged polybenzoxazole-co-imide; TR, thermally rearranged; TFN, thin film nanocomposite; TMCS, trimethylchlorosilane; TAEA, tris(2-aminoethyl) amine; TB, Tröger's Base; ZIFs, zeolitic imidazolate frameworks

* Corresponding author.
E-mail address: a-ebadi@araku.ac.ir (A. Ebadi Amooghin).

https://doi.org/10.1016/j.pmatsci.2018.11.002
Received 13 September 2017; Received in revised form 12 November 2018; Accepted 17 November 2018
Available online 20 November 2018
0079-6425/

ARTICLE INFO

Keywords:
Mixed matrix membranes
Advanced functional materials
Current challenges
Recent developments
CO_2 separation

ABSTRACT

Mixed matrix membranes (MMMs) create a new horizon for developing novel materials with desired separation properties, since conventional membranes are insufficient to fully accommodate in industrial applications and process intensifications. A broad area of researches has been dedicated to develop MMMs for CO_2 separation. MMMs are normally comprised of different kinds of fillers embedded into the polymer matrices with a final goal of surpassing the Robeson's upper boundary not only by controlling shortcomings of the available organic and inorganic membrane materials, but also through a fast upgrading of them. One of the most important aspects in the development of MMMs is an appropriate material selection for both matrix and dispersed phases to eliminate the non-ideal morphologies created at their interfaces. Development of high performance membrane materials with new functional groups and new chemistries has attracted much attention over the past few years. To have an impact on real implementations, successful MMMs are necessary to optimize multiple functions besides high porous structure and surface area, such as processability, stability, sorption kinetics, mechanical and thermal properties, while simultaneously the economic issues must be taking into account. Although, during the long years passed from applying the MMMs for CO_2 separation, various kinds of conventional porous/dense materials have made significant contributions, many novel materials have rapidly emerged over the past five years. These improvements include the extensive use of a wide range of functionalized materials, which have inexorably entered the scene to substantially promote the separation performance. Today, the range of conceivable functions for porous materials is much broader than foretime. This may be indebted to the prompt progresses in design and computing the new functions/structures, which encourages the emergence of a new way to correctly identify the best material for the specific gas separation targets. Advanced functionalized MMMs generate substantial breakthroughs in tailoring successful CO_2-selective membranes and recent progresses in functional materials create many attractive opportunities/perspectives. This review is especially devoted to describe the recent developments in methods proposed to preserve/overcome the afore-mentioned fabrication challenges of MMMs and also the progress in advanced functionalized materials used in the MMMs for CO_2 separation during the recent years.

1. Introduction

One of the most important challenges for today's environment is the emission of the CO_2 which is produced by carbon sources like fossil fuels, human activities, chemical industries and so many other factories and refineries [1]. Current global warming could be the result of the uncontrolled CO_2 emission. Intergovernmental Panel on Climate Change (IPCC) states that the atmospheric CO_2 concentration should be decreased during the 21st century [2].

Natural gas is composed of CH_4 and other heavier hydrocarbons, N_2, CO_2, H_2S, and trace amounts of other gases such as He and O_2 [3]. Gas separation and purification techniques are essential to use CH_4 as a fuel, hence they are currently one of the most popular research topics [4,5].

For reducing calorific effect produced by greenhouse gases and considering that CO_2 in sour gas together with the presence of water produces a corrosive weak acid, the CO_2 should be removed from the natural gas [6–8].

High cost, energy dissipation and environmental impact are the drawbacks of conventional technologies such as cryogenic distillation, adsorption, absorption and amine based solvent extraction for CO_2 removal. Membrane based process is preferred to conventional methods because they show higher separation performance, lower costs and less environmental challenges for gas separation performances [9–11].

In early 1960s, separation of CO_2 via a selective cellulose acetate based membrane was described for the first time [12]. However, we had to wait until 1980s for the first industrial plant for CO_2 separation to be installed [1].

Polymeric membranes could achieve commercial success because of its excellent separation performance, mechanical properties and processability [9]. But they are affected from the tradeoff effect between gas permeability and selectivity expressed typically by Robeson's "upper bound" [13,14]. As well, difficulty in finding appropriate solvents, poor chemical and thermal resistance and swelling limit the use of polymeric membranes [11,15,16].

To overcome these limitations, alternative membrane materials have been eagerly searched for. Inorganic membranes fabricated from metals, ceramics and carbon were thought to be superior for their many advantages over polymeric membranes such as intrinsically high permeability and selectivity, chemical and thermal stability, and durability under the condition of high CO_2 concentration [17]. Inorganic membranes can also withstand high temperature and pressure and can resist moisture attacks [18,19]. However, high cost and poor processability prevented their use in large-scale commercial applications.

A new type of membranes, called mixed matrix membranes (MMMs), thus emerged to overcome the aforementioned drawbacks of both polymeric and inorganic membranes, by combining excellent gas separation characteristics of inorganic materials and

acceptable mechanical properties with high economic advantages of polymers. MMMs consist of two parts, a polymer matrix and dispersed inorganic particles that might be zeolite, silica, carbon molecular sieve (CMS), carbon nanotubes, graphene or metal/nonmetal nano-sized particles. The high intrinsic gas permeation characteristics of inorganic particles allow MMMs to possess much higher permselectivity than the pristine polymeric membrane [17,18,20].

In 1970, development of MMMs for gas separation was reported for the first time, when the competitive diffusion of CO_2 and CH_4 was observed by adding zeolite 5A to polydimethylsiloxane, a rubbery polymer [21]. However, the intensive study of gas separation by means of MMMs has been carried out mostly since 2002 [18].

Inorganic fillers can produce an outstanding permeation pathway for smaller molecules and simultaneously a barrier for unwanted larger molecules, which results in a better separation. The overall separation efficiency could be considerably affected by adding even a small quantity of inorganic fillers into polymer matrix [17].

We face new challenges as the usage of polymer-based organic-inorganic membrane increases. One of them is the undesirable defects between the inorganic material and the organic matrix. To improve the interaction between polymer and molecular sieve for better adhesion, many efforts have been made [22]. Uneven dispersion of fillers is another problem [11].

Therefore, it remains as a challenge to select an appropriate type of porous material for the inorganic filler. In this respect, zeolites, MOFs, COFs, and porous polymers have emerged as novel materials in adsorption, separation, catalysis, purification, and energy storage and production [23]. However, until now, researches have been devoted to conventional fillers and polymers in MMM preparation and their modification methods [24–27]. Moreover, many critical reviews considering various viewpoints were recently emerged on MMMs based gas separation [28–38].

This review is especially devoted to explain the developments in methods proposed to preserve/overcome the fabrication challenges of MMMs and also the recent progresses in advanced functionalized materials used in the MMMs for CO_2 separation during the recent years.

2. Energy efficiency of membrane systems

All the factories and machines also all industrial processes need energy to run. Most of these energies are provided via fossil fuel, gas and oil reservoirs. Combustion of coal, petroleum, natural gas and other fossil fuels results in high CO_2 emission to the atmosphere and will cause global warming [39]. Therefore, this unwanted CO_2 should somehow be separated from the atmosphere. Conventional CO_2 absorption has operational complexity, high-energy consumption and high cost. To overcome these challenges membrane based CO_2 separation has been employed with its low overall cost, compact design, low thermal energy requirement and convenient operation procedure [40,41].

National Energy Technology Laboratory (NETL, DOE) announced that up to 2030, the cost of electricity (COE) will increased about 35% in order to remove more than 90% of CO_2 from power plants [42–44]. Although, amine absorption (monoethanolamine (MEA)) is the most considered and frequently used technology in this area, but it suffered from high CO_2 capture cost about \$40–100/ton CO_2 [42]. On the other hand, membrane gas separation can reduce this cost, if it associates with acceptable permselectivity by using high performance materials. As an example, for membrane system with CO_2 permeance about 1000–2000 GPU (1GPU = 10^{-6} $cm^3(STP)/cm^2\,s\,cmHg = 3.35 \times 10^{-10}$ $mol/m^2\,s\,Pa$) and CO_2/N_2 selectivity of about 25–50, the CO_2 capture cost is suitably decreased to \$20–23/ton CO_2 [43].

One of the most important advantages of membrane separation over conventional methods is high energy efficiency achieved by using membrane technologies [45]. Feed stream pressure and CO_2 concentration of feed gas, are two main factors will effect on energy efficiency in gas separation processes [19]. Frequently in membrane separation operations, the input feed stream should be compressed, which is an energy required process. For natural gas processing the input feed stream usually has sufficient pressure for membrane separation [41]. Moreover, high concentration of CO_2 in the feed stream will increase CO_2 diffusion rate and as a result, the membrane efficiency will be increased. In conventional CO_2 separation processes like amine absorption, high concentration of CO_2 in feed stream will increase the operation cost and energy requirements [46]. Because in amine absorption units the higher concentration required more amine circulation rate and it will result in more energy consumption [47].

Moreover, the design factors of membrane separation units such as number of stages and suitable membrane modules should be considered as effective parameters on overall energy consumption. One of the methods to enhance the membrane efficiencies is employing multiple stages operation as in single stage operation the desired separation ratio is not achieved. In multiple stage systems by repeating operation in each stage to achieve the required concentration the energy consumption will increase but it is much less than the energy used to repeat the whole process in a single stage [48]. Yang et al. [49] compared single and multiple stage systems in gas separation operations. They estimated the energy required between stages is about 107.5 KJ/m^{-3} (STP) for a two-stage membrane system. The result showed however in multiple stages more energy is consumed to generate the desired driving force after each stage but comparing to energy consumption in conventional amine absorption system which is about 600–900 KJ/m^{-3} (STP), it is not too much.

Another important factor in controlling energy consumption of membrane-based process is permeability and selectivity of the membranes. By increasing the permeability of the membrane the gas pressure drop will be decreased, consequently the energy used for compression in each stage will be decreased. On the other hand if the selectivity of the membrane is increased the circulation rate and the membrane area will be decreased and as a result the overall cost of the process will be decreased [19]. It can be concluded that by providing membranes with desirable performances for gas separation, the overall process and the energy efficiency will be improved.

Considering all of advantages mentioned for membrane separation applications up to now, but there is a limitation of their

application in industrial scale. This is more important, especially when a high volume of gases should be rectified, as it needs a large area of membrane, which is not an economic process. Baker et al. presented a schematic plot that determines in each state of CO_2 concentration and gas flow rate which separation process is the best choice (Fig. 1) [50].

Therefore by using a membrane separation system before amine absorption a hybrid system is provided which will reduce the energy consumption in CO_2 separation process [3]. Sclierf et al. [51] investigated the effect of CO_2 concentration of feed stream in a hybrid separation system comparing to a conventional amine MDEA (methyl-di-ethanolamine) absorption unit for CO_2 removal from sour gas process. They studied two different feed stream containing 10% and 50% of CO_2 concentration in a cellulose acetate membrane/amine absorption hybrid system. The result showed by using the hybrid system for the feed stream containing 50% CO_2 the weight and the volume of process unit and energy cost decreased by 80%, 50% and 30% respectively, compared to amine absorption unit. In addition, the investment costs and annual operation costs were reduced by 70% and 40%, respectively. However, the hybrid system has no advantage over amine process unit when input feed stream contains 10% CO_2 (see Fig. 2).

It can be concluded that the suitable CO_2 removal units should be designed by considering the feed stream characteristic (such as feed pressure and component concentration), the operating issues, costs and energy consumption. In addition, the membranes performances should be considered as an important factor in membrane based separation systems. Advanced MMMs as the new generation of membranes with high permselectivity and high-energy efficiency could be proper choices to this purpose.

3. Challenges and advancements of MMM fabrication

3.1. Challenges of MMM fabrication

Challenges on preparation of MMMs are classified into two categories:

I. Suitable combination and interfacial contact between filler and polymer matrix: One of the most important tasks in the development of MMMs is the material selection for both polymer matrix and sieve phases. In this respect, consideration should be given to interfacial adhesion, dispersed phase agglomerations and stress formation [10]. It is also understandable that the presence of filler particles change the structure of the surrounding polymer segments, which exerts considerable effects on the transport of larger gas molecules compared to the smaller ones [11,18,52].

Usually, the filler/polymer compatibility is poor because they are not similar in their characteristics. Ideal interfacial morphology should not allow any interfacial void spaces. The polymer layer should cover and adhere to the filler without blocking the pore of the filler particles in order to increase gas permeability and selectivity [6]. Undesirable morphologies at the polymer-filler interface will occur if the material selection is not proper causing the formation of “sieve-in-a-cage”, “leaky interface”, “matrix rigidification” and “plugged sieve” (Fig. 3) [10,17].

Various strategies such as priming and heat treatment have been adopted to overcome these non-idealities in MMM morphologies. Another effective method is preparation of ternary MMMs which will cause a defect free interface between filler and polymer phases [11].

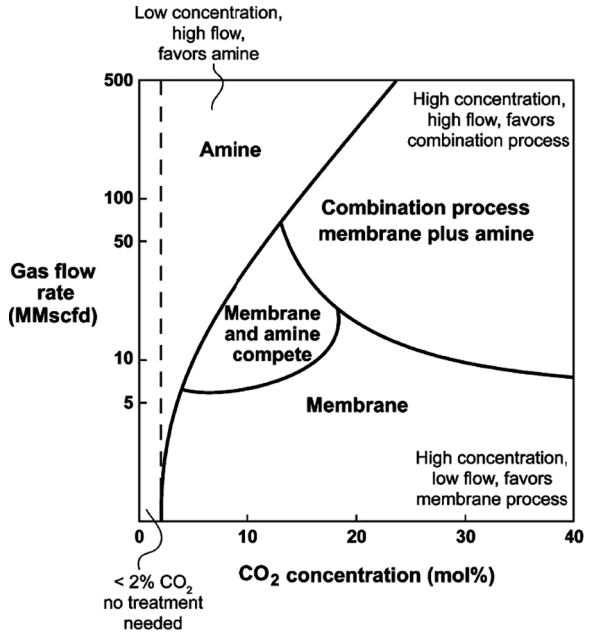

Fig. 1. A schematic view related to application of various carbon dioxide removal technologies, according to the effect of gas flow rate and carbon dioxide concentration [50]. (Copyright 2008. Reproduced with permission from American Chemical Society.)

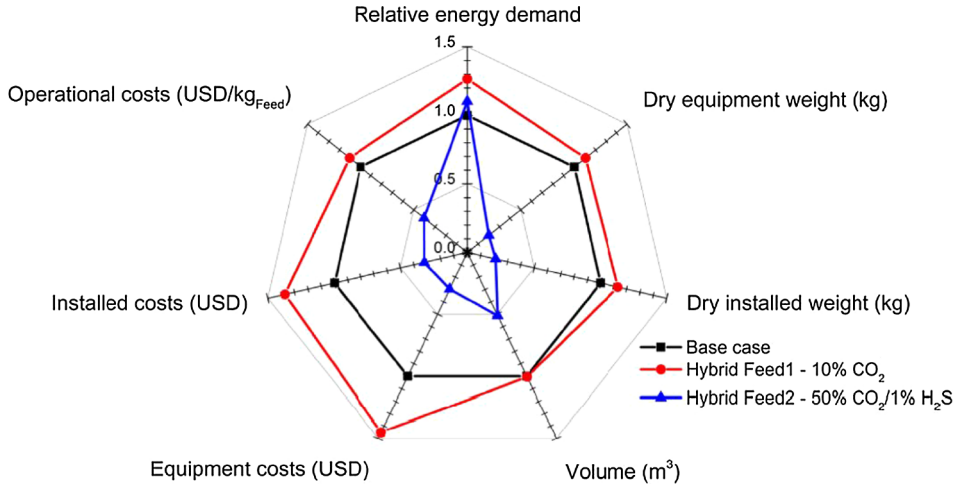

Fig. 2. Spider plot of key performance metrics for amine MDEA absorption unit and membrane/amine hybrid unit for the feed stream containing 10% and 50% of CO_2 concentration [51].

II. Dispersion of inorganic filler in polymer phase, its sedimentation and agglomeration: The properties of membrane may be negatively affected when an excessive amount of inorganic fillers are loaded. Poor dispersion of inorganic fillers leads to the sedimentation and agglomeration of particles in the polymer matrix. Particle accumulation due to the difference in physico-chemical properties such as density and polarity between the filler and the polymer may cause sedimentation or migration of fillers to the membrane surface, the prevention of which is the most serious challenge in MMM fabrication, since otherwise filler and polymer phases will not be distributed uniformly [10,11].

Different techniques like addition of surfactant and salt have been applied for stabilizing the colloidal suspensions by preventing the particles to coalesce, nucleate, aggregate, and form their agglomerates during the MMM fabrication. Ultrasonication is commonly used to help homogenous distribution of inorganic fillers in the polymer matrix. Grafting of compounds similar to the polymer matrix is another way that can help homogeneous-dispersion of particles in the polymer phase. Fig. 4 represents various techniques used to prepare defect free functional composites.

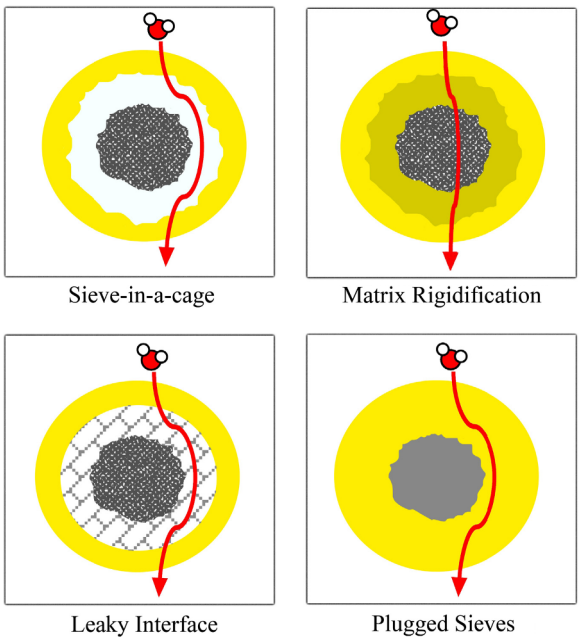

Fig. 3. Non-ideal interfacial morphologies in MMMs [10]. (Copyright 2014. Reproduced with permission from Elsevier Science Ltd.)

3.2. Development of advanced MMMs

Development of high performance membrane materials with new functional groups and new chemistries has attracted much attention over the past few years. Reasonable selection and suitable matching of polymers and fillers are of primary importance in the development of advanced hybrid membranes [6]. Designing a proper filler, modifying the filler-polymer interfacial morphology, controlling the MMM fabrication conditions, and thus, suppressing the formation of undesired defects are the matters that should be considered for the effective development of MMMs [54]. Physical aging of membrane is another defect that needs to be controlled. It can drastically reduce the initial permeability of polymer-based membranes over a quite short period of time. The use of MMMs can be one possible solution for physical aging [23].

Recently new advanced materials have been proposed for fillers such as covalent organic frameworks (COFs), organic frameworks (MOFs), carbon nanotubes (CNTs), layered silicates or graphene, which have advantages over the first generation MMMs that were provided using conventional fillers such as silica, zeolites and carbon molecular sieves [55]. The conventional inorganic fillers show weak bondings to the polymer chains, which induces nonselective defects in the resulting MMMs.

It continues to be a challenge to increase gas selectivity without compromising permeability [56]. To meet the challenges and produce high performance membranes, the methods such as acid treatment, CD (cyclodextrine) treatment, ozone mediated processes, grafting, metal depositing, solvothermal depositions, silanation, addition of ionic liquids, low molecular weight additives and ion exchange materials have been attempted [26,57–64]. One-pot synthesis is another method to scatter nanoparticles uniformly while they are being synthesized. It reduces the chance of uneven coating of a functional layer over the membrane surface. The one-pot synthesis prevents nanoparticle agglomeration that occurs if dry particles are incorporated into the membrane [10].

Sol-gel method also enables uniform dispersion of inorganic fillers. To adopt sol-gel method is especially a good choice for designing multiple functionalities. The CO_2 solubility could potentially be improved by designing the functionalized fillers with high affinity toward CO_2. Many different kinds of precursors have been used in sol-gel system such as epoxy-, amino-, mercapto-, and vinyl-containing precursors and many different functionalized organic–inorganic networks were formed to enhance the capacity to interact with polar gases like CO_2 [6,54]. Bringing CO_2-philic units into the membrane increases the CO_2 solubility, improves

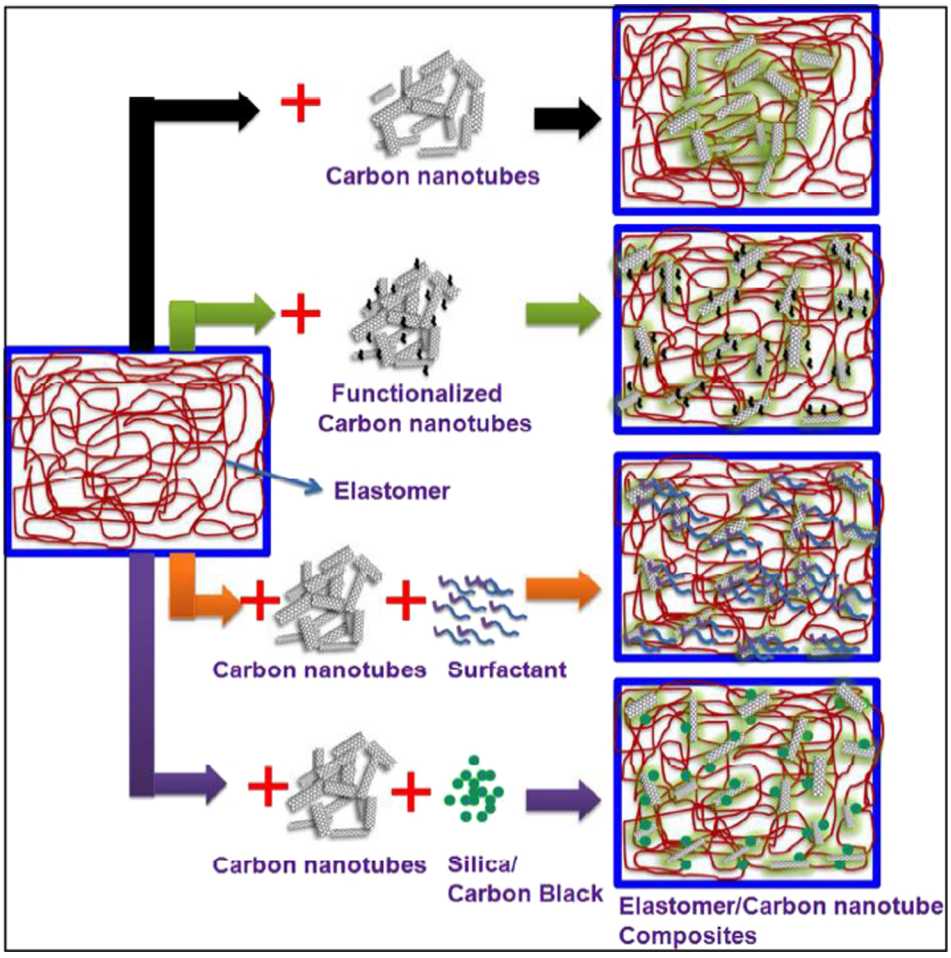

Fig. 4. Different CNT/elastomer composites [53]. (Copyright 2014. Reproduced with permission from Royal Society of Chemistry.)

facilitated transport, and consequently enhances CO_2 permeability and CO_2/gas selectivity. For this purpose the materials having strong affinity toward CO_2 are suitable choices such as ethylene oxide units, amine, phosphonium, oxadiazole and amidine groups [65].

4. Advanced functionalized materials used to prepare MMMs for CO_2 separation

4.1. Advanced functional fillers

4.1.1. Zeolite

Hydrated aluminosilicate with regular intercrystalline cavities and channels in molecular dimension possessing open three dimensional framework structures are known as zeolites [15,66]. Good thermal and chemical stabilities, well-defined microstructure and high mechanical strength make zeolites suitable for membrane fillers. Adsorption and diffusion properties of zeolites depend on the size of channel cavities. In fact, zeolite molecular sieves exhibit permeability and selectivity superior to polymeric materials, which may well compensate the high cost and the difficulties in defect-free membrane fabrication [67–75].

In fabrication of zeolitic MMMs, interphase void and incompatibility are often observed between the polymer and the filler particles. Rigidification of polymer chain may also occur due to uneven shrinkage stresses produced during solvent removal. To avoid these defects a good adhesion between filler and polymer should be achieved while maintaining chain flexibility [76–79].

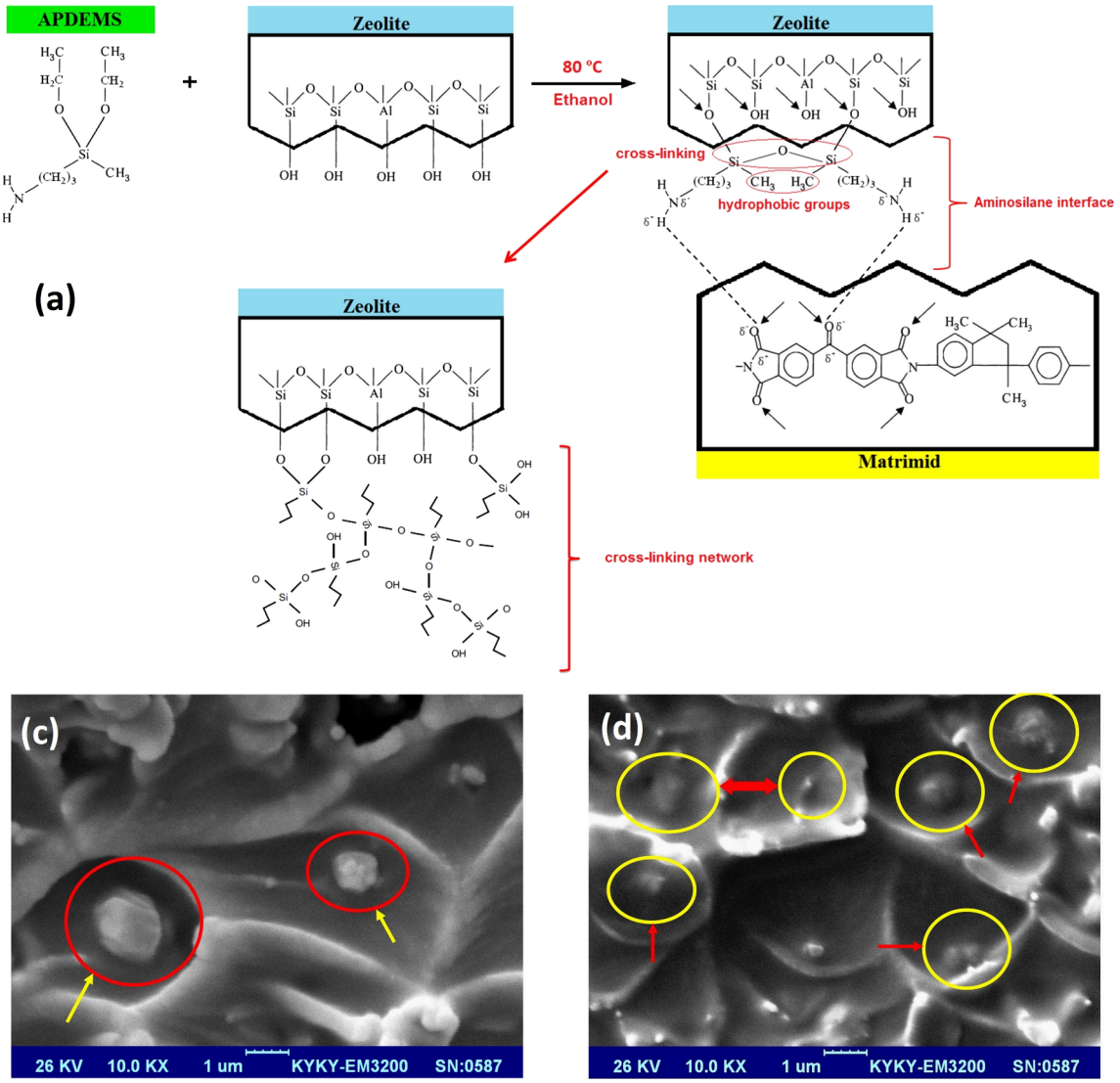

Fig. 5. (a) A schematic view of the grafting reaction mechanism between silane coupling agent-zeolite surface-Matrimid®5218. Cross-section SEM images of Matrimid based MMMs containing15 wt.% (b) NaY and (c) Silane-modified NaY (crater-like pattern) [84]. (Copyright 2015. Reproduced with permission from Elsevier Science Ltd.)

There are different techniques to eliminate the unselective voids or gaps. One of them is annealing the membrane near/above the glass transition temperature of polymer [68].

A third component, mostly a low molecular weight (LMW) organic compound can also be added to the zeolite/polymer interface. It fills the gap between the two phases more easily than the surface treatment of zeolites. The LMW materials will increase the polymer matrix stiffness owing to the decrease in polymer chain segmental motions. Thus, by appropriate choice of the ternary component, the MMM performance will be enhanced. Many LMW materials with hydroxyl and carbonyl groups that can anchor filler and polymer by hydrogen bonding are considered as good candidates [80].

Dutta and Bhatia [81] studied the CO_2 separation properties of zeolite-polyimide MMMs by equilibrium molecular dynamics (EMD) simulations. The densified polymer region was predicted in the presence of MFI zeolite in PI matrix with the thickness of about 1.2 nm. Their results also indicated that the crystal size is not significantly affecting the filler/polymer interface. The rigidified polymer resists against gas diffusion especially in the case of gas molecules with larger kinetic diameter, results in higher CO_2/CH_4 selectivity.

To modify zeolite surface for improving compatibility of inorganic fillers with matrix, different silane coupling agents are used, such as: aminopropyltriethoxy silane (APTES), 3-aminopropyltrimethoxysilane (APTMS), N-b-(aminoethyl)-aminopropyltrimethoxy silane, glycidyloxy-propyltrimethoxy silane, (3-aminopropyl)-dimethylethoxy silane, aminopropyl-diethoxymethyl silane (APDEMS), 1H,1H,2H,2H-perflourodecyltriethoxysilane (HFDS) [67,82]. They increase affinity of zeolite to the functional groups of polymer matrix and also improve surface property of zeolite. Through the modification, zeolite surface changes from hydrophilic to hydrophobic [77]. To prevent pore blockage at the zeolite surface caused by using three ethoxy-containing silane agents, such as APTES or APTMS, two ethoxy-contaning silane agents such as APDMS could be employed [15]. As compared to one ethoxy-contaning silane agents, the two ethoxy-contaning silane agents provide more adhesive linkages with the hydroxyl groups of zeolite surface. On the other hand, comparing to the three ethoxy-contaning silane agent linkages are lowered, and so the pore blockage. Aminosilanes with second reactive end groups will bond the zeolite surface to polymer chains and improve zeolite/polymer compatibilty in MMMs and can simultaneously increase the adsorption of CO_2 molecules through the interaction with amine end groups [83]. Ebadi Amooghin et al. [84] fabricated novel MMMs by grafting the aminosaline on micro-sized nanoporous NaY zeolite particles and embedding them into the Matrimid®5218 matrix. They used 3-aminopropyl(diethoxy)methylsilane (APDEMS) as the silane coupling agent. The results showed that at 15% filler loading (the optimum condition) CO_2 permeability was enhanced about 16% from 8.34 to 9.70 Barrer, and CO_2/CH_4 selectivity about 57% from 36.3 to 57.1. This increase was due to improved dispersion of the silane modified NaY particles in the Matrimid matrix. Fig. 5 shows the grafting reaction of silane coupling agent with zeolite particles and the probable interactions between the modified filler-polymer, and between the modifying agents themselves.

In another study, Gong et al. [85] successfully prepared 5A zeolite with increased surface roughness by growing nanostructured

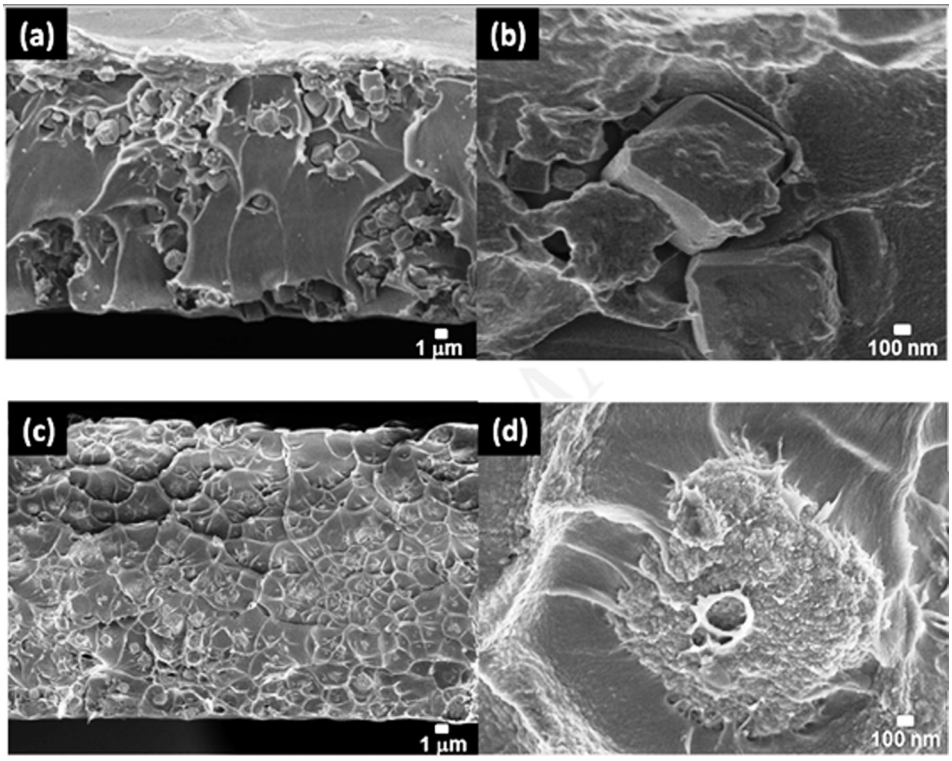

Fig. 6. Cross section FESEM images: (a) & (b) Matrimid®/bare 5A, (c) & (d) Matrimid®/surface treated 5A [85]. (Copyright 2017. Reproduced with permission from Elsevier Science Ltd.)

$Mg(OH)_2$ on the zeolite surface via a facile aqueous phase treatment. By embedding surface modified 5A zeolite into the Matrimid® matrix as filler the mechanical strength and stability of MMM was enhanced due to the improved polymer-zeolite compatibility. Moreover, CO_2 permeability increased (ca. 120%) and also CO_2/CH_4 selectivity was improved compared to the pristine polymeric membrane. Fig. 6 shows the improvement of polymer-zeolite interfacial morphology.

In order to enhance CO_2 adsorption in zeolite using mono- or di-valent ions, like Ag^+, Cu^+, Mg^{2+} and Co^{2+}, without producing considerable changes in their structure, ion exchange treatment of zeolite was attempted [86–88]. Ebadi Amooghin et al. [87] embedded Ag^+ exchanged zeolite Y into the Matrimid matrix. Inherent surface diffusion process of zeolite Y and the facilitated transport mechanism of Ag^+ ions resulted in the excellent Matrimid/Ag Y (15 wt%) MMM gas separation performance (Fig. 7).

In another work, Montes Luna et al. [89] modified natural clinoptilolite zeolite by replacing the Na^+ ions with Ca^{2+} and then fabricated a MMM by incorporating the modified zeolite into Pebax 2533 for mixed gas separation. XRD patterns indicated that the main zeolite structure is not changed through the ion exchange. Although the porosity of modified zeolite was slightly changed in terms of pore average volume and size parameters. $CH_4/CO_2/N_2$ ternary gas permeation properties at 10 bar and 35 °C revealed that the CO_2 permeability of the neat membrane was slightly increased from 332.4 to 353.3 Barrer at 10 wt% filler loading. Moreover, the CO_2/CH_4 selectivity was increased from 9.56 to 31.77. They claimed that these enhancements are related to the Ca^{2+} ions-exchanged zeolites which homogeneously scattered in the polymer matrix.

Utilization of block copolymers as polymer matrix is another idea for preparing MMMs without zeolite surface modification due to the good interaction with zeolite nanoparticles [90,91].

The permeability and selectivity data of zeolite-based MMMs reported in recent years are summarized in Table 1.

4.1.2. Silica

Silica nanoparticles are another category of inorganic fillers utilized in fabrication of MMMs. They can be divided into two groups. The first one is non-porous silica. Non-porous silica particles, when embedded into the polymer matrix, do not take part in the gas transport. Instead, it will change the molecular packing of polymer chains around the particles and consequently the gas permeability and selectivity will upgrade. Introducing non-porous silica into polymer matrix may increase polymer free volume without producing non-selective voids, which enhances the gas permeability without decreasing the selectivity. However, if the free volume is large enough to allow non-selective Knudsen transport, the selectivity decreases [15]. Another form of silica is (meso-) porous silica with different structure, pore diameters and particle sizes. MCM-41 has a 1D-pore channel structure while MCM-48 has 3D interconnected pore structure. They belong to the most popular fillers due to their desirable pore structures [10]. MCMs loaded MMMs have shown outstanding gas separation performances because of their excellent filler/polymer compatibility. Both MCM-41 and MCM-48 contain a large number of OH groups that take part in a series of reactions to produce hybrid materials with both organic and inorganic components. MCM-41 with hexagonal unidirectional structure exhibits more pore blocking and therefore less diffusion, in comparison with MCM-48 [100].

Higher separation performance and excellent interfacial compatibility are achieved by different methods such as thermal annealing [101] and surface modification. Meso-porous silica's surface modification by grafting of amine group [102–105], sulfonic acid [106], and silane coupling agents [107–109] is an easy solution to prevent formation of undesirable voids near the filler-polymer interface, which in turn improves gas separation.

Xin et al. [110] developed an efficient MMM for gas separation by embedding three different kinds of functionalized silica

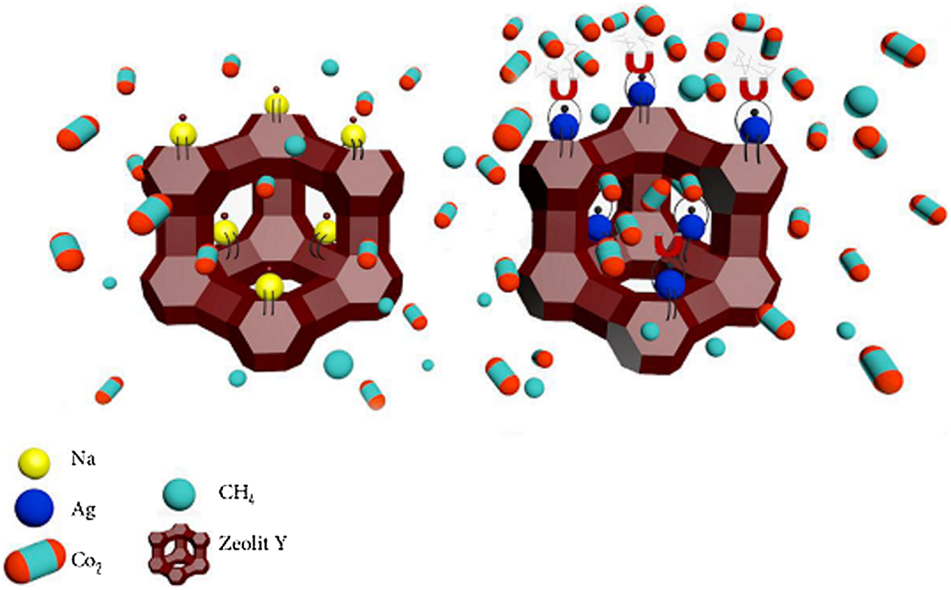

Fig. 7. CO_2 facilitated transport via Ag^+ ion exchanged zeolite Y [87]. (Copyright 2016. Reproduced with permission from Elsevier Science Ltd.)

Table 1
Different zeolite/MMMs performances for CO_2 separation.

Zeolite	Polymer	wt.% loading (best MMM performance)	Test conditions	P_{CO2} (Barrer)	CO_2/CH_4 selectivity	CO_2/N_2 selectivity	CO_2/H_2 selectivity	Ref.
SAPO34-EDA	PES	20	Room T, 2 bar	10.091	12.14	–	–	[92]
SAPO34-HA				GPU	16.09	–	–	
				0.835				
				GPU				
CHA zeolite	PTMSP	5	333 K, 2.5 bar	22,914	-	6.2	–	[93]
LTA5 zeolite				27,294	-	5.4	–	
Rho zeolite				64,920	-	5.1	–	
Zeolite A				112,627	-	4.9	–	
SAPO34	PSf	(10)	Room T, 3.48 bar	317.0	27.9	–	–	[82]
SAPO34-HFDS		(10)		GPU	38.9	–	–	
				278.8				
				GPU				
(APDEMS) silane modified zeolite (Sm-NaY)	Matrimid®5218	5	35 °C, 2 bar	7.2	34.3	–	–	[84]
		10		7.66	40.3	–	–	
		15		8.31	48.9	–	–	
		20		9.35	26.7	–	–	
Ag^+ ion-exchanged zeolite	Matrimid®5218	0	35 °C, 2 bar	8.34	36.3	–	–	[87]
		5		13.12	48.6	–	–	
		10		16.06	54.7	–	–	
		15		18.62	60.1	–	–	
		20		21.18	27.7	–		
Co^{2+} ion-exchanged zeolite	Cellulose acetate (CA)	0	Room T, 4 bar	2.28	–	25.5	–	[88]
		(15)		3.28	-	29.9		
5A zeolite	Matrimid®5218	0	40 °C, 1 bar	10.2	33.6	–	–	[85]
Surface modified 5A zeolite		10		26.7	31.3	–	–	
		20		31.0	30.8	–	–	
		10		19.6	35.4	–	–	
		20		22.4	36.4	–	–	
Bare mesoporous Ca-A	Matrimid®5218	0	40 °C, 1 bar	10.2	34	–	–	[94]
NH_2-mesoporous Ca-A		20		11.5	31	–	–	
		20		9.2	39	–	–	
NH_2-mesoporous Ca-A	XLPEO (cross-linked polyethylene oxide)	0	40 °C, 1 bar	450	15	–	–	[94]
		10		380	18	–	–	
		20		360	23	–	–	
NaY zeolite	Cellulose acetate (CA)	(20)	25 °C, 4 bar	4.87	–	25	–	[68]
(APDEMS) silane modified zeolite (Sm-NaY)	Cellulose acetate (CA)	5	25 °C, 2 bar	3.7*	-	27*	–	[83]
		10		4	-	27	–	
		15		4.1	-	26	–	
		20		4.6	-	27	–	
		25		4.8	-	25	–	
ZSM-5	Pebax	10	35 °C, 3 bar	251.5	25.1	–	–	[95]
ZSM-5/PEG200	Matrimid	5/5	35 °C,10 bar	11.53	60.1	–	–	[96]
titanosilicate ETS-10	polysulfone	10	35 °C,330 kPa	7.8	38	–	–	[97]
	polyimide 6FDA-6FpDA,	10		125	51	–	–	
TS1-100	Matrimid®	0	35 °C, 8 bar	5.0	25.5	–	–	[98]
TS1-25		10		7.2	26.8	–	–	
ETS-10		20		8.1	26.3	–	–	
		30		9.6	25.0	–	–	
		10		7.4	31.5	–	–	
		20		7.9	31.6	–	–	
		30		9.5	30.8	–	–	
		10		5.8	32.6	–	–	
		20		5.8	33.3	–	–	
		30		6.2	27.5	–	–	
SAPO34-FAS-17 (1H, 1H, 2H, 2H-perfluorodecyltrichlorosilane)	Hyflon AD60X	35	25 °C, 5 bar	155	37	12	–	[99]

* Values are approximated from plots.

microspheres into SPEEK polymer. They tailored three kinds of functionalized SiO_2 microspheres by a facile distillation-precipitation polymerization procedure to graft with carboxyl, sulfonic acid and pyridine (Fig. 8). They concluded amine functionalized SiO_2 increased the gas separation performance by producing acid-base pairs (–SO_3…H_2N–) at polymer-filler interface to work as CO_2-philic sites. The results showed the MMMs loaded by pyridine functionalized silica microspheres exhibited the best gas separation

performance by enhancing CO_2/CH_4 (N_2) selectivity from 26.7(35.1) to 64.8(68.3) and the CO_2 permeability from 525 to 2043 Barrer, compared to pristine SPEEK.

Laghaei et al. [107] fabricated MMMs from MCM-41 meso-porous silica incorporated PES and investigated the effect of two different silane coupling agents, i.e. 3-aminopropyltrimethoxysilane (APTMS) and trimethylchlorosilane (TMCS) were used one at a time in order to modify the filler surface. They reported APTMS had better interaction with PES matrix than TMCS due to hydrogen bond formation between N-H polar groups of APTMS with the sulfone groups of PES, which increased the interfacial adhesion and helped the fabrication of membranes with higher mechanical strength and also thermal stability. Furthermore, the modification of MCM-41 with APTMS enhanced the CO_2 permeability and CO_2/CH_4 selectivity about 250% and 40%, respectively.

In another study, Su et al. [111] used aminopropyl modified silica nanoparticles to make a hybrid cross-linked poly(ethylene glycol) membrane. They reported a significant increase in transport and mechanical properties. Fig. 9 shows how the silica nanoparticles undergo an aminopropyl triethoxysilane (APTES) silanization reaction.

Park et al. [112] studied the effect of incorporating 3-dimensionally disordered meso-porous silica (DMS) into different kinds of glassy polymer matrices in order to improve membrane separation performances. The hydrogen bonding between hydroxyl groups on DMS particles and functional (aryl ether or carbonyl) groups of the polymer chains and possible intrusion of polymer chains into meso-pores, provide a good sticking between the DMS particles and the polymer matrix. At nominal DMS concentration of 10 wt%, the glassy polymer-based MMMs showed the improved penetrant permeabilities due to the increase in diffusivities. Permeability of gases like CH_4, N_2, CO_2 and NF_3 were improved by DMS incorporation because of the improvement in diffusivity.

Table 2 presents the permeability and selectivity of different silica loaded MMMs.

4.1.3. MOF

Inorganic units provided by metal ions or clusters and organic linkers are new hybrid materials known as metal organic frameworks (MOFs). They are crystalline coordination compounds also called coordination networks [122,123]. With unique properties, high porosity, different pore sizes and shapes, multiple functional sites and large specific surface area they can create a large variety of final crystals with alterable properties [123–126]. Since the molecular sieving or selective adsorption of MOFs is significantly higher than the conventional particles, they attained great potential to be employed [127–129].

Composite membranes with combination of MOFs and polymers will stop trade-off between permeability and selectivity. MOF based MMMs will result in well-dispersed particles, perfect interface adhesion between polymer and MOFs as well as high gas fluxes [124,130–132]. MOFs used as fillers have potential advantages over other porous materials, because of better connection between filler and polymer chains, due to their partially organic nature. The sieve blockage morphology, which is considered as the most

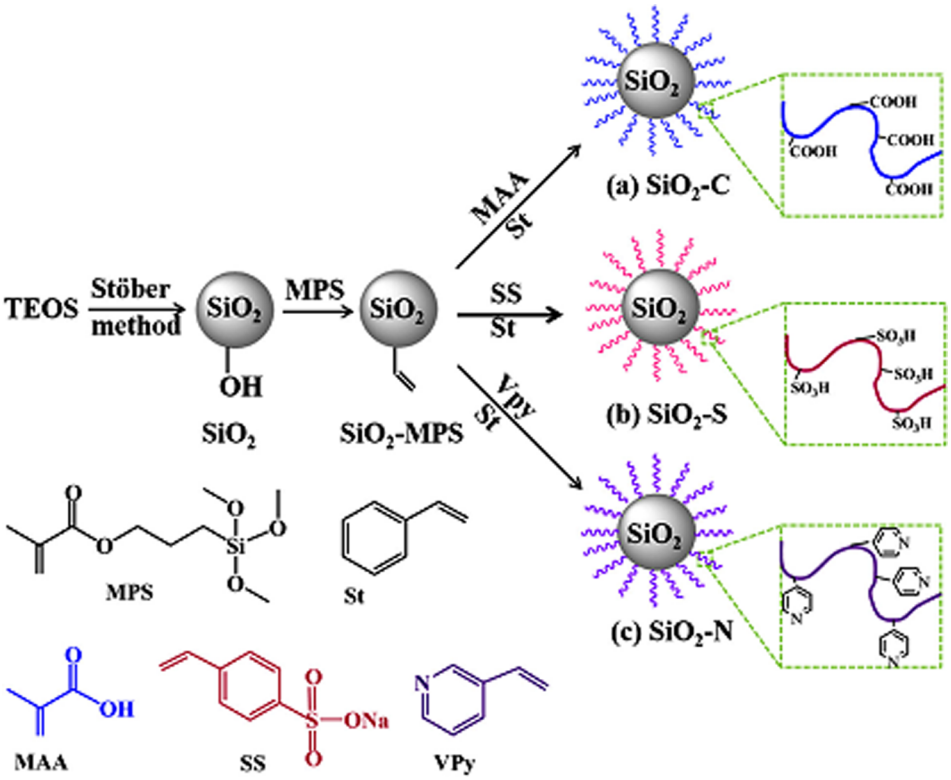

Fig. 8. Functionalization of silica microspheres by (a) Carboxyl acid, (b) Sulfonic acid and (c) Pyridine groups [110]. (Copyright 2016. Reproduced with permission from Elsevier Science Ltd.)

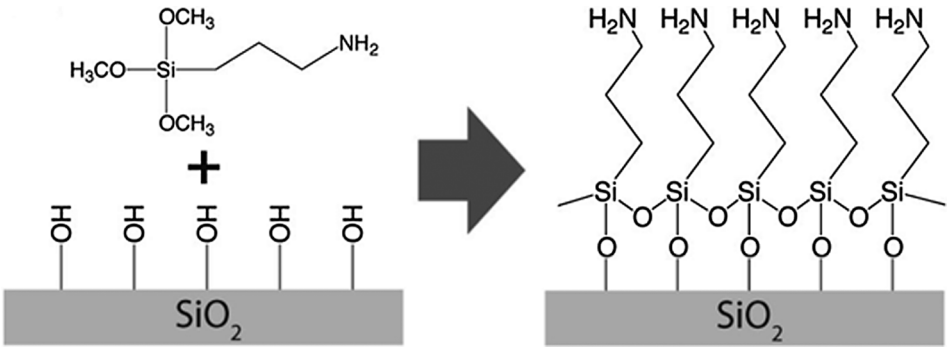

Fig. 9. Silanization of SiO_2 with APTES [111]. (Copyright 2015. Reproduced with permission from American Chemical Society.)

serious deficiency of the MMM, can also be avoided. Moreover, effects of MOF on the MMMs gas separation performances might be greater for a specific weight percentage of the filler due to their higher pore volume and less density compared to other fillers like zeolites [133,134].

The other advantage of this type of material with incomparable platforms is to compact multiple functional sites within a single system [135]. Changing synthetic conditions for initial reactants used to generate the MOF will alter the chemical structure and physical property of the MOF, which can be considered as their advantages. Presence of functional groups in a specific MOF structure will greatly affect the CO_2 removal performance [123]. Multi-functional sites (MFSs) are achieved via multiple-mono or multi-functional species of MOF materials. Established techniques for synthesis of MFS-MOFs are using various processing functional sites such as organic ligands, metal cluster and multiple guest components. The synthesis strategies used for MFS-MOFs are depicted in Fig. 10. Enzymes and metal nanoparticles (NPs), heteropoly acids are some of external molecules that provide frameworks with functional sites [135,136].

MOFs as nanofillers have great potential to be functionalized. Rodenas et al. [127] fabricated a new material which can be used as functional component for different technologies including gas separation by incorporating two-dimensional nanostructures into polymer matrix. They investigated copper 1,4-benzene dicarboxylate MOF nanosheets to make the MOF-polymer composite membrane for separation of CO_2 from CO_2/CH_4 mixtures. Remarkable increase in the CO_2/CH_4 gas mixture separation efficiency was achieved by introducing MOF nanosheets into polyimide matrix. CO_2 permeabilities were in the range of 2.8–5.8 Barrer, whereas CH_4 permeabilities were lower than 0.3 Barrer in all cases. They concluded that the two-dimensional (2D) nanostructures are suitable for advanced structures and functional materials for gas separation. Fig. 11 provides some information about synthesis/structure of the CuBDC MOF nanostructures.

Investigations have shown that incorporation of amino-functionalized MOFs into polymer matrices results in a good performance for CO_2 separation [137–140]. Sulfonate functionalization of MOFs [141] and post treatment [142] are two important strategies to enhance the MMM separation performances. As an example, Xin et al. [141] prepared MMMs by incorporating sulfonated functionalized MIL-101(Cr) into SPEEK matrix. The sulfonated MOF enhanced the CO_2 solubility and consequently the membrane selectivity improved for CO_2/CH_4 and CO_2/N_2 separation systems. On the other hand, the CO_2 permeability increased due to the diffusion of gases through the porous MOFs. The sulfonic acid groups from polymer matrix and sulfonated MOF constructed continuous CO_2 transport channels and improved CO_2 solubility selectivity.

Sabetghadam et al. [55] investigated the effect of particle morphology on the amine functionalized MOF-based MMM separation performances. They synthesized Matrimid based MMMs containing NH_2-MIL-53(Al) for CO_2/CH_4 separation of an equimolar mixture. Nanoparticles, microneedles and nanorods were the three different morphologies of amine-functionalized MOF dispersed into Matrimid. Embedding 8 wt% of NH_2-MIL-53(Al) nanoparticle as a fine performing filler into polymer matrix resulted in a higher separation performance compared to other morphologies. Distributions of the MOF particles for the 8 wt% loading MMMs are shown in Fig. 12.

Zirconium(IV)–carboxylate MOFs (Zr-MOFs which is typically known as UiO-66 and UiO-66-NH_2) have brilliant chemical and thermal stability which is due to the strong coordination bonds between Zr(IV) atoms and carboxylate oxygens (hard acid-hard base). That's why recently it has been frequently taken into consideration in MMMs fabrication.

Ma et al. [143] reported the CO_2 separation properties of novel MMMs in which UiO-66 and UiO-66-NH_2 MOFs were embedded into the poly(PEGMA-co-PEGDMA) polymer matrix. MMMs were prepared by addition of 10–35 wt% filler in the polymerization mixture and through a free radical polymerization, the dispersed crystals incorporated into the polymer network (see Fig. 13). Gas permeation results revealed that addition of 35 wt% UiO-66 octahedron resulted in increasing the CO_2 permeability from 117 to 205 Barrer and CO_2/CH_4 selectivity from 15 to 19. However, by adjusting the MOF size and shape, MMM containing 35 wt% clusters of aggregated UiO-66 revealed a 247% increase in permeability and showed the CO_2 permeability about 365 Barrer. This is due to the formation of dual transport pathways in the MMM.

Besides, Semino et al. [144] comprehensively explored the microscopic interfacial structures of Zr-based UiO-66/polymers by integration of density functional theory calculations and force field-based molecular dynamics simulations. Fig. 10 depicts the snapshots of UiO-66, various polymers and related MOF/polymer interfaces. Their results indicated that the polymer rigidity is a negative factor for MOF/polymer compatibility. They stated a fact that polymers with Young's modulus values less than 1 GPa create

Table 2
Different silica/MMMs performances for CO_2 separation.

Silica	Polymer	wt.% loading (best MMM performance)	Test conditions	P_{CO2} (Barrer)	CO_2/CH_4 selectivity	CO_2/N_2 selectivity	CO_2/H_2 selectivity	Ref.
PDA-2.2PEI-SiO_2	PEG	5	35 °C, 350 kPa	1300 GPU	–	27	–	[102]
NH_2-SiO_2	PVAm	0	298 K,	124 GPU	11.98	20.22	–	[113]
		10	0.5 MPa	119 GPU	14.08	25.85	–	
Silica-APTES	Cross-linked polyethylene glycol (XLPEG)	0	35 °C, 6 atm	116	21	62	–	[111]
		2.7		134	21	63		
		6.6		130	21	62		
		10.2		125	20	62		
		16.2		109	21	64		
TEOS/protamine	Pebax®1657	10	25 °C, 1 atm	161.5	65.5	82.8	–	[103]
			25 °C, 10 atm	160.5	63.8	81.6	–	
			65 °C, 1 atm	515.2	8.1	39.89	–	
Carboxyl functionalized silica microspheres	Sulfonated poly(ether ether ketone) (SPEEK)	20	25 °C, 1 bar	1400*	54*	57*	–	[110]
Sulfonic acid functionalized silica microspheres		20		1300	50	54	–	
Pyridine functionalized silica microspheres		20		2000	64	68	–	
PEI-MCM-41	Pebax®1657	5	25 °C, 2 bar	699	25	61	–	[105]
		10		810	29	78	–	
		15		1015	32	94	–	
		20		1521	41	102	–	
DMS	PS	10	35 °C, 1 atm	12.81	23.7	28.5	–	[112]
	PS	20		28.51	19.4	23.8	–	
	6FDA-DAM:DABA	10		202.9	36.2	22.2	–	
	6FDA-DAM:DABA	20		364.96	33	20.8	–	
CSM-18.4	Matrimid®	30	35 °C, 9 bar	38.9(CO_2–CH_4)	41.9	38.1	–	[114]
				37.7(CO_2–N_2)			–	
CSM-23.3	Matrimid®	30	35 °C, 9 bar	48.6(CO_2/CH_4)	38	37.6	–	[114]
				52.6(CO_2/N_2)			–	
SO_3H-MCM-41	Matrimid	10	25 °C, 10 bar	7.1*	36*	29.5*	–	[106]
		20		8.2	37	30	–	
		30		10	37.5	31	–	
Cis-9-octadecenoic acid-SiO_2	PEBA	(8)	25 °C, 2 bar		17	45	124	[115]
APTMS-modified MCM-41	PES	5	25 °C, 8 bar	1.97	28.8	26.2	–	[107]
		10		2.55	31.3	28.5	–	
		15		3.03	35.1	30.8	–	
		20		3.44	35.6	31.2	–	
TMCS-modified MCM-41	PES	5	25 °C, 8 bar	1.78	30.5	26.0	–	[107]
		10		2.25	29.8	25.6	–	
		15		2.51	27.8	23.9	–	
		20		2.72	25.9	22.2	–	
Titanosilicate ETS-10	Polysulfone	10	35 °C, 330 kPa	7.8	38	–	–	[97]
	Polyimide 6FDA-6FpDA,	10		125	51	–	–	
SiO_2	PBO(6FAHP-OBC)	0		67.7	40	–	–	[116]
		10		103	41	–	–	
		20		168	41	–	–	
		30		206	49	–	–	
SiO_2	PBO(6FAHP-BTC)	0		67.7	40	–	–	[116]
		10		103	40	–	–	
		20		16	41	–	–	
Cloisite15A(C15A)	Polysulfone(PSF)	1	25 °C, 5 bar	18.72	20.98	–	–	[117]
Cloisite15A(C15A)	PES	1	25 °C, 3 bar	3.71	46.89	–	–	[118]
Cloisite15A(C15A)	PSF	0.05	25 °C, 5 bar	56.25	40.26	–	–	[119]
Attapulgite (ATP)	Pebax®1657	1.4	35 °C, 4 bar	69	–	–	42	[120]
		1.7		77	–	–	52	
		3.5		73	–	–	52	
		6.3		63	–	–	43	
		11.1		33	–	–	29	
		21.0		30	–	–	19	

(*continued on next page*)

Table 2 (*continued*)

Silica	Polymer	wt.% loading (best MMM performance)	Test conditions	P_{CO2} (Barrer)	CO_2/CH_4 selectivity	CO_2/N_2 selectivity	CO_2/H_2 selectivity	Ref.
SiO	PVA/PEG/PEI/ triethylenetetramine	3.34	100 °C, 2.5 atm	710	–	300	–	[121]

* Values are approximated from plots.

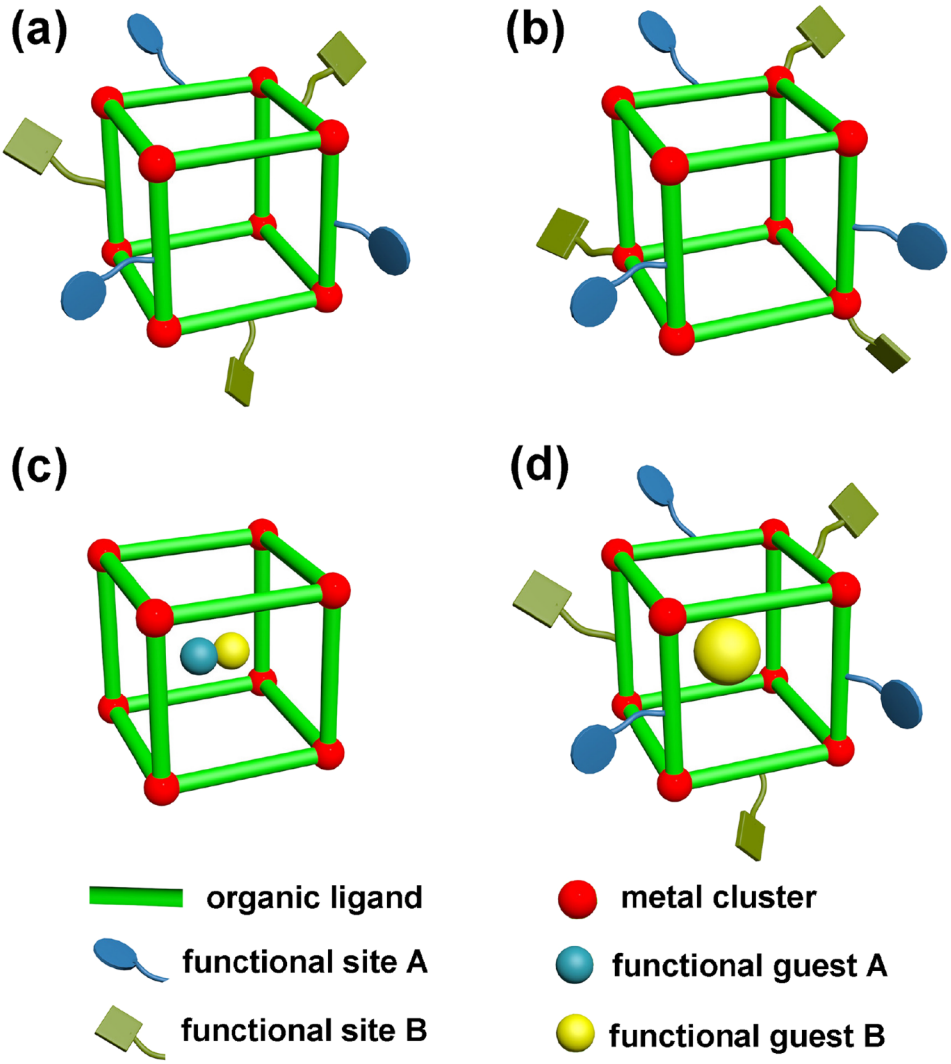

Fig. 10. Various strategies investigated in the synthetic of MFS–MOFs [135]. (Copyright 2016. Reproduced with permission from Elsevier Science Ltd.)

extremely compatible systems. Indeed, in these polymers, chain ends can better penetrate in the MOF pores and also can fill the pockets created by the atomic roughness of the surface. Among the various surveyed systems, UiO-66/PVDF and UiO-66/PEG MMMs revealed better interfacial compatibility with the MOFs (Fig. 14III-c and d). On the other hand, incompatible systems, UiO-66/PS and UiO-66/PIM-1, contained some interfacial voids with brittle and fragile structures (Fig. 14III-c and d). Achieved results were finally suggested that two parameters should be tuned in successful MOF-based MMMs: enough compatibility to achieve a sturdy structure in simultaneous with controlling interactions to avoid the occurrence of pore blocking.

In another work, Gao et al. [145] presented a new approach to prepare the mechanically robust-high performance MMMs (Fig. 15). They covalently attached the norbornene modified UiO66-NH_2 MOF and cis-5-norbornene-exo-2,3-dicarboxylic anhydride (ND) by ring-opening metathesis polymerization (ROMP) method in a very short time. Their approach resulted in exceptional

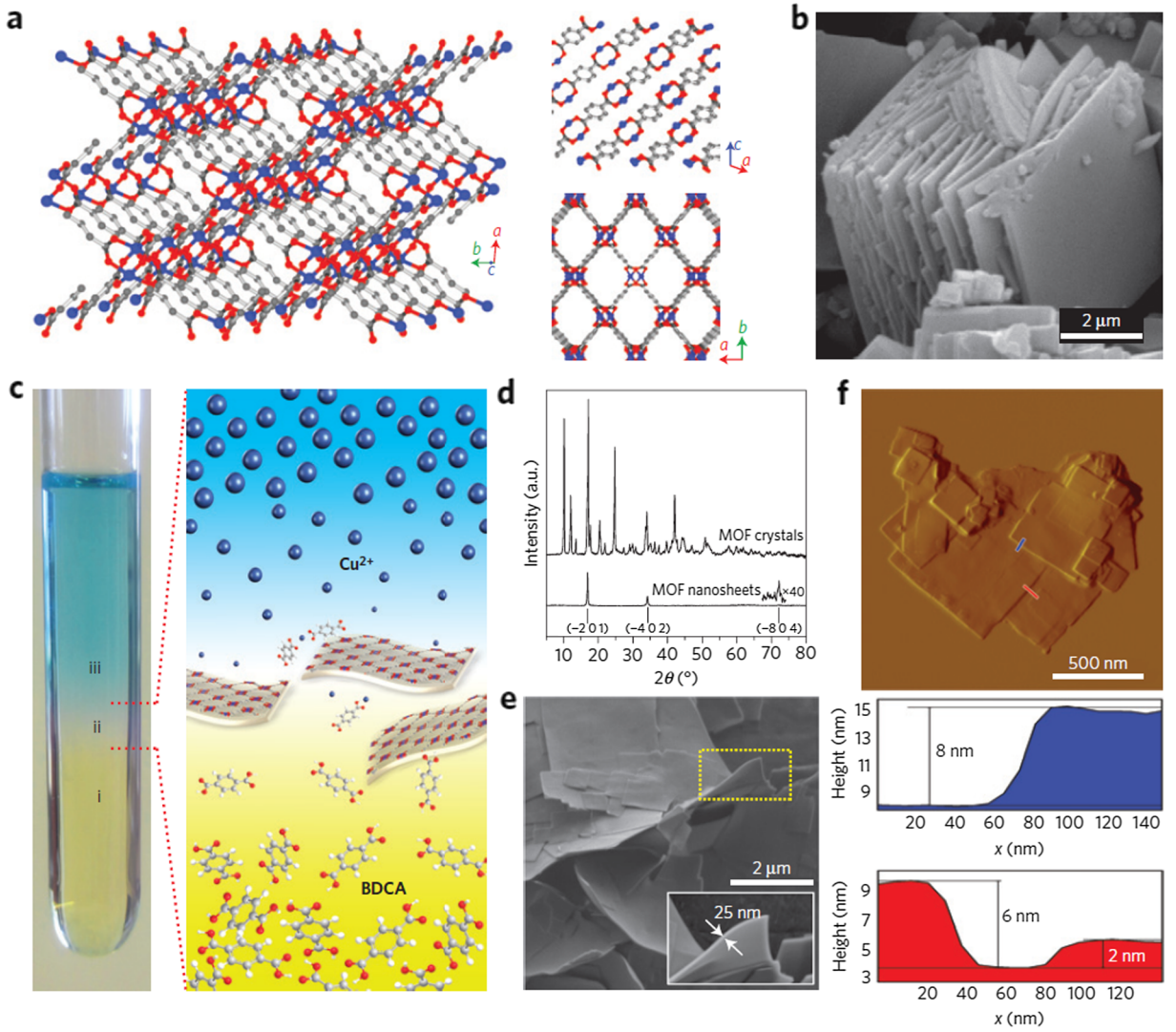

Fig. 11. Synthesis/structure of the CuBDC MOF nanostructures: a – A 3D crystalline structure of MOF which from left to right are respectively front, top and bottom view. b – SEM images of the bulk-type crystals. c – The spatial arrangement of various liquid layers during the nanosheets synthesis which are respectively a benzene 1,4-dicarboxylic acid (BDCA) Solution (yellow), the solvent spacer layer (white) and the solution of Cu^{2+} ions (blue). d – X-ray patterns the bulk-type and nanosheet MOF. e, f – SEM and AFM images of synthesized nanosheets [127]. (Copyright 2015. Reproduced with permission from Springer Nature.)

mechanical toughness (52 MJ/m^3) of MMM containing 20 wt% of filler in comparison with neat membrane (0.1 MJ/m^3). The gas permeation results revealed that fabricated MMMs surpass the Robeson upper bound by the H_2 permeability ranged from 91 to 230 Barrer and H_2/N_2 and H_2/CO_2 selectivities more than 1000 and 6 to 7, respectively.

Venna et al. [146], in order to improve the MMM gas separation characteristics of UiO-66-NH_2 loaded Matrimid®, applied three kinds of functional groups for surface modification of the MOFs, including aromatic (phenyl acetyl), aliphatic (decanoyl acetyl) and acid (succinic acid) groups. The transport properties of the MMMs with the surface-functionalized MOFs were investigated. The results showed using aliphatic and acid functional groups worsened the transport and mechanical properties of MMMs, due to the poor interaction between functional groups and the polymer and the formation of unobservable defects at the Matrimid®/MOF interface. However, the aromatic functionalized MOF embedded in polymer matrix resulted in the ideal selectivity to enhance compared to the neat polymer. These performances are due to the Matrimid® structure, which contains aromatic and imide groups, enabling two kinds of linkages with functional group of MOF surface. One is π-π stacking between the aromatic group of the polymer and the aromatic ring of the phenyl acetyl group, and the other is hydrogen bonding between the imide groups in the polymer and the amine group of functionalized MOF (Fig. 16) [146].

The gas permeation properties for different MOF-based MMMs are given in Table 3.

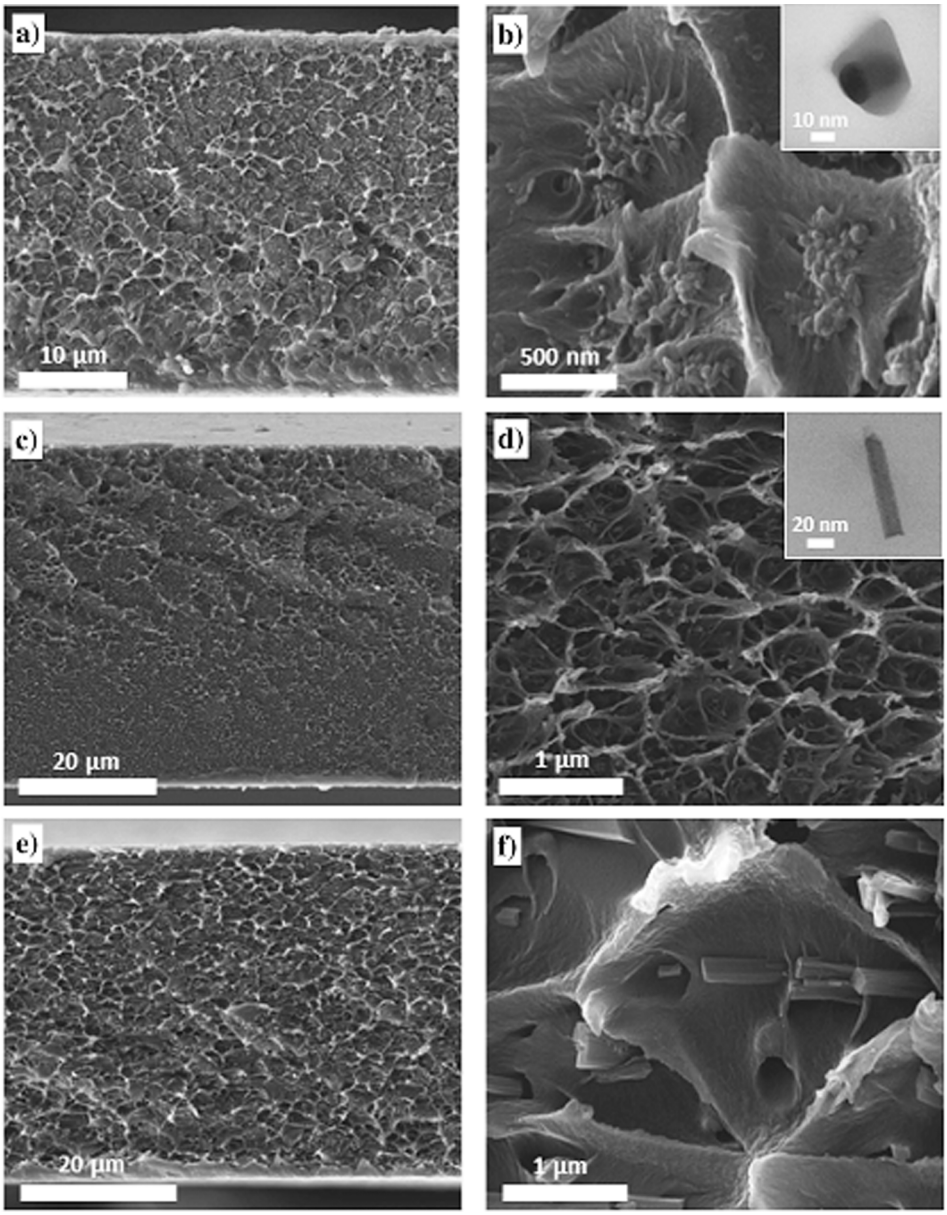

Fig. 12. SEM images of 8 wt% NH_2-MIL-53(Al)-Matimid MMMs prepared using the three different crystal morphologies: (a, b) nanoparticles, (c, d) nanorods and (e, f) microneedles [55]. (Copyright 2016. Reproduced with permission from John Wiley and Sons.)

4.1.4. ZIF

Zeolitic imidazolate frameworks (ZIFs) are a sub-category of metal-organic frameworks (MOFs) which are formed by joining metal clusters like Co and Zn with imidazole linkers. They have better properties like higher thermal, chemical, and moisture stability compared with other MOFs. ZIFs have smaller pores exhibiting zeotype design such as SOD, RHO or LTA. ZIFs are topologically isomorphic with zeolites [187,188]. SOD and RHO topologies are obtained by using benzimidazole and LTA topology obtains when the carbon atom in 5- or 5- and 7-positions on benzimidazole is replaced with a nitrogen atom [189]. Varieties of ZIFs are available such as ZIF7, ZIF8, ZIF11, ZIF22, ZIF69, ZIF78, ZIF90, ZIF93, ZIF95, ZIF100 and ZIF301 [190–194]. Among these, ZIF8 is probably one of the most popular ZIF to produce MMMs. ZIF-8 is comprised of a metal cation of Zn^{2+} in conjunction with molecules of organic linkers, which provides SOD zeolitic topology comprised of large cavities. Therefore, it is suitable to be used in gas storage and gas separation processes [195–200]. It provides high thermal and chemical solidity and is suitable for usage in the MMMs as fillers [201,202].

To increase CO_2-philicity of ZIF-8 ammonia-based modification has been attempted. This is a difficult task as modification may cause the pores to be blocked, which in turn would worsen the MMM performances. More investigations are necessary for the performance of the modified ZIF particles as dispersed phase in MMM [203]. Nordin et al. [203] synthesized ZIF-8 under ammonia

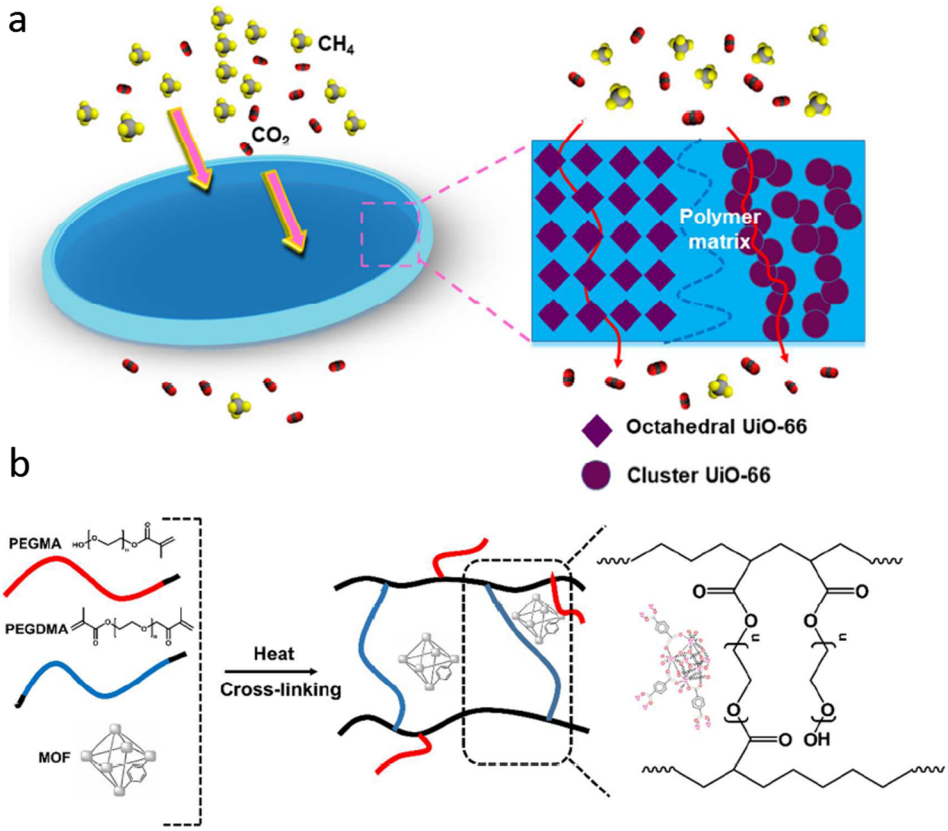

Fig. 13. a – Schematic view of dual transport pathway creates in MOF-based MMMs. b – Synthesis method employed for preparing the crosslinked poly[(ethylene glycol) methacrylate] and metal-organic framework (MOF) [143]. (Copyright 2018. Reproduced with permission from American Chemical Society.)

modification with various ammonia solutions. The performance exhibited remarkable enhancement of micropore volume, phase crystallinity and BET surface area. The addition of modified and unmodified ZIF-8 into PSf matrix showed that this type of modification for ZIF-8 caused CO_2 permeance to decrease while CO_2/CH_4 selectivity increases. This was due to the decrease in mesopore contribution and the increase of micropore contribution to the gas pathway. The adherence of N-H group to CO_2 in modified ZIF-8 will cause the CO_2 permeance to increase (Fig. 17).

Kertik et al. [204] employed the in-situ controlled thermal treatment for Matrimid/ZIF-8 MMM at 350 °C for 24 h and found that this membrane revealed extraordinary CO_2/CH_4 mixed gas selectivity. This may be due to the excellent interfacial adhesion between MOF and polymer which are covalently bounded. They also confirmed these results employing ultramicrotomy by advanced TEM imaging and showed that MOF-polymer crosslinking which successfully sealed the grain boundary at the polymer/filler interface. Hence, the amorphous MMM showed an excellent gas separation performance under real condition. The thermally treated MMM (in air at 350 °C), Matrimid/ZIF-8 (40 wt%), exhibited the CO_2 permeability about 1.9 Barrer and CO_2/CH_4 selectivity about 134 under real condition (40 bar, 35 °C, and 50 vol% CO_2/50 vol% CH_4). Hwang et al. [205] was studied the variation of CO_2 concentration in ZIF-8@6FDA-DAM MMM employing the microimaging by IR microscopy. Time-resolved images illustrated that gas molecules pass through the ZIF-8 to the surrounding polymer. Indeed, the gas molecules are cumulated in filler/polymer interface microvoids and this proves the importance of the interfacial compatibility on separation performance (see Fig. 18).

Li et al. [206] employed a new strategy of chelation-assisted interfacial reaction to embed the vertically oriented fillers into the polymer matrix. Indeed, a novel membrane was fabricated by incorporating the ZIF-L into the cross-linked network of poly(vinylamine) PVAm/polyvinyl alcohol (PVA) blended membrane. Indeed, a continuous vertically-aligned PVAm/PVA-ZIF-L MMMs were fabricated on functionalized PS membranes. The fabricated membrane revealed superior filler/polymer interfacial adhesion without any non-selective microvoids due to the high capacity of PVAm to complex formation with Zn^{2+}. As a result, the composite membrane showed the high flexibility and tensile strength. The pristine PS membrane demonstrated the tensile strength of 13.20 MPa, Young's module of 120.36 MPa and breaking elongation of about 10.96%, while these results achieved for the PVA/PVAm membrane about 40.01 MPa, 177.69 MPa and 22.52%, respectively. Moreover, in the case of PVA/PVAm-ZIF-L composite membrane, these results were acquired about 44.70 MPa, 194.50 MPa and 22.98%. This indicates the great mechanical property of PVAm/PVA-ZIF-L membrane. In addition, the fabricated membranes showed a reversed selectivity of CO_2/N_2 gas pair with the N_2 permeance of 174.9 GPU and N_2/CO_2 selectivity of about 51.9 (Fig. 19).

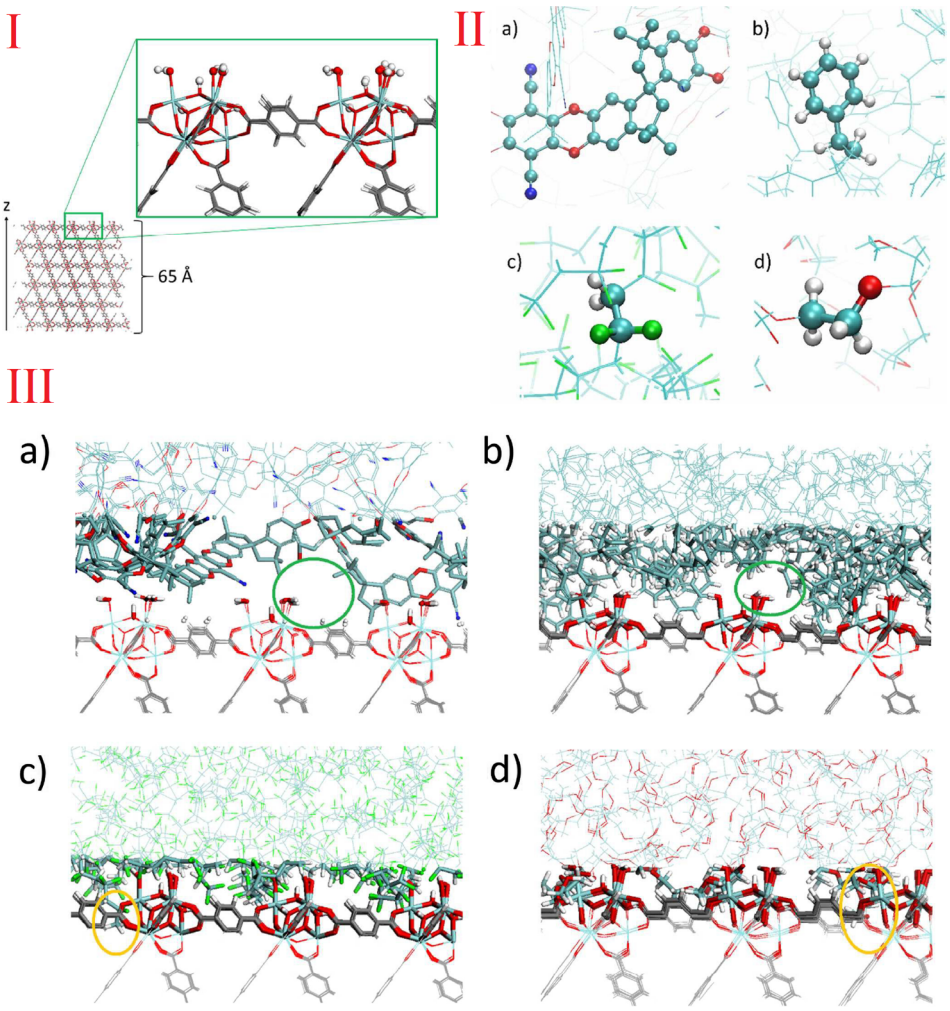

Fig. 14. I – Snapshot of UiO-66 surface model. II – Schematic view of the atomistic models for various polymers investigated which are respectively: (a) PIM-1, (b) PS, (c) PVDF, and d) PEG. III – Schematic illustration of the interfaces for: (a) UiO-66/PIM-1, (b) UiO-66/PS, (c) UiO-66/PVDF, and (d) UiO-66/PEG MMMs [144].

The permeability and selectivity for various ZIF-based MMMs are summarized in Table 4.

4.1.5. COF

Covalent organic frameworks (COFs) as a new class of the porous crystalline materials are pure organic polymers composed of covalent bonds with light elements such as B, C, N, O, Si and with pre-designable porous structure [221,222]. The COFs integrate organic units with atomic precision into periodic structures [223]. These solid materials are constructed by the covalent bonds of tough and constant organic builders to form novel strong porous COFs. Light elements are held together by strong covalent bonds to make robust porous materials having the advantages of predictable structures and tunable pore functionality and metrics [224]. COFs are highly crystalline while the traditional polymers were shapeless and semicrystalline. Reversible covalent bond formation reactions will automatically correct structural defects toward thermally stable crystalline structures. The TGA results revealed that NUS-2 and NUS-3 COFs are thermally stable up to 300 °C [222]. Biswal et al. [225] demonstrated that both TpPa-1 and TpBD COFs have no visible weight loss until 350 °C. Moreover, the hybrid membranes which formed by the addition of these solids into polybenzimidazole showed good thermal stability up to approximately 400 °C, a temperature between the thermal stability of particles and polymer. Shan et al. [226] have also demonstrated the stability of ACOF-1 up to 300 °C. Concluding from the works, COFs have high thermal stability (more than 300 °C) and the COF-based MMMs as compared to the MOF-based MMMs constructed by a same polymer matrix are more stable, even at high COF loadings.

COFs maintain excellent properties such as foreseen and various structures, adjustable aperture volumes and easy-modified scaffolding and also have high affinity to polymer matrix due to similarity and intermiscibility, as they are porous material and organic polymer at the same time [45,227]. These COF characteristics make them suitable choices for gas storage and separation processes.

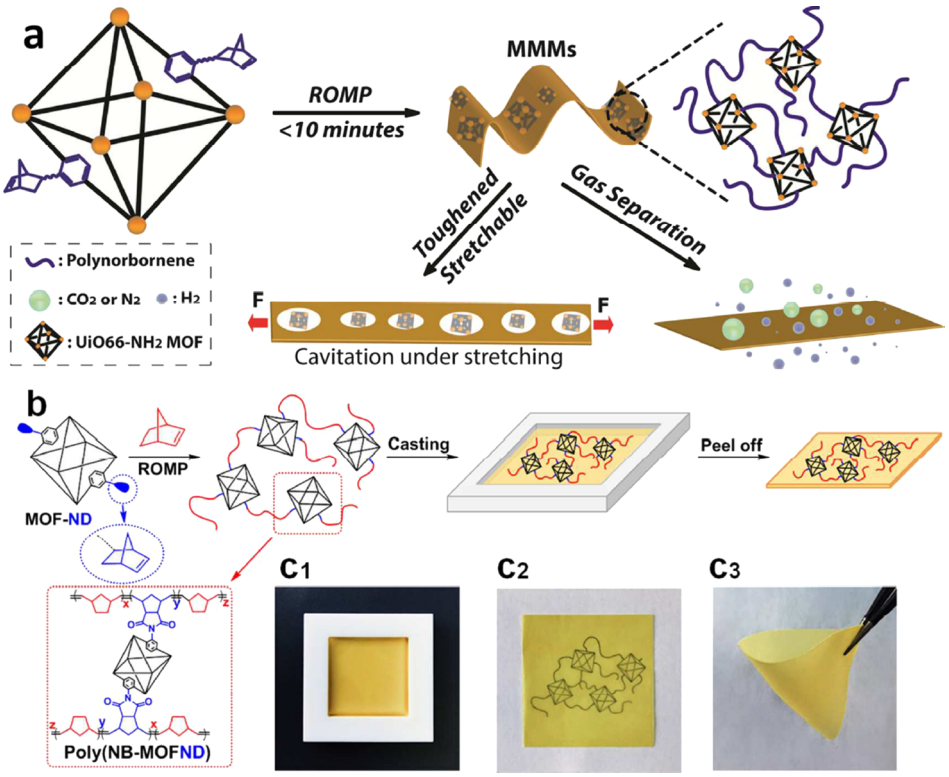

Fig. 15. a – Ring-opening metathesis polymerization (ROMP) method for tailoring of mechanically robust MMMs. b – Mechanically tough MMMs preparation by covalently attaching of UiO66-NH_2 in polymer. C_1 – Fabricated MMMs in Teflon mold. C_2 – on a paper to illustrate transparency and C_3 – A simple test to show the membrane flexibility [145]. (Copyright 2018. Reproduced with permission from American Chemical Society.)

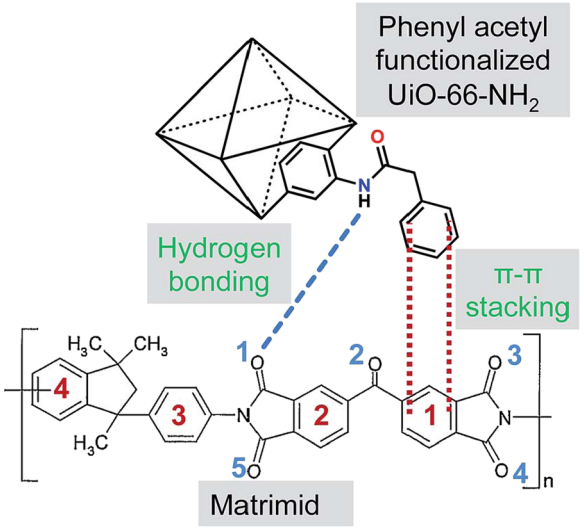

Fig. 16. A favorable interactions between the Matrimid and phenyl acetyl functionalized MOF [146]. (Copyright 2015. Reproduced with permission from Royal Society of Chemistry.)

Among COFs those named as porous aromatic framework (PAFs) are more strong and stable than traditional COFs or even MOFs. The PAFs keep inherent natural electron rich structure having high porosity and being capable to be functionalized. PAFs have purely organic construction but unshaped internal structure compared to crystalline COFs and have good physico-chemical characteristics for gas capture [228]. Volkov et al. [229] incorporated PAF-11 into PTSMP membrane in order to prevent its physical aging. In a sample containing 10 wt% of PAF-11, the stable gas transport characteristics were maintained as a result of annealing for a period of 100–200 h at 100 °C which has the best result among other samples. However, for all other samples containing less than 5 wt% of

Table 3
Different MOF/MMMs performances for CO_2 separation.

MOF	Polymer	wt.% loading (best MMM performance)	Test conditions	P_{CO2} (Barrer)	CO_2/CH_4 selectivity	CO_2/N_2 selectivity	CO_2/H_2 selectivity	Ref.
NH_2-UiO-66	PEBA	(10)	20 °C, 1 atm		–		–	[147]
			Dry state	87		66		
			Humid state	130		72		
NH_2-UiO-66	Matrimid®	(30)	35 °C, 9 bar	37.9	47.7	–	–	[148]
neat UiO-66-NH_2 (I)	Matrimid®	(23)	Room T, 20	23.5*	-	36.5*	-	[146]
aromatic-modified I (I_{PA})		(23)	psia	29	-	37	-	
aliphatic C_{10}-modified I (IC_{10})		(23)		22	-	27.5	-	
acid-modified I (I_{SA})		(23)		20	-	30	-	
NH_2-MIL-125(Ti)	PSf	0	303 K, 3 bar	9.5	22.0	–	–	[137]
		10		18.5	28.3			
		20		29.3	29.5			
		30		40.0	29.2			
NH_2-MIL-125(Ti)	Matrimid®9725	15	35 °C, 9 bar	17	50	–	–	[138]
		30		50	37	-	-	
NH_2-MIL-53(Al)	Matrimid®	8	25 °C, 3 bar	7.5*	36*	–	–	[55]
		16		9.2	42			
NH_2-MIL-53(Al)	PMP	30	30 °C, 8 bar	339.5	22.8	–	–	[139]
UiO-66(Hf)-(OH)2	PBI	0			–	–	–	[149]
		10						
		20						
		30						
NH_2-MIL-53(Al)	PI(polyimide)	15	35 °C, 1 bar	8.2*	31.5*	-	-	[150]
		20		8.8	32.5	-	-	
		25		9	33	-	-	
	PSf	15		5.1	24	-	-	
		20		4.5	26	-	-	
		25		5.4	28	-	-	
APTMS-MIL-53(Al)	Ultem	0	298 K, 5 bar	9.1 GPU	-	31.0	-	[151]
		2		12.4 GPU	-	36.7	-	
		6		17.8 GPU	-	41.8	-	
		10		24.1 GPU	-	41.1	-	
		15		27.7 GPU	-	33.6	-	
NH_2-MIL-101(Al)	PI(polyimide)	8	35 °C, 1 bar	10*	35*	-	-	[150]
		15		9.5	36	-	-	
	PSf	8		5.5	24.5	-	-	
		15		7	25	-	-	
		25		8.5	29	-	-	
S-MIL-101(Cr)	SPEEK	40	30 °C, 1 bar	34.33	40	39	–	[141]
PEI@MIL-101(Cr)	SPEEK	40	25 °C, 1 bar	2490	71.8	80	–	[152]
MIL-68(Al)	polyimide	10	373 K, 1 bar	279.6	79.0	–	–	[153]
Ni_2(dobdc)	Cellulose acetate	23	35 °C, 1 bar	3.78	30.3	-	-	[154]
	Matrimid®	23		9.31	29.5	-	-	
	6FDA-DAT	15		63.9	51.9	-	-	
	6FDA-DAM:DAT	18		220	30.5	-	-	
	6FDA-DAM	23		715	14.5	-	-	
	6FDA-durene	21		1035	12.3	-	-	
$Cu_3(BTC)_2$	ODPA–TMPDA	20	35 °C, 2 atm	24.8	37.8	–	–	[142]
Sod-ZMOF	Matrimid	0	35 °C, 4 bar	7.16	30.8	-	-	[155]
		5		6.96	36.6	-	-	
		10		7.05	37.7	-	-	
		20		13.79	43.4	-	-	
Cu-MOF1	polyoxazoline (POZ)	0	Room T	7* GPU	-	2*	-	[156]
		5		2 GPU	-	5	-	
		10		2 GPU	-	8	-	
		15		3 GPU	-	55	-	
Cu-MOF2		20		70 GPU	-	35	-	
		0		7 GPU	-	2	-	
		5		3 GPU	-	3	-	
		10		2 GPU	-	2	-	
		15		4 GPU	-	7	-	
		20		70 GPU	-	4	-	
Cd-6F	6FDA-ODA	10	Up to 30 bar	37.8	44.8	35.1	–	[157]

(*continued on next page*)

Table 3 (*continued*)

MOF	Polymer	wt.% loading (best MMM performance)	Test conditions	P_{CO2} (Barrer)	CO_2/CH_4 selectivity	CO_2/N_2 selectivity	CO_2/H_2 selectivity	Ref.
T-MOF-5	PEI	0	25 °C, 6 bar	1.7	18.67	-	-	[158]
		5		1.9	18	-	-	
		15		2.1	19.19	-	-	
		25		3	22.57			
CuBTC	PVDF	5		1.067	24.81	-	-	[140]
		10		2.002	41.70	-	-	
		15		3.206	40.07	-	-	
CuBDC		5		1.126	26.18	-	-	
		10		1.602	35.60	-	-	
		15		1.987	45.15	-	-	
MIL-53(Al)		5		1.210	21.22	-	-	
		10		1.553	20.98	-	-	
NH_2-MIL-53(AL)		5		1.107	23.06	-	-	
		10		1.406	26.03	-	-	
MIL-53	FDH-11	0	35 °C, 150	54.1	18.0	-	-	[159]
		10	psia	61.4	15.7	-	-	
		15		71.1	15.1	-	-	
NH_2-MIL-53		10		47.1	78.5	-	-	
		15		46.7	58.4	-	-	
		20		44.3	27.7	-	-	
UiO-66	Matrimid	(11)	Room T, 10 bar	22	–	24	–	[160]
UiO-66-CH═CH_2	PEO-250:PETM:EDDT	0	35 °C, 5 atm	80.7	15.6	50.5	–	[161]
		35		83.4	17.9	39.9		
		60		467.7	8.00	14.1		
UiO-66	PMP/Pebax-1657	2	25 °C, 5 bar	369.3	31.3	–	–	[162]
NH_2-UiO-66		1.5		393.4	39.8			
UiO-66	Matrimid	10	35 °C, 4 atm	7.8	–	29.4	–	[163]
Azo-UiO-66		20		13		40		
UiO-66-MA	PEO	2	35 °C, 3.5 atm	1450	–	45.8	–	[164]
UiO-66-NH_2@ICA	Matrimid	10	25 °C, 3 atm	40.1	64.7	–	–	[165]
UiO-66-NH_2	Pebax-1657	50	25 °C, 2 bar	338 GPU	–	57	–	[166]
UiO-66-$(COOH)_2$		50		240 GPU		50		
GMA–UiO-66	PMMA	28	25 °C, 4 bar	1.1	152	110	–	[167]
MIL-101(Cr)	Matrimid/PVDF	10	35 °C, 7 bar	14.87	62	–	–	[168]
NH2-MIL-53(Al)	CA	15	25 °C, 3 bar	52.6	28.7	23.4	–	[169]
NH2-MIL-53(Al)	Pebax-1657	10	35 °C, 10 bar	149	20.5	55.5	10.6	[170]
MIL-53-NHCOH	Pebax-1657	15	10 °C, 1 atm	4.6 GPU	–	65.02	–	[171]
MIL-53(Al)	PSf	8	Room T, 2.75 bar	4.89	–	22.74	–	[172]
MIL-53-PC	PPO-PEG	20	30 °C, 3 bar	912	44.7	–	–	[173]
CuBDC	Polyactive™	16	25 °C, 2 bar	3.3 GPU	–	66	–	[174]
CuBDC	Matrimid	8	–, 4 bar	4	–	48	–	[175]
Fe-BTC	Pebax-1657	30	25 °C, 3 bar	402.69	21.5	–	–	[176]
Fe-BTC	Matrimid	30	80 °C, 1 bar	217.9	–	23.1	–	[177]
Sub-NH_2-Cu-BTC	Pebax-1657	3	25 °C, 1 bar	108.5	29.05	66.27	–	[178]
CuBTC	MP/HFBAA	30	30 °C, 10 bar	208.7	35.4	43.5	–	[179]
Ni_2(L-asp)$_2$bipy	Pebax-1657	20	35 °C, 1 bar	120.2	37.06	39.38	32.88	[180]
Ni_2(L-asp)$_2$pz		20		89.66	23.14	28.88	30.96	
Bio-MOF-1	PSf	30	25 °C, 10 bar	16.57	42.6	45.6	–	[181]
PEI-CAU-1	XLPEO	30	35 °C, 3 bar	546	27.8	–	–	[182]
CuCoMOF-5	PI	5	Room T, 1 bar	4.17	9.59	–	–	[183]
T-MOF-5	CA	9	25 °C, 6 bar	3.19	–	–	0.52	[184]
Al-fum	Matrimid	24	25 °C, 3 bar	13.9	52.1	–	–	[185]
Al-fum(DMSO)		24		5.0	50.6			
ZnCo-MOFs	Pebax-1657	8	25 °C, 2 bar	510.1	56.8	–	–	[186]

* Values are approximated from plots.

PAF-11, gas permeability slowly decreased with time.

COFs serve as a fascinating design medium for gas adsorption and storage because of their structural regularity and discrete pore size [223]. Compatibility at the filler-polymer interface will be improved when COFs are used as fillers in MMMs. They are also able to carry several types of functionalities [59,222,227].

Imine-linked COFs and azine-linked COFs are stable under various conditions and therefore are suitable for CO_2 adsorption [226,227].

Shan et al. [230] synthesized the azine-linked covalent organic framework (ACOF-1) and incorporated it into three polymers

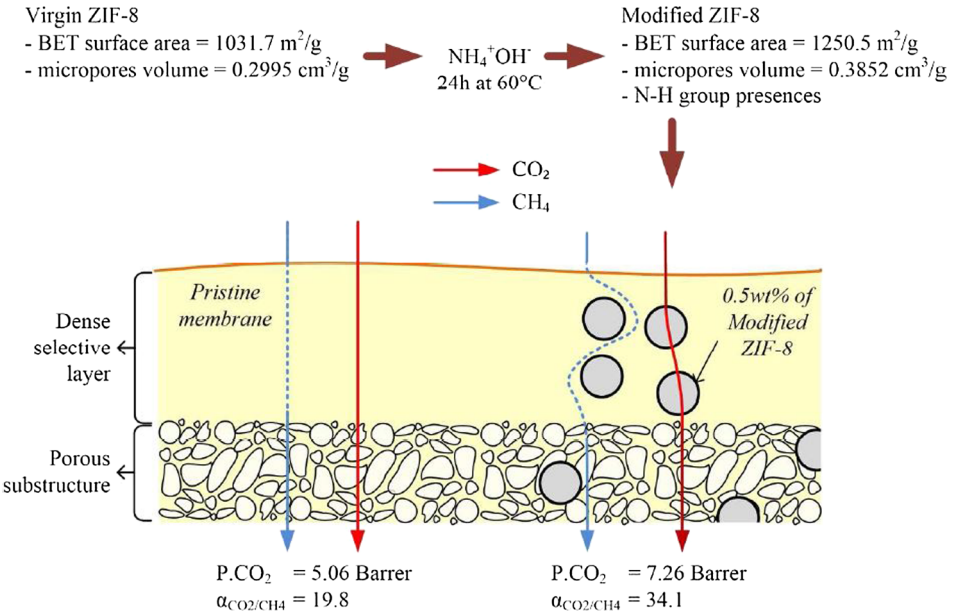

Fig. 17. Increasing trend of BET surface area and micropore volume of ammonia-modified ZIF-8 particles in the presence of N-H group [203]. (Copyright 2015. Reproduced with permission from Royal Society of Chemistry.)

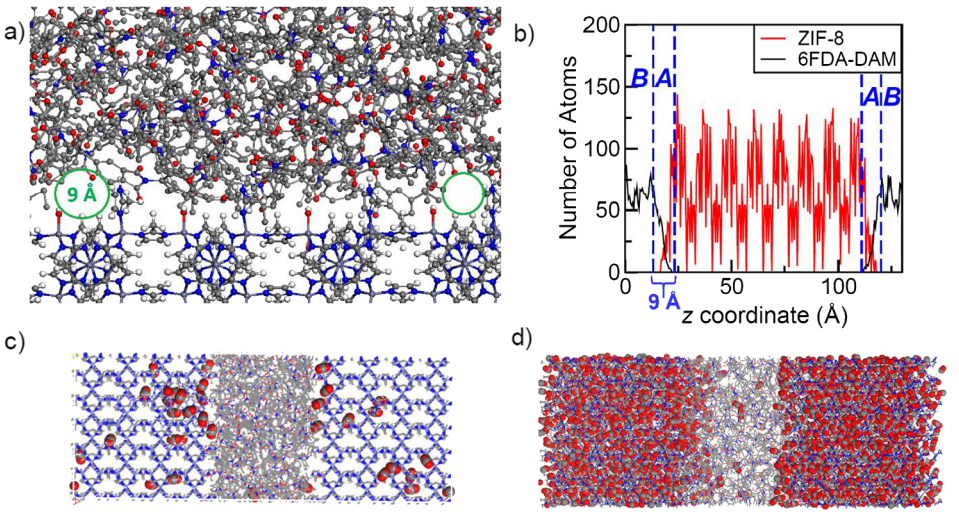

Fig. 18. (a) The snapshot related to microvoids creates at filler/polymer interface. (b) Atomic density of filler and polymer as a function of the coordinate perpendicular to the filler surface. (c, d) Two configurations of the ZIF-8-filled MMM models at low and high pressures [205]. (Copyright 2018. Reproduced with permission from John Wiley and Sons.)

(Matrimid, 6FDA:DAM and Polyactive™) with different gas permeation behaviors to fabricate MMMs Fig. 20. The SEM results demonstrated that ACOF-1 had a good adhesion with polymer matrices. Gas permeation results also indicated that for Matrimid and 6FDA:DAM based MMMs permeability enhances in comparison with the pure membranes. While, in the case of Polyactive™, filler partial pore blockage was occurred by the more flexible polymeric chains, which resulted in permeability decrease. Indeed, these results support the issue that filler/polymer compatibility is still the key factor in successful MMMs.

Kang et al. [222] synthesized NUS-2 and NUS-3 the two water-stable COFs comprising of two-dimensional layered forms with hexagonal channels and various pore sizes. They are able to be exfoliated into nanosheets and have excellent compatibility to polymeric matrix. They prepared new MMMs by embedding these frameworks into polybenzimidazole and observed a defect free structure. Also the COF-containing MMMs showed increased gas permeability and selectivity.

In another study, Cao et al. [227] embedded an imine-based COF with a 2D network into poly(vinylamine) (PVAm) to increase membrane performance for CO_2/H_2 separation. By embedding 10 wt% COF into the polymer matrix, a CO_2 permeance of 396 GPU and CO_2/H_2 selectivity of 15 were achieved at 0.15 MPa. It can be concluded that COFs with different structures have potential to

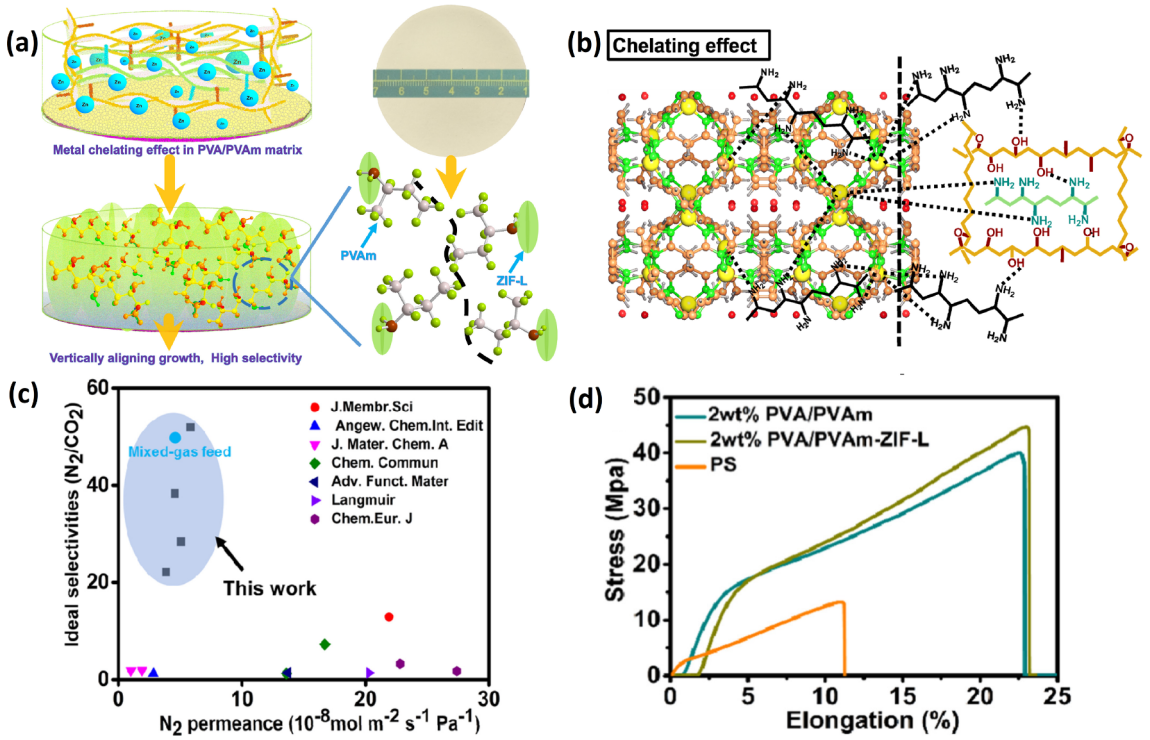

Fig. 19. (a) Schematic illustration of oriented ZIF-L within PVAm/PVA matrix. (b) Interfacial interaction between ZIF-L crystals and polymer matrix, (c) Comparison of the gas permeation results of synthesized membrane with other literatures (d) Mechanical properties of synthesized membranes [206]. (Copyright 2019. Reproduced with permission from Elsevier Science Ltd.)

have good compatibility with polymers and to reveal MMMs with privileged performance.

4.1.6. Graphene

A single layer of sp2 carbon atoms joined securely into hexagonal network structure provides the two-dimensional nanomaterial known as graphene. Graphene is the main structural unit for all graphitic carbon forms like carbon nanotubes, graphite and fullerenes. Monolayer graphene has superior mechanical characteristics and high clearness and also it is gas-impermeable [231,232]. Continuously fabricated films from few to hundreds of graphenes and graphene oxide (GO) exfoliate stuck on top of each other exhibit selective properties for various separations because of the space between graphene sheets and/or holes produced during the oxidation step [233].

When there is a good compatibility between a filler and polymer matrix, permeability is expected to decrease. Due to the weak compatibility between graphene and polymer, the polymer chains will not stick tightly to the nanosheets of graphene. Therefore, gas molecules instead of passing through graphene are moving among narrow aperture or through polymer matrix. Thus, the MMM exhibits a low separation performance [231,234].

The graphene surface modification is a suitable choice to resolve this drawback. Functionalization in order to increase compatibility of graphene with the polymer matrix might be suitable for construction of MMMs [231].

Another graphene subsidiary which consists of a remarkable number of covalently bonded oxygen-containing groups like carbonyl and carboxyl groups, hydroxyl and epoxy groups on its basal plane and edges, is graphene oxide. Graphene oxide is a suitable nanofiller for MMMs due to its high aspect ratio (> 1000) and simple surface functionalization. GO's nanosheets are sufficiently hydrophilic and compatibe with polymers. Exfoliated GO particles supply transport channels for CO_2 separation [235–242]. By surface modification of GO, there are possibilities to provide composite materials with novel structure and unique properties. Attachment of polyamines covalently to GO layers will leave some unreacted amine groups which can rather react with CO_2, and in turn, provide outstanding separation of CO_2 from gas streams [232].

Dai et al. [243] prepared MMMs by incorporating imidazole functionalized graphene oxide (ImGO) into a poly(ether-b-amide) (Pebax) matrix. The MMM containing 0.8 wt% ImGO revealed the best CO_2 separation performance with CO_2 permeability of 76.2 Barrer along with CO_2/N_2 selectivity about 105.5, which exceeds the Robeson upper bound of 2008. It was attributed to proper interaction between CO_2 and imidazole groups. Moreover, the results exhibited that the T_g of MMMs increased and accordingly the mechanical properties were enhanced.

Li et al. [244] fabricated novel MMMs by embedding GO nanosheets, which were functionalized with ether linkages of polyethylene glycol (PEG) and with amines of polyethylenimine (PEI), into the commercial Pebax matrix in order to increase the diffusivity selectivity, solubility selectivity and reactivity selectivity of the membrane. The CO_2 permeability and CO_2/CH_4 and CO_2/N_2

Table 4
Different ZIF/MMMs performances for CO_2 separation.

ZIF	Polymer	wt.% loading (best MMM performance)	Test conditions	P_{CO2} (Barrer)	CO_2/CH_4 selectivity	CO_2/N_2 selectivity	CO_2/H_2 selectivity	Ref.
ZIF-8	Matrimid	10	35 °C, 5 bar	13*	43*	–	–	[195]
		20		18	48	–	–	
		30		25	52	–	–	
		40		45	42	–	–	
ZIF-8	PVAm	9 (13) 23	22 °C	297 GPU	–	83	–	[197]
PDA@ZIF-8	Pebax	0	25 °C, 1 bar	94.56	–	29.36	–	[207]
		5	Dry state	158.16	–	46.11	–	
		10		187.08	–	50.68	–	
		15		220.06	–	56.14	–	
		0	Humid state	113.96	–	30.12	–	
		5		196.69	–	49.02	–	
		10		233.13	–	56.65	–	
		15		267.74	–	62.65	–	
Ammonia modified ZIF-8	PSf	0.5	27 °C, 4 bar	7.26	34.09	–	–	[203]
ZIF-8@GO	Pebax	(6)	25 °C, 1 bar	249	–	47.6	–	[208]
H-ZIF-8 (Hollow ZIF)	PVC-g-POEM	0	35 °C	70.0	13.7	–	–	[196]
		10		170.1	12.2	–	–	
		20		495.4	10.8	–	–	
		30		623.0	11.2			
ZIF-8	PVC-g-POEM	0	35 °C	70.2	14.0	30.5	–	[209]
		10		197.6	14.4	31.4	–	
		20		446.3	14.2	32.1	–	
		30		687.7	12.4	34.9	–	
		40		1195.4	10.9	26.1	–	
ZIF301	PSf	0	298 K, 2 bar	6.32	–	26.33	–	[192]
		10		10.17	–	29.06	–	
		20		13.75	–	30.56	–	
		30		17.12	–	28.07	–	
		40		21.36		22.72		
ZIF-8	Pebax-2533	0	Room T, 2 bar	351	8.3	33.8	–	[198]
		5		365	8.1	29.6	–	
		10		427	8.5	31.4	–	
		15		574	10.4	30.3	–	
		20		854	9.2	28.9	–	
		25		1082	8.5	31.3	–	
		30		1176	8.7	31.6	–	
		35		1287	9.0	32.3	–	
ZIF-8	Ultem®	0	35 °C	1.535	37.9	26.52	–	[210]
		30		11.1	40.4	31.11	–	
ZIF-11	Pebax-2533	70	20 °C, 2 bar	402.89	12.49	–	–	[211]
ZIF-11	6FDA-DAM	0	30 °C, 4 bar	20.60	32.69	–	–	[212]
		10		109.70	31.34	–	–	
		20		257.50	31.02	–	–	
		30		73.05	30.44	–	–	
PEI-g-ZIF-8	PVAm	16.7	35 °C, 3 bar	656.7	–	79.9	–	[213]
ZIF-8	P84	27	25 °C, 3 bar	10.92	92.6	–	–	[214]
Zn/Ni-ZIF-8	Pebax-2533	10	25 °C, 2 bar	321	–	42.8	–	[215]
ZIF-8	PEGMEA	1.5	35 °C, 2 bar	730.8	13.3	–	–	[216]
ZIF-8	XLPEGDA	20	35 °C, 2 bar	840	16.0	48.0	9.2	[217]
ZIF-7/8 core-shell	PBI	32	250 °C, 3 bar	141.2	–	–	0.018	[218]
ZIF-302	Ultrason® S 6010	40	25 °C, 2 bar	13	–	33	–	[219]
ZIF-11	Matrimid	30	35 °C, 4 bar	31.36	42.95	–	–	[220]

* Values are approximated from plots.

selectivities of the Pebax/(PEG-PEI-GO) 10 wt% membrane, respectively, were enhanced about 2.7 and 2.4 folds, as compared to pure Pebax. The gas diffusion was enhanced due to the indirect paths, which were produced by the presence of GO nanosheets in polymer matrix. Presence of ether groups in PEG and the amine groups in PEI respectively increase the solubility selectivity and reactivity selectivity. Thus, the prepared MMMs provide excellent CO_2 permeability and CO_2/gas selectivity (Fig. 21). This method will simplify the genetic strategy for MMMs design/preparation with multi-permselectivity to increase CO_2 capture.

Peng et al. [245] modified GO nanosheets with zinc ion (Zn^{2+}) by applying dopamine-mediated complexation reaction. They provided a new facilitated transport membrane (FTMs) by embedding nanosheets of zinc ion-modified graphene (GO-DA-Zn^{2+}) into a Pebax matrix. The results showed 49% and 78% increase, respectively, in CO_2 permeability and CO_2/CH_4 selectivity in comparison with pristine Pebax membrane. This is due to the π-complexation reaction which results in the higher permeability and selectivity of

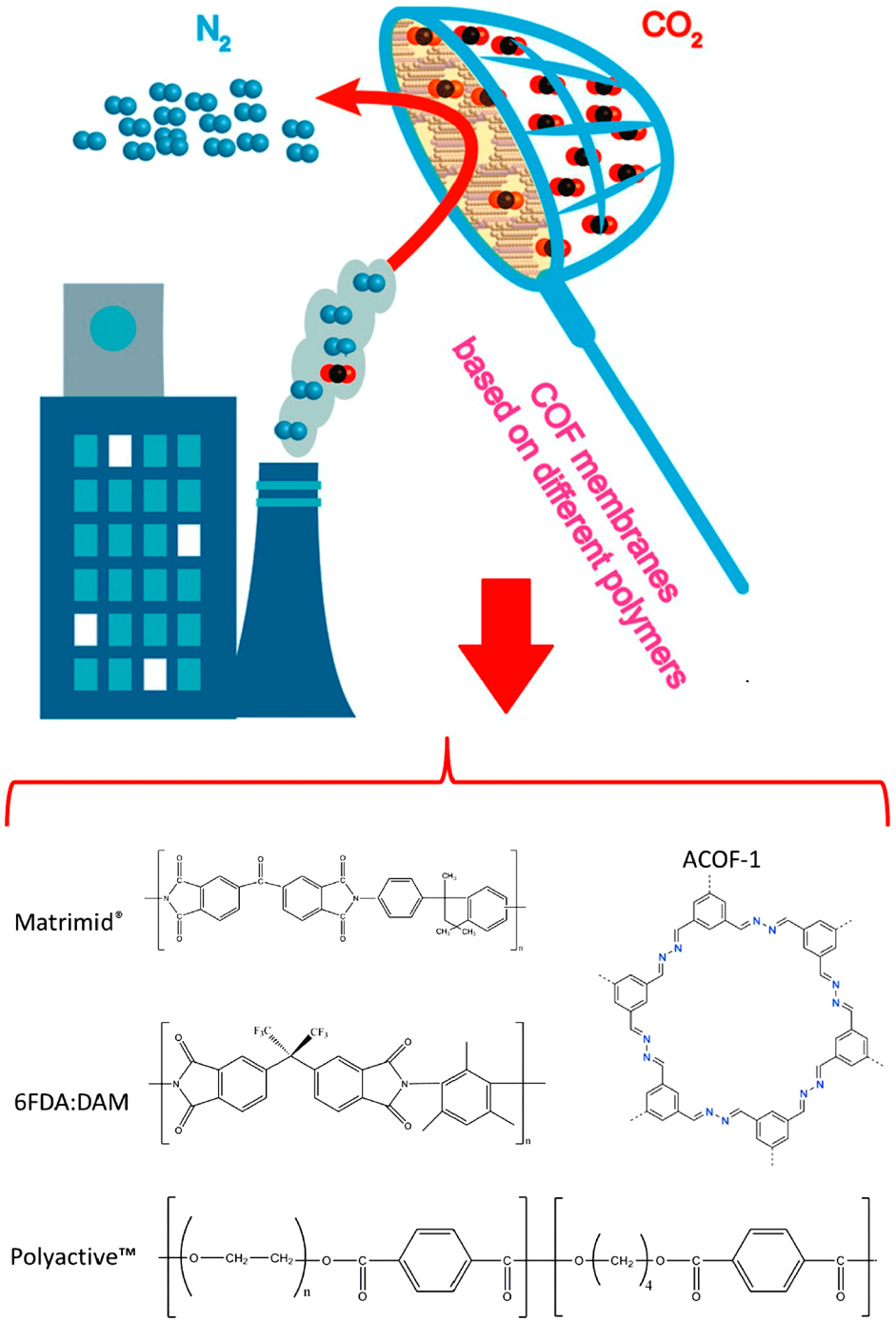

Fig. 20. (a) – ACOF-1 and various polymer materials considered in synthesis of MMMs for CO_2/N_2 separation [230]. (Copyright 2018. Reproduced with permission from Elsevier Science Ltd.)

CO_2 over CH_4. Also, incorporation of GO nanosheets produced more tortuous channels to prevent the transport of larger CH_4 molecules, leading to increase in the CO_2/CH_4 selectivity. Due to the increase of the fractional free volume of MMM the permeability of CO_2 was increased (Fig. 22) [245].

Huang et al. [246] investigated the effect of addition ionic liquid functionalized graphene oxide on the gas separation performance of MMMs. They effectively incorporated the 1-(3-aminopropyl)-3-methylimidazolium bromide ionic liquid (IL-NH_2) covalently functionalized GO (GO-IL) into the Pebax-1657 matrix. Fig. 23 illustrates the MMM preparation method considered in this work. Intrinsic properties of synthesized GO-IL such as excellent dispersibility and high-aspect ratio, interfacial compatibility with

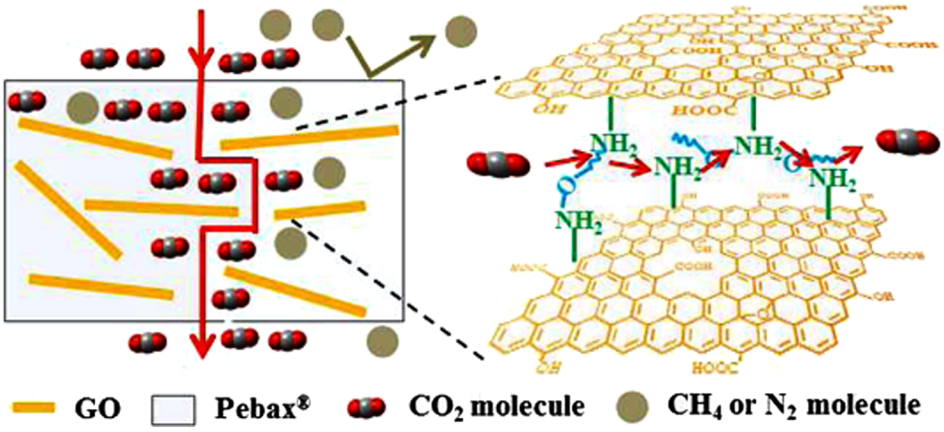

Fig. 21. Schematic of Pebax®-PEG-PEI-GO membrane separation mechanism [244]. (Copyright 2015. Reproduced with permission from American Chemical Society.)

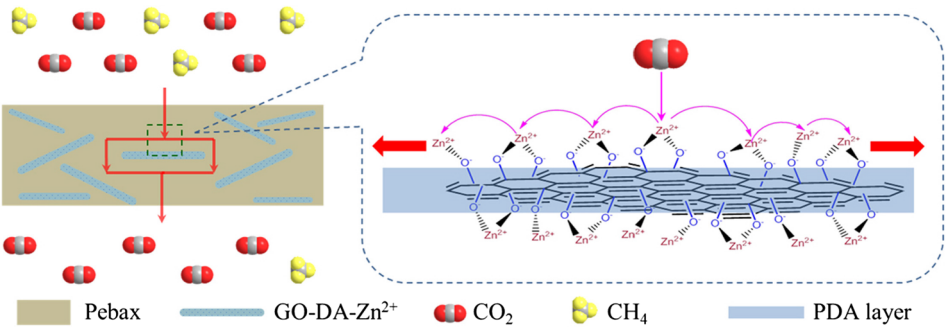

Fig. 22. Schematic of CO_2 transport mechanism in GO-DA-Zn^{2+}/Pebax membrane [245]. (Copyright 2017. Reproduced with permission from Elsevier Science Ltd.)

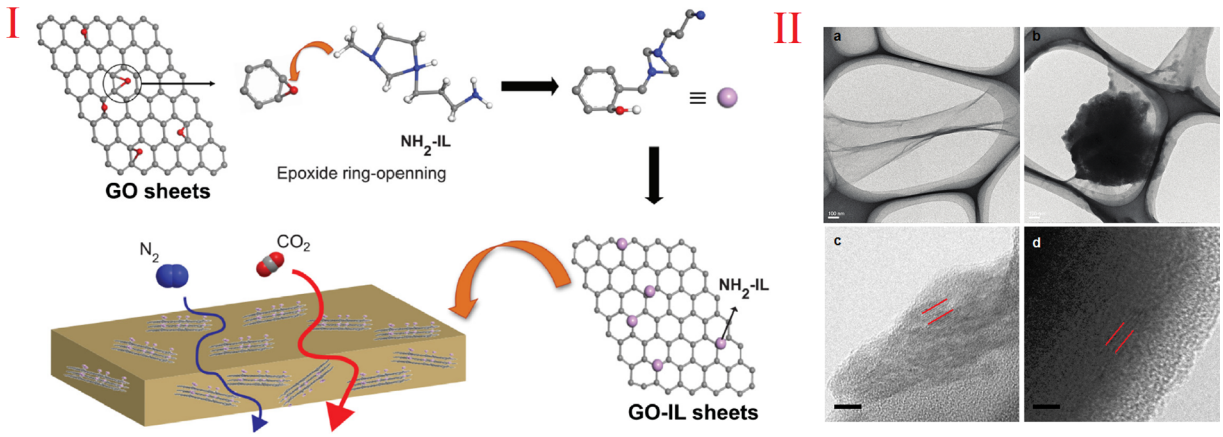

Fig. 23. I – Schematic illustration of the synthesis of GO-IL based MMMs. II – TEM images of (a) GO nanosheets, (b) GO-IL nanosheets, (c) MMM containing 0.2 wt% GO nanosheets and (d) MMM containing 0.2 wt% GO-IL nanosheets [246]. (Copyright 2018. Reproduced with permission from Elsevier Science Ltd.)

polymer and good affinity with gas molecules are severely affected the CO_2 separation properties. TEM images confirmed that the lateral size of GO and GO-IL sheets were 1–2 μm with a thickness of ca. 1–1.5 nm. A 0.05 wt% GO-IL loaded Pebax MMM exhibited the CO_2 permeance of 905.4 GPU and CO_2/N_2 and CO_2/H_2 selectivities of about 44.8 and 5.8, respectively.

Table 5 summarizes gas separation properties of MMMs containing graphene.

4.1.7. CNT

Carbon nanotubes (CNTs) are graphitic carbon material sheets rolled into a hollow and seamless tube cylinder [257]. This

Table 5
Different graphene/MMMs performances for CO_2 separation.

Graphene	Polymer	Wt.% loading (best MMM performance)	Test conditions	P_{CO2} (Barrer)	CO_2/CH_4 selectivity	CO_2/N_2 selectivity	CO_2/H_2 selectivity	Ref.
PEG-PEI-GO	Pebax	(10)	30 °C, 2 bar	1330	45	120	–	[244]
Imidazole functionalized-GO	Pebax	0.8	25 °C, 0.4 MPa	64	25.1	90.3	14.1	[243]
GO-DA-Zn^{2+}	Pebax	1	30 °C, 2 bar	137.9	28.8	–	–	[245]
Amine-functionalized GO	PES	0	5 bar	7.13 GPU	29.7	–	–	[232]
		0.5		9.61 GPU	35.59	–	–	
		1		11.86 GPU	35.93	–	–	
		3		13.26 GPU	37.88	–	–	
		5		17.81 GPU	34.25	–	–	
		10		21.54 GPU	32.14	–	–	
GO	PES	0	5 bar	7.13	29.7	–	–	[232]
		0.5		8.43	33.72	–	–	
		1		10.15	33.83	–	–	
		3		11.9	36.06	–	–	
		5		14.15	32.9	–	–	
		10		17.59GPU	30.32	–	–	
Porous reduced GO	Pebax	(5)	30 °C, 0.2 MPa	119	–	104	–	[247]
GO	HPEI/TMC	0	30 °C,	6.4 GPU	–	51.4	–	[237]
		(0.33)	0.1 MPa	9.7 GPU	–	81.3	–	
HPEI-GO	Polyvinyl amine (PVAm) and chitosan (Cs)	2	25 °C,	36 GPU	–	–	–	[235]
		3	0.1 MPa	–	–	107	–	
GO	Telechelic PDMS	8	35 °C, 10 atm	27.7	–	24	–	[236]
GO	PSf	0	25 °C, 5 bar	65.24 GPU	17.15	17.26	–	[248]
		0.25		74.47 GPU	29.90	44.4	–	
GO	PVDF	0.5	Room T,	0.90	40.63	–	–	[249]
	M-PVDF		5 bar	1.52	31.5			
POP-GO	Pebax-1657	10	35 °C, 1 atm	696	–	51.2	–	[250]
GNP	CS/SG	0.5	90 °C, 2 atm	159	–	93	–	[251]
GO	PPO_{dm}	5	Room T, 3.5 bar	80.95	40.27	–	–	[252]
WS_2 (a graphene-like material)	FPPO	10	18 °C, 0.7 atm	473	29.6	39.4	–	[253]
GO	Matrimid	0.57	Room T, 0.01 bar	45.7	–	–	0.51	[254]
Fe_3O_4–GO	Pebax-1657	3	Room T, 2 bar	538	47	75	–	[255]
NH_2-GO	BTDA-DMMDA	3	15 °C, 1 bar	12.34	–	38.56	–	[256]

*Values are approximated from plots.

cylinder is with the diameter ranging from a few to tens of nanometer and its length reaches several millimeters [15]. There are two kinds of CNTs. One is a single tube or single walled carbon nanotubes (SWCNTs) and another is composed of a series of graphitic layer which rolled around an axis known as multi walled carbon nanotubes (MWCNTs). SWCNTs consist of one graphite sheet wound on it. Moreover, it's both ends can be closed by a semi-fullerene molecule. MWCNTs consist of a tube surrounded by graphitic layers spacing 0.34 nm from each other [257].

Since CNTs were first introduced in 1991 [258] CNTs have been under special consideration in different field of science such as chemistry. CNTs of good gas separation and mechanical properties are very suitable choices in commercial separation processes. The gas transport of CNTs is faster than any other known materials due to their natural smoothness [259]. CNTs have smooth internal surface, great length to diameter ratio, very exact diameter, and excellent thermal stability [260]. Hence they are very suitable for MMM developments.

Difficulty in dispersing the CNTs in uniform orientation is an obstacle in developing polymer-CNT composites. Further applications of the MMM definitely depend on dispersion of the CNTs in a polymer matrix. Setting the CNTs vertically into the membrane surface, quick diffusion of the gases through the channels of the nanotubes will occur, which leads to high gas permeability without compromising selectivity [15,257]. Formation of complicated or uneven accumulation of CNTs in polymer matrix because of the presence of Van der Waals forces is a problem. However, it is possible to earn fine and even spreading of the CNTs in polymer matrix by using functional groups. Weak dispersion of CNTs in organic solvent is also a problem for their usage in industry. Therefore, many efforts are carried out to modify CNTs and improve their dispersion ability [259,261,262].

As the nature of carbon atoms is naturally inert, a proper CNT functionalization is difficult. End tips and sidewalls have different properties. Sidewalls functionalization is more difficult because of less chemical reactivity of hexagons on the sidewall compared to pentagons at the end tips. To turn CNTs more hydrophilic and soluble, chemical functionalization is preferred (Fig. 24) [261,263].

Different methods are available for MWNT functionalization. One of them is amino functionalization [264]. Since the amino

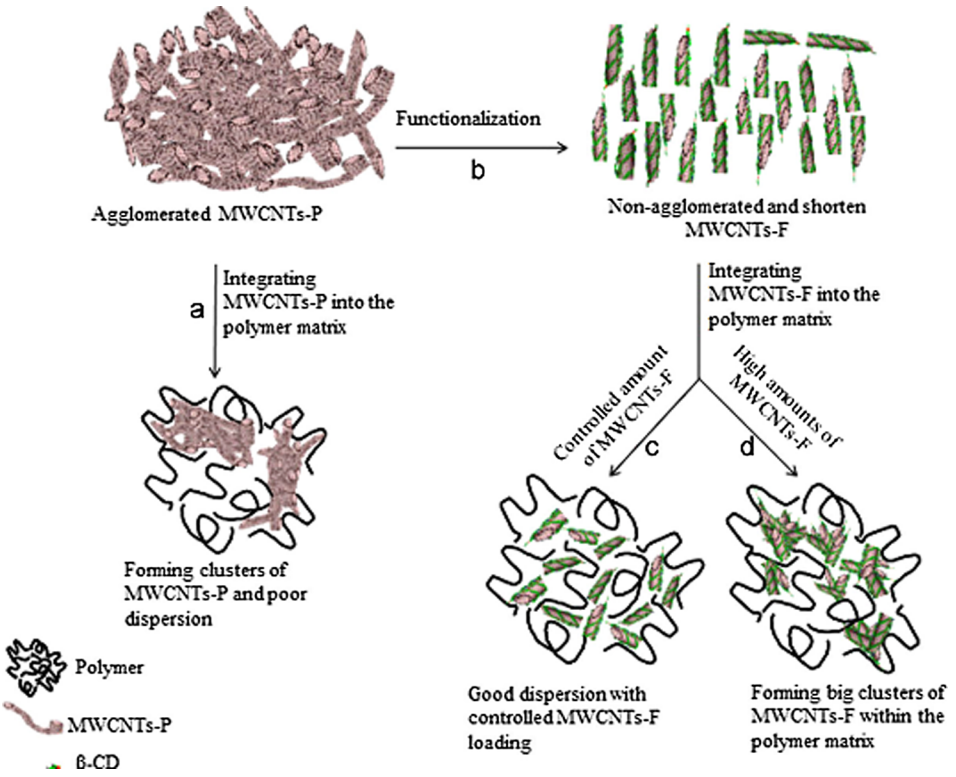

Fig. 24. Schematic view of the effect of MWCNTs-P functionalization on integrating the filler/polymer matrix (a) MWCNTs-P, (b) functionalized MWCNTs-P structure, (c) integrating controlled amount of MWCNTs-F, and (d) integrating high amounts of MWCNTs-F [261]. (Copyright 2014. Reproduced with permission from Elsevier Science Ltd.)

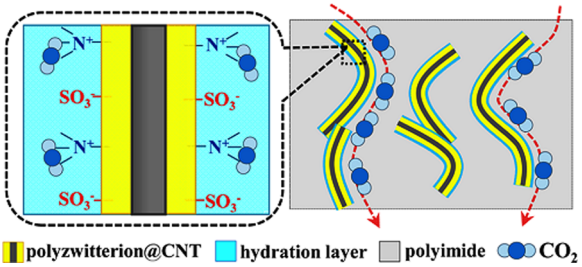

Fig. 25. Schematic of separation performance of the polyzwitterion coated carbon nanotubes hybrid membrane [267]. (Copyright 2014. Reproduced with permission from American Chemical Society.)

group has strong affinity toward CO_2, aminofunctionalization could enhance the CO_2 solubility selectivity. The dispersion of amino functionalized MWNTs is more uniform due to the presence of amino groups [265]. Zhao et al. [259] found that the normalized N_2, CH_4, and CO_2 permeability had increased almost equally with increasing MWNT–NH_2 content. In comparison with pristine Pebax membrane, CO_2 permeability remarkably increased from 133 Barrer to 361 Barrer for Pebax/MWNT-NH_2 MMMs with 33 wt% filler loading. Gas permeability increment was mostly due to the rapid diffusion of gases through CNTs and the reduction of crystallinity of the polymer phase.

N-isopropylacrylamide coated carbon nanotube (NIPAM@CNT) is another form of functionalized CNT prepared to increase CO_2 permeability [266]. Polyzwitterion coated carbon nanotube (SBMA@CNT) was also used for the same purpose. Liu et al. [267] prepared new hybrid membranes by incorporating polyzwitterion coated carbon nanotubes (SBMA@CNT) into polyimide matrix for CO_2 separation. By precipitation polymerization method, composite particles of polyzwitterion coated carbon nanotubes (SBMA@CNT) were provided. The MMM containing 5 wt% SBMA@CNT exhibited the maximum CO_2 permeability of 103 Barrer with a CO_2/CH_4 selectivity of 36. This improvement is because of interconnected channels for CO_2 transportation. In addition, SBMA@CNT was further modified by water uptake (Fig. 25).

The other method is the oxidation of nanotubes with oxidizing acid by which numerous functional groups such as hydroxyl (OH), carboxyl (COOH), and carbonyl (CO) are produced on the surface of the nanotubes. These surface functional groups will increase the specific surface area of the nanotubes [260,263,264,268–270]. Ranjbaran et al. [260] fabricated novel MMMs by embedding MWNTs

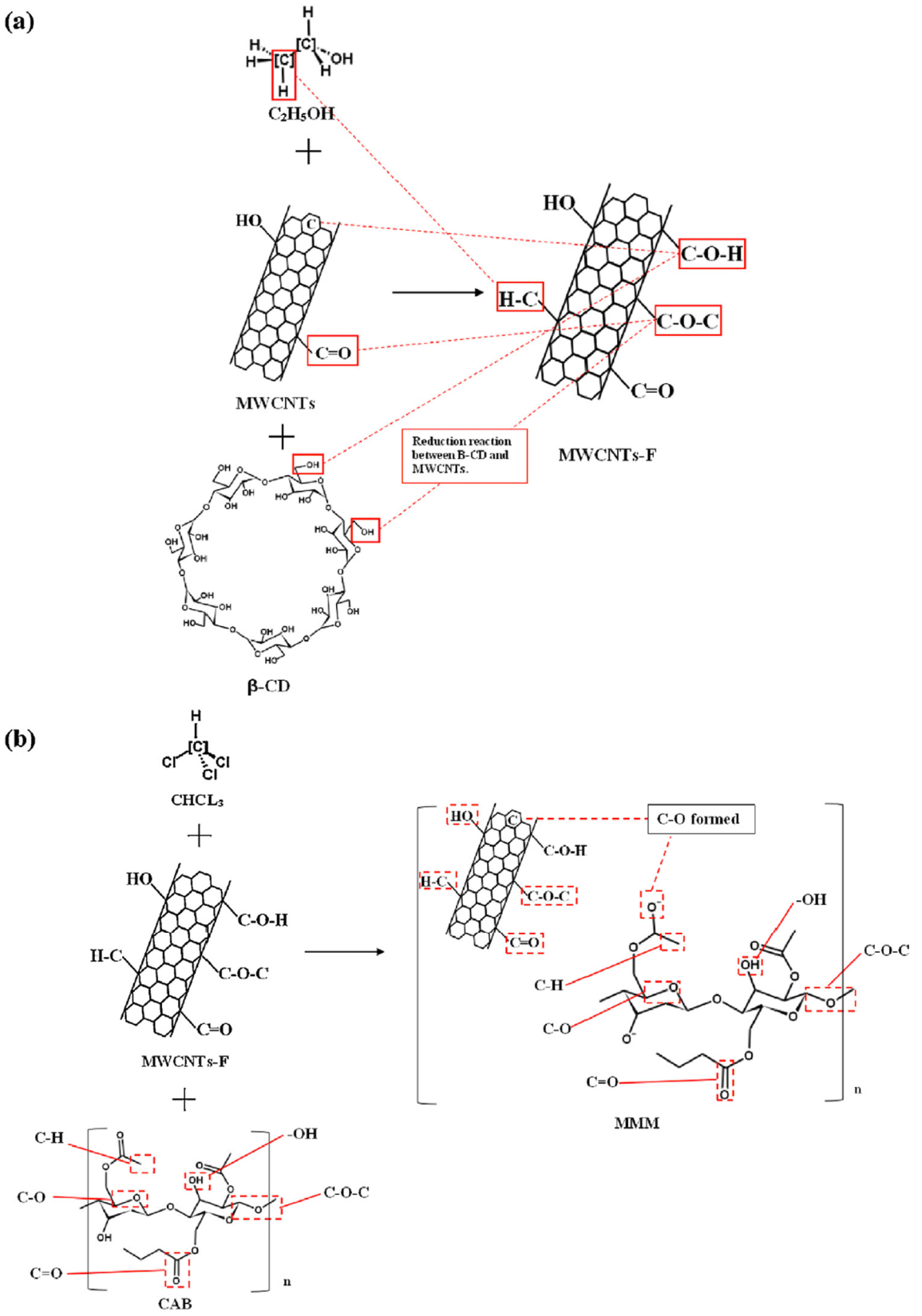

Fig. 26. Schematic illustration of the interactions between (a) MWCNTs and β-CD, and (b) MWCNTs-F and CAB [273]. (Copyright 2018. Reproduced with permission from Elsevier Science Ltd.)

Table 6
Different CNT/MMMs performances for CO_2 separation.

CNT	Polymer	wt.% loading (best MMM performance)	Test conditions	P_{CO2} (Barrer)	CO_2/CH_4 selectivity	CO_2/N_2 selectivity	CO_2/H_2 selectivity	Ref.
Carboxyl, Hydroxyl, Carbonyl functionalized MWCNT	Kapton–polysulfone (50/50 wt%)	0	30 °C, 10 bar	4.462	20.67	3.68	–	[268]
		2.5		4.714	19.47	3.598	–	
		5		5.146	19.05	3.571	–	
		8		5.434	16.98	3.25	–	
	Kapton–polysulfone (25/75 wt%)	0		5.298	21.01	–	–	
		2.5		5.432	20.81	–	–	
		5		5.89	19.97	–	–	
		8		6.2	17.71	–	–	
Amino functionalized MWCNT	Polyvinylalcohol-polysiloxane/amine blend	2.1	107 °C, 15 bar	957	264	384	56	[265]
Acid-treated MWCNT	PVA containing amines	2	380.15 K, 1.52 MPa	758	–	–	49.8	[269]
		4		896	–	–	50.9	
		6		903.8	–	–	50.0	
		8		812.5	–	–	48.2	
Amino modified MWCNT	Pebax 1657	(33)	35 °C, 0.7 MPa	361	16	52	9	[259]
Acid-treated MWCNT	Elvaloy4170	0	35 °C, 2 bar	80.69	6.57	–	–	[260]
		(1)		102.78	5.95	–	–	
		2		76.92	5.97	–	–	
		3		71.26	6.18	–	–	
		4		64.31	7.38	–	–	
SBMA@CNT	Polyimide	(5)	30 °C, 2 bar	103	36	–	–	[267]
NIPAM@CNT	Pebax	5	25 °C, 2 atm	567	35	70	–	[266]
β-CD (Cyclodextrine) – MWCNT	Cellulose acetate (CA)	0.00	300 kPa	400.93	–	32.92	–	[261]
		0.05		GPU	–	31.92	–	
		(0.10)		511.56	–	40.17	–	
		0.20		GPU	–	8.39	–	
				741.67 GPU				
				138.37 GPU				
PDA-TiNTs	PPO	6	–	127.78	14.52	20.81	0.148	[274]
	PBI	6		0.275	16.18	11.00	0.095	

*Values are approximated from plots.

into Elvaloy4170. This was done for the first time to use Elvaloy4170-based membrane for gas separation. The commercial Elvaloy4170 polymer is a reactive ethylene terpolymer, comprised of epoxide functional group, polyethylene group and polar methylmethacrylate group. The nanotube was functionalized with sulfuric/nitric acid treatment. Compared to the bare polymeric membrane, the MMM with 1 wt% of f-MWNTs exhibited 30% and 40% higher CO_2 and CH_4 permeability, respectively. A small loss in the CO_2/CH_4 selectivity was noticed as the f-MWNT content increased from 1 to 4 wt% in the polymer matrix.

Covalent functionalization often results in constructional changes in the CNTs, therefore the non-covalent methods are more desired. Chemical functionalization is performed by the covalent linkage of functional units with the carbon scaffold of CNTs at the end tips or sidewalls. Introducing saturated sp^3 carbon atoms, covalent functionalization can disrupt the π-bonding system and causes to symmetry-breaking effect. Hence, covalent functionalization often results in severe damages of CNTs, changes in intrinsic properties by breaking the carbon–carbon bonds and changes in the surface structure [271,272].

Formation of covalent linkage between functional groups and CNT framework at the end or sidewalls is the base of covalent functionalization [271]. Non-covalent functionaliztion done by noncovalent attachment of molecules such as beta-cyclodextrins (β-CD) and gamma-cyclodextrins (γ-CD) significantly enhances the CNT distribution [261].

Lee et al. [273] developed the MMMs by embedding the functionalized multi-walled carbon nanotubes (MWCNTs-F) into the cellulose acetate butyrate (CAB) matrix to study the CO_2/N_2 separation. A schematic illustration of the interactions between MWCNTs/beta-cyclodextrin (β-CD) and MWCNTs-F/CAB depicts in Fig. 26. As can be seen in Fig. 26a, MWCNTs with −OH and C═O groups is functionalized with β-CD with C−H and −OH groups. In this approach, the C−O−C group on the surface of MWCNTs-F is formed through an oxidation–reduction reaction. Also, the C−H group forms due to the presence of ethanol (a non-aqueous media). Moreover, the C−O−H stretching vibration of α-pyranose is also attached the MWCNTs-F surface. On the other hand, the functional groups of CAB-M are C═O, C−O, C−O−C, C−H and −OH which their transmittance peaks in the provided ATR-FTIR spectra are intensified by similar functional groups of MWCNTs-F in the MMM (Fig. 26b). Since carboxyl (C═O) and hydroxyl (O−H) groups are main effective polar groups for CO_2 separation, this MMM should have a superior separation performance. Accordingly, the MMM containing 4 wt% of MWCNTs-F revealed a superior CO_2 permeability about 3581 Barrer but quite low CO_2/N_2 selectivity of 11.

Table 6 summarizes the permeability and selectivity of MMMs containing CNTs.

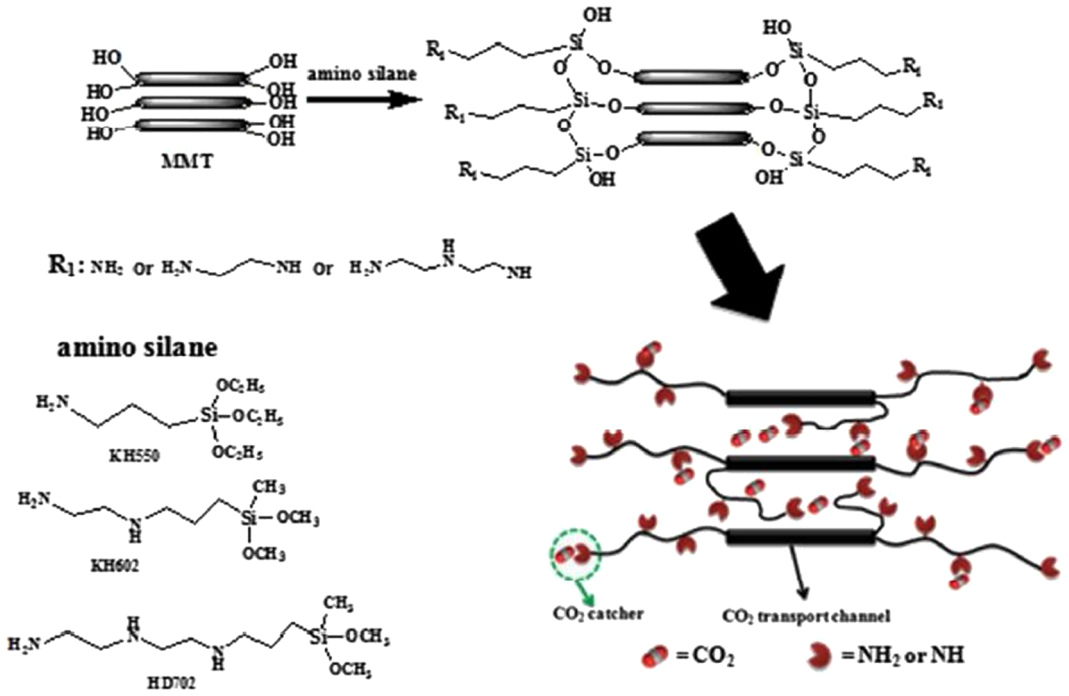

Fig. 27. CO_2 transport mechanism of functionalized montmorillonite [275]. (Copyright 2016. Reproduced with permission from American Chemical Society.)

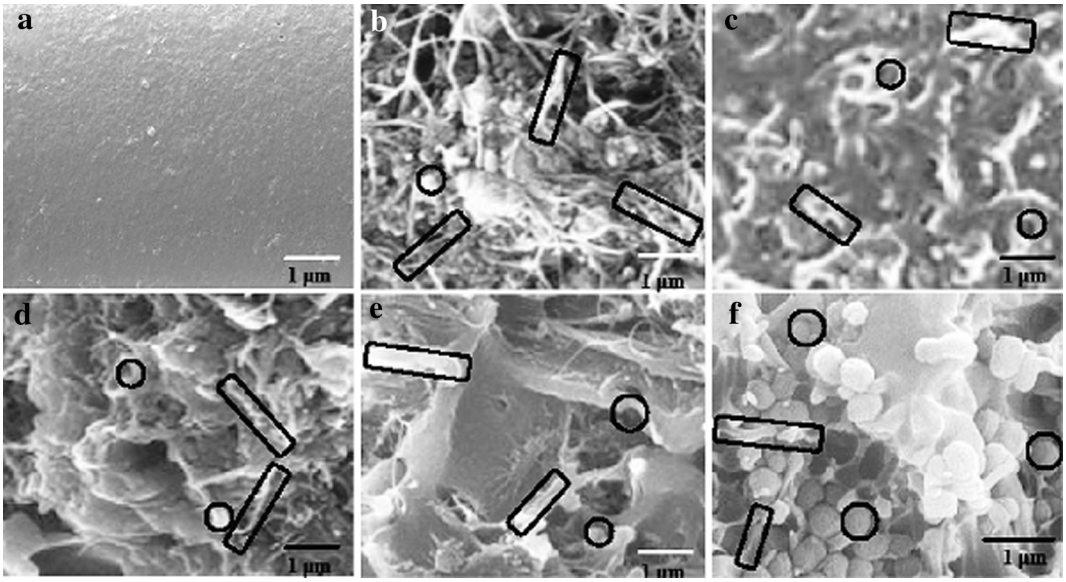

Fig. 28. SEM images of bare PSF (a), PSF/CNTs(10)/ZIF-302(6) (b), PSF/CNTs(8)/ZIF-302(12) (c), PSF/CNTs(6)/ZIF-302(18) (d), PSF/CNTs(4)/ZIF-302(24) (e), and PSF/CNTs(2)/ZIF-302(30) (f) MMMs containing different loadings of CNTs (enclosed by rectangles) and ZIF-302 nanocrystals (surrounded by circles) [277]. (Copyright 2016. Reproduced with permission from Springer.)

4.1.8. Filler combination and ternary systems

Adding two different fillers at the same time may increase the membrane selectivity due to different separation characteristics of the fillers. Regardless of impurity effects, this combination provides situations for hierarchical structures and synergic effects. Silanization can improve adhesion and interaction between inorganic filler and polymer phase via formation of ternary MMM. To produce this type of MMMs via chemical or physical modification a third component is added between inorganic filler and polymer phase. Usually the chemical silanization process causes the surface of inorganic filler to be modified [10,11]. Silanization for different types of filler was investigated on previous sections. Dong et al. [275] functionalized the montmorillonite (MMT) with PEG and

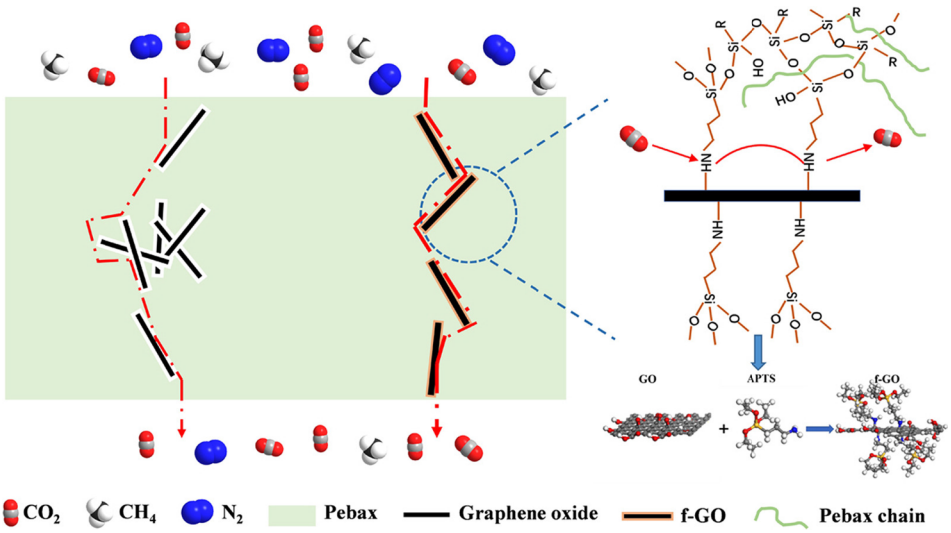

Fig. 29. Schematic illustration of grafting the APTES on GO, and a facilitated transport pathway through the embedded f-GO into the polymer matrix [283]. (Copyright 2019. Reproduced with permission from Elsevier Science Ltd.)

Table 7
CO_2 separation performances of MMMs containing filler combination and ternary systems.

Fillers/Modifier	Polymer	wt.% loading (best MMM performance)	Test conditions	P_{CO2} (Barrer)	CO_2/CH_4 selectivity	CO_2/N_2 selectivity	CO_2/H_2 selectivity	Ref.
mHNTs/PRG^{FC}	Pebax-1657	7.5 (fillers mass ratio)	30 °C, 3 bar	124	–	118	–	[284]
DA-PEI/TiO2^{TS}	Pebax-1657	1 (modifier mass ratio)-3	20 °C, 3 bar	67	–	101	–	[285]
pNA/ZIF-8^{TS}	PES	4–10	35 °C, 10 bar	2.66	43.6	–	–	[286]
ZIF-8/ns-CuBDC^{FC}	ODPA-TMPDA	10–2	25 °C, 1 bar	131	47	–	–	[287]
PEG 200/ZIF-8^{TS}	Matrimid	4–30	25 °C, 8 bar	33.1	15.4	–	–	[288]
APTMS/MIL-53^{TS}	Ultem®1000	15	35 °C, 5 bar	31.37	–	35.56	–	[289]
CuBTC/GO^{FC}	PVDF	9.5–0.5	25 °C, 5 bar	3.316	–	66.32	–	[290]
BPPO/UiO-66-NH_2^{TS}	PES	20	25 °C, 1 bar	125.6	–	50.2	–	[291]
TEOS/Silica^{TS}	Matrimid	15	35 °C, 10 bar	12.1	77.5	57.6	–	[292]
PEG 400/ZnO^{TS}	Pebax-1657	40–4	25 °C, 7 bar	94.49	31.58	–	–	[293]
ZIF-300/GO^{FC}	Ultrason® S 6010	30–1	25 °C, 1 bar	21	–	61	–	[294]
AS/TiO2^{TS}	Pebax-1657	3	25 °C, 20 bar	188.6	–	84.9	–	[295]
CMC/TiO2^{TS}		3		194.6		82.4		
ZIF-8/PG^{TS}	PVA	5	80 °C, 2.5 atm	344	–	370	–	[121]

FC: Filler Combination.
TS: Ternary System.

aminosilane coupling agents and fabricated a new MMM by incorporating functional MMT in poly(ether-block-amide) (PEBA) matrix. This kind of functional MMM exhibited good CO_2 permeability and CO_2/N_2 selectivity due to the CO_2-philicity of PEG and also the reaction between CO_2 and amine groups, which facilitates the CO_2 transport more than N_2 transport (Fig. 27). This functional MMM with 40 wt% of MMT-HD702-PEG5000 exhibited superior gas separation properties, i.e. CO_2 permeability of 448.45 Barrer and CO_2/N_2 selectivity of 70.73.

Li et al. [276] applied a combination of carbon nanotube (CNT) and graphene oxide (GO) into a Matrimid® matrix for CO_2 separation. The mixture of GO and CNT exhibited desirable effect on the membrane performances. CNT increases the permeability because it offers transfer pathways of CO_2 and GO nanosheets enhance the selectivity due to the presence of hydroxyl and carboxyl groups. Sarfraz et al. [277] prepared MMMs to separate CO_2 from post combustion gas streams by combining MWCNTs and zeolitic imidazole framework (ZIF-302) into glassy polysulfone (PSf). The membrane including 8 wt% MWCNTs and 12 wt% ZIF-302 nanofillers exhibited the best performance with a CO_2 permeability of 18 Barrers and CO_2/N_2 selectivity of 35 (Fig. 28).

In some other works, filler combinations like CNT/MOF [278], MIL-101(Cr)/ZIF-8 [279], GO/UiO-66 [280] and GO/ZIF-302 [281] were employed to provide MMMs, resulting in excellent CO_2 separation performances.

Loloei et al. [96] investigated the effect of LMW polyethylene glycol (PEG 200) as a CO_2-philic polymer on Matrimid® 5218/ZSM-5 MMMs separation performances. By combining Matrimid® 5218, PEG 200 and calcined ZSM-5, a new CO_2 selective ternary MMM was fabricated. LMW PEG was added to improve CO_2 selectivity by eliminating filler/polymer interfacial voids. They reported incorporating the zeolite and PEG decreased the Matrimid crystallinity due to the increase in polymer intra/inter segmental

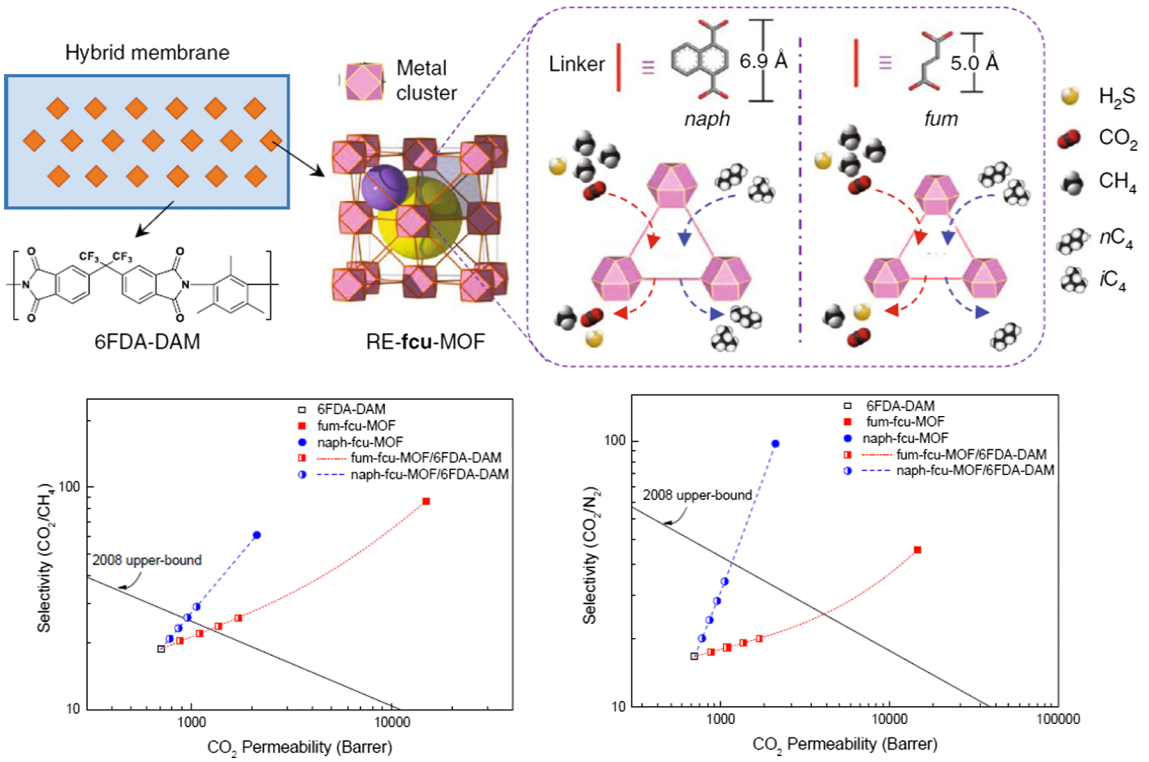

Fig. 30. A schematic of fabricating the MMM based on embedding the RE-fcu-MOF fillers into 6FDA-DAM polymer matrix (RE is yttrium for the fum linker or europium for the naph linker) and CO_2/CH_4 and CO_2/N_2 separation performances Y-fum-fcu-MOF/6FDA-DAM and Eu-naph-fcu-MOF/6FDA-DAM [296]. (Copyright 2018. Reproduced with permission from Springer Nature.)

distances. 5 wt% of PEG and ZSM-5 embedded in the polymer matrix, provided the best performance membrane, increasing CO_2 permeability and CO_2/CH_4 selectivity, respectively, from 7.68 to 11.53 Barrer and from 34.9 to 60.1. Khosravi et al. [282] prepared a new ternary system for CO_2 separation. They modified the Pebax/PSf membrane by using CuBTC and poly(ethylene glycol)-ran-poly (propylene glycol) (PEG-ran-PPG) in order to increase the selectivity and permeability. They reported 620% increase in CO_2 permeability and 43% enhancement in CO_2/CH_4 selectivity by using the MMM containing 32.76 wt% of PEG-ran-PPG and 20 wt% of CuBTC. Zhang et al. [283] functionalized the GO nanosheets by an oxygen-containing functional groups with 3-aminopropyltriethoxysilane (APTES). Afterwards, they prepared novel MMMs by incorporating the aminosilane functionalized nanosheets (f-GO) into the Pebax-1657 for CO_2 separation. Fabricated MMMs revealed outstanding mechanical properties in comparison with neat membrane (1.7-times higher Young's modulus). Organosilane acted as a linker between filler surface and polymer chains and increased the interfacial adhesion and uniformity of the filler distribution in the polymer matrix. On the other hand, amino groups on the f-GO surface provided the facilitated transport pathway at the filler/polymer interface (Fig. 29). Therefore, the elevated CO_2 permeability of about 934.3 Barrer, CO_2/N_2 and CO_2/CH_4 selectivities of 71.1 and 40.9 were achieved by the MMMs.

Table 7. summarizes the permeability and selectivity of MMMs containing filler combination and ternary systems.

4.1.9. New emerging fillers

In recent years, with the growth of synthetic organic/inorganic membrane materials, some new emerging materials have been developed to use as high performance fillers in mixed MMMs for gas separation. These can be divided into four categories: **(I)** microstructural design and changing the assembly of the present advanced fillers (like MOF, GO, ZIF, etc.), **(II)** co-synthesis of advanced fillers (like ZIF-8@GO), **(III)** synthesis of innovative organometallic nano-structures (like coordinated ligands, porous coordination polymers (PCPs), ion-loaded macromolecules, metal organic polyhedra (MOPs), micro-porous organic/inorganic hybrids, etc.) and **(IV)** developing the porous organic frameworks (POFs) such as covalent organic frameworks (COFs), conjugated microporous polymers (CMPs), porous aromatic frameworks (PAFs) and covalent triazinebased frameworks (CTFs). Some research works in these categories are discussed in the following:

4.1.9.1. Category I. Liu et al. [296] introduced a new kind of rare-earth (RE) based MOF fillers with face-centered cubic (fcu) topology for preparing novel MMMs. These kind of fine-tuned MOFs have triangular pore-apertures which are precisely constrained by some di-topic linkers such as 1,4-naphthalenedicarboxylate (naph) and or fumarate (fum) (Fig. 30). Synthesized fillers were embedded into the 6FDA-DAM matrix for CO_2/CH_4 and CO_2/N_2 separations. Achieved results indicated that by increment in fillers loading, Y-fum-fcu-MOF/6FDA-DAM is more permeable, while the Eu-naph-fcu-MOF/6FDA-DAM reveals higher gas pair selectivities.

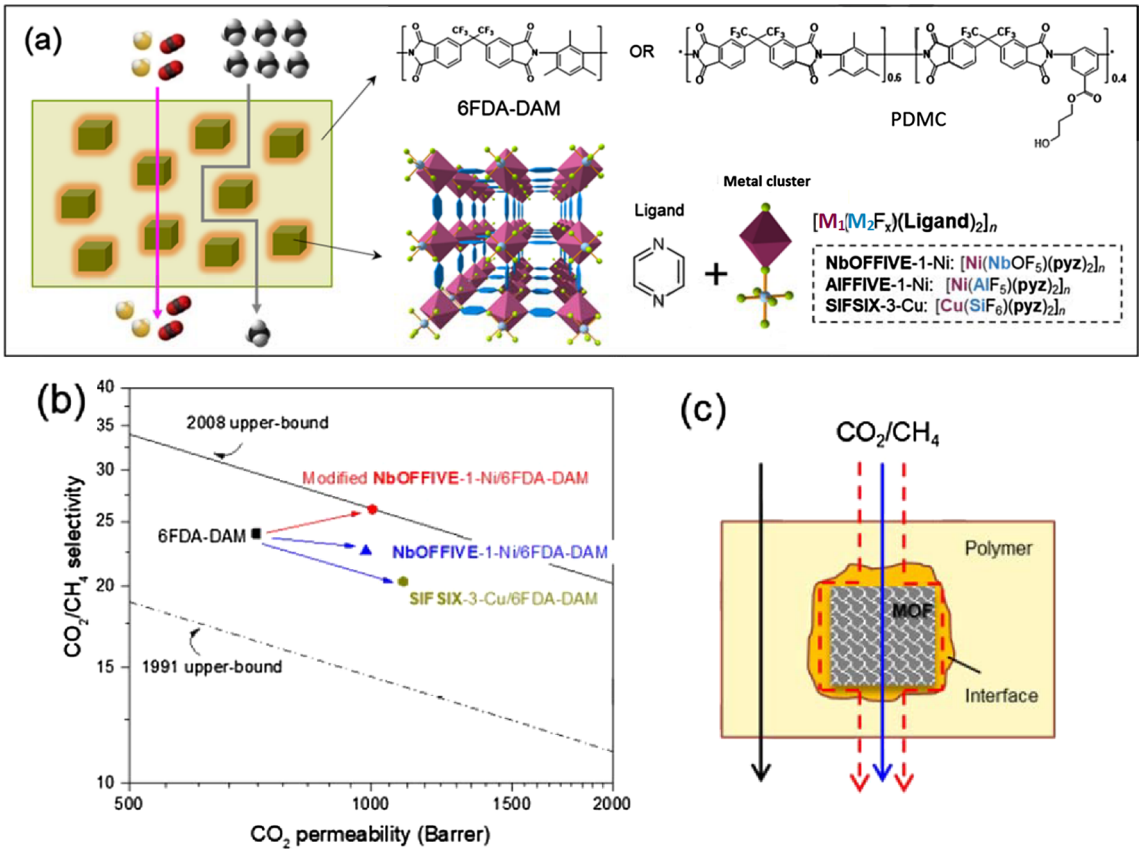

Fig. 31. (a) Schematic illustration of fabricating the fluorinated MOF-based MMMs. (b) Gas separation performance of 6FDA-DAM-base MMMs embedded by SIFSIX-3-Cu, pristine NbOFFIVE-1-Ni and modified NbOFFIVE-1-Ni. (c) Schematic view of CO_2/CH_4 permeation through NbOFFIVE-1-Ni/6FDA-DAM MMM [298]. (Copyright 2018. Reproduced with permission from John Wiley and Sons.)

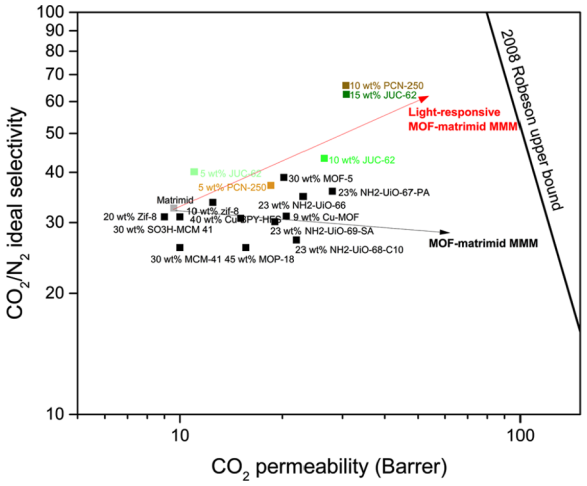

Fig. 32. A trajectory for enhancement the CO_2/N_2 gas separation performance of light-responsive MOF loaded Matrimid MMMs [299].

In another work, Liu et al. [297] explored the CO_2/CH_4 separation of Y-fum-fcu-MOF/6FDA-DAM MMM in a wide range of operating temperature. Their results showed that by decreasing the temperature from +35 to −40 °C, the CO_2/CH_4 selectivity increased to 130 and permeability was slightly decreased to 1050 Barrer.

With a new perspective, they also tailored a new fluorinated MOFs which have a with tunable channel apertures by adjusting the metal pillars/organic liker. Synthesized fillers were than incorporated into the synthesized polymer, 6FDA–DAM to form a novel MMMs for acid gas removal performance for natural gas [298]. Ultramicroporous fluorinated MOFs such as SIFSIX, NbOFFIVE and

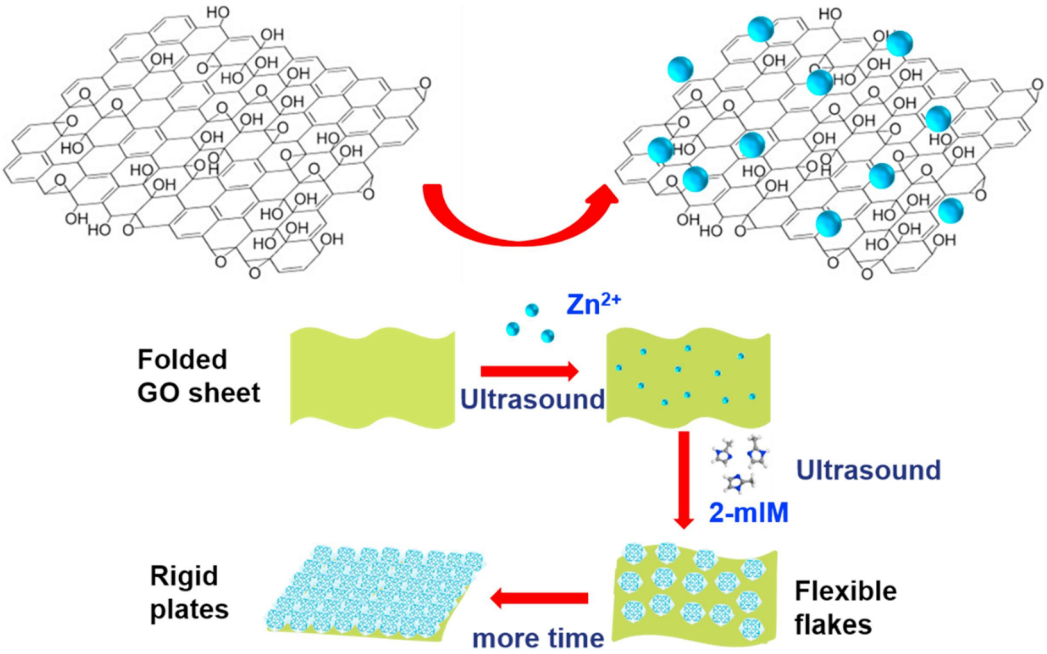

Fig. 33. Co-synthesis approach for the growth of ZIF-8 on the GO sheets for preparation of ZIF-8@GO nano-filler [300]. (Copyright 2019. Reproduced with permission from Elsevier Science Ltd.)

AlFFIVE, present two-dimensional nets based on linked metal nodes that are pillared through an inorganic molecular building block in a third dimension (Fig. 31a). As can be seen in Fig. 31b, addition of this class of fillers causes to dramatically enhance the CO_2 permeability of bare membrane. In the case of modified 6FDA–DAM/NbOFFIVE-1-Ni (20 wt%), CO_2 permeability of about 1000 Barrer and CO_2/CH_4 selectivity of 26 were achieved.

Light-responsive MOFs have attracted attentions for low-energy CO_2 capture and storage. Based on the host-guest interaction between the framework and photo-responsive guest molecule, three classes of the particles were investigated [163]. These materials have azo-functionality which makes them appropriate for low energy CO_2 capture because a difference behavior in the exposure of UV and visible light. For example, CO_2 adsorption capacity of JUC-62 and PCN-250 (Fig. 32), as two light-responsive MOFs, considerably decrease upon exposure to UV light. Therefore, during the regeneration process, they require low energy and hence can be good candidates for CO_2 separation [299].

4.1.9.2. Category II. GO sheets in the MMMs enhance the gas diffusivity selectivity due to high aspect ratio of the sheets that makes a longer and tortuous path for gas penetrants. On the other hand, ZIF-8 with ultra-microporosity and high gas permeability can be chemically synthesized on the surface of GO nano-sheets (a co-synthesis approach) (Fig. 33). The resultant ZIF-8@GO nano-filler incorporated in ethyl cellulose (EC) in which at 20 wt% filler content, CO_2 permeability and CO_2/N_2 selectivity increased respectively by 139% and 65% [300]. In another works, Lee et al. [301] have also considered a similar way for growing ZIF-8 on GO template and incorporated the co-synthesized particles into the Pebax matrix and obtained a considerable increase in permeability of gases. Huang et al. [302] with 20 wt% ZIF-8@GO loading to a polyimide matrix reached in a CO_2 permeability of 238 Barrer and CO_2/N_2 selectivity of 65, surpassing Robeson upper bound.

Zhang et al. [303] synthesized novel filler, ZIF-8@LDH by in-situ growth of ZIF-8 on LDH (ZnAl-CO_3) and then embedded them into Pebax-1657 to prepare a new MMM for CO_2/CH_4 separation. Fig. 34 is schematically illustrates the MMM synthesis routes and also gas separation mechanism. As can be seen in Fig. 34b, both physical and chemical selectivities are severely incorporated in separation factor improvement. First, an increase in physical selectivity is owing to the good affinity of CO_2 molecules with ZIF-8 and LDH hydroxyl groups. Second, ZIF-8 with oriented distribution increases the CO_2 concentration in the vicinity of LDH moiety and enhances the chemical selectivity due to the CO_2 facilitated transport. Pebax/ZIF-8@LDH (2 wt%) was the optimum MMM with the mixed gas CO_2 permeability of 1307 Barrer and CO_2/CH_4 selectivity of 31.6.

In another work, Lee et al. [304] fabricated a novel MMM by incorporating the hollow ZIF-8 (H-ZIF) polyhedral nanocrystals into the PVC-g-POEM graft copolymer. The polyhedral nanocrystals were synthesized through the use of seed crystals, epitaxial ZIF-8 growth, and excavation of ZIF-67 sacrificial templates. Fig. 35 shows SEM/TEM images of synthesized filler and also a schematic view of the MMM synthesis method. Their results indicated that the synthesized filler has internally hollow structures with a Zn-rich, dense and thin outer shell. Moreover, the best performance MMM, PVC-g-POEM/H-ZIF (10 wt%) showed the CO_2 permeability of 210.6 Barrer and the CO_2/CH_4 selectivity of 14.3.

4.1.9.3. Category III. Some biomimetic functional materials have been synthesized by inspiration from enzyme catalysts to promote

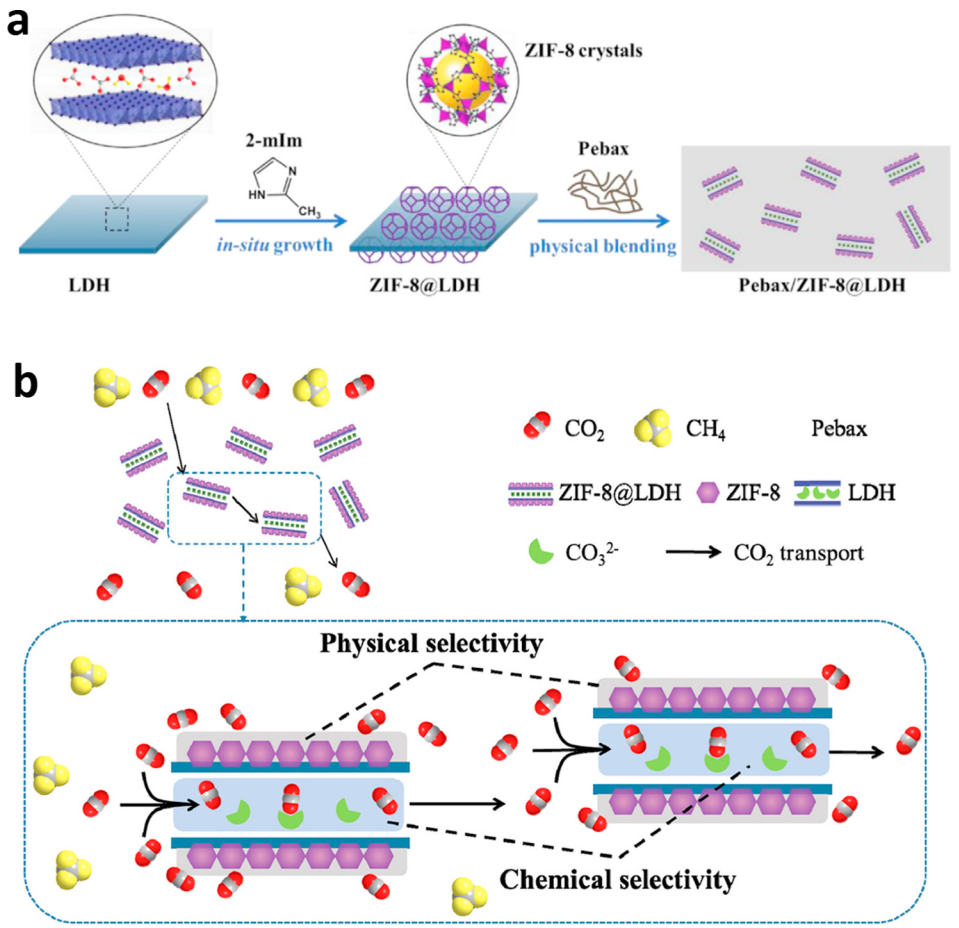

Fig. 34. a – Synthesis method employed for heterostructured ZIF-8@LDH and Pebax-based MMM. b – Coordination of physical and chemical selectivities in CO_2/CH_4 separation [303]. (Copyright 2018. Reproduced with permission from Elsevier Science Ltd.)

the MMM efficiently. These materials should be tailored as to be active at harsh environment, like implementation in the reversible reactions for acidic CO_2 capture. Zhang et al. [305] synthesized biomimetic filler (cobalt ion (Co^{2+}), 6-Bis (2-benzimidazolyl) pyridine, CoBBP) with a similar molecular structure with carbonic anhydrase (CA) enzyme and incorporated it in the Pebax matrix. With a little loading of the CoBBP (1.33 wt%), a surprising increase in CO_2 permeability of Pebax (from ~100 to 675.5 Barrer) in simultaneous with a proper increase in CO_2/N_2 selectivity (from ~40 to 62) was attained. Moreover, the mechanical strength, thermal stability and long-term durability of the MMMs were enhanced due to the proper interactions between the particles and membrane matrix.

Transient metal ion-functionalized nanofibers were also used to fabricate MMMs. CO_2 can reversibly react with the transient metal ions to form a π-bond complex that facilitate the CO_2 transfer from the MMMs. In addition, the anionic polymers like the sulfonated polyphenylene sulfone (sPPSU) and these ions can form metallic cation-polymeric anion complex ligands which thoroughly form excellent hydrogen bonding and electrostatic interactions with CO_2. Sulfonated pitch (SP), a hydrophilic polymer containing more than 10 wt% sulfonated groups, and zinc (Zn) ions were applied to synthesized SP-Zn^{2+} nano-fiber powders to incorporate into the Pebax matrix (Fig. 36). The hybrid membrane with 2 wt% SP-Zn^{2+} nanofillers enhances the CO_2 permeability and CO_2/CH_4 selectivity up to 104% and 70.2%, respectively [306].

Metal organic polyhedra (MOPs) are synthesized similar to MOFs via a self-assembly reaction through a metal ligand formation, with an only difference in structure where they have a discrete structure instead of infinite frameworks of MOFs. Fulong et al. [307] synthesized CuMOP, PdMOP and FeMOP, respectively by Cu^{2+}, Pd^{2+} and Fe^{2+} metal ions and embedded them into PVDF matrix. Both the polymer and metal-MOPs were soluble in each other that resulted in homogeneity of the MMMs. This coincided with a better thermal stability, significant decrease in crystallinity, superior gas transport properties, especially for CO_2/N_2 selectivity by the FeMOP. In another work, Yun et al. [308] developed Cu^{2+}-MOPs which functionalized by CO_2-philic triethylene glycol pendant groups (EG_3-MOP) and incorporated them into the cross-linked polyethylene oxide (XLPEO) to fabricate MMMs. With 2.5 wt% loading of the EG_3-MOP into the polymer matrix, CO_2 permeability increased ~25% and CO_2/N_2 selectivity increased surprisingly more than 35%.

Ship-in-a-bottle (SIB) is an advanced synthesis strategy which is currently investigated to develop the advanced MMMs. Indeed,

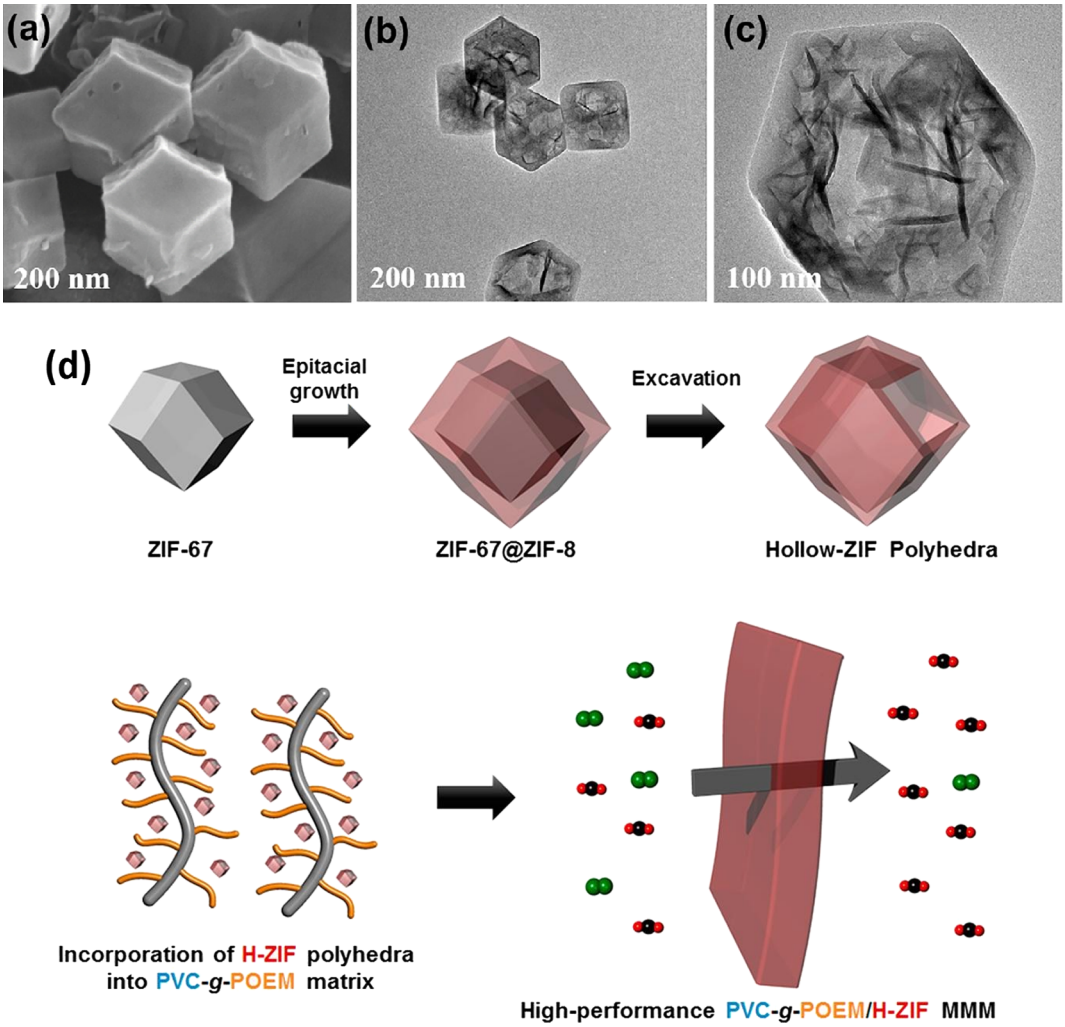

Fig. 35. a – SEM image, b, c – TEM images of H-ZIF-8 polyhedral nanocrystals. d – Synthesis method employed for the hollow ZIF-8 (H-ZIF) polyhedral nanocrystals and related MMM synthesis [304]. (Copyright 2018. Reproduced with permission from Elsevier Science Ltd.)

this method can be employed for designing novel nano-porous hybrid fillers through the encapsulation of various types of metal-ligand complexes into micro-porous fillers such as zeolites. Ebadi Amooghin et al. [309] synthesized a new filler type by encapsulating a polyaza macrocyclic metal–ligand complex (a metal-organic complex of a transient metal such as cobalt (Co)) into the zeolite Y cavities through the three-step SIB synthesis method. These steps are as follows: (1) ion exchange reaction (in which results in a product named as Co-1), (2) complex formation reaction with diamine (named as Co-2) and (3) complete the complex formation reaction with diketone through a template condensation reaction (named as Co-3). Fig. 37 illustrates the schematic view of the steps of SIB synthesis.

The new synthesized filler was then embedded in Matrimid@5218 polymer to prepare the related MMMs for gas separation. The results indicated that incorporating the encapsulated fillers into the polymer matrix drastically enhances the CO_2/CH_4 selectivity. Indeed, an additional mechanism of transport was offered in addition to intrinsic mechanism of inorganic filler/organic polymers, which is the insertion of additional electrostatic forces through the gas molecules/metal-organic complex interactions. The fabricated MMMs were considered in both single- and mixed-gas experiments. Finally, the results revealed that the insertion of 15 wt% filler into Matrimid leads to reach in a surprisingly high performance membrane with CO_2 permeability of 18.96 Barrer and CO_2/CH_4 selectivity of 111.7, which were respectively more than two and three-fold superior than pristine polymer (Fig. 38).

Suitable mechanical properties are vital for any industrial implementation of MMMs. Therefore, mechanical properties of the selected MMM were compared with pure Matrimid membrane. Achieved results indicated that Matrimid/Co-3 (15 wt%) had a highest tensile strength. As compared to pure Matrimid, this membrane revealed the highest Young's modulus which is a sign for excellent interfacial adhesion between encapsulated filler and polymer chains.

Results were also simulated by molecular dynamics method to find the most feasible/stable complex, as can be seen in Fig. 38. It was found that the probable stable molecular structures for the Co^{2+} metal-organic complex is formed with coordination number of

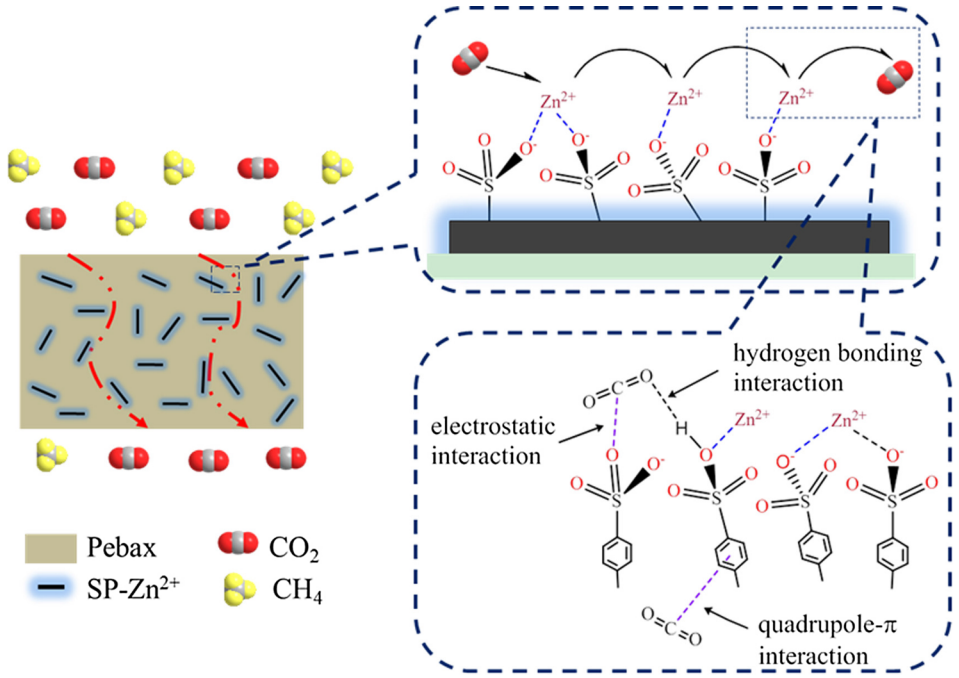

Fig. 36. Schematic representation of the CO_2 transfer mechanism in the SP-Zn^{2+} nanofiller incorporated Pebax MMM [306]. (Copyright 2018. Reproduced with permission from Elsevier Science Ltd.)

4. Also, the simulation results revealed that 4-coordinated Co^{2+} complex has a higher dipole moment in comparison with 6-coordinated one, indicating that this complex molecule has a higher intermolecular interaction with CO_2.

Lim et al. [310] applied an ionic polymer matrix to diffusion-control synthesis of iconic metal organic frameworks. In this case, anionic alginate polymer with metal ion-exchangeable sites considered as a platform for synthesis of iconic MOFs, HKUST-1 and MOF-74(Zn). They claimed that this in situ synthesis can enhance chemical stability of the MOF by encapsulating them inside polymer matrix.

4.1.9.4. Category IV. POFs with various porosities, excellent chemical resistance and thermal stabilities, and the inherent light weight are favorable candidates for using as fillers in MMMs for CO_2 separation. Tessema et al. [311] synthesized different polyimide-based, highly cross-linked benzimidazole linked polymers (BILPs) as new POF fillers with high surface area and good CO_2 adsorption capacity. They incorporated the synthesized fillers in Matrimid, and with 15 wt% BILP loading, obtained 34% higher CO_2/N_2 selectivity as compared to the neat Matrimid. This is comprises from the physical sorption affinity of the fillers for CO_2 through Lewis acid-base (N···CO_2) and aryl (CH···O═C═O) in BILPs. In addition, they stated that the structural similarities of the two BILPs with the same functional groups lead to similar performance of two Matrimid/BILP-4 and Matrimid/BILP-101 MMMs (Fig. 39), despite the remarkable difference in physical properties of the filler materials. Indeed, the BET surface area and CO_2 adsorption of BILP-4 (1079 m^2/g, 158 mg/g at 1 bar and 25 °C) were significantly higher than those of BILP-101 (536 m^2/g, 108 mg/g at 1 bar and 25 °C).

In another work, Shan et al. [312] investigated the effect of BILP porosity on CO_2/N_2 separation performance of the Matrimid/BILP-101 MMM. Moreover, they synthesized the room temperature (RT) BILP (RT-BILP-101) with lower porosity than the corresponding BIPL-101 and showed 2.8-fold higher CO_2 permeability as compared to the neat Matrimid with 24 wt% RT-BILP-101 particle loading. At a same loading, RT-BILP-101 showed also a higher permeability than the BILP-101 due to its lower partial pore blockage by the Matrimid chains in the MMMs.

Hollow polyamide nanoparticles (HPNs, average diameter of 42 nm) with dense shell were synthesized by Ding et al. [313] and incorporated in polyethylene oxide (PEO) to prepare PEO/HPN MMMs. Fig. 40 illustrates the chemical structures and properties of two polyimide-based BILPs. Through the incorporation of 1.0 wt% HPNs into PEO matrix, mechanical strength of the MMM was surprisingly increase (12.5 fold as compared to pure PEO). In addition, CO_2 permeability and CO_2/N_2 selectivity were increased respectively up to 1898 Barrer and 43.9, which surpasses the Robeson upper limit. This was attributed to significant increase in solubility of condensable CO_2 molecules in the nano-composite because the capillary condensation in hollow spaces. Moreover, the amino groups in the HPNs play the role of CO_2 carrier to facilitate its transport through the MMMs.

4.2. Advanced polymers

Advanced polymer matrices, which were used in MMM fabrication, can be divided into three groups:

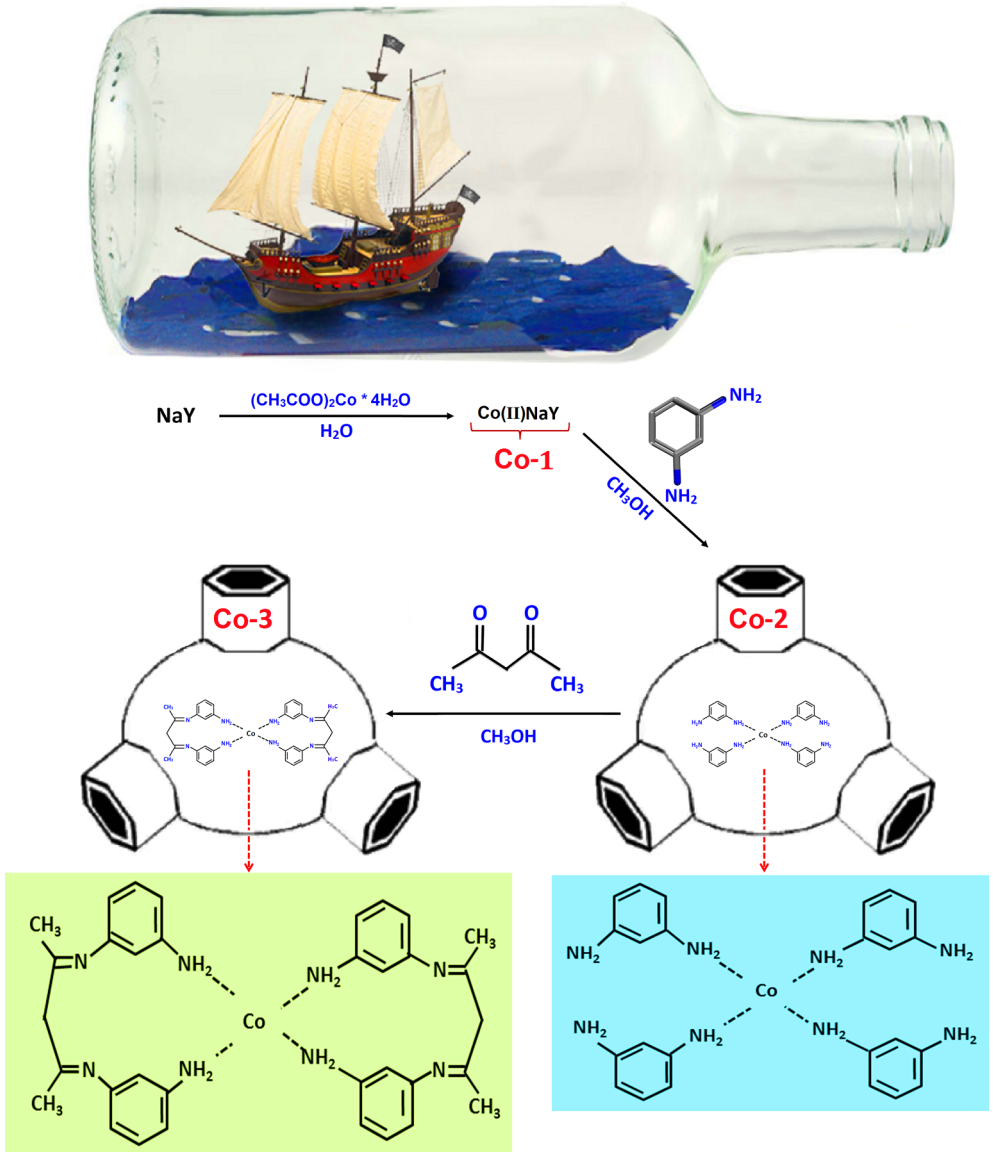

Fig. 37. A schematic view of the mechanism of the ship-in-a-bottle (SIB) synthesis [309]. (Copyright 2018. Reproduced with permission from Royal Society of Chemistry.)

Advanced highly permeable polymers such as polymers of intrinsic microporosity (PIMs), polyimides, thermally rearranged (TR) polymers, polyurethanes and polyacetylenes.
Polymers with moderate gas permeability but high selectivity, such as polyimide, polysulfone, cellulose acetate, and etc.
Ionic liquid/poly ionic liquids with high permeability and high selectivity.

Rigid backbone (polybenzodioxane) of PIMs decreases molecular packing of the polymers and thus improves the free volume, and consequently, the separation properties. PIM membranes are examples of microporous polymers with high gas permeability and selectivity [314] owing to large surface area, free volume elements and good pore alignment and size distributions. This new series of microporous polymer membranes could be widely used in extensive measure applications for gas separation, resulting in their extra ordinary gas fluxes for light gases and also satisfying economic cost requirements [56,315]. For example, a high value of Young's modulus for PIM-1 (530 MPa) was considerably increased (640 MPa) with the insertion of only 3 wt% f-MWCNT into the matrix. In this case, the CO_2 permeability was significantly enhanced from 6211 to 15,721 Barrer, while the CO_2/N_2 selectivity decreased from 22.2 to 16.5 [244].

Strategies to improve CO_2 separation properties are designing rigid polymer chains with contorted structure and frustrated chain-packing, incorporating CO_2-philic functional groups in polymers and finally designing facilitated transport membranes and MMM materials [316,317]. In this section, different advanced polymers used in MMMs as matrixes and the related functionalization

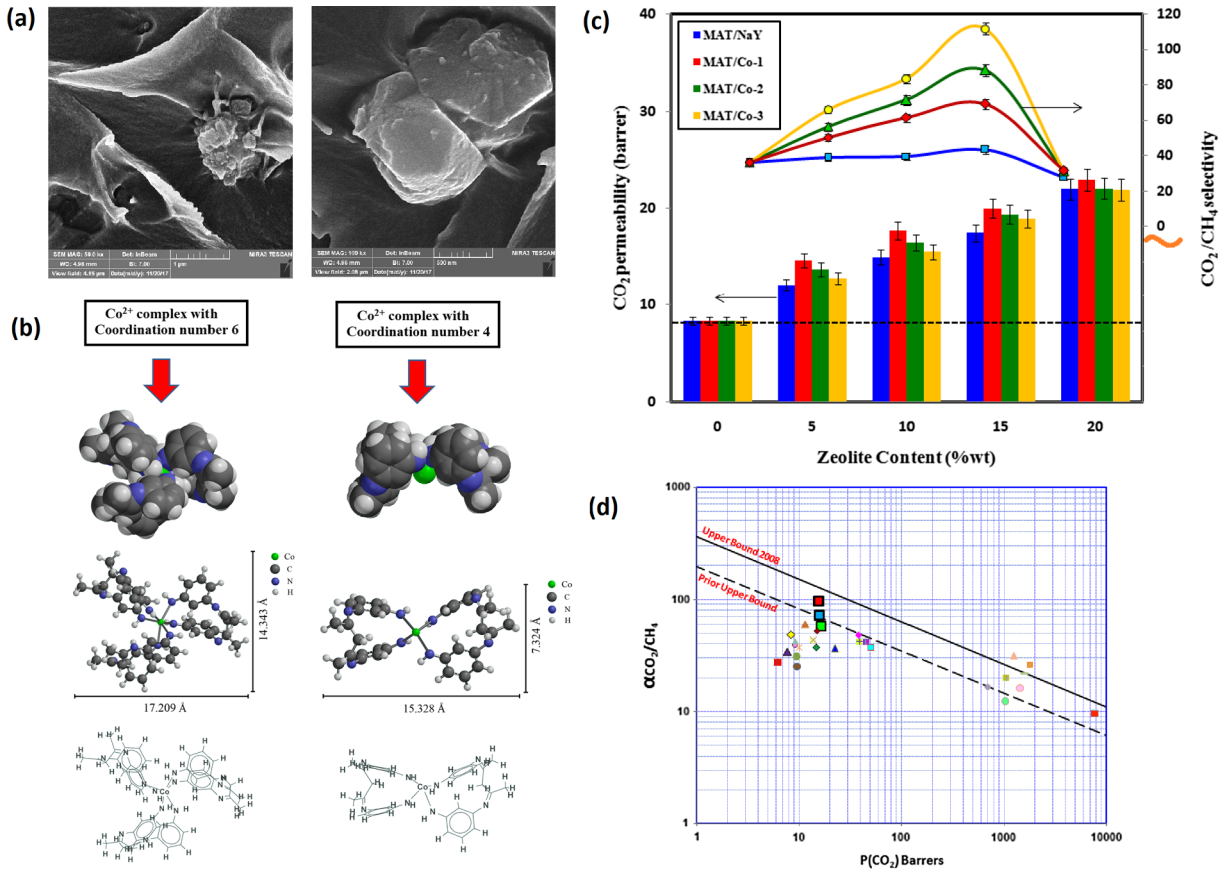

Fig. 38. Schematic illustration showing the (a) cross-sectional SEM images of Matrimid/Co-3 (15 wt%) in two magnifications, (b) Possible structures of cobalt-based synthesized complex molecules with the coordination numbers 4 and 6. (c) Effect of filler loading on gas permeation properties of Matrimid at 35 °C and 2 bar. (d) Robeson plot showing the superior performance of the MMMs containing SIB synthesized fillers in comparison with the other polyimide-based MMMs [309]. (Copyright 2018. Reproduced with permission from Royal Society of Chemistry.)

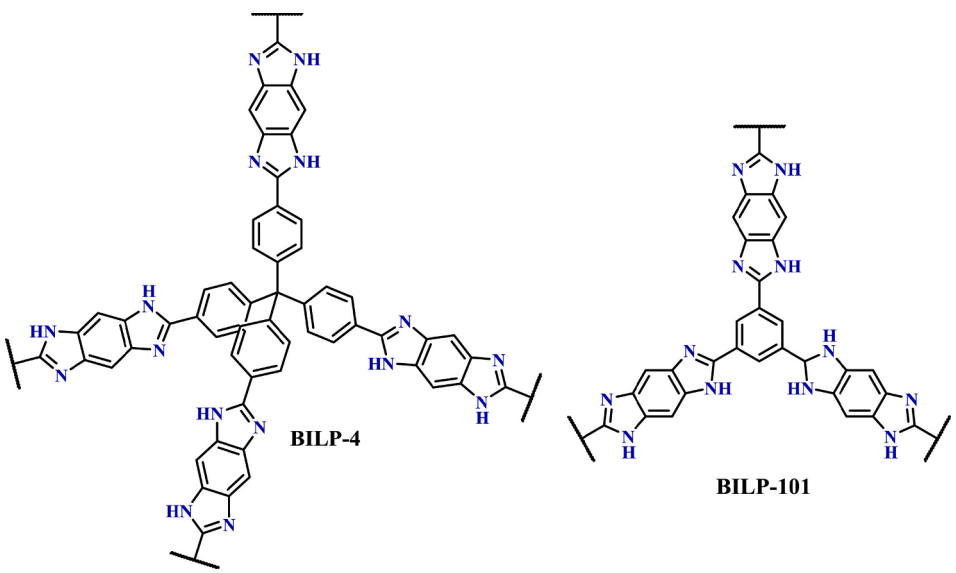

Fig. 39. Chemical structures and properties of two polyimide-based BILPs [311]. (Copyright 2018. Reproduced with permission from Elsevier Science Ltd.)

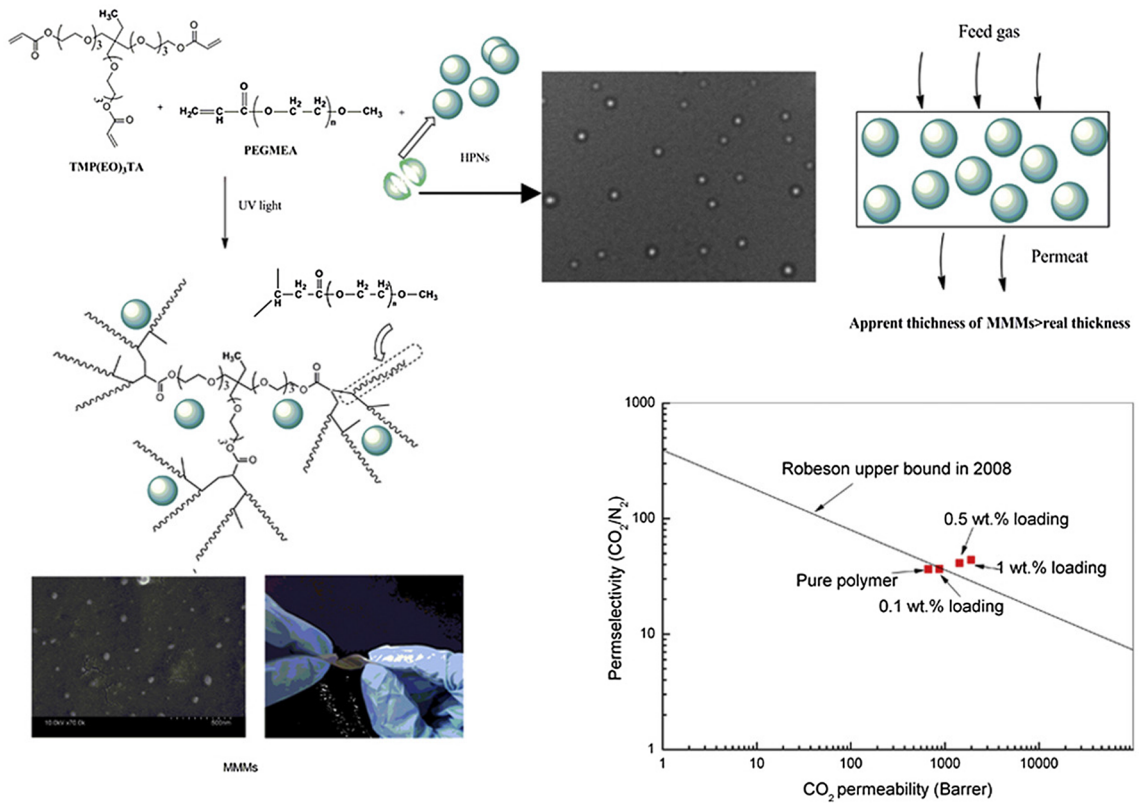

Fig. 40. Chemical structures and properties of two polyimide-based BILPs [313]. (Copyright 2019. Reproduced with permission from Elsevier Science Ltd.)

methods will be studied.

4.2.1. PIMs

Polymers of intrinsic microporosity (PIMs) are excellent membrane materials due to their excellent properties such as high specific surface, thermal resistance and superior chemical resistance [318].

PIMs, the amorphous glassy polymers with properties of a microporous material, were supposed to have interconnected regions of large interchains' free volume, which might be identified in some sense as "pores" (pore size < 2 nm, as defined by IUPAC) [319]. These ladder type polymers are prepared by a benzodioxane formation reaction between proper monomers [320]. It was reported in 2002 for the first time by McKeown et al. [321,322] as a new type of polymer. Subsequently, Budd et al. [323,324] confirmed that PIMs have suitable characteristics to make them proper choices for membrane fabrication.

Good solubility and high processability are advantages of PIMs in the role of membrane materials [325]. PIMs and their derivatives could also be suitable absorbents for efficient gas separation and have very high CO_2 permeabilities. Hence, they could be used for acid gas removal in membrane based systems [47]. PIMs preparation parameters including monomer purities, type of solvent and especially methanol post-treatment could alter their gas transport properties [56,326]. PIM-1 and PIM-7 with high selectivity and excellent permeability surpassed the Robeson's upper bound for gas separation [56].

PIMs have unique ability to combine the microporosity properties of inorganic materials with functional adjustability. Post-polymerization modification can introduce CO_2-philic functionalities onto the main chain through amine modification [327,328], amidoxime modification [329], etc. Amine–PIM-1 exhibited higher CO_2 uptake and higher CO_2/N_2 sorption selectivity than the original polymer, with very obvious dual-mode sorption behavior (Fig. 41) [327].

Physical aging is a main challenge for glassy polymers. To overcome the challenge "freezing in" the free volume is considered. Rigidifying the initial polymer structure by means of surface modification, co-polymerization [318,330], or cross-linking can be a useful step. These methods reduced aging, but often faced with a major loss in permeability. Incorporating another porous material such as zeolites, porous organic cages or MOFs, to form a MMM, is another way to suppress the physical aging and also increase the membrane performance [325,331–335]. Mitra et al. [336] introduced a hypercross-linked polymer (HCP) "sponge" as an economical alternative filler into PIM-1. By adding the filler, membrane permeability and CO_2/N_2 selectivity was increased while aging was strongly delayed. Introducing the HCP filler increased the CO_2 permeability up to 250% while it decreased 39.9% over 150 days of operation. In another similar study, Lau et al. [337] solved the aging problem of super glassy polymers such as PIM-1 by adding an ultraporous additive (PAF-1). It also improves membrane permeability and selectivity. Polymer chains absorbed within the PAF-1

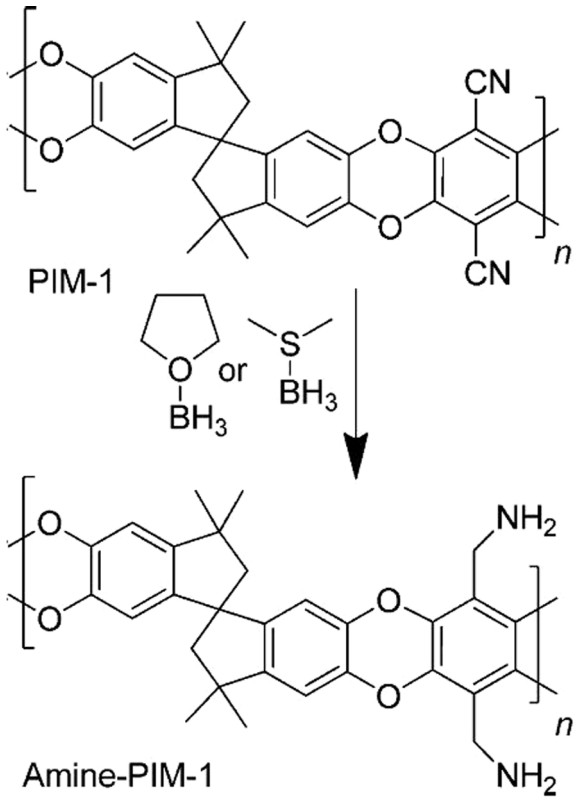

Fig. 41. Amine modification of PIM-1 [327]. (Copyright 2014. Reproduced with permission from American Chemical Society.)

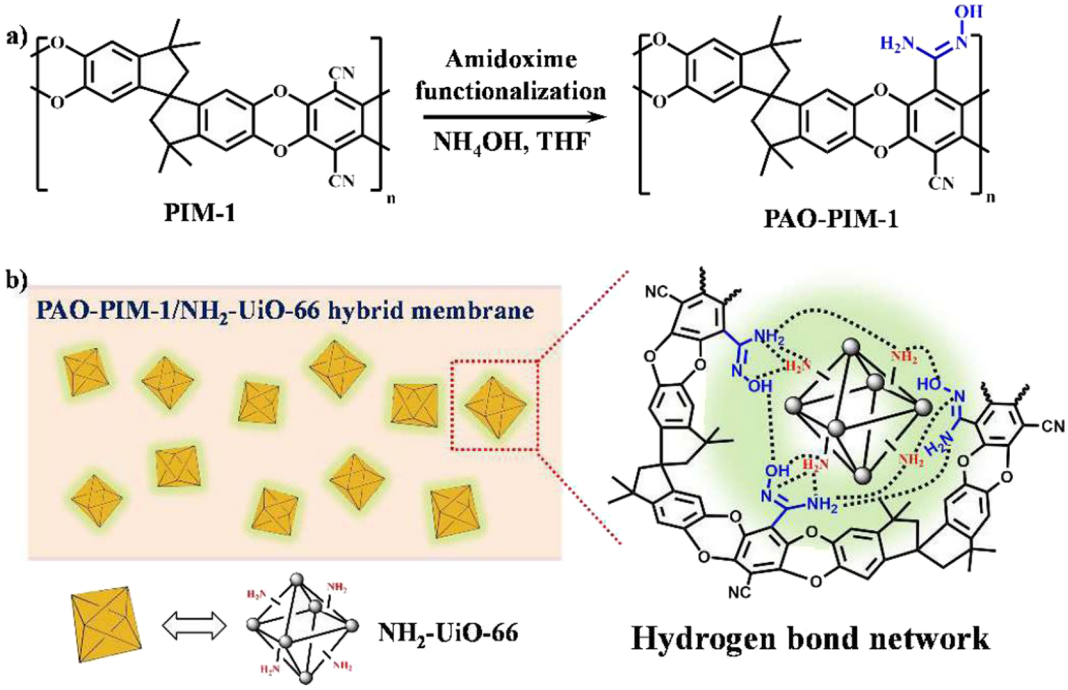

Fig. 42. Schematic view of: (a) PAO-PIM-1 synthetic procedure and (b) interfacial design of MMM by hydrogen bond network [338]. (Copyright 2017. Reproduced with permission from Royal Society of Chemistry.)

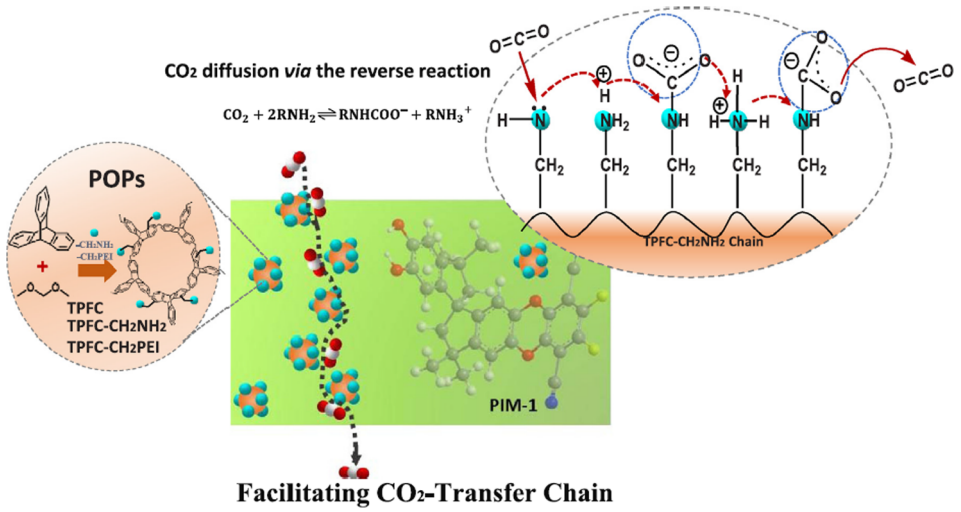

Fig. 43. Chemical structures of triptyene based POP fillers and PIM-1, and mechanism of a facilitating CO_2-transfer chain reveals in PIM-TPFC-CH_2NH_2 MMM for superior CO_2 [339]. (Copyright 2018. Reproduced with permission from Elsevier Science Ltd.)

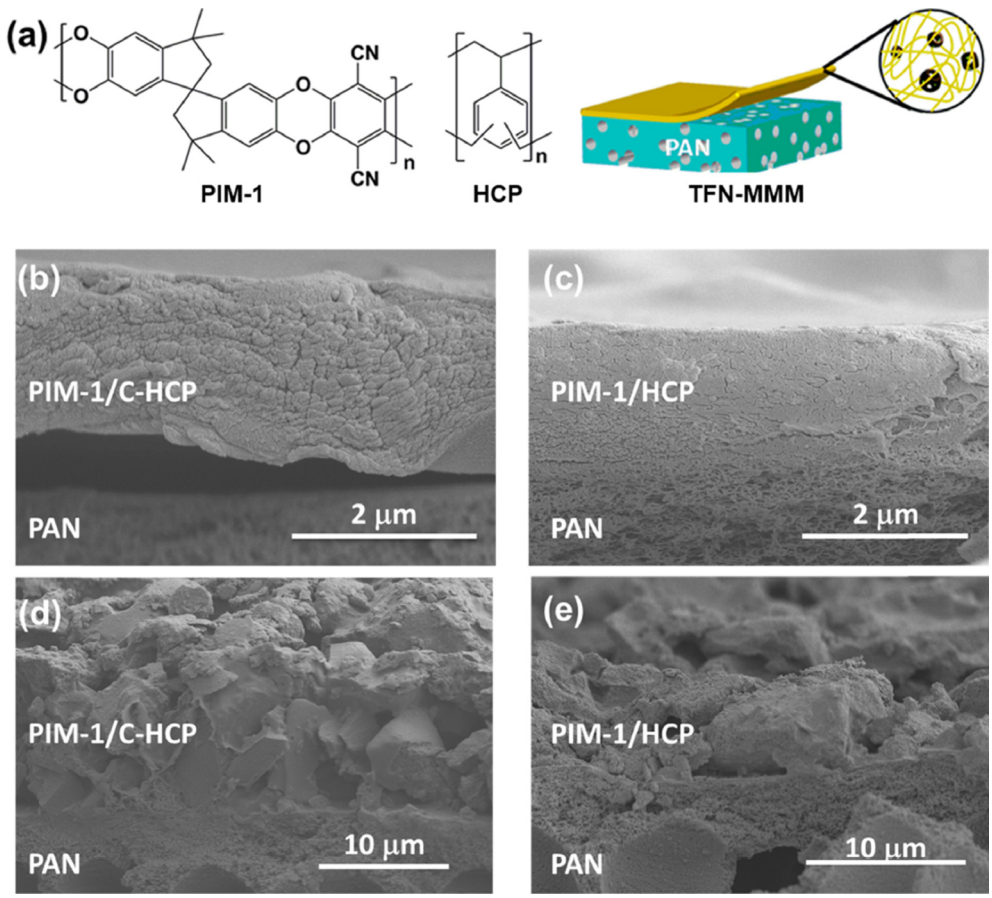

Fig. 44. (a) Chemical structures of PIM-1 and HCP employed in TFN synthesis, SEM images of (b, d) PIM-1/C-HCP TFN MMM with 10 and 60 wt% filler loading, respectively, and (c, e) PIM-1/HCP TFN MMM with 10 and 60 wt% filler loading, respectively [340].

pores will cause them to remain in their open position and overcome the polymer aging. The addition of PAF-1 into PIM-1 enhanced the CO_2 permeability about 320%. Moreover, it would practically stop aging and the CO_2 permeability decrease was only less than 7% over 240 days.

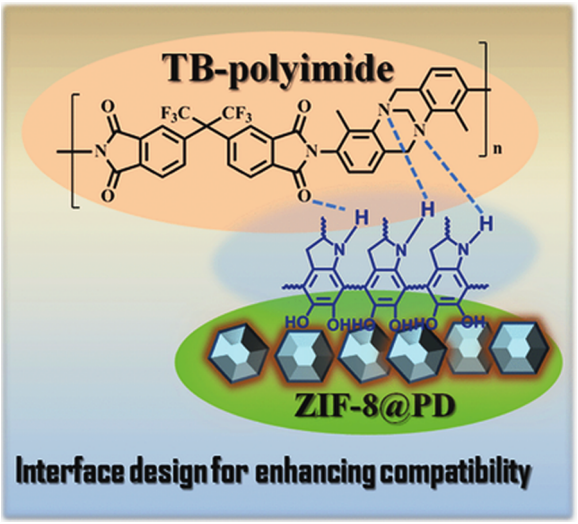

Fig. 45. Interface design of ZIF-8@PD-PI MMM [349]. (Copyright 2016. Reproduced with permission from John Wiley and Sons.)

Wang et al. [338] designed a defect free filler/polymer interface by embedding an amine functionalized MOF into amidoxime functionalized PIM-1matrix. Fig. 42 depicts the hydrogen bond network between functionalized filler and PIM-1, which makes a good compatibility between them. Prepared PAO-PIM-1/NH_2-UiO-66 (30 wt%) MMM, showed a superior gas separation performance of 8425 barrer for CO_2 permeability, 27.5 for CO_2/N_2 selectivity and 23.0 for CO_2/CH_4 selectivity.

Wang et al. [339] synthesized two different amine functionalized triptyene-based POP with the titles of TPFC-CH_2NH_2 and TPFC-CH_2PEI, and afterwards embedded them into the PIM-1 to prepare novel MMMs for CO_2/light gas separations. Authors claimed that the 15 wt% filler loaded MMM have the superior performance through the most reported state-of-the-art membranes with the CO_2 permeability of 7730 barrer, CO_2/CH_4 and CO_2/N_2 selectivities of about 36.4 and 45.9, respectively. They also attributed this result to a facilitating CO_2-transfer chain mechanism in MMMs. FTIR results showed that the peak at 1666 cm^{-1} is attributed to the HNCOO− group is the best sign for reversible amine reaction for CO_2 adsorption. As can be seen in Fig. 43, by introducing the modified POP fillers with homogenous pattern into the PIM-1, an amine network with specific transport chains for CO_2 facilitating transport is embedded in the membrane structure. This directly affects the MMM ability for CO_2 separation.

In another work, Bhavsar et al. [340] studied the effect of the addition of the hypercrosslinked polystyrene (HCP) and its carbonized form (C-HCP) on gas permeation properties of PIM-1. Both thin film nanocomposite (TFN) membranes and MMMs were prepared with the thickness of 2 μm and 40–90 μm, respectively. Obtained results showed that robust MMMs prepared in the moderate filler loadings, but in the case of TFN, higher dispersion was achieved up to 60 wt%. SEM images of TFN membranes which was prepared by coating of MMM on a porous polyacrylonitrile (PAN) support, depict in Fig. 44. As can be seen, at higher filler loadings (60 wt%) an irregular surface layer with varying thickness was created. TFN MMM with 60 wt% of C-HCP demonstrated a CO_2 permeance and CO_2/N_2 selectivity about 9300 GPU 11, respectively.

4.2.2. Polyimides

Polyimides composed of diamines and dianhydrides are widely used for gas separation due to their physical properties such as high thermal (> 500 °C) and mechanical stability (excellent mechanical strength properties which is about seven times stronger than steel), outstanding chemical and solvent resistance. The “type of bridging groups”, “linkage” and “polar groups” in polyimide structures can affect the polyimide-based membranes performances [1,341].

A wide variety of diamines and dianhydrides are used to prepare the glassy polyimides. Particularly the large array of 4,4′-(hexafluoroisopropylidene) diphthalic anhydride (6FDA)-based polyimides offer high solubility in common solvents. Moreover, they have fabulous inherent CO_2/CH_4 separation properties, in terms of good permeability and selectivity. They also have excellent mechanical properties [342,343]. On the contrary, the CO_2 or H_2S separation efficiencies of polyimide membranes are limited due to the acid gas-induced “plasticization”. Condensable acid gases like CO_2 and H_2S will lead to excessive swelling of the glassy polymer structure and increase in the segmental mobility [39]. The higher the segmental mobility, the more transport of unwanted gases will occur together with the desired gases, wherein a lower selectivity is resulted.

Cross-linked polyimides utilization for membrane preparation will increase permeability without sacrificing the selectivity. Cross-linked polyimides are achieved by different techniques including UV irradiation, thermal treatment and using cross-linker compounds [39,344–346].

Wang et al. [347] successfully combined two kinds of anhydrides with Tröger’s Base (TB) diamines to increase the permeability of polyimides. The permeability of polyimides was increased by TB unit comprised of rigid and in-built amine structure and high selectivity was maintained at the same time. Gas separation performance was improved by TB-polyimide membranes for H_2/CH_4, H_2/N_2, He/CH_4, and CO_2/CH_4 gas pairs.

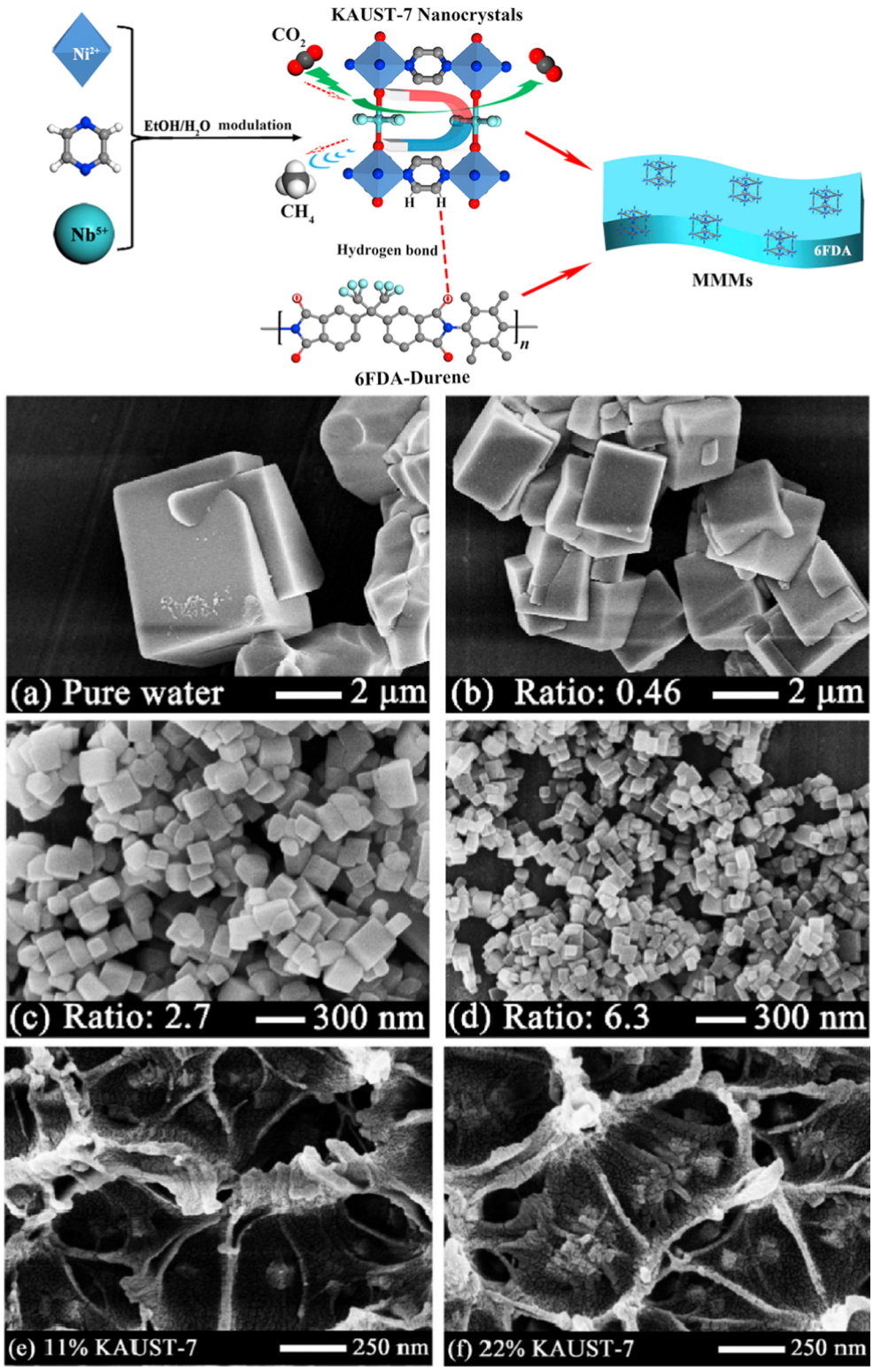

Fig. 46. The chemical structure of MMM species and SEM images (a–d) the effect altering the ethanol-to-water ratios on synthesized KAUST-7 crystals and (e, f) cross section images of 6FDA-Durene/KAUST-7 MMMs containing 11 and 22 wt% nnalocrystals with the average diameter of 80 nm [354]. (Copyright 2018. Reproduced with permission from Elsevier Science Ltd.)

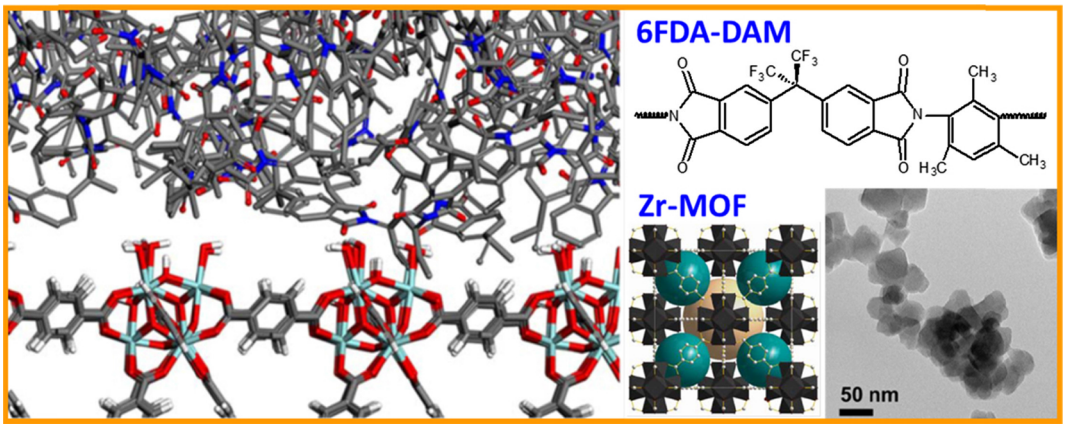

Fig. 47. The snapshot the polymer/filler structure at the interface and TEM image of UiO-66 [355]. (Copyright 2018. Reproduced with permission from Elsevier Science Ltd.)

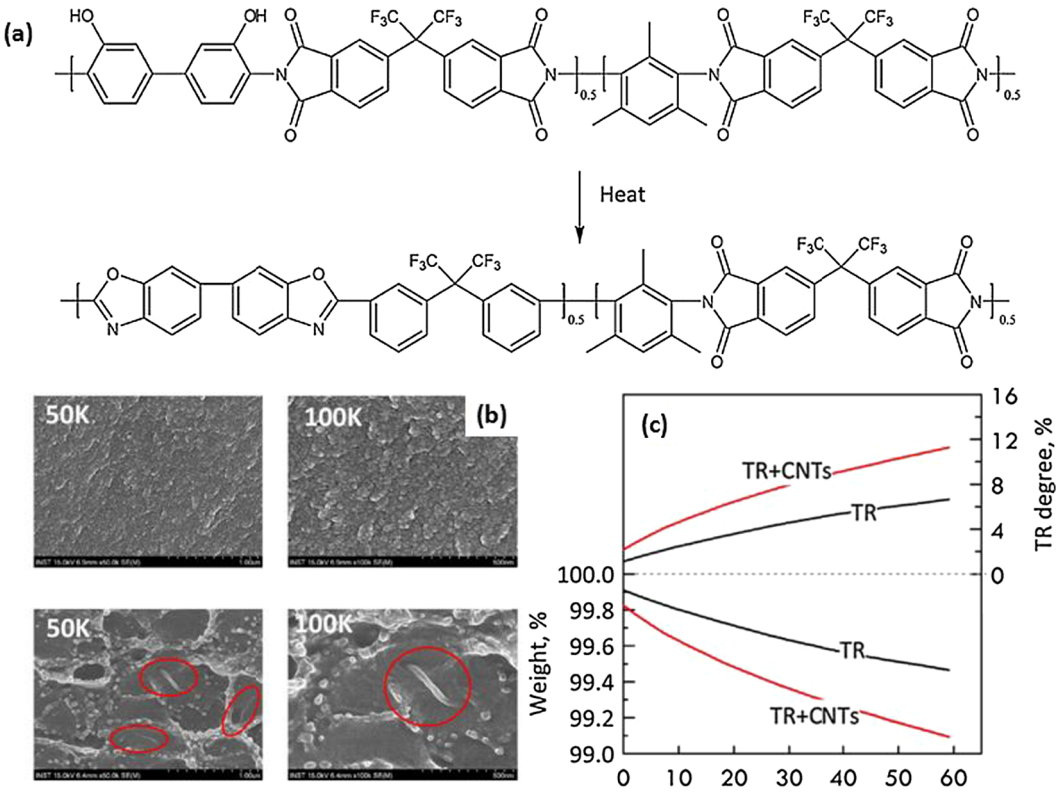

Fig. 48. (a) Precursor hydroxyl copolyimide and poly(benzoxazole-co-imide) chemical structures. (b) The neat TR and TR + CNTs membranes cross-sectional SEM images (treated at 375 °C). Red circles underline the disperse CNTs. (c) Weight and degree of thermal rearrangement as a function of time [362]. (Copyright 2017. Reproduced with permission from Elsevier Science Ltd.)

Incorporation of inorganic/organic fillers such as zeolites, silicas, carbon nanotubes and MOFs into polyimides is another method employed to provide the MMMs with high membrane performance [348–353]. Wang et al. [349] fabricated MMMs by using a bio-inspired interface design to improve filler/polymer compatibility. The surface of ZIF-8 nanocrystals was coated by a thin poly-dopamine (PD) layer keeping constant thickness via dopamine self-polymerization process. Permeability of CO_2 increased significantly from 285 Barrer for pure PI membrane to 380, 702 and 1056 Barrer respectively for ZIF-8@PD-PI (7%), ZIF-8@PD-PI (20%), and ZIF-8@PD-PI (30%). CO_2/CH_4 selectivities were 25, 23 and 20 respectively for the aforementioned membranes. Moreover, the CO_2/N_2 ideal selectivity was enhanced from 12 for ZIF-8-PI (30%) to 14 for ZIF-8@PD-PI (30%). The selectivity values increased due to the development of filler/polymer interface (Fig. 45).

Chen et al. [354] synthesized a CO_2-philic NbOFFIVE-1-Ni MOFs (KAUST-7) and embedded them into the 6FDA-Durene

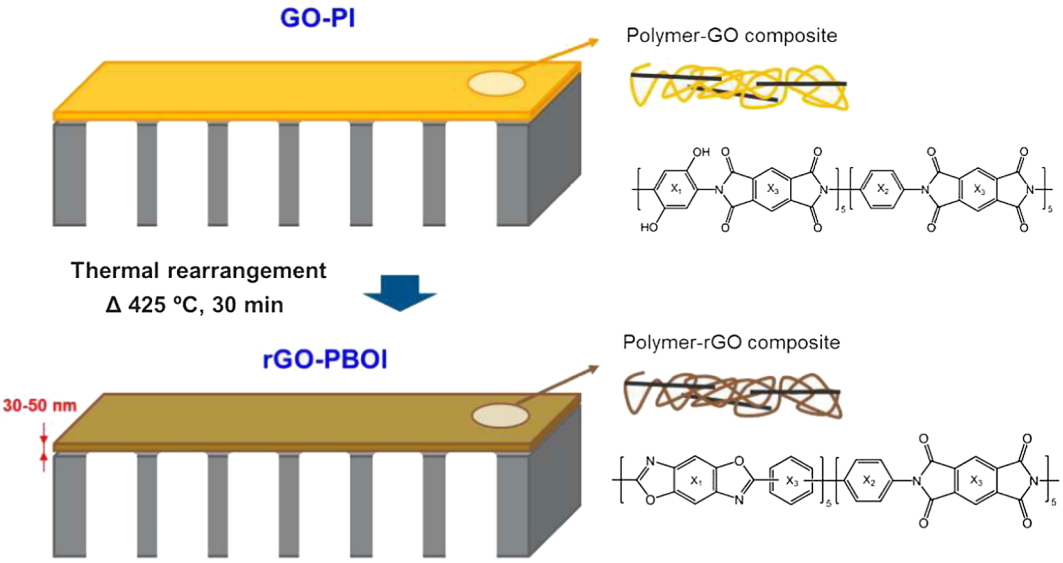

Fig. 49. Schematic of the GO-PBOI ultrathin selective layers on AAO) substrate [363]. (Copyright 2018. Reproduced with permission from Royal Society of Chemistry.)

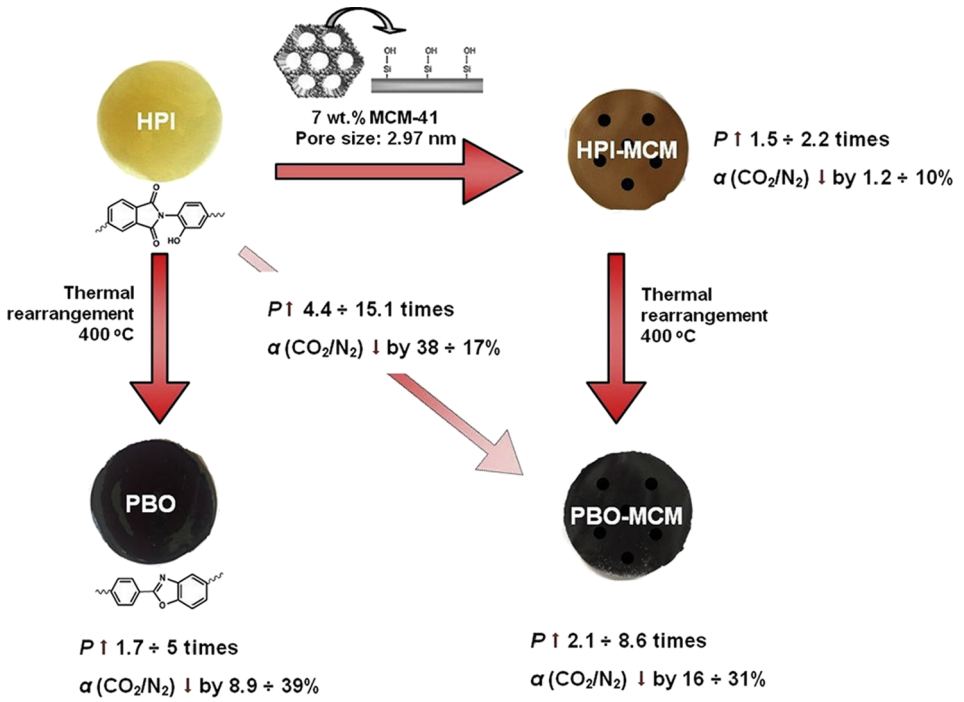

Fig. 50. Illustration of MCM/HPI and MCM-PBO MMMS through the thermal conversion process [364]. (Copyright 2018. Reproduced with permission from Elsevier Science Ltd.)

polyimide. Gas permeation results indicated a significant increase in permselectivity, especially at higher filler loadings. MMM based on 33 wt% filer loading revealed the CO_2 permability of 1030 Barrer and CO_2/CH_4 selectivity of 33, which were higher than that of pure polymer. Fig. 46 presents the chemical structure of MMM species and also SEM images of synthesized fillers and fabricated MMMs. Various KAUST-7 were synthesized by altering the ethanol-to-water ratio in solution. As can be observed in Fig. 46a–d, the as-synthesized square-shaped fillers were changed with the diameter of 3 μm (pure water used as solvent) to 80 nm (a solvent used with the ethanol-to-water ratio of 6.3). The decrease in filler sizes is attributed to hindering the crystal growth due to the preferential adsorption of ethanol molecules to its structure. Moreover, the cross sectional images of MMMs containing 11 and 22 wt% of KAUST-7 (Fig. 46e and f), also indicates a sieve-in-a-cage morphology with no any detectible voids which confirms the interfacial compatibility of 6FDA-Durene/KAUST-7 MMM.

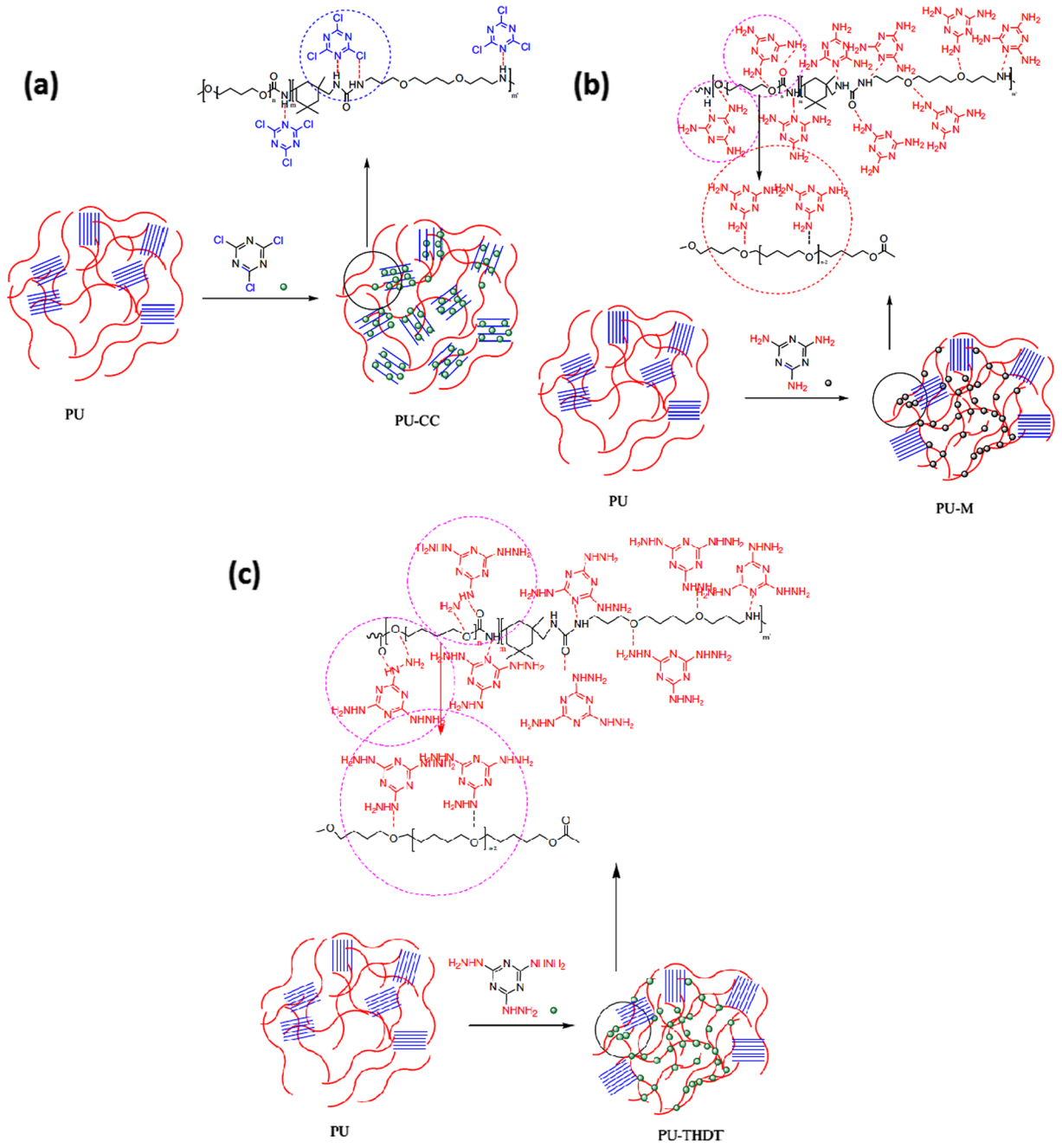

Fig. 51. Fillers dispersion in the PU chains, and also possible hydrogen bonds between the polymer backbone and nanoparticles (a) CC/PU, (b) M/PU and (c) THDT/PU [377]. (Copyright 2018. Reproduced with permission from Elsevier Science Ltd.)

Zamidi Ahmad et al. [355] considered the effect of UiO-66, UiO-66-NH_2 and UiO-66-NH-$COCH_3$ MOFs on highly permeable polymer 6FDA-DAM. They found that the best performance MMM was the 6FDA-DAM/UiO-66 (14 wt%) with CO_2 permeability of 1912 Barrer and CO_2/CH_4 selectivity of 31. They also employed the atomistic modeling as illustrated in Fig. 47 and showed that the surface of UiO-66 is relatively covered by polymer and also the polymer chains are not penetrate into the filler pores.

4.2.3. TR polymers

Thermally rearranged (TR) polymers are another member of high permeable polymers family, prepared by a thermal post-membrane conversion procedure from aromatic polyimide precursors [1]. TR polymers characteristic for membrane gas separation are reported for the first time by Park et al. [356].

Functionalized polyimides used as precursors have different functional groups at ortho position such as –OH, –SH or –NH_2 which

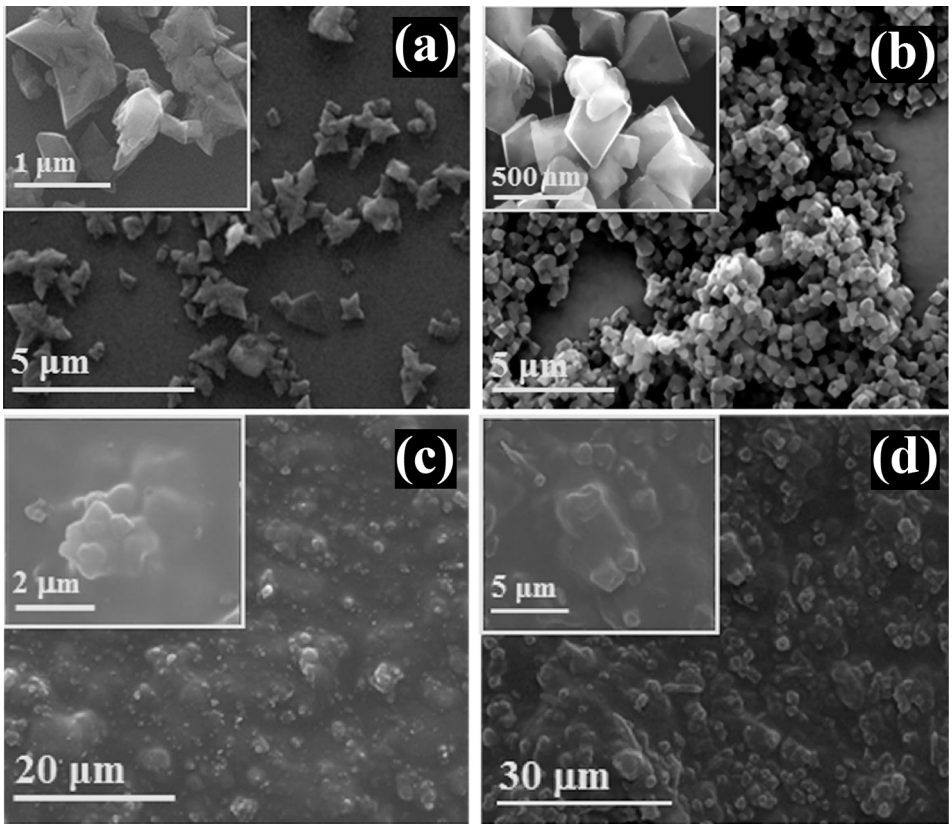

Fig. 52. SEM images of (a) UiO-66 (Zr) powder, (b) MIL-101 (Cr) powder, (c) PU/UiO-66 (28 wt%) surface and (d) PU/MIL-101 (28 wt%) surface [378]. (Copyright 2018. Reproduced with permission from Elsevier Science Ltd.)

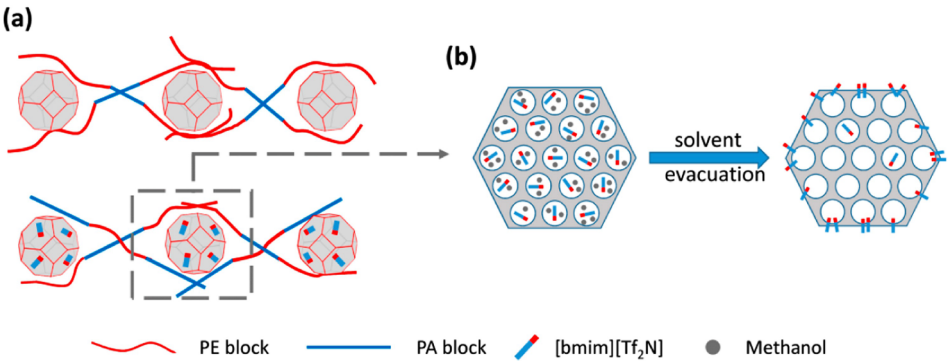

Fig. 53. Schematic view of the probable mechanism related to the toughening of IL@ZIF-8-polymer interface: (a) the favored adsorption of PA block on IL@ZIF-8 and (b) the aggregation of [bmim][Tf_2N] at the filler/polymer interface [394]. (Copyright 2016. Reproduced with permission from Elsevier Science Ltd.)

cause the TR polymers preparation with different structures comprising polybenzoxazoles (PBO), polybenzothiazoles (PBZ), polypyrrolone (PPL) and polybenzimidazoles (PBI) [56,357].

TR-polymers have excellent characteristics for gas separation performance including high selectivity as good as permeability, which is overcoming the trade-off relationship [314,358]. The structure of molecules and preparation conditions adjust the cavity size and make various types of TR polymers. TR membranes also have high plasticization resistance for mixed gas separation [359].

It should be mentioned that due to thermal rearrangement process during the formation, TR polymers have brittle structure which limits their usage in gas separation process. The higher the rearrangement temperature usually the more brittleness of the TR sample is attained. For example, tensile strength of HAB-6FDA polyimide was measured as 153 MPa that it was reduced for the corresponding TR polymers to 107, 85 and 62 MPa, which respectively synthesized at rearrangement temperatures of 350, 400 and 500 °C. In recent researches different strategies have been carried out to overcome the brittleness (to enhance the stiffness) of the TR polymers. For

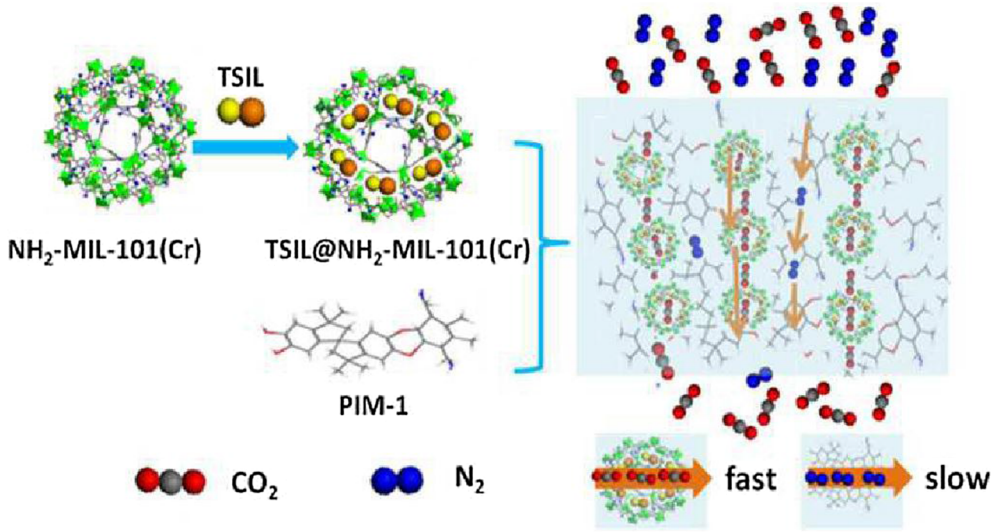

Fig. 54. A schematic representation of TSIL@NH_2-MIL-101(Cr)/PIM-1 MMM gas separation performance [395]. (Copyright 2016. Reproduced with permission from Royal Society of Chemistry.)

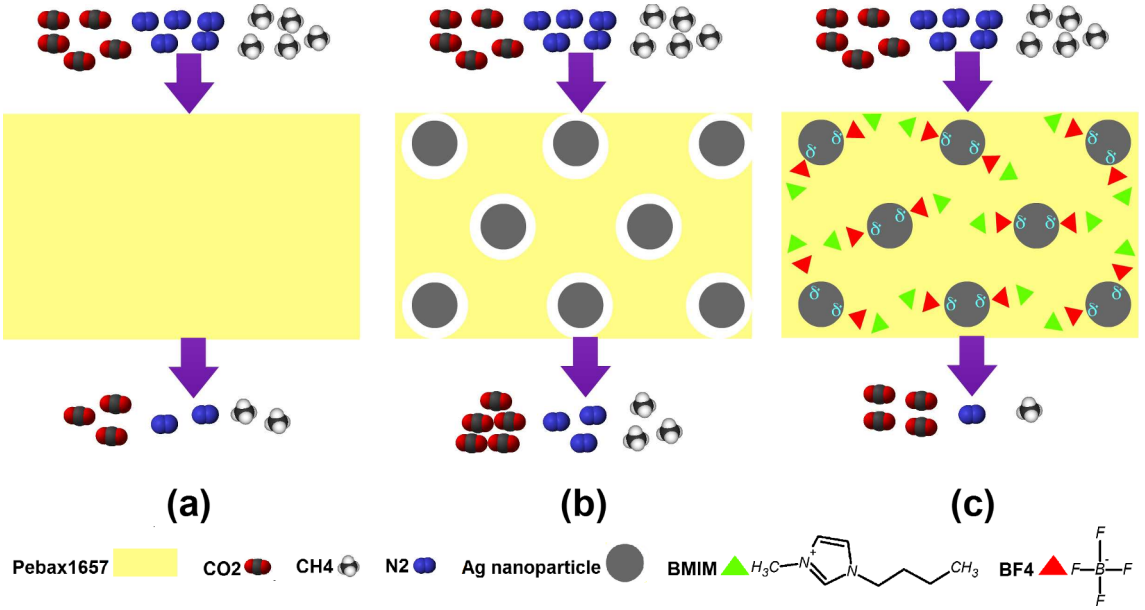

Fig. 55. A schematic view of the complexation through the (a) neat Pebax 1657 membrane, (b) Pebax 1657/Ag MMM, and (c) Pebax 1657/Ag/IL ternary MMM [398]. (Copyright 2017. Reproduced with permission from American Chemical Society.)

instance introducing spirobisindane in the TR-PBO membrane or blending with different polyimides could improve the mechanical properties of TR polymers [360]. Jo et al. [361] used different TR-able (bisAPAF, HAB) and non TR-able (DAM, ODA) diamines to prepare poly-(benzoxazole-co-imide) membranes (TR-BPOI) and investigated the mechanical properties (tensile strength and elongation at break) of these membranes. The result showed the TR-BPOI membranes have better mechanical properties respect to TR-BPO and also the gas separation performance was improved. Among various diamines, HAB-ODA has the best result in improving the tensile strength and elongation at break up to 70%. It comes from the fact that thermal rearrangement deforms the benzoxazole chains and lowers the mechanical strength of TR membranes. On the other hand, non-TR-able diamines (ODA, DAM) do not undergo the same TR process, and hence, they form membranes with superior properties.

However, TR polymers have noticeable gas separation performances, their application as a polymer matrix in MMMs have been seldom. Recently, Brunetti et al. [362] prepared new MMMs by incorporating oxidized multi-wall carbon nanotubes (0.5 wt%) into thermally rearranged polybenzoxazole-co-imide (TR-PBOI) matrix and studied the gas separation performance and aging behavior of MMMs (Fig. 48). The result of gas separation tests showed an increase of 17.1% in CO_2 permeability and 16.5% in CO_2/N_2 selectivity

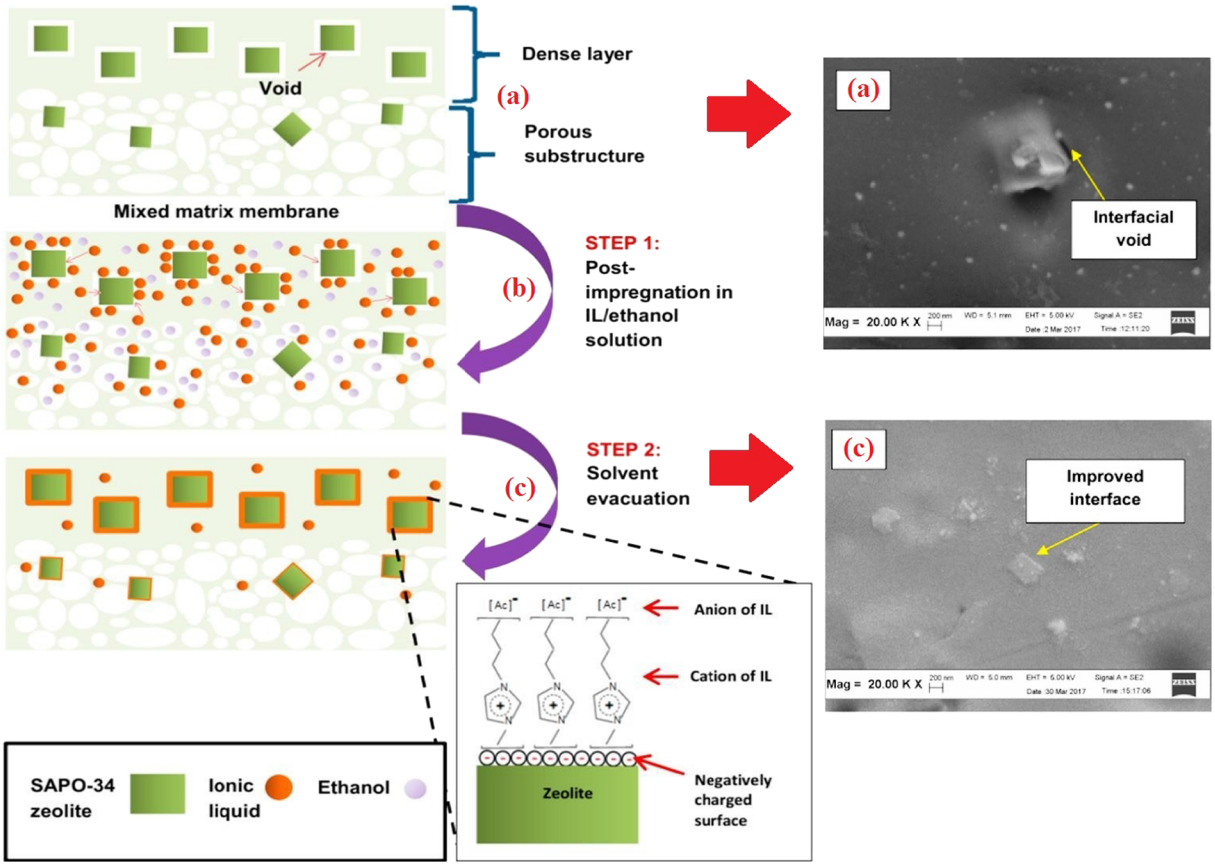

Fig. 56. The effect of post-impregnation of MMMs with IL on surface morphology of MMMs (a) PSf/SP5, (c) PSf/SP5-0.6 M membranes [399]. (Copyright 2018. Reproduced with permission from Elsevier Science Ltd.)

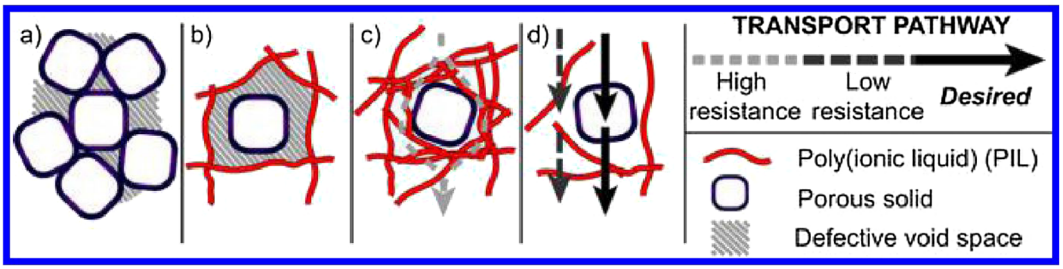

Fig. 57. Various defects frequently encountered in MMM fabrication by embedding porous solid into a polymer matrix: (a) solid/solid interface; (b) solid/polymer interface; (c) matrix accumulation around the porous solid fillers; and (d) transport through the MMM matrix [402]. (Copyright 2016. Reproduced with permission from American Chemical Society.)

compared to the pure TR membrane.

Tailoring the ultrathin TR-based MMMs is an important issue for practical implementation of MMMs. Kim et al. [363] fabricated a novel MMM by incorporating the 2D GO nanosheets into the thermally rearranged polybenzoxazole-co-imide (TR-PBOI) to prepare the ultrathin selective layer with the thickness of less than 40 nm on an anodic aluminum oxide (AAO) substrate (Fig. 49). Embedding the GO nanosheets into the MMM caused to enhance the mechanical robustness. The 1 wt% filler-based MMM revealed the CO_2 permeance of and a CO_2/CH_4 selectivity of 1784 GPU and 32, respectively.

In another work, Wolińska-Grabczyk et al. [364] prepared the poly(hydroxyimide)s (HPI)/mesoporous MCM-41 silica MMMs for CO_2 separation. Both bare and MCM-41 filled poly(hydroxyimide)s precursors were employed to achieve thermally rearranged (TR) polybenzoxazoles (PBO). Various synthesized polyimides were acquired as HPI-1 (BPDA/HAB), HPI-2 (BPDA/DAR), and HPI-3 (BPDA/DAP). Afterwards, a thermal treatment under an argon atmosphere in a tube furnace was used to convert the HPIs and MMMs to PBO films (dark membranes). Mechanical results indicated that tensile strengths, elongation at break and Young's modulus of

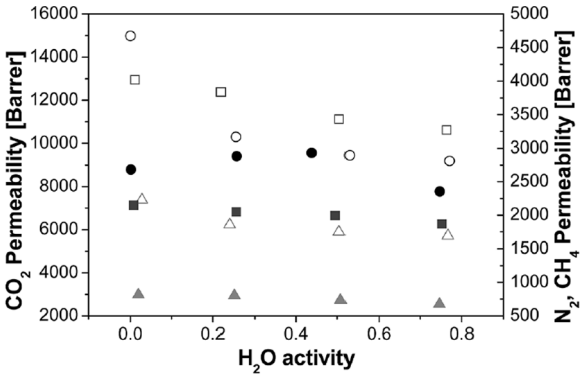

Fig. 58. PTMSP/zeolite 4A permeability variation in terms of relative humidity [408].

unfilled membranes were respectively about 12–38 MPa, 8.1–16% and 0.6–1 GPa. On the other hand, strength and modulus were considerably enhanced only in HPI-1 and HPI-2 based MMMs. This may be due to the better dispersion of MCM in HAB and DAR based HPIs in comparison with lower hydroxyl groups ones, HPI-3. Moreover, through the thermal conversion of HPIs, strength and modulus were enhanced, while the elongation at break was decreased. They also concluded that the presence of MCM via thermal conversion process caused to weakening the chain interactions and reducing the tensile strength of PBOs MMMs. However, excellent filler/polymer interfacial adhesion caused to not only slight decrease in elongation at break, but also some enhancement in Young's modulus. In addition, the gas permeability results showed a 1.5–2.2 times increase for 7 wt% filled HPI precursors and also 4.4–15.1times increase for 7 wt% filled PBOs, compared to neat HPIs (Fig. 50).

4.2.4. Polyurethanes

Other types of polymers with rubbery behavior are polyurethanes (PUs), which extensively have been used for gas separation. They consist of two segments at the micro phase level. One is a soft segment consisting of diols that can be made of a polyester or polyether to provide flexible chain structures for good gas permeability. The other one is a hard segment, which is formed by extension reaction of a terminal diisocyanate group with a low molecular weight diol. In brief, the glassy segments form a constructional framework which provides mechanical strength for PU polymers. Since the rubbery segments normally conform continuous microdomains and the gas transport is allowed by the flexible chain structure, they provide a good permeability [47,365].

PUs are one of the important categories of specific polymers and are employed to prepare different kinds of membranes. High thermal stability, chemical resistance, mechanical strength, wear resistance, fine gas permeability, good elasticity and good oil resistance are properties of PUs, which make them ideal for membrane separation performance [366,367]. PU membranes are used for separation of various gas mixtures consisting of both polar/non-polar components [47].

The structure of hard segment [368–371] and chain extender type [372,373], the type of polyol [374] and its molecular weight [375] have effects on membrane separation performances, which have been studied by many different investigators. On the other hand, incorporating nanoparticles as filler into PU matrix for MMM fabrications could improve the membrane selectivity [367,376].

Sadeghi et al. [377] studied the effect of surface functionalized groups on filer dispersion control in hard/soft segments of a PU polymer. In this way, three different MMMs were fabricated by embedding the cyanuric chloride and its derivatives, melamine, and 2,4,6-trihydazino-1,3,5-triazine (THDT) nanoparticles into the PU matrix. Results revealed that cyanuric chloride was distributed in the hard segments of PU, while melamine and the THDT were dispersed in the soft domains. Fig. 51 presents the fillers dispersion in the PU chains, and also possible hydrogen bonds between the polymer backbone and nanoparticles. As can be seen, cyanuric chlorides create hydrogen bonds with hard segments of PU (urethane amine groups). On the other hand, NH-functionalized fillers (melamine and THDT) are willing to disperse in the soft segment of PU (ethereal groups). Finally, the best performance MMM was PU-THDT (10 wt%) with CO_2 permeability, CO_2/N_2 and CO_2/CH_4 selectivities of 87.9 Barrer, 46.3 and 12.4, respectively.

Rodrigues et al. [378] investigated the effect of synthesized UiO-66 (Zr) and MIL-101 (Cr) on structure and gas permeation properties of PU membrane. PU/UiO-66 (Zr) (28 wt%) revealed the CO_2 permeability of 75.2 Barrer and CO_2/N_2 selectivity of 34.2. On the other hand, the permselectivity of PU/MIL-101 (Cr) (28 wt%) were about 83.1 Barrer and 42.4. Fig. 52 depicts the SEM images of synthesized fillers and PU based MMMs. In the case of UiO-66 (Zr), a well-defined tetrahedral structure with crystals size ranged from 1 to 5 μm was achieved (Fig. 52a). But in the case of MIL-101 (Cr), well-defined/uniform rhombohedra structures were obtained (Fig. 52b). Filler/polymer interface of fabricated MMMs are shown in Fig. 52c and d. As can be seen, there is a very good interfacial adhesion between polymer and filler, especially in the case of MMM which contains the MIL-101 (Cr). EDS analysis of MMMs also indicated that MIL-101 (Cr) was more efficiently dispersed in PU polymer matrix, compared with UiO-66 (Zr). Results which demonstrated the metal (Cr) content also indicated that the various regions in PU/MIL-101 (Cr) (28 wt%) had a similar composition.

4.2.5. Ionic liquids/poly ionic liquids

A salt with an organic cation mixed with an inorganic or organic anion is known as ionic liquid (IL). High thermal and chemical stability, low vapor pressure, non-flammability, nontoxicity, low volatility, low melting point, tunable physicochemical

Table 8
Different advanced polymer-based MMMs performances for CO_2 separation.

Filler	Polymer	wt.% loading (best MMM performance)	Test conditions	P_{CO2} (Barrer)	CO_2/CH_4 selectivity	CO_2/N_2 selectivity	CO_2/H_2 selectivity	Ref.
POSS	PIM-1	2	298 K	6730	12	13	–	[409]
		10		1562	17	19	–	
HCP-Polystyrene	PIM-1(ethanol treated)	5.7		12,500	–	12.5	–	[336]
		16.67		16,000	–	12	–	
		21.3		20,000	–	9.5	–	
PAO-PIM-1	NH_2-UiO-66	0	35 °C, 1 bar	2902	24.0	28.0	–	[338]
		7		3825	24.3	30.0	–	
		15		4832	22.9	28.9	–	
		30		8425	23.0	27.5	–	
PAO-PIM-1	UiO-66	30	35 °C, 1 bar	8126	18.4	22.5	–	[338]
PIM-1	NH_2-UiO-66	30	35 °C, 1 bar	9420	12.3	15.6	–	[338]
PEG functionalized MWCNT	PIM	0.5	30 °C	7535	10.8	23.9	–	[332]
		1		7813	9.9	18.7	–	
		(2)		12,274	8.3	17.2	–	
		3		4816	16.3	22.2	–	
g-C_3N_4 nanosheets	PIM-1	0.5	30 °C, 2 bar	3946	12.4	19.9	–	[331]
		(1)		5785	11.5	16.3	–	
		1.5		4062	11.7	15.6	–	
		2		3381	14.4	19.8	–	
Graphene	PIM-1	0.00096	25 °C, 1 bar	12,700	8.76	15.60	–	[325]
		0.0018		9840	12.30	17.26	–	
		0.0034		7830	14.24	19.10	–	
		0.0071		3410	21.31	20.06	–	
UiO-66	PIM-1	5	298 K,	5340	–	20	–	[333]
Ti Exchanged UiO-66		5	1 atm	13,540	–	24	–	
MOF-74	PIM-1	0	25 °C, 2 bar	6576	12.3	18.7	–	[410]
		10		9400	14.3	21.2	–	
		15		15,064	17.4	29.5	–	
		20		21,269	19.1	28.7	–	
BILP-101	PIM-1	0	40 °C	4700	–	19.3	–	[411]
		17		6300	–	15.1	–	
		(30)		7200	–	15.3	–	
		40		5100	–	17.4	–	
ZIF-71	PIM-1	0	35C,	3294.7	10.2	20.1	–	[334]
		10	3.5 atm	4271.0	11.3	19.4	–	
		20		5942.0	11.9	20.0	–	
		30		8377.1	11.2	18.3	–	
ZIF-71	PIM-1, UV treated	0	35 °C,	1233.2	34.1	29.8	–	[334]
		10	3.5 atm	1909.3	35.5	29.1	–	
		20		2545.7	35.3	27.2	–	
		30		3458.6	35.6	26.9	–	
NDPC	PIM-1/ILs	–	35 °C, 2 atm	31,807	–	14.1	–	[412]
UiO-66-NH_2	PIM-1	20	25 °C, 2 bar	12,498	31.9	54.2	–	[413]
GO	PIM-1	20	30 °C, 4 bar	6169	–	123.5	–	[414]
GO-ODA	PIM-1	0.05	25 °C, 3 bar	3000	23.7	–	–	[415]
rGO-ODA		0.05		2400	29.1			
rGO-OA		0.05		3500	22.4			
NH_2-MIL-53(Al)	PIM-1/Matrimid	25	25 °C, 2 bar	4390	–	25.0	–	[416]
ZIF-94(Zn)		25		3730		27.1		
UiO-66-NH_2	PIM-1	5	25 °C, 4 bar	2952	27.3	26.9	–	[417]
ZIF-71	6FDA–Durene	5	35 °C	472	–	–	–	[418]
	TAEA vapor cross-linked	10		540	–	–	–	
		20		581	–	–	–	
ZIF-8	PI	7	35 °C	560	27	20	–	[349]
		20		896	21	16	–	
		30		1437	16	12	–	
ZIF-8@PD	PI	7	35 °C	380	25	19	–	[349]
		20		702	23	18	–	
		30		1056	20	14	–	
Ni_2(dobdc)	6FDA-durene	21	35 °C, 1 bar	1035	12.3	–	–	[154]
Modified Si	6FDA-durene	6.3	Room T,	1783	26	29	–	[351]
		8.7	2 bar	1967	28	29	–	
		11.7		2439	34	30	–	
		21.0		3293	43	31	–	
		30.5		3785	46	31	–	

(*continued on next page*)

Table 8 (*continued*)

Filler	Polymer	wt.% loading (best MMM performance)	Test conditions	P_{CO2} (Barrer)	CO_2/CH_4 selectivity	CO_2/N_2 selectivity	CO_2/H_2 selectivity	Ref.
ZIF-8	6FDA-durene	0	30 °C,	468.01	7.03	–	–	[419]
		5	3.5 bar	693.54	16.54	–	–	
ZIF-8	6FDA-durene	3	2 bar	1593.4	21.9	25.7	–	[350]
		5		1695.0	20.1	22.7	–	
		7		1773.5	19.4	22.1	–	
		10		1881.7	19.0	20.5	–	
		15		1940.4	18.1	18.6	–	
		20		2027.6	16.9	17.5	–	
		30		2185.5	17.1	17.0	–	
ZIF-71	6FDA-durene	0	35 °C,	959	16.4	14.7	–	[348]
		10	3.5 atm	1805	16.1	14.9	–	
		20		4006	12.8	12.9	–	
		30		7750	9.53	11.5	–	
Mg-MS	6FDA-DAM	8	35 °C 200 kPa	1245	31.5	24.4	–	[352]
MOP-15	6FDA–DAM	1.6	25 °C, 1 bar	1413	–	26.7	–	[420]
Mg_2(dobdc)	6FDA-durene	51	35 °C, 1 bar	157	–	28	–	[421]
		27		179	18	–		
ZMOF	6FDA-DAM	20	35 °C, 3.5 bar	1512	30	–	–	[422]
MFM-300(Al)	6FDADurene-DABA	25	30 °C, 0.75 bar	911	30	–	–	[423]
ZIF-8	6FDA-bisP	15	25 °C, 5 bar	81.2	35	–	–	[424]
ZIF-94	6FDA–DAM	40	25 °C, 1 bar	2310	–	22	–	[425]
ZIF-L	PI	2	Room T, 1 bar	119.2	37.8	21.4	–	[426]
UiO-66	6FDA-BisP	17	35 °C, 2 bar	108	41.9	–	–	[355]
	6FDA-ODA	7		43.3	57			
	6FDA-DAM	8		1728	32			
MIL-96(Al)	6FDA–DAM	25	25 °C, 2 bar	1052	–	26	–	[427]
$Cu_3(BTC)_2$	6FDA/TMPDA	20	35 °C, 3.5 bar	1560	18.76	–	–	[428]
MWCNT	TR-BPOI(HD5 precursor)	0	35 °C, 7 bar	105	23.8	11.4	–	[362]
		0.5		126	25.8	13.6	–	
Al_2O_3	BDO-based PU	0	10 atm	135.12	7.77	25.84	–	[429]
		2.5		123	8.97	35.04	–	
		5		110	11.58	40.74	–	
		10		96.6	14.53	47.82	–	
		20		85.5	18.08	52.45	–	
Al_2O_3		30		78.28	19.82	61.64	–	
	MPD-based PU	0		120.6	8.18	27.1	–	
		2.5		111	10	38.27	–	
		5		100.2	12.51	47.71	–	
		10		88.35	15.61	49.92	–	
		20		81.13	20.44	58.79	–	
		30		74.67	23.48	67.88	–	
epoxy	PU	0	25 °C,	186.5	9.6	25.0	–	[430]
		10	10 bar	165.0	16.3	55.5	–	
		20		134.0	16.4	60.1	–	
		30		109.0	15.8	62.3	–	
Silica	PDMS-PU	0	25 °C,	68.4	5.1	22.0	–	[366]
		1	10 bar	72.0	5.8	25.7	–	
		2		75.0	6.4	34.0	–	
		5		84.3	8.3	44.3	–	
		10		96.7	10.6	64.4	–	
Silica	PU	0	20 °C,	86.27	15.40	34.10	–	[431]
		2.5	10 bar	66.76	18.44	42.79	–	
		5		62.11	17.49	45.00	–	
		10		59.12	18.30	45.47	–	
		20		53.58	18.60	54.12	–	
		30		41.27	19.11	62.53	–	
NiO	PU	5	30 °C, 1 bar	321	24.76	67.72	–	[432]
MWCNT-TEPA	PU	10	35 °C, 5 bar	396.5	7.0	–	–	[433]
ZSM 5	PU	15.64	30 °C, 4 bar	164.7	7.8	20.6	–	[434]
Silica/Pluronic-PVA	PU	10	25 °C, 10 bar	64.7	7.7	91.4	–	[435]
SAPO-34	PU	20		28.71	25.63	58.59	–	[436]

(*continued on next page*)

Table 8 (*continued*)

Filler	Polymer	wt.% loading (best MMM performance)	Test conditions	P_{CO2} (Barrer)	CO_2/CH_4 selectivity	CO_2/N_2 selectivity	CO_2/H_2 selectivity	Ref.
			Room T, 12 bar					
SAPO-34	[C_2mim][Tf_2N]	10		477	19	35	–	[437]
	poly(RTIL)	10		13.9	35	35	–	
	poly(RTIL)–[C_2mim][Tf_2N]	10		72	30	44	–	
[emim][TF_2N] @SAPO-34	PSf	0.361–5	Room T	7.24GPU	20.4	18.8	–	[391]
([bmim][Tf_2N])@ZIF-8	PSf	6	30 °C, 6 bar	300*	39*	–	–	[438]
ZIF-8	P[vbim][NTf_2]/[emim][NTf_2]	0	35 °C, 3.5 bar	300.1	14.8	23.6	–	[439]
		9.9		367.1	13.0	21.1	–	
		18.8		623.2	13.0	20.4	–	
		23.7		693.6	12.1	19.6	–	
ZIF-8	P[vbim][NTf_2]/[emim][$B(CN)_4$]	0	35 °C, 3.5 bar	365.4	15.8	29.9	–	[439]
		9.9		734.9	14.4	28.2	–	
		20.0		907.4	13.7	25.0	–	
		25.8		1062.4	12.3	24.2	–	
ZIF-8	P[vbim][NTf_2]/[emim][BF_4]	0	35 °C, 3.5 bar	233.2	17.1	30.7	–	[439]
		10.1		241.3	16.4	31.3	–	
		19.7		294.1	16.5	28.8	–	
		26.4		340.0	16.6	29.1	–	
Ag nanoparticles	([bmim][BF_4])/ Pebax1657	0.5Ag/50IL	35 °C 10 bar	180	61.0	187.5	–	[398]
[C_3NH_2bim][Tf_2N]@ NH_2-MIL-101(Cr)	PIM-1	5	298 K, 3 bar	2979	–	37	–	[395]
[emim][Tf_2N]-SAPO-34	poly([smim][Tf_2N])	16–20	25 °C, 2 atm	155	74	–	–	[401]
		20–30		260	90	–	–	
		30–40		680	38	–	–	
[bmim][Tf_2N]@ZIF-8	Pebax1675	15	25 °C, 1 bar	104.9	34.8	83.9	–	[394]
ZIF-8	[emim][Ac]/CS	10	50 °C, 2 bar	5413	–	11.5	–	[390]
HKUST-1	[emim][Ac]/CS	5	50 °C, 2 bar	4754	–	19.3	–	[390]
[EMIM][BF_4]-GO	Pebax-1657	0.5	35 °C, 3 bar	642 GPU	–	34	–	[440]
[emim][Tf_2N]-hexylamine functionalized SAPO-34	PES	20	Room T, 4 bar	0.033 GPU	37.23			[441]
[APTMS][Ac]@zeolite 4A	PSf	20	25 °C, 10 bar	11	30	34.3	–	[442]
Silica	IXPE (poly(ionic liquid)s and poly(trimethylene ether)glycol (PTMEG)	30	25 °C, 2.5 bar	121.6	–	42.4	–	[443]
CHA zeolite	PTMSP	5	333 K, 2.5 bar	22,914	–	6.2	–	[93]
LTA5 zeolite		5		27,294	–	5.4	–	
Rho zeolite		5		64,920	–	5.1	–	
Zeolite A		5		112,627	–	4.9	–	
GO	PTMSP	0	30 °C	21,000*	2.5*	5.3*	–	[407]
IND G		1		22,000	2.3	5.2	–	
M60		1		18,000	2.7	5.6	–	
		1		19,000	2.2	5.1	–	
PAF-1	PTMSP	10	298 K, 1 atm	28,400			–	[403]
PAF-1-NH2				35,100			–	
PAF-1-SO3H				32,400			–	
PAF-1-C60				25,800			–	
PAF-1-Li6C60				50,600			–	

* Values are approximated from plots.

characteristics and high selectivity are special features of ILs, which make them suitable materials for separation processes [379–381]. Combining different cations and anions or adding functional groups in ILs will provide electrical charges which make a desirable interaction with CO_2 molecules due to quadrupole moment characteristic of CO_2 [382]. Combining the effects of ILs with the inorganic fillers in the MMMs induces a synergistic effect on gas separation performance of polymer matrices [379,383]. The first approach is to immobilize ILs in membrane to enable facilitated transport of CO_2 through the membrane [384,385]. Semi-solid IL gel membrane is another form of IL based membranes. This kind of membrane is provided by a large amount of IL filled in an interlaced network formed by chemical cross-linking of polymers such as polymeric ILs (PILs) [386]. Polymerization of IL monomers and chemical modification of available polymers are two methods to produce PILs which have the polymer properties and also ILs characteristics [379].

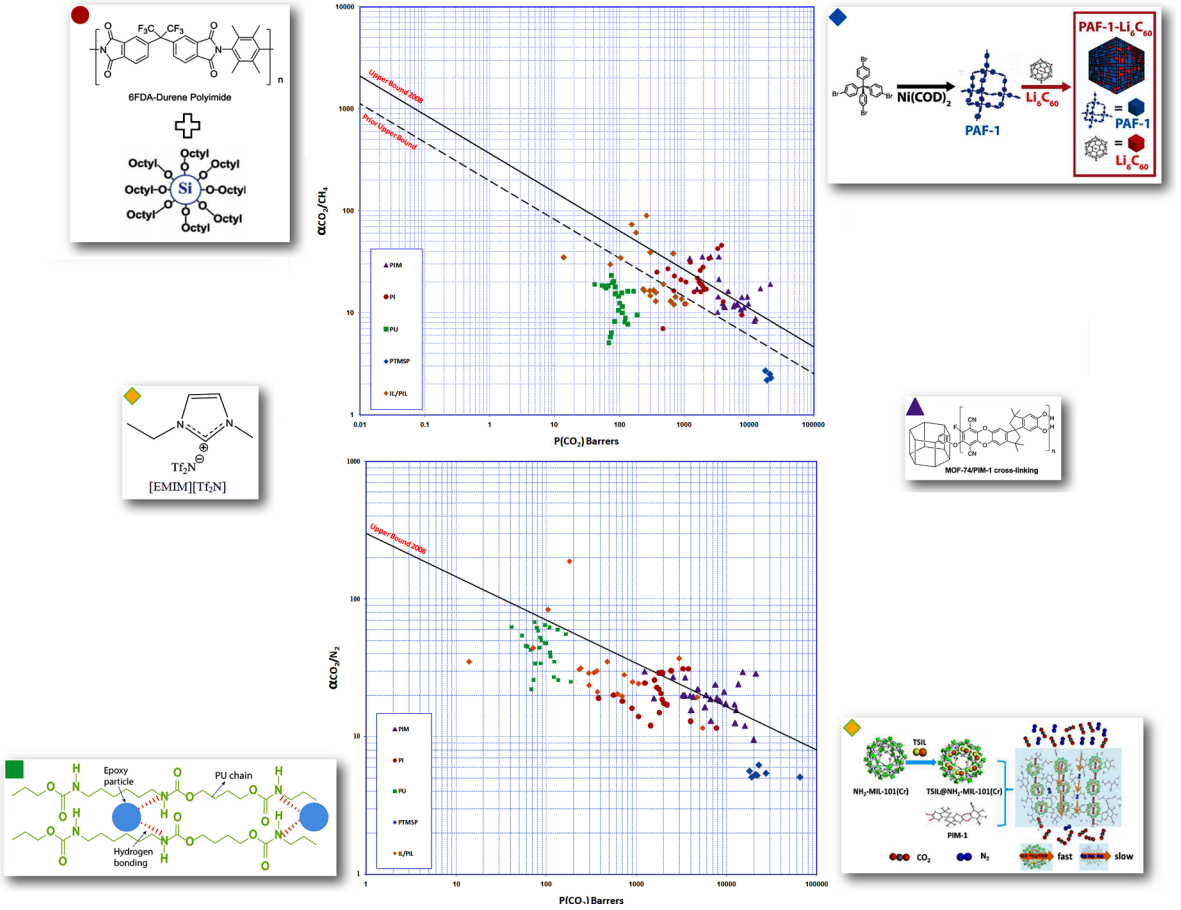

Fig. 59. Robeson's upper bound limit for CO_2/CH_4 and CO_2/N_2 separation and various polymeric MMMs performances. The chemical structures of the best performance MMMs containing PIM [410], PI [351], PU [430], PTMSP [403], IL/PIL [395,401] are magnified. (Copyright year. Reproduced with permission from All Publishers.)

Room temperature ionic liquids (RTILs) and task specific ionic liquids (TSILs) are two categories of ionic liquids. In RTILs known as conventional ILs, the solubility of gases will increase with increase in the pressure. TSILs can be provided by modification of cations or anions with proper functional groups and are capable of absorbing CO_2 at lower pressure by chemical reaction [387]. In brief, the RTILs are used to capture CO_2 in the spaces between ions (physical adsorption) and the TSILs are used to increase the overall absorption capacity by chemical reactions [382]. The main purpose of using ionic liquids as functional materials is designing and creating new polymer materials with incomparable improvements in their physical properties [388–393].

Li et al. [394] presented a new strategy to form toughened MOF-polymer linkages by introducing an RTIL, 1-butyl-3-methylimidazolium bis (trifluoromethylsulfonyl) imide ([bmim][Tf_2N]), into ZIF-8. The results showed remarkable improvement in IL@ZIF-8/Pebax membrane performances and molecular sieving properties of the MMMs. This was due to the better filler/polymer compatibility and the reduction in effective pore size of ZIF-8 (Fig. 53).

Ma et al. [395] provided a size selective and CO_2-carrier containing nano-porous composite material by adding an TSIL, N-aminopropyil-3-butyl imidazolium bis (trifluoromethyl -sulfonyl)imide ([C_3NH_2bim][Tf_2N]), into an MOF, the NH_2-MIL-101(Cr). The TSIL@NH_2-MIL-101(Cr)/PIM-1 membrane showed 116% and 119% enhancements in CO_2/N_2 separation selectivities compared to NH_2-MIL101(Cr)/PIM-1 and PIM-1 membranes, respectively. This increase in selectivity is due to more amine functional groups available in TSIL@NH_2-MIL-101(Cr). Also loading of the TSIL into NH_2-MIL101(Cr) led to better dispersion of the TSIL in polymeric matrix (Fig. 54).

In another investigation, Mohshim et al. [396] fabricated PES membranes with different imidazolium-based ionic liquids via a dry-phase inversion method. They found membranes with addition of emim[Tf_2N] resulted in higher CO_2 permeation. It was also noticed that membranes with emim[CF_3SO_3] offered higher CO_2/CH_4 selectivity. While emim[Tf_2N] enhanced permeation of both CO_2 and CH_4, the emim[CF_3SO_3] increased only CO_2 permeation significantly.

McDonald et al. [397] used organic ionic plastic crystals (OIPCs) to fabricate MMMs for separation of light gases such as CO_2. OIPCs are a subclass of plastic crystals having structures as ILs. They prepared membranes by incorporating methyl(diethyl)isobutylphosphonium hexafluorophosphate ([P_{122i4}][PF_6]) and N-methyl-N-ethylpyrrolidinium tetrafluoroborate ([C_2mpyr][BF_4]) as

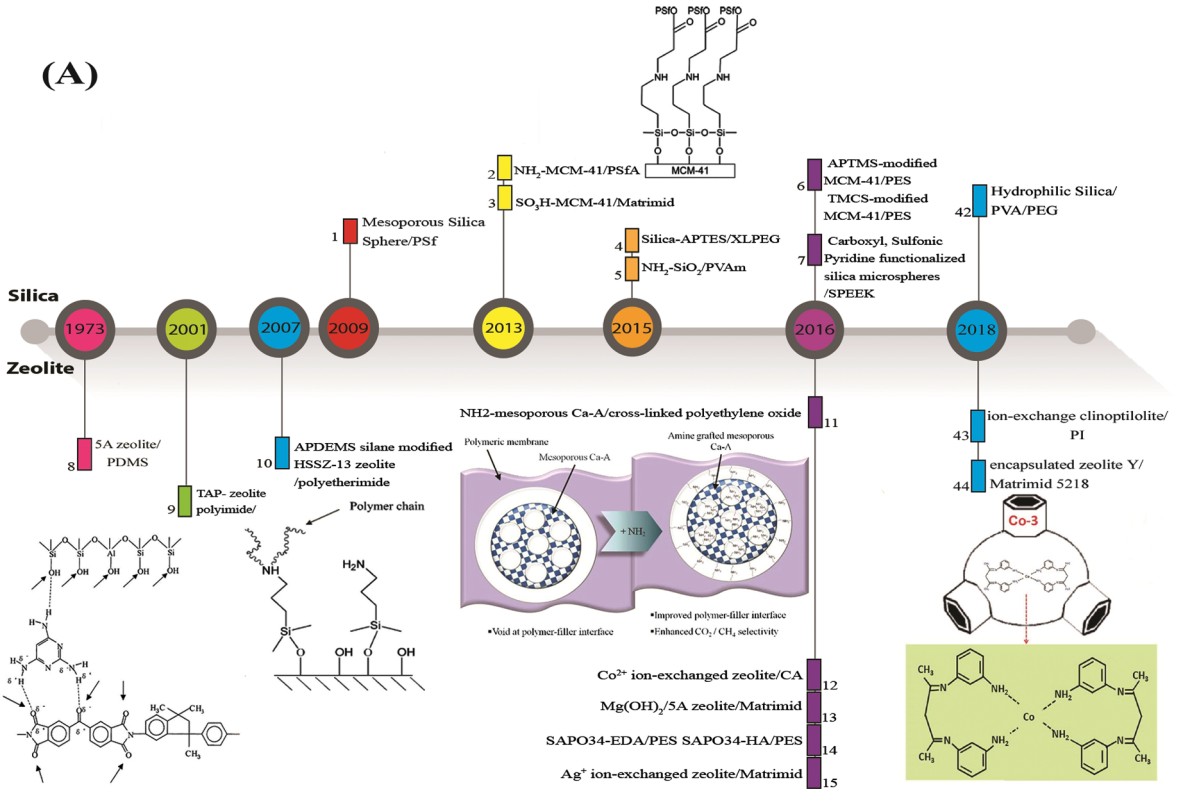

Fig. 60. Timeline of career achievement/research output of advanced functionalized fillers employed for MMMs (A) Silica 1 [445] 2 [104] 3 [106] 4 [111] 5 [113] 6 [107] 7 [110] 42 [121], Zeolite 8 [21] 9 [446] 10 [447] 11 [94] 12 [88] 13 [85] 14 [92] 15 [87] 43 [89] 44 [309], (B) ZIF 16 [448] 17 [203] 18 [208] 19 [207] 45 [303] 46 [304], MOF 20 [449] 21 [450] 22 [157] 23 [137] 24 [141] 25 [152] 26 [151] 47 [296], (C) COF 27 [403] 28 [222] 29 [227] 30 [229] 48 [230], (D) Graphene 31 [244] 32 [407] 33 [243] 34 [232] 35 [245] 49 [250], CNT 36 [451] 37 [452] 38 [261] 39 [265] 40 [264] 41 [266] 50 [273]. (Copyright year. Reproduced with permission from All Publishers.)

OIPC into PVDF polymer. The gas separation results exhibited that OIPC/PVDF MMMs have an excellent characteristic with CO_2/N_2 ideal selectivity of about 30.

Ghasemi Estahbanati et al. [398] prepared novel ternary MMMs by adding 1-Butyl-3-methylimidazolium tetrafluoroborate ([bmim][BF_4]) ionic liquid to silver nanoparticles/Pebax1657 membranes. The filler/polymer interface was improved by using the IL, which removes the non-selective voids and makes a selective layer around Ag particles for CO_2 separation (Fig. 55). The gas permeation results of ternary MMM (Pebax 1657/0.5%Ag/50%IL) showed an increment in CO_2 permeability (from 110 Barrer to 180), CO_2/CH_4 selectivity (from 20.8 to 61.0) and CO_2/N_2 selectivity (from 78.6 to 187.5) compared to the neat membrane.

Ahmad et al. [399] used the 1-butyl-3-methylimidazolium acetate ([bmim][Ac]) to functionalize PSf/SAPO-34 zeolite interface and prepared an asymmetric MMM. Indeed, after fabrication of PSf/SAPO-34 MMMs, the prepared MMMs were post-impregnated by immersing in acetate-based IL solution with various IL concentrations. Results achieved by EDX spectra and FTIR analysis confirmed that the IL was effectively incorporated into MMM. Fig. 56 illustrates the effect of post-impregnation method on morphology of prepared membranes. As can be seen, non-selective voids appear in unmodified MMM, which indicates the poor adhesion between filler/polymer interfaces. However, IL-modified MMMs revealed excellent interfacial adhesion without any voids. Indeed, due to the hydrophilic nature of [bmim][Ac], it could be simply attached on the hydrophilic surface of PSf/SP5 MMM, confirmed by water contact angle about 70.7°. In othe words, cations of IL could be attached to the negative charged surface of SAPO-34 and improves the polymer/filler interface. The best performance MMM containing 5 wt% SAPO-34 with the post-treatment in 3.95 wt% IL solution, exhibited the CO_2 permeance of 1.98 GPU and CO_2/N_2 selectivity 39.60.

In some recent investigations for MMM fabrication, RTILs were loaded in polyRTILs matrix [400–402]. PolyRTIL/RTIL composite membranes have good stability due to the Coulombic attraction between non-polymerizable IL and polyRTIL matrix [385]. Cowan et al. [402] prepared high-performance PIL/IL/zeolite ion gel MMMs and found that the tailored MMMs have high gas separation performance with ideal CO_2 permeability of about 261 Barrer and CO_2/CH_4 selectivity of about 93. They investigated the defects encountered in development of MMMs (Fig. 57) and explained the methods to remove these defects.

4.2.6. Substituted polyacetylenes

Microporous organic polymers (MOPs) are the new advanced classes of materials for gas storage and separation applications. Polyacetylenes is one of the most well-known MOPs families. Polymerization of acetylenic monomers by the use of transition metal

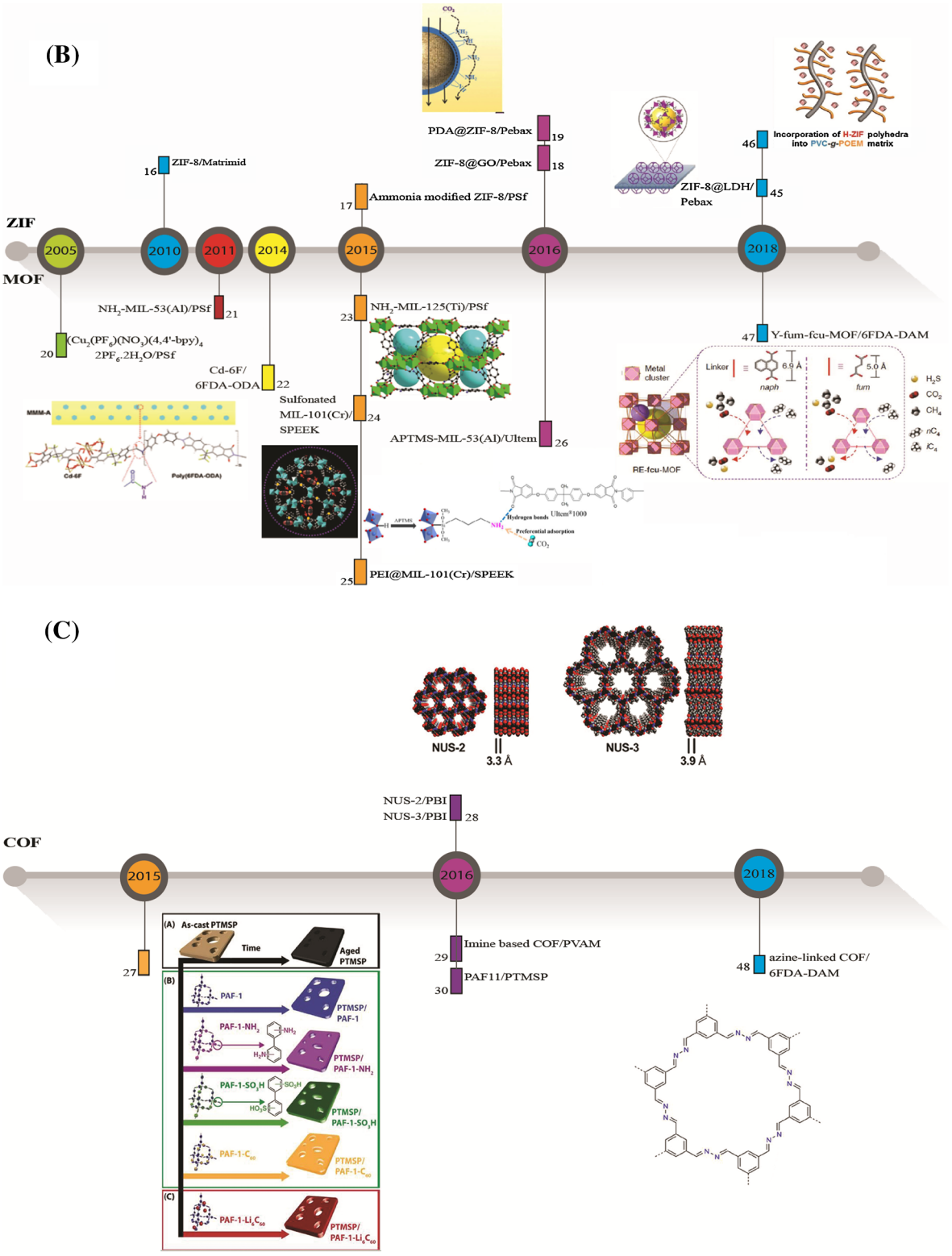

Fig. 60. (*continued*)

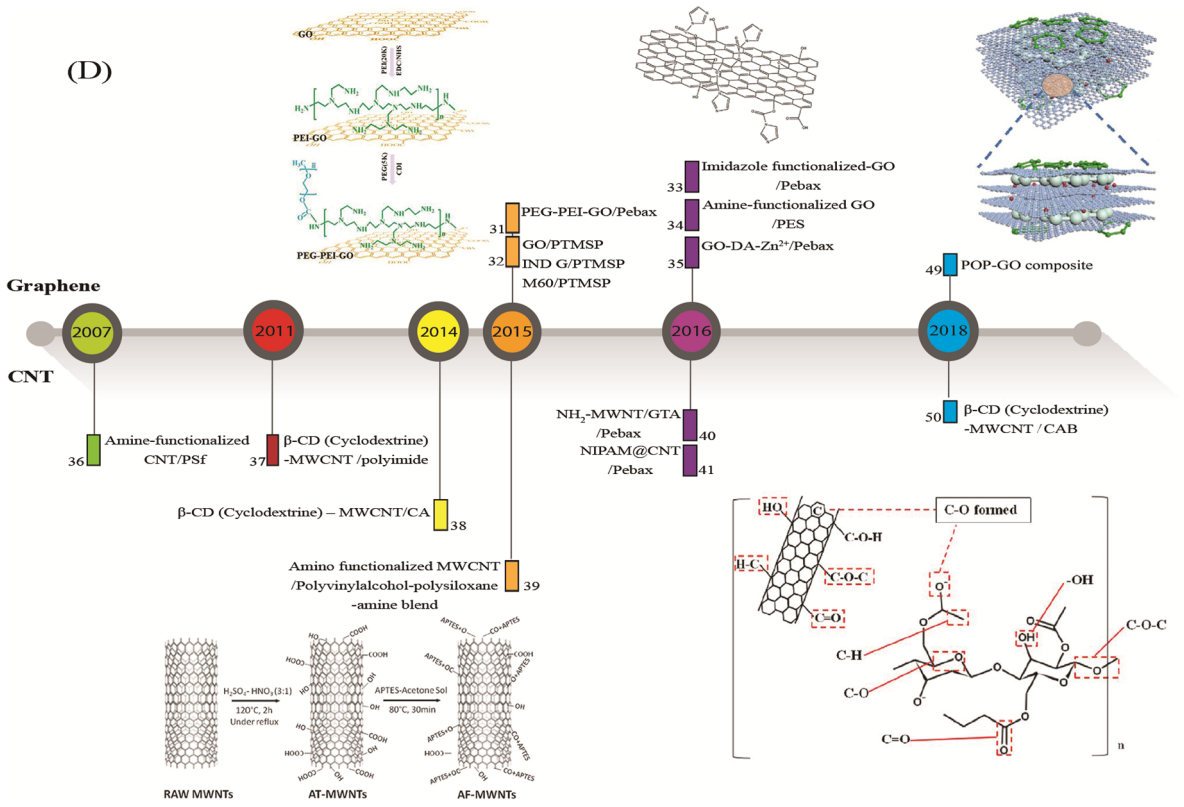

Fig. 60. (*continued*)

catalysts resulted in production of the substituted polyacetylenes, the highly permeable polymers which contain different molecular scale voids, formed by the presence of bulky pendant groups [1,333].

Substituted polyacetylenes have high permeability and low selectivity. Excessive aging problem in polyacetylenes is a substantial challenge that hinders their application in large scale. Polyacetylene-based membranes have high CO_2 permeability but are not suitable for CO_2 separations due to their high physical aging and poor selectivity [1,403]. Poly(1-trimethylsilyl-1-propyne) (PTMSP) is known as the highest gas-permeable polymer among MOPs. PTMSP is a convenient material for high temperature membrane separations. As already mentioned, the problem is loss of permselectivity with time because of physical aging and CO_2 plasticization [404].

Many efforts have been made to obtain long lasting and stable MOP membranes such as cross-linking, substitution of functional groups, blending, reversing aging by methanol treatment and fabricating mixed matrix membranes (MMMs) [405,406]. Proper selection of inorganic fillers such as zeolites, graphene and graphene oxide could increase membrane selectivity with no serious challenges [93,407]. Fernandez et al. [93] successfully performed this modification technique. They put small-pore zeolites of various topologies, all with silica to aluminum ratio of 5, into highly permeable PTMSP in order to enhance its selectivity, thermal stability and mechanical strength. The MMMs charged with 5 wt% zeolite surpassed the Robeson's upper bound for CO_2/N_2 separation, without significant reduction in the permeability.

In a recent work, Fernández-Barquín et al. [408] evaluated the water vapor effect on CO_2 separation properties of MMM comprising the hydrophilic porous filler into the hydrophobic polymer. The relative humidity (R. H.) ranged from range 0–75% was considered on the performance of PTMSP/zeolite 4A (20 wt%). Results of this work demonstrated that the gas permeability of CO_2, CH_4 and N_2 gases declined in PTMSP membrane at 50% R. H. However, in the case of MMMs, CO_2 permeability increased about 10% in comparison with dry state and CH_4 and N_2 permeabilities were decreased. The result may be attributed to increase in the rigidity and decrease in free volume of MMM compared to pristine one. This also confirmed by the adsorption test which the presence of water could not directly affect the CO_2 adsorption on zeolite 4A, while this was also in contrary for CH_4 and N_2. Fig. 58 depicts the permeability variation of gases in terms of relative humidity. As can be seen, the best state was achieved at 50% R.H. in which the CO_2 permeability was 9570 Barrer with the CO_2/N_2 and CO_2/CH_4 selectivities were about 30 and 4.8, respectively.

The values of permeability and selectivity recently reported for different advanced polymer-based MMMs are summarized in Table 8. In addition, these values are compared to the Robeson's upper bound in Fig. 59.

5. Future outlooks and conclusions

BACKGROUND: Development of mixed matrix membranes (MMMs) for CO_2 separation is recognized as a broad area of research.

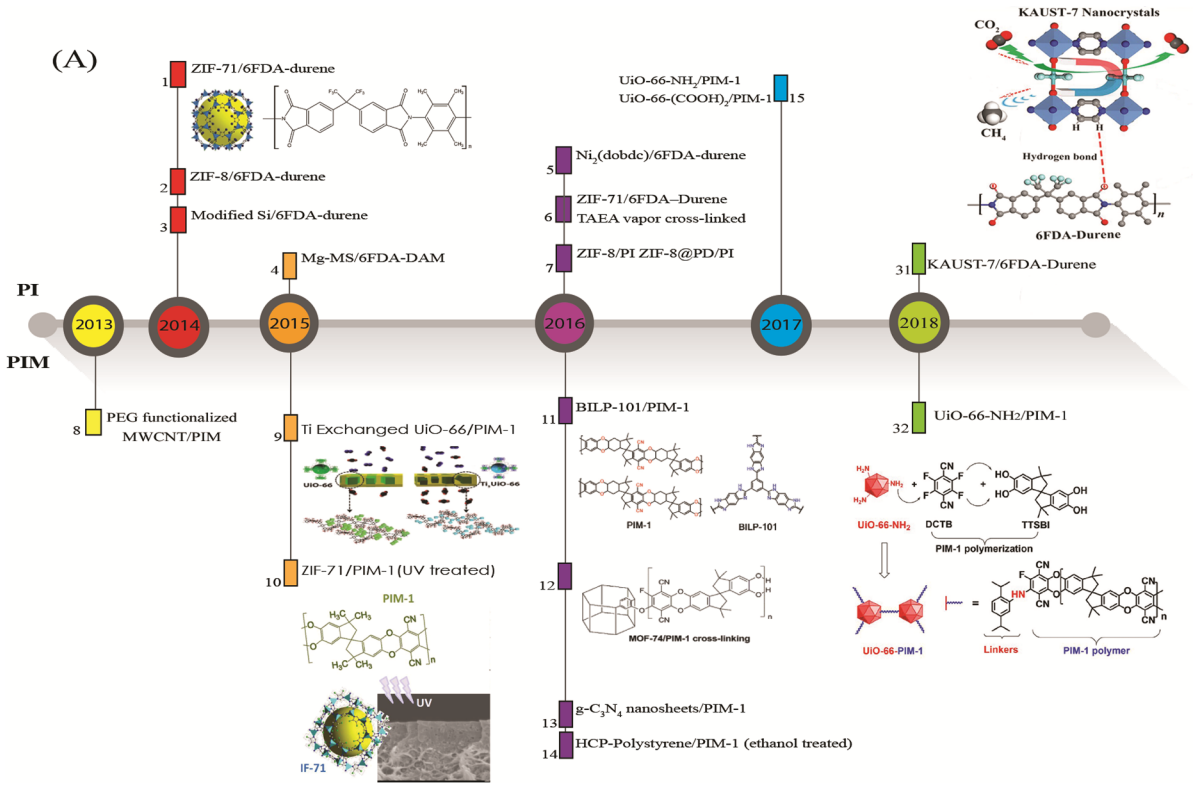

Fig. 61. Timeline of career achievement/research output of advanced functionalized polymers employed for MMMs (A) PI 1 [348] 2 [350] 3 [351] 4 [352] 5 [154] 6 [418] 7 [349] 31 [354], PIM 8 [332] 9 [333] 10 [334] 11 [411] 12 [410] 13 [331] 14 [336] 15 [328] 32 [413], (B) PU 16 [431] 17 [366] 18 [429] 19 [430] 33 [377], PTMSP 20 [407] 21 [403] 22 [93], (C) IL/PIL 23 [437] 24 [390] 25 [398] 26 [453] 27 [439] 28 [394] 29 [401] 30 [395] 34 [440] 35 [399]. (Copyright year. Reproduced with permission from All Publishers.)

MMMs used for gas separation are normally comprised of different inorganic/organic fillers embedded into the polymer matrix with the final aim of passing the Robeson's trade-off boundary. Different researches have already been carried out for combination of different fillers and different kinds of polymers. Inorganic fillers with define pore sizes will increase the transport of gas molecules and as a result to enhance the overall selectivity. One of the most important aspects in the development of MMMs is an appropriate material selection for both the matrix and sieve phases. Interfacial adhesion, dispersed phase agglomeration and stress formation are very important unsolved problems to be considered. The existence of filler particles will vary the dynamic structure, the composition of polymer chains close to its surface and the diffusion of large molecules as compared to the smaller ones. Poor dispersion of inorganic fillers causes agglomeration and sedimentation of particles in the polymer matrix. Particle accumulation due to the difference in physico-chemical properties such as density and polarity between filler and polymer leads to solid sedimentation or migration to the surface, which are the most serious challenges for the MMM fabrication. To have an impact on real commercial applications, successful MMMs are necessary to optimize multiple functions in addition to pore structure and surface area of the filler. The processability, stability, sorption kinetics, mechanical and thermal properties will together affect the economics of MMM applications. Therefore, it remains as a challenge to select an appropriate type of porous material for a given purpose. Until now many researches have been devoted to implementation of conventional fillers and polymers in MMM preparation and their modification [8,24–27,58,444]. Particularly, surface and structural modifications of the fillers are important since the surface and interfacial properties of the filler can strongly affect the final performance of membrane in many applications. Up to now, different techniques have been attempted for filler modifications in respect to the MMM developments. To see which technique has given the best results, comparing their gas separation performances would be more effective. On the other hand, copolymerization, blending, grafting, cross-linking and some other methods were tried to produce new polymer matrices in order to overcome swelling, plasticization and other polymer challenges. Finding new fillers, knowing the filler size effect, finding new coupling agents, and exploring different MMM formation methods are some of the main key factors that must be considered in rational MMM designs.

ADVANCES: Although, during the long years of using MMMs for CO_2 separation, various kinds of conventional porous/dense materials have the largest contribution, but many developments have rapidly emerged over the past five years. These improvements include the extensive use of a wide range of functionalized materials which are inexorably entered the scene to substantially promote the separation performance. Today, the range of functions that can be expected for the porous materials is much broader than before. This may be in part ascribed to the prompt progresses made in computing capacity to design and propose new functions/structures, which encourages the emergence of a new way to correctly identifying the best material for the specific gas separation targets. The

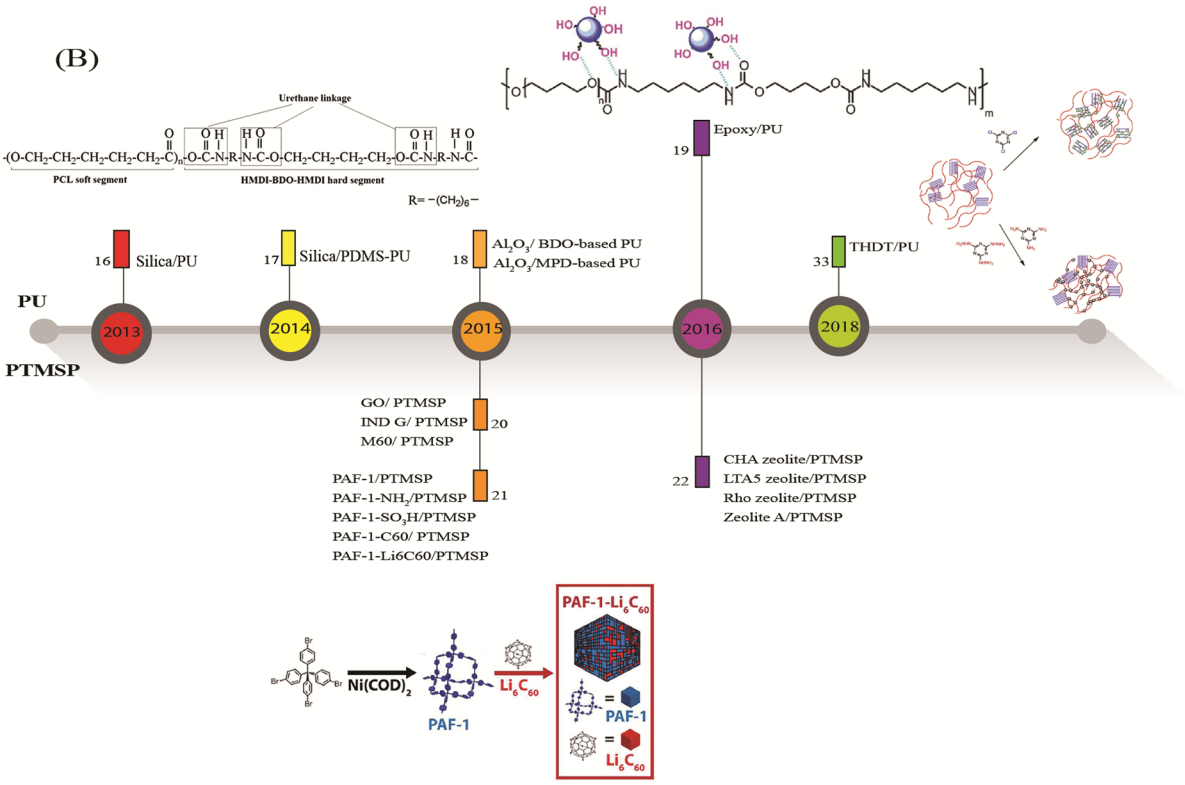

Fig. 61. (*continued*)

functionalized filler materials include functionalized zeolites, silica, metal-organic frameworks (MOFs), zeolitic imidazolate frameworks (ZIFs), covalent organic frameworks (COFs), graphene and carbon nanotubes (CNTs). In addition to these newly emerging fillers, other classes of novel advanced functionalized materials have been proposed in the recent years, such as polymers of intrinsic microporosity (PIMs), polyimides, polyurethanes, microporous organic polymers (MOPs) and ionic liquids/poly ionic liquids. Figs. 60 and 61 depict the timeline of career achievement/research output of advanced functionalized materials employed for MMMs. Many recently, some new emerging materials with engineering the structures or molecular designing of the combined inorganic/organic materials have been gradually grown that is expected the future perspective of researches in MMM materials will be dedicated to them. Some of the proposed materials with outstanding gas sorption and physic-chemical properties are: the new two dimensional mono-elemental crystals like silicene, germanene, stanene, and phosphorene (2D-Xenes), transition metal carbides and nitrides (MXenes), co-synthesized advanced particles (like ZIF-8@GO), innovative organometallic nano-structures (like coordinated ligands, porous coordination polymers (PCPs), ion-loaded macromolecules, metal organic polyhedra (MOPs), micro-porous organic/inorganic hybrids that are generated through the SIB synthesis approach), the porous organic frameworks (POFs) such as covalent organic frameworks (COFs), conjugated microporous polymers (CMPs), porous aromatic frameworks (PAFs) and covalent triazinebased frameworks (CTFs).

OUTLOOKS: Although advanced MMMs enabled substantial breakthroughs in tailoring successful CO_2-selective membranes, these improvements are not necessarily contributed to the large-scale industrial/commercial development in membrane technology. Nevertheless, recent progresses in functional materials offer many attractive opportunities/perspectives, compared to a decade ago. In fact, many functional porous materials have already been examined. However, the main challenges are to actually obtain anticipated effects from the real MMM performance experiments. As can be seen in Figs. 60 and 61, although many effective MMMs were designed for CO_2 separation, proper selection of materials and functions in a systematic way is not yet possible.

Permeability and selectivity of MMMs are higher than pristine polymeric membranes because of the better intrinsic characteristics of inorganic fillers. There is no doubt that the development of MMMs is the best approach to improve the gas separation performance of polymeric membranes. The next hurdle to overcome is re-engineering and large-scale implementation of functionalized materials. Because the scale-up is costly, the use of low cost-sustainable blocks/structures materials is essential while maintaining excellent separation properties. In the case of CO_2 separation with megatons of emission per day, without a doubt advanced functionalized MMMs have an enormous benefit, if the barriers to commercialization are removed. As mentioned above the use of inexpensive material with a long service lifetime is necessary for this purpose. It is needless to say the utilization of specific molecular interactions to control structure, morphology and performance plays a pivotal role in MMM design but outstanding physical, mechanical,

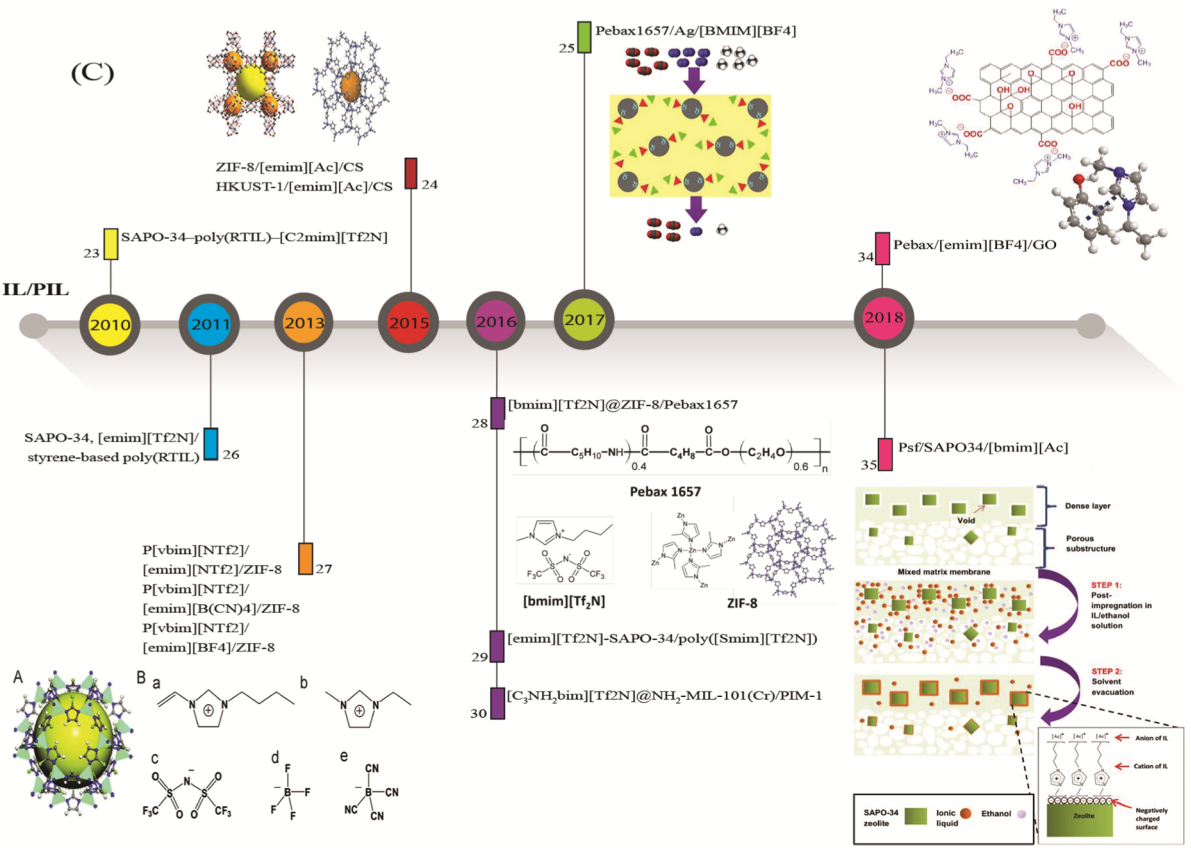

Fig. 61. (*continued*)

chemical and thermal properties are equally important in producing composite membrane. Economics and energy efficiency are the primary advantages of membrane-based separation. Hence, they should not be compromised by any type of novel membranes to be used in commercial scale.

References

[1] Du N, Park HB, Dal-Cin MM, Guiver MD. Advances in high permeability polymeric membrane materials for CO_2 separations. Energy Environ Sci 2012;5:7306–22.
[2] UNEP W. IPCC third assessment report 'climate change 2001'. Contributions of working groups I II, and III to the third assessment report of the intergovernmental panel on climate change. Cambridge and New York: Cambridge University Press; 2001.
[3] Scholes CA, Stevens GW, Kentish SE. Membrane gas separation applications in natural gas processing. Fuel 2012;96:15–28.
[4] Jeon Y-W, Lee D-H. Gas membranes for CO_2/CH_4 (biogas) separation: a review. Environ Eng Sci 2015;32:71–85.
[5] Chen XY, Vinh-Thang H, Ramirez AA, Rodrigue D, Kaliaguine S. Membrane gas separation technologies for biogas upgrading. RSC Adv 2015;5:24399–448.
[6] Wang S, Li X, Wu H, Tian Z, Xin Q, He G, et al. Advances in high permeability polymer-based membrane materials for CO_2 separations. Energy Environ Sci 2016;9:1863–90.
[7] Ramasubramanian K, Zhao Y, Winston Ho W. CO_2 capture and H_2 purification: prospects for CO_2-selective membrane processes. AIChE J 2013;59:1033–45.
[8] Ebadi Amooghin A, Sanaeepur H, Moghadassi A, Kargari A, Ghanbari D, Mehrabadi ZS. Modification of ABS membrane by PEG for capturing carbon dioxide from CO_2/N_2 streams. Sep Sci Technol 2010;45:1385–94.
[9] Tul Muntha S, Kausar A, Siddiq M. Progress in application of polymer-based membranes in gas separation technology. Polym-Plast Technol Eng 2016;55:1282–98.
[10] Rezakazemi M, Ebadi Amooghin A, Montazer-Rahmati MM, Ismail AF, Matsuura T. State-of-the-art membrane based CO_2 separation using mixed matrix membranes (MMMs): an overview on current status and future directions. Prog Polym Sci 2014;39:817–61.
[11] Jusoh N, Yeong YF, Chew TL, Lau KK, Shariff AM. Current development and challenges of mixed matrix membranes for CO_2/CH_4 separation. Sep Purif Rev 2016;45:321–44.
[12] Watson ER, Rowley GV, Wunderlich CR. Method and apparatus for continuous fabrication of desalination membrane. US patent, 34325851969.
[13] Robeson LM. Correlation of separation factor versus permeability for polymeric membranes. J Membr Sci 1991;62:165–85.
[14] Robeson LM. The upper bound revisited. J Membr Sci 2008;320:390–400.
[15] Goh PS, Ismail AF, Sanip SM, Ng BC, Aziz M. Recent advances of inorganic fillers in mixed matrix membrane for gas separation. Sep Purif Technol 2011;81:243–64.
[16] Rezakazemi M, Sadrzadeh M, Matsuura T. Thermally stable polymers for advanced high-performance gas separation membranes. Prog Energy Combust Sci 2018;66:1–41.
[17] Chung T-S, Jiang LY, Li Y, Kulprathipanja S. Mixed matrix membranes (MMMs) comprising organic polymers with dispersed inorganic fillers for gas separation. Prog Polym Sci 2007;32:483–507.
[18] Nasir R, Mukhtar H, Man Z, Mohshim DF. Material advancements in fabrication of mixed-matrix membranes. Chem Eng Technol 2013;36:717–27.
[19] Luis P, Van Gerven T, Van der Bruggen B. Recent developments in membrane-based technologies for CO_2 capture. Prog Energy Combust Sci 2012;38:419–48.

[20] Sanaeepur H, Amooghin AE, Bandehali S. Theoretical gas permeation models for mixed matrix membranes. Beau Bassin: Mauritius LAP Lambert Academic Publishing; 2018.
[21] Paul D, Kemp D. The diffusion time lag in polymer membranes containing adsorptive fillers. J Polym Sci: Polym Symp: Wiley Online Library 1973:79–93.
[22] Yang H-C, Hou J, Chen V, Xu Z-K. Surface and interface engineering for organic–inorganic composite membranes. J Mater Chem A 2016;4:9716–29.
[23] Slater AG, Cooper AI. Function-led design of new porous materials. Science 2015;348:aaa8075.
[24] Shehni PM, Ebadi Amooghin A, Ghadimi A, Sadrzadeh M, Mohammadi T. Modeling of unsteady-state permeation of gas mixture through a self-synthesized PDMS membranes. Sep Purif Technol 2011;76:385–99.
[25] Liu Y, Li X, Qin Y, Guo R, Zhang J. Pebax–polydopamine microsphere mixed-matrix membranes for efficient CO_2 separation. J Appl Polym Sci 2017;134:44564.
[26] Shen Y, Wang H, Zhang X, Zhang Y. MoS_2 nanosheets functionalized composite mixed matrix membrane for enhanced CO_2 capture via surface drop-coating method. ACS Appl Mater Interfaces 2016;8:23371–8.
[27] Wong K, Goh P, Ismail A. Thin film nanocomposite: the next generation selective membrane for CO_2 removal. J Mater Chem A 2016;4:15726–48.
[28] Vinoba M, Bhagiyalakshmi M, Alqaheem Y, Alomair AA, Pérez A, Rana MS. Recent progress of fillers in mixed matrix membranes for CO_2 separation: a review. Sep Purif Technol 2017;188:431–50.
[29] Chuah CY, Goh K, Yang Y, Gong H, Li W, Karahan HE, et al. Harnessing filler materials for enhancing biogas separation membranes. Chem Rev 2018;118:8655–769.
[30] Cheng Y, Wang Z, Zhao D. Mixed matrix membranes for natural gas upgrading: current status and opportunities. Ind Eng Chem Res 2018;57:4139–69.
[31] Echaide-Górriz C, Clément C, Cacho-Bailo F, Téllez C, Coronas J. New strategies based on microfluidics for the synthesis of metal–organic frameworks and their membranes. J Mater Chem A 2018;6:5485–506.
[32] Castro-Muñoz R, Fíla V. Progress on incorporating zeolites in Matrimid® 5218 mixed matrix membranes towards gas separation. Membranes 2018;8.
[33] Wang M, Wang Z, Zhao S, Wang J, Wang S. Recent advances on mixed matrix membranes for CO_2 separation. Chin J Chem Eng 2017;25:1581–97.
[34] Arabi Shamsabadi A, Riazi H, Soroush M. Mixed matrix membranes for CO_2 separations: membrane preparation, properties, and separation performance evaluation. In: Basile A, Favvas EP, editors. Current trends and future developments on (bio-) membranes. Elsevier; 2018. p. 103–53 [chapter 4].
[35] Zhu J, Hou J, Uliana A, Zhang Y, Tian M, Van der Bruggen B. The rapid emergence of two-dimensional nanomaterials for high-performance separation membranes. J Mater Chem A 2018;6:3773–92.
[36] Lin R, Villacorta Hernandez B, Ge L, Zhu Z. Metal organic framework based mixed matrix membranes: an overview on filler/polymer interfaces. J Mater Chem A 2018;6:293–312.
[37] Cheng Y, Ying Y, Japip S, Jiang S-D, Chung T-S, Zhang S, et al. Advanced porous materials in mixed matrix membranes. Adv Mater 2018;30:1802401.
[38] Liu M, Gurr PA, Fu Q, Webley PA, Qiao GG. Two-dimensional nanosheet-based gas separation membranes. J Mater Chem A 2018;6:23169–96.
[39] Sanders DF, Smith ZP, Guo R, Robeson LM, McGrath JE, Paul DR, et al. Energy-efficient polymeric gas separation membranes for a sustainable future: a review. Polymer 2013;54:4729–61.
[40] Otani A, Zhang Y, Matsuki T, Kamio E, Matsuyama H, Maginn EJ. Molecular design of high CO_2 reactivity and low viscosity ionic liquids for CO_2 separative facilitated transport membranes. Ind Eng Chem Res 2016;55:2821–30.
[41] Rufford TE, Smart S, Watson GCY, Graham BF, Boxall J, Diniz da Costa JC, et al. The removal of CO_2 and N_2 from natural gas: a review of conventional and emerging process technologies. J Petrol Sci Eng 2012;94:123–54.
[42] Figueroa JD, Fout T, Plasynski S, McIlvried H. Srivastava RD. Advances in CO_2 capture technology—The U.S. Department of Energy's carbon sequestration program. Int J Greenhouse Gas Control 2008;2:9–20.
[43] Merkel TC, Lin H, Wei X, Baker R. Power plant post-combustion carbon dioxide capture: an opportunity for membranes. J Membr Sci 2010;359:126–39.
[44] Ciferno J, Litynski J, Plasynski S, Murphy J, Vaux G, Munson R, et al. DOE/NETL carbon dioxide capture and storage RD&D roadmap. Pittsburgh: US DOE National Energy Technology Laboratory; 2010. p. 67.
[45] Fu J, Das S, Xing G, Ben T, Valtchev V, Qiu S. Fabrication of COF-MOF composite membranes and their highly selective separation of H_2/CO_2. J Am Chem Soc 2016;138(24):7673–80.
[46] Budhathoki S, Ajayi O, Steckel JA, Wilmer CE. High-throughput computational prediction of the cost of carbon capture using mixed matrix membranes. Energy Environ Sci 2019.
[47] George G, Bhoria N, AlHallaq S, Abdala A, Mittal V. Polymer membranes for acid gas removal from natural gas. Sep Purif Technol 2016;158:333–56.
[48] He X, Nieto DR, Lindbråthen A, Hägg MB. Membrane system design for CO_2 capture. Process systems and materials for CO_2 capture: modelling, design, control and integration. John Wiley & Sons; 2018. p. 249–81.
[49] Yang D, Wang Z, Wang J, Wang S. Parametric study of the membrane process for carbon dioxide removal from natural gas. Ind Eng Chem Res 2009;48:9013–22.
[50] Baker RW, Lokhandwala K. Natural gas processing with membranes: an overview. Ind Eng Chem Res 2008;47:2109–21.
[51] Sclierf M, Rufford TE. A technical evaluation of hybrid membrane-absorption processes for acid gas removal. International petroleum technology conference.
[52] Schneider D, Mehlhorn D, Zeigermann P, Karger J, Valiullin R. Transport properties of hierarchical micro-mesoporous materials. Chem Soc Rev 2016;45:3439–67.
[53] Ponnamma D, Sadasivuni KK, Grohens Y, Guo Q, Thomas S. Carbon nanotube based elastomer composites–an approach towards multifunctional materials. J Mater Chem C 2014;2:8446–85.
[54] Li Y, He G, Wang S, Yu S, Pan F, Wu H, et al. Recent advances in the fabrication of advanced composite membranes. J Mater Chem A 2013;1:10058–77.
[55] Sabetghadam A, Seoane B, Keskin D, Duim N, Rodenas T, Shahid S, et al. Metal organic framework crystals in mixed-matrix membranes: impact of the filler morphology on the gas separation performance. Adv Funct Mater 2016;26:3154–63.
[56] Kim S, Lee YM. Rigid and microporous polymers for gas separation membranes. Prog Polym Sci 2015;43:1–32.
[57] Ahmad R, Naimah N, Mukhtar H, Mohshim DF, Nasir R, Man Z. Surface modification in inorganic filler of mixed matrix membrane for enhancing the gas separation performance. Rev Chem Eng 2016;32:181–200.
[58] Ansaloni L, Salas-Gay J, Ligi S, Baschetti MG. Nanocellulose-based membranes for CO_2 capture. J Membr Sci 2017;522:216–25.
[59] Ying Y, Liu D, Ma J, Tong M, Zhang W, Huang H, et al. A GO-assisted method for the preparation of ultrathin covalent organic framework membranes for gas separation. J Mater Chem A 2016;4:13444–9.
[60] Loloei M, Moghadassi A, Omidkhah M, Ebadi Amooghin A. Improved CO_2 separation performance of Matrimid® 5218 membrane by addition of low molecular weight polyethylene glycol. Greenhouse Gases Sci Technol 2015;5:530–44.
[61] Pedram MZ, Omidkhah M, Ebadi Amooghin A, Yegani R. Facilitated transport by amine-mediated poly(vinyl alcohol) membranes for CO_2 removal from natural gas. Polym Eng Sci 2014;54:1268–79.
[62] Pedram MZ, Omidkhah M, Ebadi Amooghin A. Synthesis and characterization of diethanolamine-impregnated cross-linked polyvinylalcohol/glutaraldehyde membranes for CO_2/CH_4 separation. J Ind Eng Chem 2014;20:74–82.
[63] Ebadi Amooghin A, Pedram MZ, Omidkhah M, Yegani R. A novel CO_2-selective synthesized amine-impregnated cross-linked polyvinylalcohol/glutaraldehyde membrane: fabrication, characterization, and gas permeation study. Greenhouse Gases Sci Technol 2013;3:378–91.
[64] Omidkhah M, Pedram MZ, Amooghin AE. Facilitated transport of CO_2 through EA-mediated poly(vinyl alcohol) membrane cross-linked by formaldehyde. J Membr Sci Technol 2013;3:119.
[65] Jia R, Jin J, Lin S, Wang Y. Application of CO_2-favored organic units in CO2 separation membranes. Curr Org Chem 2016;20:1945–54.
[66] W-g Kim, Zhang X, Lee JS, Tsapatsis M, Nair S. Epitaxially grown layered MFI–bulk MFI hybrid zeolitic materials. ACS Nano 2012;6:9978–88.
[67] Bastani D, Esmaeili N, Asadollahi M. Polymeric mixed matrix membranes containing zeolites as a filler for gas separation applications: a review. J Ind Eng Chem 2013;19:375–93.
[68] Sanaeepur H, Nasernejad B, Kargari A. Cellulose acetate/nano-porous zeolite mixed matrix membrane for CO_2 separation. Greenhouse Gases Sci Technol 2015;5:291–304.
[69] Snider MT, Verweij H. Gas sorption studies on zeolite Y membrane materials for post-combustion CO_2 capture in coal-fired plants. Microporous Mesoporous

Mater 2014;192:3–7.
[70] Kim SJ, Tan S, Taborga Claure M, Briones Gil L, More KL, Liu Y, et al. One-step synthesis of zeolite membranes containing catalytic metal nanoclusters. ACS Appl Mater Interface. 2016;8:24671–81.
[71] Ebadi Amooghin A, Omidkhah M, Kargari A. Enhanced CO_2 transport properties of membranes by embedding nano-porous zeolite particles into Matrimid® 5218 matrix. RSC Adv 2015;5:8552–65.
[72] Zhang H, Xiao Q, Guo X, Li N, Kumar P, Rangnekar N, et al. Open-pore two-dimensional MFI zeolite nanosheets for the fabrication of hydrocarbon-isomer-selective membranes on porous polymer supports. Angew Chem Int Ed 2016;55:7184–7.
[73] Rezakazemi M, Shahidi K, Mohammadi T. Hydrogen separation and purification using crosslinkable PDMS/zeolite A nanoparticles mixed matrix membranes. Int J Hydrogen Energy 2012;37:14576–89.
[74] Rostamizadeh M, Rezakazemi M, Shahidi K, Mohammadi T. Gas permeation through H_2-selective mixed matrix membranes: experimental and neural network modeling. Int J Hydrogen Energy 2013;38:1128–35.
[75] Rezakazemi M, Shahidi K, Mohammadi T. Sorption properties of hydrogen-selective PDMS/zeolite 4A mixed matrix membrane. Int J Hydrogen Energy 2012;37:17275–84.
[76] Khulbe K, Matsuura T, Feng C, Ismail A. Recent development on the effect of water/moisture on the performance of zeolite membrane and MMMs containing zeolite for gas separation; review. RSC Adv 2016;6:42943–61.
[77] Ahmad N, Leo C, Junaidi M, Ahmad A. PVDF/PBI membrane incorporated with SAPO-34 zeolite for membrane gas absorption. J Taiwan Inst Chem Eng 2016;63:143–50.
[78] Li Y, Guan H-M, Chung T-S, Kulprathipanja S. Effects of novel silane modification of zeolite surface on polymer chain rigidification and partial pore blockage in polyethersulfone (PES)–zeolite A mixed matrix membranes. J Membr Sci 2006;275:17–28.
[79] Rezakazemi M, Dashti A, Asghari M, Shirazian S. H2-selective mixed matrix membranes modeling using ANFIS, PSO-ANFIS, GA-ANFIS. Int J Hydrogen Energy 2017;42:15211–25.
[80] Şen D, Kalıpçılar H, Yilmaz L. Development of polycarbonate based zeolite 4A filled mixed matrix gas separation membranes. J Membr Sci 2007;303:194–203.
[81] Dutta RC, Bhatia SK. Structure and gas transport at the polymer-zeolite interface: insights from molecular dynamics simulations. ACS Appl Mater Interfaces 2018;10:5992–6005.
[82] Junaidi M, Leo C, Ahmad A, Ahmad N. Fluorocarbon functionalized SAPO-34 zeolite incorporated in asymmetric mixed matrix membranes for carbon dioxide separation in wet gases. Microporous Mesoporous Mater 2015;206:23–33.
[83] Sanaeepur H, Kargari A, Nasernejad B. Aminosilane-functionalization of a nanoporous Y-type zeolite for application in a cellulose acetate based mixed matrix membrane for CO_2 separation. RSC Adv 2014;4:63966–76.
[84] Ebadi Amooghin A, Omidkhah M, Kargari A. The effects of aminosilane grafting on NaY zeolite–Matrimid® 5218 mixed matrix membranes for CO_2/CH_4 separation. J Membr Sci 2015;490:364–79.
[85] Gong H, Lee SS, Bae T-H. Mixed-matrix membranes containing inorganically surface-modified 5A zeolite for enhanced CO_2/CH_4 separation. Microporous Mesoporous Mater 2017;237:82–9.
[86] Pakizeh M, Hokmabadi S. Experimental study of the effect of zeolite 4A treated with magnesium hydroxide on the characteristics and gas-permeation properties of polysulfone-based mixed-matrix membranes. J Appl Polym Sci 2017;134:44329.
[87] Ebadi Amooghin A, Omidkhah M, Sanaeepur H, Kargari A. Preparation and characterization of Ag^+ ion-exchanged zeolite-Matrimid® 5218 mixed matrix membrane for CO_2/CH_4 separation. J Energy Chem 2016;25:450–62.
[88] Sanaeepur H, Kargari A, Nasernejad B, Ebadi Amooghin A, Omidkhah M. A novel Co^{2+} exchanged zeolite Y/cellulose acetate mixed matrix membrane for CO_2/N_2 separation. J Taiwan Inst Chem Eng 2016;60:403–13.
[89] Montes Luna AdJ, Castruita de León G, García Rodríguez SP, Fuentes López NC, Pérez Camacho O, Perera Mercado YA. Na^+/Ca^{2+} aqueous ion exchange in natural clinoptilolite zeolite for polymer-zeolite composite membranes production and their $CH_4/CO_2/N_2$ separation performance. J Nat Gas Sci Eng 2018;54:47–53.
[90] Pechar TW, Kim S, Vaughan B, Marand E, Baranauskas V, Riffle J, et al. Preparation and characterization of a poly(imide siloxane) and zeolite L mixed matrix membrane. J Membr Sci 2006;277:210–8.
[91] Han J, Lee W, Choi JM, Patel R, Min B-R. Characterization of polyethersulfone/polyimide blend membranes prepared by a dry/wet phase inversion: precipitation kinetics, morphology and gas separation. J Membr Sci 2010;351:141–8.
[92] Ahmad N, Mukhtar H, Mohshim D, Nasir R, Man Z. Effect of different organic amino cations on SAPO-34 for PES/SAPO-34 mixed matrix membranes toward CO_2/CH_4 separation. J Appl Polym Sci 2016;133:43387.
[93] Fernández-Barquín A, Casado-Coterillo C, Palomino M, Valencia S, Irabien A. Permselectivity improvement in membranes for CO_2/N_2 separation. Sep Purif Technol 2016;157:102–11.
[94] Nguyen TH, Gong H, Lee SS, Bae T-H. Amine-appended hierarchical Ca-A zeolite for enhancing CO_2/CH_4 selectivity of mixed-matrix membranes. ChemPhysChem 2016;17:3165–9.
[95] Hosseinzadeh Beiragh H, Omidkhah M, Abedini R, Khosravi T, Pakseresht S. Synthesis and characterization of poly (ether-block-amide) mixed matrix membranes incorporated by nanoporous ZSM-5 particles for CO_2/CH_4 separation. Asia-Pac J Chem Eng 2016;11:522–32.
[96] Loloei M, Omidkhah M, Moghadassi A, Ebadi Amooghin A. Preparation and characterization of Matrimid® 5218 based binary and ternary mixed matrix membranes for CO_2 separation. Int J Greenhouse Gas Control 2015;39:225–35.
[97] Sorribas S, Comesaña-Gándara B, Lozano AE, Zornoza B, Téllez C, Coronas J. Insight into ETS-10 synthesis for the preparation of mixed matrix membranes for CO_2/CH_4 gas separation. RSC Adv 2015;5:102392–8.
[98] Martin-Gil V, López A, Hrabanek P, Mallada R, Vankelecom I, Fila V. Study of different titanosilicate (TS-1 and ETS-10) as fillers for mixed matrix membranes for CO_2/CH_4 gas separation applications. J Membr Sci 2017;523:24–35.
[99] Santaniello A, Golemme G. Interfacial control in perfluoropolymer mixed matrix membranes for natural gas sweetening. J Ind Eng Chem 2018;60:169–76.
[100] Meléndez-Ortiz HI, Perera-Mercado Y, Mercado-Silva JA, Olivares-Maldonado Y, Castruita G, García-Cerda LA. Functionalization with amine-containing organosilane of mesoporous silica MCM-41 and MCM-48 obtained at room temperature. Ceram Int 2014;40:9701–7.
[101] Zhuang G-L, Wey M-Y, Tseng H-H. The density and crystallinity properties of PPO-silica mixed-matrix membranes produced via the in situ sol-gel method for H_2/CO_2 separation. II: Effect of thermal annealing treatment. Chem Eng Res Des 2015;104:319–32.
[102] Kim J, Fu Q, Xie K, Scofield JM, Kentish SE, Qiao GG. CO_2 separation using surface-functionalized SiO_2 nanoparticles incorporated ultra-thin film composite mixed matrix membranes for post-combustion carbon capture. J Membr Sci 2016;515:54–62.
[103] Xin Q, Zhang Y, Huo T, Ye H, Ding X, Lin L, et al. Mixed matrix membranes fabricated by a facile in situ biomimetic mineralization approach for efficient CO_2 separation. J Membr Sci 2016;508:84–93.
[104] Khan AL, Klaysom C, Gahlaut A, Vankelecom IF. Polysulfone acrylate membranes containing functionalized mesoporous MCM-41 for CO_2 separation. J Membr Sci 2013;436:145–53.
[105] Wu H, Li X, Li Y, Wang S, Guo R, Jiang Z, et al. Facilitated transport mixed matrix membranes incorporated with amine functionalized MCM-41 for enhanced gas separation properties. J Membr Sci 2014;465:78–90.
[106] Khan AL, Klaysom C, Gahlaut A, Khan AU, Vankelecom IF. Mixed matrix membranes comprising of Matrimid and–SO_3H functionalized mesoporous MCM-41 for gas separation. J Membr Sci 2013;447:73–9.
[107] Laghaei M, Sadeghi M, Ghalei B, Shahrooz M. The role of compatibility between polymeric matrix and silane coupling agents on the performance of mixed matrix membranes: polyethersulfone/MCM-41. J Membr Sci 2016;513:20–32.
[108] Tzi ECN, Ching OP. Surface modification of AMH-3 for development of mixed matrix membranes. Procedia Eng 2016;148:86–92.
[109] Waheed N, Mushtaq A, Tabassum S, Gilani MA, Ilyas A, Ashraf F, et al. Mixed matrix membranes based on polysulfone and rice husk extracted silica for CO_2 separation. Sep Purif Technol 2016;170:122–9.

[110] Xin Q, Zhang Y, Shi Y, Ye H, Lin L, Ding X, et al. Tuning the performance of CO_2 separation membranes by incorporating multifunctional modified silica microspheres into polymer matrix. J Membr Sci 2016;514:73–85.
[111] Su NC, Buss HG, McCloskey BD, Urban JJ. Enhancing separation and mechanical performance of hybrid membranes through nanoparticle surface modification. ACS Macro Lett 2015;4:1239–43.
[112] Park S, Bang J, Choi J, Lee SH, Lee J-H, Lee JS. 3-Dimensionally disordered mesoporous silica (DMS)-containing mixed matrix membranes for CO_2 and non-CO_2 greenhouse gas separations. Sep Purif Technol 2014;136:286–95.
[113] Wang M, Wang Z, Li N, Liao J, Zhao S, Wang J, et al. Relationship between polymer–filler interfaces in separation layers and gas transport properties of mixed matrix composite membranes. J Membr Sci 2015;495:252–68.
[114] Anjum MW, de Clippel F, Didden J, Khan AL, Couck S, Baron GV, et al. Polyimide mixed matrix membranes for CO_2 separations using carbon–silica nano-composite fillers. J Membr Sci 2015;495:121–9.
[115] Ghadimi A, Mohammadi T, Kasiri N. Gas permeation, sorption and diffusion through PEBA/SiO_2 nanocomposite membranes (chemical surface modification of nanoparticles). Int J Hydrogen Energy 2015;40:9723–32.
[116] Suzuki T, Takenaka M, Yamada Y. Synthesis and gas transport properties of hyperbranched polybenzoxazole – silica hybrid membranes. J Membr Sci 2017;521:10–7.
[117] Zulhairun A, Ismail A, Matsuura T, Abdullah M, Mustafa A. Asymmetric mixed matrix membrane incorporating organically modified clay particle for gas separation. Chem Eng J 2014;241:495–503.
[118] Ismail N, Ismail A, Mustafa A, Zulhairun A, Nordin N. Enhanced carbon dioxide separation by polyethersulfone (PES) mixed matrix membranes deposited with clay. J Polym Eng 2016;36:65–78.
[119] Zulhairun A, Ng B, Ismail A, Murali RS, Abdullah M. Production of mixed matrix hollow fiber membrane for CO_2/CH_4 separation. Sep Purif Technol 2014;137:1–12.
[120] Xiang L, Pan Y, Zeng G, Jiang J, Chen J, Wang C. Preparation of poly (ether-block-amide)/attapulgite mixed matrix membranes for CO_2/N_2 separation. J Membr Sci 2016;500:66–75.
[121] Barooah M, Mandal B. Enhanced CO_2 separation performance by PVA/PEG/silica mixed matrix membrane. J Appl Polym Sci 2018;135:46481.
[122] Seoane B, Castellanos S, Dikhtiarenko A, Kapteijn F, Gascon J. Multi-scale crystal engineering of metal organic frameworks. Coord Chem Rev 2016;307:147–87.
[123] Andirova D, Cogswell CF, Lei Y, Choi S. Effect of the structural constituents of metal organic frameworks on carbon dioxide capture. Microporous Mesoporous Mater 2016;219:276–305.
[124] Zhang Y, Feng X, Yuan S, Zhou J, Wang B. Challenges and recent advances in MOF–polymer composite membranes for gas separation. Inorg Chem Front 2016;3:896–909.
[125] Ma J, Ying Y, Yang Q, Ban Y, Huang H, Guo X, et al. Mixed-matrix membranes containing functionalized porous metal–organic polyhedrons for the effective separation of CO 2–CH 4 mixture. Chem Commun 2015;51:4249–51.
[126] Rui Z, James JB, Kasik A, Lin Y. Metal-organic framework membrane process for high purity CO_2 production. AIChE J 2016;62:3836–41.
[127] Rodenas T, Luz I, Prieto G, Seoane B, Miro H, Corma A, et al. Metal–organic framework nanosheets in polymer composite materials for gas separation. Nat Mater 2015;14:48–55.
[128] Abu Ghalia M, Dahman Y. Development and evaluation of zeolites and metal-organic frameworks for carbon dioxide separation and capture. Energy Technol 2017;5:356–72.
[129] Yao BJ, Jiang WL, Dong Y, Liu ZX, Dong YB. Post-synthetic polymerization of UiO-66-NH2 nanoparticles and polyurethane oligomer toward stand-alone membranes for dye removal and separation. Chem-Eur J 2016;22:10565–71.
[130] Kanehashi S, Chen GQ, Scholes CA, Ozcelik B, Hua C, Ciddor L, et al. Enhancing gas permeability in mixed matrix membranes through tuning the nanoparticle properties. J Membr Sci 2015;482:49–55.
[131] Duan C, Kang G, Liu D, Wang L, Jiang C, Cao Y, et al. Enhanced gas separation properties of metal organic frameworks/polyetherimide mixed matrix membranes. J Appl Polym Sci 2014;131:40719.
[132] Gong H, Nguyen TH, Wang R, Bae T-H. Separations of binary mixtures of CO_2/CH_4 and CO_2/N_2 with mixed-matrix membranes containing Zn $(pyrz)_2$ (SiF_6) metal-organic framework. J Membr Sci 2015;495:169–75.
[133] Seoane B, Coronas J, Gascon I, Benavides ME, Karvan O, Caro J, et al. Metal–organic framework based mixed matrix membranes: a solution for highly efficient CO_2 capture? Chem Soc Rev 2015;44:2421–54.
[134] Dorosti F, Omidkhah M, Abedini R. Enhanced CO_2/CH_4 separation properties of asymmetric mixed matrix membrane by incorporating nano-porous ZSM-5 and MIL-53 particles into Matrimid® 5218. J Nat Gas Sci Eng 2015;25:88–102.
[135] Li B, Chrzanowski M, Zhang Y, Ma S. Applications of metal-organic frameworks featuring multi-functional sites. Coord Chem Rev 2016;307:106–29.
[136] Yang Y, Lin R, Ge L, Hou L, Bernhardt P, Rufford TE, et al. Synthesis and characterization of three amino-functionalized metal–organic frameworks based on the 2-aminoterephthalic ligand. Dalton Trans 2015;44:8190–7.
[137] Guo X, Huang H, Ban Y, Yang Q, Xiao Y, Li Y, et al. Mixed matrix membranes incorporated with amine-functionalized titanium-based metal-organic framework for CO_2/CH_4 separation. J Membr Sci 2015;478:130–9.
[138] Anjum MW, Bueken B, De Vos D, Vankelecom IF. MIL-125 (Ti) based mixed matrix membranes for CO_2 separation from CH_4 and N_2. J Membr Sci 2016;502:21–8.
[139] Abedini R, Omidkhah M, Dorosti F. Highly permeable poly (4-methyl-1-pentyne)/NH_2-MIL 53 (Al) mixed matrix membrane for CO_2/CH_4 separation. RSC Adv 2014;4:36522–37.
[140] Feijani EA, Mahdavi H, Tavasoli A. Poly (vinylidene fluoride) based mixed matrix membranes comprising metal organic frameworks for gas separation applications. Chem Eng Res Des 2015;96:87–102.
[141] Xin Q, Liu T, Li Z, Wang S, Li Y, Li Z, et al. Mixed matrix membranes composed of sulfonated poly (ether ether ketone) and a sulfonated metal–organic framework for gas separation. J Membr Sci 2015;488:67–78.
[142] Duan C, Jie X, Liu D, Cao Y, Yuan Q. Post-treatment effect on gas separation property of mixed matrix membranes containing metal organic frameworks. J Membr Sci 2014;466:92–102.
[143] Ma L, Svec F, Tan T, Lv Y. Mixed matrix membrane based on cross-linked poly[(ethylene glycol) methacrylate] and metal-organic framework for efficient separation of carbon dioxide and methane. ACS Appl Nano Mater 2018;1:2808–18.
[144] Semino R, Moreton JC, Ramsahye NA, Cohen SM, Maurin G. Understanding the origins of metal–organic framework/polymer compatibility. Chem Sci 2018;9:315–24.
[145] Gao X, Zhang J, Huang K, Zhang J. ROMP for metal-organic frameworks: an efficient technique toward robust and high-separation performance membranes. ACS Appl Mater Interfaces 2018;10:34640–5.
[146] Venna SR, Lartey M, Li T, Spore A, Kumar S, Nulwala HB, et al. Fabrication of MMMs with improved gas separation properties using externally-functionalized MOF particles. J Mater Chem A 2015;3:5014–22.
[147] Shen J, Liu G, Huang K, Li Q, Guan K, Li Y, et al. UiO-66-polyether block amide mixed matrix membranes for CO_2 separation. J Membr Sci 2016;513:155–65.
[148] Anjum MW, Vermoortele F, Khan AL, Bueken B, De Vos DE, Vankelecom IF. Modulated UiO-66-based mixed-matrix membranes for CO_2 separation. ACS Appl Mater Interfaces 2015;7:25193–201.
[149] Hu Z, Kang Z, Qian Y, Peng Y, Wang X, Chi C, et al. Mixed matrix membranes containing UiO-66 (Hf)-$(OH)_2$ metal-organic framework nanoparticles for efficient H_2/CO_2 separation. Ind Eng Chem Res 2016;55:7933–40.
[150] Rodenas T, van Dalen M, Serra-Crespo P, Kapteijn F, Gascon J. Mixed matrix membranes based on NH_2-functionalized MIL-type MOFs: Influence of structural and operational parameters on the CO_2/CH_4 separation performance. Microporous Mesoporous Mater 2014;192:35–42.
[151] Zhu H, Wang L, Jie X, Liu D, Cao Y. Improved interfacial affinity and CO_2 separation performance of asymmetric mixed matrix membranes by incorporating post-modified MIL-53 (Al). ACS Appl Mater Interfaces 2016;8:22696–704.

[152] Xin Q, Ouyang J, Liu T, Li Z, Li Z, Liu Y, et al. Enhanced interfacial interaction and CO_2 separation performance of mixed matrix membrane by incorporating polyethylenimine-decorated metal-organic frameworks. ACS Appl Mater Interfaces 2015;7:1065–77.
[153] Dong X, Liu Q, Huang A. Highly permselective MIL-68 (Al)/matrimid mixed matrix membranes for CO_2/CH_4 separation. J Appl Polym Sci 2016;133.
[154] Bachman JE, Long JR. Plasticization-resistant Ni_2(dobdc)/polyimide composite membranes for the removal of CO_2 from natural gas. Energy Environ Sci 2016;9:2031–6.
[155] Kılıç A, Atalay-Oral Ç, Sirkecioğlu A, Tantekin-Ersolmaz ŞB, Ahunbay MG. Sod-ZMOF/Matrimid® mixed matrix membranes for CO_2 separation. J Membr Sci 2015;489:81–9.
[156] Lim SY, Choi J, Kim H-Y, Kim Y, Kim S-J, Kang YS, et al. New CO_2 separation membranes containing gas-selective Cu-MOFs. J Membr Sci 2014;467:67–72.
[157] Lin R, Ge L, Hou L, Strounina E, Rudolph V, Zhu Z. Mixed matrix membranes with strengthened MOFs/polymer interfacial interaction and improved membrane performance. ACS Appl Mater Interfaces 2014;6:5609–18.
[158] Arjmandi M, Pakizeh M, Pirouzram O. The role of tetragonal-metal-organic framework-5 loadings with extra ZnO molecule on the gas separation performance of mixed matrix membrane. Korean J Chem Eng 2015;32:1178–87.
[159] Tien-Binh N, Vinh-Thang H, Chen XY, Rodrigue D, Kaliaguine S. Polymer functionalization to enhance interface quality of mixed matrix membranes for high CO_2/CH_4 gas separation. J Mater Chem A 2015;3:15202–13.
[160] Marti AM, Venna SR, Roth EA, Culp JT, Hopkinson DP. Simple fabrication method for mixed matrix membranes with in situ MOF growth for gas separation. ACS Appl Mater Interfaces 2018;10:24784–90.
[161] Satheeshkumar C, Yu HJ, Park H, Kim M, Lee JS, Seo M. Thiol–ene photopolymerization of vinyl-functionalized metal–organic frameworks towards mixed-matrix membranes. J Mater Chem A 2018;6:21961–8.
[162] Mozafari M, Abedini R, Rahimpour A. Zr-MOFs-incorporated thin film nanocomposite Pebax 1657 membranes dip-coated on polymethylpentyne layer for efficient separation of CO_2/CH_4. J Mater Chem A 2018;6:12380–92.
[163] Prasetya N, Donose BC, Ladewig BP. A new and highly robust light-responsive Azo-UiO-66 for highly selective and low energy post-combustion CO_2 capture and its application in a mixed matrix membrane for CO_2/N_2 separation. J Mater Chem A 2018;6:16390–402.
[164] Jiang X, Li S, He S, Bai Y, Shao L. Interface manipulation of CO_2–philic composite membranes containing designed UiO-66 derivatives towards highly efficient CO_2 capture. J Mater Chem A 2018;6:15064–73.
[165] Jiang Y, Liu C, Caro J, Huang A. A new UiO-66-NH_2 based mixed-matrix membranes with high CO_2/CH_4 separation performance. Microporous Mesoporous Mater 2019;274:203–11.
[166] Sutrisna PD, Hou J, Zulkifli MY, Li H, Zhang Y, Liang W, et al. Surface functionalized UiO-66/Pebax-based ultrathin composite hollow fiber gas separation membranes. J Mater Chem A 2018;6:918–31.
[167] Molavi H, Shojaei A, Mousavi SA. Improving mixed-matrix membrane performance via PMMA grafting from functionalized NH_2–UiO-66. J Mater Chem A 2018;6:2775–91.
[168] Rajati H, Navarchian AH, Tangestaninejad S. Preparation and characterization of mixed matrix membranes based on Matrimid/PVDF blend and MIL-101(Cr) as filler for CO_2/CH_4 separation. Chem Eng Sci 2018;185:92–104.
[169] Mubashir M, Yeong YF, Lau KK, Chew TL, Norwahyu J. Efficient CO_2/N_2 and CO_2/CH_4 separation using NH_2-MIL-53(Al)/cellulose acetate (CA) mixed matrix membranes. Sep Purif Technol 2018;199:140–51.
[170] Meshkat S, Kaliaguine S, Rodrigue D. Mixed matrix membranes based on amine and non-amine MIL-53(Al) in Pebax® MH-1657 for CO_2 separation. Sep Purif Technol 2018;200:177–90.
[171] Li Q, Duan J, Jin W. Efficient CO_2/N_2 separation by mixed matrix membrane with amide functionalized porous coordination polymer filler. Chin Chem Lett 2018;29:854–6.
[172] Chang Y-W, Chang BK. Influence of casting solvents on sedimentation and performance in metal–organic framework mixed-matrix membranes. J Taiwan Inst Chem Eng 2018;89:224–33.
[173] Zhang W, Liu D, Guo X, Huang H, Zhong C. Fabrication of mixed-matrix membranes with MOF-derived porous carbon for CO_2 separation. AIChE J 2018;64:3400–9.
[174] Sabetghadam A, Liu X, Gottmer S, Chu L, Gascon J, Kapteijn F. Thin mixed matrix and dual layer membranes containing metal-organic framework nanosheets and Polyactive™ for CO_2 capture. J Membr Sci 2019;570–571:226–35.
[175] Shete M, Kumar P, Bachman JE, Ma X, Smith ZP, Xu W, et al. On the direct synthesis of Cu(BDC) MOF nanosheets and their performance in mixed matrix membranes. J Membr Sci 2018;549:312–20.
[176] Dorosti F, Alizadehdakhel A. Fabrication and investigation of PEBAX/Fe-BTC, a high permeable and CO_2 selective mixed matrix membrane. Chem Eng Res Des 2018;136:119–28.
[177] Nabais AR, Ribeiro RPPL, Mota JPB, Alves VD, Esteves IAAC, Neves LA. CO_2/N_2 gas separation using Fe(BTC)-based mixed matrix membranes: a view on the adsorptive and filler properties of metal-organic frameworks. Sep Purif Technol 2018;202:174–84.
[178] Ge B, Xu Y, Zhao H, Sun H, Guo Y, Wang W. High performance gas separation mixed matrix membrane fabricated by incorporation of functionalized sub-micrometer-sized metal-organic framework. Materials 2018;11:1421.
[179] Abedini R, Mosayebi A, Mokhtari M. Improved CO_2 separation of azide cross-linked PMP mixed matrix membrane embedded by nano-CuBTC metal organic framework. Process Saf Environ Prot 2018;114:229–39.
[180] Fan L, Kang Z, Shen Y, Wang S, Zhao H, Sun H, et al. Mixed matrix membranes based on metal-organic frameworks with tunable pore size for CO_2 separation. Cryst Growth Des 2018;18:4365–71.
[181] Ishaq S, Tamime R, Bilad MR, Khan AL. Mixed matrix membranes comprising of polysulfone and microporous Bio-MOF-1: preparation and gas separation properties. Sep Purif Technol 2019;210:442–51.
[182] Guo X, Huang H, Liu D, Zhong C. Improving particle dispersity and CO_2 separation performance of amine-functionalized CAU-1 based mixed matrix membranes with polyethyleneimine-grafting modification. Chem Eng Sci 2018;189:277–85.
[183] Ozen HA, Ozturk B. Gas separation characteristic of mixed matrix membrane prepared by MOF-5 including different metals. Sep Purif Technol 2019;211:514–21.
[184] Arjmandi M, Pakizeh M, Saghi M, Arjmandi A. Study of separation behavior of activated and non-activated MOF-5 as filler on MOF-based mixed-matrix membranes in H_2/CO_2 separation. Pet Chem 2018;58:317–29.
[185] Nuhnen A, Dietrich D, Millan S, Janiak C. Role of filler porosity and filler/polymer interface volume in metal-organic framework/polymer mixed-matrix membranes for gas separation. ACS Appl Mater Interfaces 2018;10:33589–600.
[186] Wang Z, Hou J, Guo R, Li X. Efficient CO_2 separation in mixed matrix membranes with a hierarchical pore carbon nanostructure. J Chin Chem Soc 2018;65:1347–55.
[187] Yeo ZY, Chai S-P, Zhu PW, Mohamed AR. An overview: synthesis of thin films/membranes of metal organic frameworks and its gas separation performances. RSC Adv 2014;4:54322–34.
[188] Lee Y-R, Kim J, Ahn W-S. Synthesis of metal-organic frameworks: a mini review. Korean J Chem Eng 2013;30:1667–80.
[189] Eddaoudi M, Sava DF, Eubank JF, Adil K, Guillerm V. Zeolite-like metal–organic frameworks (ZMOFs): design, synthesis, and properties. Chem Soc Rev 2015;44:228–49.
[190] Zhang C, Koros WJ. Zeolitic imidazolate framework-enabled membranes: challenges and opportunities. J Phys Chem Lett 2015;6:3841–9.
[191] Matsumoto M, Kitaoka T. Ultraselective gas separation by nanoporous metal-organic frameworks embedded in gas-barrier nanocellulose films. Adv Mater 2016;28:1765–9.
[192] Sarfraz M, Ba-Shammakh M. A novel zeolitic imidazolate framework based mixed-matrix membrane for efficient CO_2 separation under wet conditions. J Taiwan Inst Chem Eng 2016;65:427–36.
[193] Friebe S, Diestel L, Knebel A, Wollbrink A, Caro J. MOF-based mixed-matrix membranes in gas separation-mystery and reality. Chem Ing Tech

2016;88:1788–97.
[194] Sánchez-Laínez J, Zornoza B, Ariso CT, Coronas J. On the chemical filler-polymer interaction of nano-and micro-sized ZIF-11 in PBI mixed matrix membranes and their application for H_2/CO_2 separation. J Mater Chem A 2016;4:14334–41.
[195] Shahid S, Nijmeijer K, Nehache S, Vankelecom I, Deratani A, Quemener D. MOF-mixed matrix membranes: precise dispersion of MOF particles with better compatibility via a particle fusion approach for enhanced gas separation properties. J Membr Sci 2015;492:21–31.
[196] Hwang S, Chi WS, Lee SJ, Im SH, Kim JH, Kim J. Hollow ZIF-8 nanoparticles improve the permeability of mixed matrix membranes for CO_2/CH_4 gas separation. J Membr Sci 2015;480:11–9.
[197] Zhao S, Cao X, Ma Z, Wang Z, Qiao Z, Wang J, et al. Mixed-matrix membranes for CO_2/N_2 separation comprising a poly(vinylamine) matrix and metal-organic frameworks. Ind Eng Chem Res 2015;54:5139–48.
[198] Nafisi V, Hägg M-B. Development of dual layer of ZIF-8/PEBAX-2533 mixed matrix membrane for CO_2 capture. J Membr Sci 2014;459:244–55.
[199] Cacho-Bailo F, Matito-Martos I, Perez-Carbajo J, Etxeberría-Benavides M, Karvan O, Sebastián V, et al. On the molecular mechanisms for the H_2/CO_2 separation performance of zeolite imidazolate framework two-layered membranes. Chem Sci 2017;8:325–33.
[200] Hess SC, Grass RN, Stark WJ. MOF channels within porous polymer film: flexible, self-supporting ZIF-8 polyethersulfone composite membrane. Chem Mater 2016;28:7638–44.
[201] Mahdi E, Tan J-C. Mixed-matrix membranes of zeolitic imidazolate framework (ZIF-8)/matrimid nanocomposite: Thermo-mechanical stability and viscoelasticity underpinning membrane separation performance. J Membr Sci 2016;498:276–90.
[202] Kertik A, Khan AL, Vankelecom IF. Mixed matrix membranes prepared from non-dried MOFs for CO_2/CH_4 separations. RSC Adv 2016;6:114505–12.
[203] Nordin NAHM, Racha SM, Matsuura T, Misdan N, Sani NAA, Ismail AF, et al. Facile modification of ZIF-8 mixed matrix membrane for CO_2/CH_4 separation: synthesis and preparation. RSC Adv 2015;5:43110–20.
[204] Kertik A, Wee LH, Pfannmöller M, Bals S, Martens JA, Vankelecom IFJ. Highly selective gas separation membrane using in situ amorphised metal–organic frameworks. Energy Environ Sci 2017;10:2342–51.
[205] Hwang S, Semino R, Seoane B, Zahan M, Chmelik C, Valiullin R, et al. Revealing the transient concentration of CO_2 in a mixed-matrix membrane by ir microimaging and molecular modeling. Angew Chem Int Ed 2018;57:5156–60.
[206] Li H, Han L, Hou J, Liu J, Zhang Y. Oriented zeolitic imidazolate framework membranes within polymeric matrices for effective N_2/CO_2 separation. J Membr Sci 2019;572:82–91.
[207] Dong L, Chen M, Wu X, Shi D, Dong W, Zhang H, et al. Multi-functional polydopamine coating: simultaneous enhancement of interfacial adhesion and CO_2 separation performance of mixed matrix membranes. New J Chem 2016;40:9148–59.
[208] Dong L, Chen M, Li J, Shi D, Dong W, Li X, et al. Metal-organic framework-graphene oxide composites: a facile method to highly improve the CO_2 separation performance of mixed matrix membranes. J Membr Sci 2016;520:801–11.
[209] Chi WS, Kim SJ, Lee SJ, Bae YS, Kim JH. Enhanced performance of mixed-matrix membranes through a graft copolymer-directed interface and interaction tuning approach. ChemSusChem 2015;8:650–8.
[210] Eiras D, Labreche Y, Pessan LA. Ultem® /ZIF-8 mixed matrix membranes for gas separation: transport and physical properties. Mater Res 2016;19:220–8.
[211] Ehsani A, Pakizeh M. Synthesis, characterization and gas permeation study of ZIF-11/Pebax® 2533 mixed matrix membranes. J Taiwan Inst Chem Eng 2016;66:414–23.
[212] Boroglu MS, Yumru AB. Gas separation performance of 6FDA-DAM-ZIF-11 mixed-matrix membranes for H_2/CH_4 and CO_2/CH_4 separation. Sep Purif Technol 2016;173:269–79.
[213] Gao Y, Qiao Z, Zhao S, Wang Z, Wang J. In situ synthesis of polymer grafted ZIFs and application in mixed matrix membrane for CO_2 separation. J Mater Chem A 2018;6:3151–61.
[214] Guo A, Ban Y, Yang K, Yang W. Metal-organic framework-based mixed matrix membranes: Synergetic effect of adsorption and diffusion for CO_2/CH_4 separation. J Membr Sci 2018;562:76–84.
[215] Zhang X, Zhang T, Wang Y, Li J, Liu C, Li N, et al. Mixed-matrix membranes based on Zn/Ni-ZIF-8-PEBA for high performance CO_2 separation. J Membr Sci 2018;560:38–46.
[216] Ding X, Li X, Zhao H, Wang R, Zhao R, Li H, et al. Partial pore blockage and polymer chain rigidification phenomena in PEO/ZIF-8 mixed matrix membranes synthesized by in situ polymerization. Chin J Chem Eng 2018;26:501–8.
[217] Hu L, Liu J, Zhu L, Hou X, Huang L, Lin H, et al. Highly permeable mixed matrix materials comprising ZIF-8 nanoparticles in rubbery amorphous poly(ethylene oxide) for CO_2 capture. Sep Purif Technol 2018;205:58–65.
[218] Sánchez-Laínez J, Veiga A, Zornoza B, Balestra SRG, Hamad S, Ruiz-Salvador AR, et al. Tuning the separation properties of zeolitic imidazolate framework core–shell structures via post-synthetic modification. J Mater Chem A 2017;5:25601–8.
[219] Sarfraz M, Ba-Shammakh M. ZIF-based water-stable mixed-matrix membranes for effective CO_2 separation from humid flue gas. Can J Chem Eng 2018;96:2475–83.
[220] Yumru AB, Safak Boroglu M, Boz I. ZIF-11/Matrimid® mixed matrix membranes for efficient CO_2, CH_4, and H_2 separations. Greenhouse Gases Sci Technol 2018;8:529–41.
[221] Huang N, Krishna R, Jiang D. Tailor-made pore surface engineering in covalent organic frameworks: systematic functionalization for performance screening. J Am Chem Soc 2015;137:7079–82.
[222] Kang Z, Peng Y, Qian Y, Yuan D, Addicoat MA, Heine T, et al. Mixed matrix membranes (MMMs) comprising exfoliated 2D covalent organic frameworks (COFs) for efficient CO_2 separation. Chem Mater 2016;28:1277–85.
[223] Chen X, Addicoat M, Jin E, Zhai L, Xu H, Huang N, et al. Locking covalent organic frameworks with hydrogen bonds: general and remarkable effects on crystalline structure, physical properties, and photochemical activity. J Am Chem Soc 2015;137:3241–7.
[224] Waller PJ, Gándara F, Yaghi OM. Chemistry of covalent organic frameworks. Acc Chem Res 2015;48:3053–63.
[225] Biswal BP, Chaudhari HD, Banerjee R, Kharul UK. Chemically stable covalent organic framework (COF)-polybenzimidazole hybrid membranes: enhanced gas separation through pore modulation. Chem–Eur J 2016;22:4695–9.
[226] Shan M, Seoane B, Rozhko E, Dikhtiarenko A, Clet G, Kapteijn F, et al. Azine-linked covalent organic framework (COF)-based mixed-matrix membranes for CO_2/CH_4 separation. Chem-Eur J 2016;22:14467–70.
[227] Cao X, Qiao Z, Wang Z, Zhao S, Li P, Wang J, et al. Enhanced performance of mixed matrix membrane by incorporating a highly compatible covalent organic framework into poly (vinylamine) for hydrogen purification. Int J Hydrogen Energy 2016;41:9167–74.
[228] Díaz U, Corma A. Ordered covalent organic frameworks, COFs and PAFs. From preparation to application. Coord Chem Rev 2016;311:85–124.
[229] Volkov A, Bakhtin D, Kulikov L, Terenina M, Golubev G, Bondarenko G, et al. Stabilization of gas transport properties of PTMSP with porous aromatic framework: effect of annealing. J Membr Sci 2016;517:80–90.
[230] Shan M, Seoane B, Andres-Garcia E, Kapteijn F, Gascon J. Mixed-matrix membranes containing an azine-linked covalent organic framework: Influence of the polymeric matrix on post-combustion CO_2-capture. J Membr Sci 2018;549:377–84.
[231] Cui Y, Kundalwal S, Kumar S. Gas barrier performance of graphene/polymer nanocomposites. Carbon 2016;98:313–33.
[232] Ebrahimi S, Mollaiy-Berneti S, Asadi H, Peydayesh M, Akhlaghian F, Mohammadi T. PVA/PES-amine-functional graphene oxide mixed matrix membranes for CO_2/CH_4 separation: experimental and modeling. Chem Eng Res Des 2016;109:647–56.
[233] Rubio C, Zornoza B, Gorgojo P, Tellez C, Coronas J. Separation of H_2 and CO_2 containing mixtures with mixed matrix membranes based on layered materials. Curr Org Chem 2014;18:2351–63.
[234] Miculescu M, Thakur VK, Miculescu F, Voicu SI. Graphene-based polymer nanocomposite membranes: a review. Polym Adv Technol 2016;27:844–59.
[235] Shen Y, Wang H, Liu J, Zhang Y. Enhanced performance of a novel polyvinyl amine/chitosan/graphene oxide mixed matrix membrane for CO_2 capture. ACS Sustain Chem Eng 2015;3:1819–29.
[236] Ha H, Park J, Ando S, Kim CB, Nagai K, Freeman BD, et al. Gas permeation and selectivity of poly(dimethylsiloxane)/graphene oxide composite elastomer

membranes. J Membr Sci 2016;518:131–40.
[237] Dong G, Zhang Y, Hou J, Shen J, Chen V. Graphene oxide nanosheets based novel facilitated transport membranes for efficient CO_2 capture. Ind Eng Chem Res 2016;55:5403–14.
[238] Zhao D, Ren J, Qiu Y, Li H, Hua K, Li X, et al. Effect of graphene oxide on the behavior of poly (amide-6-b-ethylene oxide)/graphene oxide mixed-matrix membranes in the permeation process. J Appl Polym Sci 2015;132.
[239] Shen J, Liu G, Huang K, Jin W, Lee KR, Xu N. Membranes with fast and selective gas-transport channels of laminar graphene oxide for efficient CO_2 capture. Angew Chem 2015;127:588–92.
[240] Wang S, Wu Y, Zhang N, He G, Xin Q, Wu X, et al. A highly permeable graphene oxide membrane with fast and selective transport nanochannels for efficient carbon capture. Energy Environ Sci 2016;9:3107–12.
[241] Shen J, Zhang M, Liu G, Guan K, Jin W. Size effects of graphene oxide on mixed matrix membranes for CO_2 separation. AIChE J 2016;62:2843–52.
[242] Quan S, Li SW, Xiao YC, Shao L. CO_2-selective mixed matrix membranes (MMMs) containing graphene oxide (GO) for enhancing sustainable CO_2 capture. Int J Greenhouse Gas Control 2017;56:22–9.
[243] Dai Y, Ruan X, Yan Z, Yang K, Yu M, Li H, et al. Imidazole functionalized graphene oxide/PEBAX mixed matrix membranes for efficient CO_2 capture. Sep Purif Technol 2016;166:171–80.
[244] Li X, Cheng Y, Zhang H, Wang S, Jiang Z, Guo R, et al. Efficient CO_2 capture by functionalized graphene oxide nanosheets as fillers to fabricate multi-permselective mixed matrix membranes. ACS Appl Mater Interfaces 2015;7:5528–37.
[245] Peng D, Wang S, Tian Z, Wu X, Wu Y, Wu H, et al. Facilitated transport membranes by incorporating graphene nanosheets with high zinc ion loading for enhanced CO_2 separation. J Membr Sci 2017;522:351–62.
[246] Huang G, Isfahani AP, Muchtar A, Sakurai K, Shrestha BB, Qin D, et al. Pebax/ionic liquid modified graphene oxide mixed matrix membranes for enhanced CO_2 capture. J Membr Sci 2018;565:370–9.
[247] Dong G, Hou J, Wang J, Chen V, Liu J. Enhanced CO_2/N_2 separation by porous reduced graphene oxide/Pebax mixed matrix membranes. J Membr Sci 2016;520:860–8.
[248] Zahri K, Wong K, Goh P, Ismail A. Graphene oxide/polysulfone hollow fiber mixed matrix membranes for gas separation. RSC Adv 2016;6:89130–9.
[249] Feijani EA, Tavassoli A, Mahdavi H, Molavi H. Effective gas separation through graphene oxide containing mixed matrix membranes. J Appl Polym Sci 2018;135:46271.
[250] Cong S, Li H, Shen X, Wang J, Zhu J, Liu J, et al. Construction of graphene oxide based mixed matrix membranes with CO_2-philic sieving gas-transport channels through strong π–π interactions. J Mater Chem A 2018;6:17854–60.
[251] Prasad B, Mandal B. Graphene-incorporated biopolymeric mixed-matrix membrane for enhanced CO_2 separation by regulating the support pore filling. ACS Appl Mater Interfaces 2018;10:27810–20.
[252] Murugiah PS, Oh PC, Lau KK. Facilitated transport graphene oxide based PPOdm mixed matrix membrane for CO_2 separation. Mater Today: Proc 2018;5:21818–24.
[253] Geng Z, Song Q, Zhang X, Yu B, Shen Y, Cong H. Mixed matrix membranes composed of WS_2 nanosheets and fluorinated poly(2,6-dimethyl-1,4-phenylene oxide) via Suzuki reaction for improved CO_2 separation. J Membr Sci 2018;565:226–32.
[254] Melicchio A, Favvas EP. Preparation and characterization of graphene oxide as a candidate filler material for the preparation of mixed matrix polyimide membranes. Surf Coat Technol 2018;349:1058–68.
[255] Zhu W, Qin Y, Wang Z, Zhang J, Guo R, Li X. Incorporating the magnetic alignment of GO composites into Pebax matrix for gas separation. J Energy Chem 2019.
[256] Ge B-S, Wang T, Sun H-X, Gao W, Zhao H-R. Preparation of mixed matrix membranes based on polyimide and aminated graphene oxide for CO_2 separation. Polym Adv Technol 2018;29:1334–43.
[257] Oueiny C, Berlioz S, Perrin F-X. Carbon nanotube–polyaniline composites. Prog Polym Sci 2014;39:707–48.
[258] Iijima S. Helical microtubules of graphitic carbon. Nature 1991;354:56–8.
[259] Zhao D, Ren J, Li H, Li X, Deng M. Gas separation properties of poly (amide-6-b-ethylene oxide)/amino modified multi-walled carbon nanotubes mixed matrix membranes. J Membr Sci 2014;467:41–7.
[260] Ranjbaran F, Omidkhah MR, Ebadi Amooghin A. The novel Elvaloy4170/functionalized multi-walled carbon nanotubes mixed matrix membranes: fabrication, characterization and gas separation study. J Taiwan Inst Chem Eng 2015;49:220–8.
[261] Ahmad A, Jawad Z, Low S, Zein S. A cellulose acetate/multi-walled carbon nanotube mixed matrix membrane for CO_2/N_2 separation. J Membr Sci 2014;451:55–66.
[262] Rajabi Z, Afshar Taromi F, Kargari A, Sanaeepur H. CO_2/N_2 Gas separation using nanocomposite membranes comprised of ethylene-propylene-diene monomer/multi-walled carbon nano ethylene-propylene-diene monomer/multi-walled carbon nanotubes (EPDM/MWCNT). Iran J Polym Sci Technol (PERSIAN) 2015;28:211–24.
[263] Morales-Torres S, Silva TL, Pastrana-Martínez LM, Brandão AT, Figueiredo JL, Silva AM. Modification of the surface chemistry of single-and multi-walled carbon nanotubes by HNO_3 and H_2SO_4 hydrothermal oxidation for application in direct contact membrane distillation. PCCP 2014;16:12237–50.
[264] Zhao D, Ren J, Wang Y, Qiu Y, Li H, Hua K, et al. High CO_2 separation performance of Pebax® /CNTs/GTA mixed matrix membranes. J Membr Sci 2017;521:104–13.
[265] Ansaloni L, Zhao Y, Jung BT, Ramasubramanian K, Baschetti MG, Ho WW. Facilitated transport membranes containing amino-functionalized multi-walled carbon nanotubes for high-pressure CO_2 separations. J Membr Sci 2015;490:18–28.
[266] Zhang H, Guo R, Hou J, Wei Z, Li X. Mixed matrix membranes containing carbon nanotubes composite with hydrogel for efficient CO_2 separation. ACS Appl Mater Interfaces 2016;8(42):29044–51.
[267] Liu Y, Peng D, He G, Wang S, Li Y, Wu H, et al. Enhanced CO_2 permeability of membranes by incorporating polyzwitterion@ CNT composite particles into polyimide matrix. ACS Appl Mater Interfaces 2014;6:13051–60.
[268] Soleymanipour SF, Dehaghani AHS, Pirouzfar V, Alihosseini A. The morphology and gas-separation performance of membranes comprising multiwalled carbon nanotubes/polysulfone–Kapton. J Appl Polym Sci 2016;133:43839.
[269] Zhao Y, Jung BT, Ansaloni L, Ho WW. Multiwalled carbon nanotube mixed matrix membranes containing amines for high pressure CO_2/H_2 separation. J Membr Sci 2014;459:233–43.
[270] Favvas EP, Stefanopoulos KL, Nolan JW, Papageorgiou SK, Mitropoulos AC, Lairez D. Mixed matrix hollow fiber membranes with enhanced gas permeation properties. Sep Purif Technol 2014;132:336–45.
[271] Ma P-C, Siddiqui NA, Marom G, Kim J-K. Dispersion and functionalization of carbon nanotubes for polymer-based nanocomposites: a review. Compos A Appl Sci Manuf 2010;41:1345–67.
[272] Ma P-C, Kim J-K. Carbon nanotubes for polymer reinforcement. CRC Press; 2011.
[273] Lee RJ, Jawad ZA, Ahmad AL, Chua HB. Incorporation of functionalized multi-walled carbon nanotubes (MWCNTs) into cellulose acetate butyrate (CAB) polymeric matrix to improve the CO_2/N_2 separation. Process Saf Environ Prot 2018;117:159–67.
[274] Giel V, Perchacz M, Kredatusová J, Pientka Z. Gas transport properties of polybenzimidazole and poly(phenylene oxide) mixed matrix membranes incorporated with PDA-functionalised titanate nanotubes. Nanoscale Res Lett 2017;12:3.
[275] Dong L, Zhang C, Bai Y, Shi D, Li X, Zhang H, et al. High-performance PEBA2533-functional MMT mixed matrix membrane containing high-speed facilitated transport channels for CO_2/N_2 separation. ACS Sustainable Chem Eng 2016;4:3486–96.
[276] Li X, Ma L, Zhang H, Wang S, Jiang Z, Guo R, et al. Synergistic effect of combining carbon nanotubes and graphene oxide in mixed matrix membranes for efficient CO_2 separation. J Membr Sci 2015;479:1–10.
[277] Sarfraz M, Ba-Shammakh M. Combined effect of CNTs with ZIF-302 into polysulfone to fabricate MMMs for enhanced CO_2 separation from flue gases. Arab J Sci Eng 2016;41:2573–82.

[278] Lin R, Ge L, Liu S, Rudolph V, Zhu Z. Mixed-matrix membranes with metal-organic framework-decorated CNT fillers for efficient CO_2 separation. ACS Appl Mater Interfaces 2015;7:14750–7.
[279] Tanh Jeazet HB, Sorribas S, Román-Marín JM, Zornoza B, Téllez C, Coronas J, et al. Increased selectivity in CO_2/CH_4 separation with mixed-matrix membranes of polysulfone and mixed-MOFs MIL-101 (Cr) and ZIF-8. Eur J Inorg Chem 2016;2016:4363–7.
[280] Castarlenas S, Téllez C, Coronas J. Gas separation with mixed matrix membranes obtained from MOF UiO-66-graphite oxide hybrids. J Membr Sci 2017;526:205–11.
[281] Sarfraz M, Ba-Shammakh M. Synergistic effect of incorporating ZIF-302 and graphene oxide to polysulfone to develop highly selective mixed-matrix membranes for carbon dioxide separation from wet post-combustion flue gases. J Ind Eng Chem 2016;36:154–62.
[282] Khosravi T, Omidkhah M. Preparation of CO_2 selective composite membranes using Pebax/CuBTC/PEG-ran-PPG ternary system. J Energy Chem 2017;26:530–9.
[283] Zhang J, Xin Q, Li X, Yun M, Xu R, Wang S, et al. Mixed matrix membranes comprising aminosilane-functionalized graphene oxide for enhanced CO_2 separation. J Membr Sci 2019;570–571:343–54.
[284] Dong G, Zhang X, Zhang Y, Tsuru T. Enhanced permeation through CO_2-stable dual-inorganic composite membranes with tunable nanoarchitectured channels. ACS Sustain Chem Eng 2018;6:8515–24.
[285] Zhu H, Yuan J, Zhao J, Liu G, Jin W. Enhanced CO_2/N_2 separation performance by using dopamine/polyethyleneimine-grafted TiO_2 nanoparticles filled PEBA mixed-matrix membranes. Sep Purif Technol 2019.
[286] Ayas İ, Yilmaz L, Kalipcilar H. The gas permeation characteristics of ternary component mixed matrix membranes prepared using ZIF-8 with a large range of average particle size. Ind Eng Chem Res 2018;57:16041–50.
[287] Samarasinghe SASC, Chuah CY, Yang Y, Bae T-H. Tailoring CO_2/CH_4 separation properties of mixed-matrix membranes via combined use of two- and three-dimensional metal-organic frameworks. J Membr Sci 2018;557:30–7.
[288] Castro-Muñoz R, Fíla V, Martin-Gil V, Muller C. Enhanced CO_2 permeability in Matrimid® 5218 mixed matrix membranes for separating binary CO_2/CH_4 mixtures. Sep Purif Technol 2019;210:553–62.
[289] Zhu H, Jie X, Wang L, Kang G, Liu D, Cao Y. Enhanced gas separation performance of mixed matrix hollow fiber membranes containing post-functionalized S-MIL-53. J Energy Chem 2018;27:781–90.
[290] Feijani EA, Mahdavi H, Tavassoli A. Synthesis and gas permselectivity of CuBTC–GO–PVDF mixed matrix membranes. New J Chem 2018;42:12013–23.
[291] Jia M, Feng Y, Qiu J, Lin X, Yao J. Bromomethylated poly(phenylene oxide) (BPPO)-assisted fabrication of UiO-66-NH_2/BPPO/polyethersulfone mixed matrix membrane for enhanced gas separation. J Appl Polym Sci 2018;135:46759.
[292] Nezhadmoghadam E, Chenar MP, Omidkhah M, Nezhadmoghadam A, Abedini R. Aminosilane grafted Matrimid 5218/nano-silica mixed matrix membrane for CO_2/light gases separation. Korean J Chem Eng 2018;35:526–34.
[293] Jazebizadeh MH, Khazraei S. Investigation of methane and carbon dioxide gases permeability through PEBAX/PEG/ZnO nanoparticle mixed matrix membrane. Silicon 2017;9:775–84.
[294] Sarfraz M, Ba-Shammakh M. Pursuit of efficient CO_2-capture membranes: graphene oxide- and MOF-integrated Ultrason® membranes. Polym Bull 2018;75:5039–59.
[295] Shamsabadi AA, Seidi F, Salehi E, Nozari M, Rahimpour A, Soroush M. Efficient CO_2-removal using novel mixed-matrix membranes with modified TiO_2 nanoparticles. J Mater Chem A 2017;5:4011–25.
[296] Liu G, Chernikova V, Liu Y, Zhang K, Belmabkhout Y, Shekhah O, et al. Mixed matrix formulations with MOF molecular sieving for key energy-intensive separations. Nat Mater 2018;17:283–9.
[297] Liu Y, Liu G, Zhang C, Qiu W, Yi S, Chernikova V, et al. Enhanced CO_2/CH_4 separation performance of a mixed matrix membrane based on tailored MOF-polymer formulations. Adv Sci 2018;5:1800982.
[298] Liu G, Cadiau A, Liu Y, Adil K, Chernikova V, Carja I-D, et al. Enabling fluorinated MOF-based membranes for simultaneous removal of H_2S and CO_2 from natural gas. Angew Chem Int Ed 2018;57:14811–6.
[299] Prasetya N, Teck AA, Ladewig BP. Matrimid-JUC-62 and Matrimid-PCN-250 mixed matrix membranes displaying light-responsive gas separation and beneficial ageing characteristics for CO_2/N_2 separation. Sci Rep 2018;8:2944.
[300] Yang K, Dai Y, Zheng W, Ruan X, Li H, He G. ZIFs-modified GO plates for enhanced CO_2 separation performance of ethyl cellulose based mixed matrix membranesf. Sep Purif Technol 2019.
[301] Lee H, Park SC, Roh JS, Moon GH, Shin JE, Kang YS, et al. Metal–organic frameworks grown on a porous planar template with an exceptionally high surface area: promising nanofiller platforms for CO_2 separation. J Mater Chem A 2017;5:22500–5.
[302] Huang D, Xin Q, Ni Y, Shuai Y, Wang S, Li Y, et al. Synergistic effects of zeolite imidazole framework@graphene oxide composites in humidified mixed matrix membranes on CO_2 separation. RSC Adv 2018;8:6099–109.
[303] Zhang N, Wu H, Li F, Dong S, Yang L, Ren Y, et al. Heterostructured filler in mixed matrix membranes to coordinate physical and chemical selectivities for enhanced CO_2 separation. J Membr Sci 2018;567:272–80.
[304] Lee JH, Kwon HT, Bae S, Kim J, Kim JH. Mixed-matrix membranes containing nanocage-like hollow ZIF-8 polyhedral nanocrystals in graft copolymers for carbon dioxide/methane separation. Sep Purif Technol 2018;207:427–34.
[305] Zhang Y, Wang H, Zhou S, Wang J, He X, Liu J, et al. Biomimetic material functionalized mixed matrix membranes for enhanced carbon dioxide capture. J Mater Chem A 2018;6:15585–92.
[306] Zhang N, Peng D, Wu H, Ren Y, Yang L, Wu X, et al. Significantly enhanced CO_2 capture properties by synergy of zinc ion and sulfonate in Pebax-pitch hybrid membranes. J Membr Sci 2018;549:670–9.
[307] Fulong CRP, Liu J, Pastore VJ, Lin H, Cook TR. Mixed-matrix materials using metal–organic polyhedra with enhanced compatibility for membrane gas separation. Dalton Trans 2018;47:7905–15.
[308] Yun YN, Sohail M, Moon J-H, Kim TW, Park KM, Chun DH, et al. Mixed-matrix membranes with hydrophilic metal-organic polyhedra for efficient carbon dioxide separation. Chem – Asian J 2018;13:631–5.
[309] Ebadi Amooghin A, Sanaeepur H, Omidkhah M, Kargari A. "Ship-in-a-bottle", a new synthesis strategy for preparing novel hybrid host–guest nanocomposites for highly selective membrane gas separation. J Mater Chem A 2018;6:1751–71.
[310] Lim J, Lee EJ, Choi JS, Jeong NC. Diffusion control in the in situ synthesis of iconic metal-organic frameworks within an ionic polymer matrix. ACS Appl Mater Interfaces 2018;10:3793–800.
[311] Tessema TDM, Venna SR, Dahe G, Hopkinson DP, El-Kaderi HM, Sekizkardes AK. Incorporation of benzimidazole linked polymers into Matrimid to yield mixed matrix membranes with enhanced CO_2/N_2 selectivity. J Membr Sci 2018;554:90–6.
[312] Shan M, Seoane B, Pustovarenko A, Wang X, Liu X, Yarulina I, et al. Benzimidazole linked polymers (BILPs) in mixed-matrix membranes: influence of filler porosity on the CO_2/N_2 separation performance. J Membr Sci 2018;566:213–22.
[313] Ding X, Tan F, Zhao H, Hua M, Wang M, Xin Q, et al. Enhancing gas permeation and separation performance of polymeric membrane by incorporating hollow polyamide nanoparticles with dense shell. J Membr Sci 2019;570–571:53–60.
[314] Robeson LM, Dose ME, Freeman BD, Paul DR. Analysis of the transport properties of thermally rearranged (TR) polymers and polymers of intrinsic microporosity (PIM) relative to upper bound performance. J Membr Sci 2017;525:18–24.
[315] Guiver MD, Lee YM. Polymer rigidity improves microporous membranes. Science 2013;339:284–5.
[316] Liu J, Hou X, Park HB, Lin H. High-performance polymers for membrane CO_2/N_2 separation. Chem-Eur J 2016;22:15980–90.
[317] Ebadi Amooghin A, Sanaeepur H, Omidkhah M, Kargari A. New advances in polymeric membranes for CO_2 separation. In: Méndez-Vilas A, Solano-Martín A, editors. Polymer science: research advances, practical applications and educational aspects. Spain: FORMATEX; 2016. p. 354–68.
[318] Wu XM, Zhang QG, Lin PJ, Qu Y, Zhu AM, Liu QL. Towards enhanced CO_2 selectivity of the PIM-1 membrane by blending with polyethylene glycol. J Membr Sci 2015;493:147–55.

[319] Li P, Chung T, Paul D. Gas sorption and permeation in PIM-1. J Membr Sci 2013;432:50–7.
[320] Castro-Muñoz R, Fíla V, Dung CT. Mixed matrix membranes based on PIMs for gas permeation: principles, synthesis, and current status. Chem Eng Commun 2016;204:295–309.
[321] McKeown NB, Hanif S, Msayib K, Tattershall CE, Budd PM. Porphyrin-based nanoporous network polymers. Chem Commun 2002:2782–3.
[322] McKeown NB, Makhseed S, Budd PM. Phthalocyanine-based nanoporous network polymers. Chem Commun 2002:2780–1.
[323] Budd PM, Elabas ES, Ghanem BS, Makhseed S, McKeown NB, Msayib KJ, et al. Solution-processed, organophilic membrane derived from a polymer of intrinsic microporosity. Adv Mater 2004;16:456–9.
[324] Budd PM, Ghanem BS, Makhseed S, McKeown NB, Msayib KJ, Tattershall CE. Polymers of intrinsic microporosity (PIMs): robust, solution-processable, organic nanoporous materials. Chem Commun 2004:230–1.
[325] Althumayri K, Harrison WJ, Shin Y, Gardiner JM, Casiraghi C, Budd PM, et al. The influence of few-layer graphene on the gas permeability of the high-free-volume polymer PIM-1. Phil Trans R Soc A 2016;374:20150031.
[326] Xiao Y, Liling Z, Xu L, Chung T-S. Molecular design of Tröger's base-based polymers with intrinsic microporosity for gas separation. J Membr Sci 2017;521:65–72.
[327] Mason CR, Maynard-Atem L, Heard KW, Satilmis B, Budd PM, Friess K, et al. Enhancement of CO_2 affinity in a polymer of intrinsic microporosity by amine modification. Macromolecules 2014;47:1021–9.
[328] Khdhayyer MR, Esposito E, Fuoco A, Monteleone M, Giorno L, Jansen JC, et al. Mixed matrix membranes based on UiO-66 MOFs in the polymer of intrinsic microporosity PIM-1. Sep Purif Technol 2017;173:304–13.
[329] Swaidan R, Ghanem BS, Litwiller E, Pinnau I. Pure-and mixed-gas CO_2/CH_4 separation properties of PIM-1 and an amidoxime-functionalized PIM-1. J Membr Sci 2014;457:95–102.
[330] Pang SH, Jue ML, Leisen J, Jones CW, Lively RP. PIM-1 as a solution-processable "Molecular Basket" for CO_2 capture from dilute sources. ACS Macro Lett 2015;4:1415–9.
[331] Tian Z, Wang S, Wang Y, Ma X, Cao K, Peng D, et al. Enhanced gas separation performance of mixed matrix membranes from graphitic carbon nitride nanosheets and polymers of intrinsic microporosity. J Membr Sci 2016;514:15–24.
[332] Khan MM, Filiz V, Bengtson G, Shishatskiy S, Rahman MM, Lillepaerg J, et al. Enhanced gas permeability by fabricating mixed matrix membranes of functionalized multiwalled carbon nanotubes and polymers of intrinsic microporosity (PIM). J Membr Sci 2013;436:109–20.
[333] Smith SJ, Ladewig BP, Hill AJ, Lau CH, Hill MR. Post-synthetic Ti exchanged UiO-66 metal-organic frameworks that deliver exceptional gas permeability in mixed matrix membranes. Sci Rep 2015;5:7823.
[334] Hao L, Liao K-S, Chung T-S. Photo-oxidative PIM-1 based mixed matrix membranes with superior gas separation performance. J Mater Chem A 2015;3:17273–81.
[335] Evans JD, Huang DM, Hill MR, Sumby CJ, Thornton AW, Doonan CJ. Feasibility of mixed matrix membrane gas separations employing porous organic cages. J Phys Chem C 2014;118:1523–9.
[336] Mitra T, Bhavsar RS, Adams DJ, Budd PM, Cooper AI. PIM-1 mixed matrix membranes for gas separations using cost-effective hypercrosslinked nanoparticle fillers. Chem Commun 2016;52:5581–4.
[337] Lau CH, Nguyen PT, Hill MR, Thornton AW, Konstas K, Doherty CM, et al. Ending aging in super glassy polymer membranes. Angew Chem Int Ed 2014;53:5322–6.
[338] Wang ZG, Ren H, Zhang S, Zhang F, Jin J. Polymer of Intrinsic microporosity/metal organic framework hybrid membrane with improved interfacial interaction for high-performance CO_2 separation. J Mater Chem A 2017;5:10968–77.
[339] Wang C, Guo F, Li H, Xu J, Hu J, Liu H. Porous organic polymer as fillers for fabrication of defect-free PIM-1 based mixed matrix membranes with facilitating CO_2-transfer chain. J Membr Sci 2018;564:115–22.
[340] Bhavsar RS, Mitra T, Adams DJ, Cooper AI, Budd PM. Ultrahigh-permeance PIM-1 based thin film nanocomposite membranes on PAN supports for CO_2 separation. J Membr Sci 2018;564:878–86.
[341] Swaidan R, Ghanem B, Al-Saeedi M, Litwiller E, Pinnau I. Role of intrachain rigidity in the plasticization of intrinsically microporous triptycene-based polyimide membranes in mixed-gas CO_2/CH_4 separations. Macromolecules 2014;47:7453–62.
[342] Eguchi H, Kim DJ, Koros WJ. Chemically cross-linkable polyimide membranes for improved transport plasticization resistance for natural gas separation. Polymer 2015;58:121–9.
[343] Zhuang Y, Seong JG, Do YS, Jo HJ, Cui Z, Lee J, et al. Intrinsically microporous soluble polyimides incorporating tröger's base for membrane gas separation. Macromolecules 2014;47:3254–62.
[344] Askari M, Chua ML, Chung T-S. Permeability, solubility, diffusivity, and PALS data of cross-linkable 6FDA-based copolyimides. Ind Eng Chem Res 2014;53:2449–60.
[345] Jeon E, Moon SY, Bae JS, Park JW. In situ generation of reticulate micropores through covalent network/polymer nanocomposite membranes for reverse-selective separation of carbon dioxide. Angew Chem 2016;128:1340–5.
[346] Liu G, Li N, Miller SJ, Kim D, Yi S, Labreche Y, et al. Molecularly designed stabilized asymmetric hollow fiber membranes for aggressive natural gas separation. Angew Chem 2016;128:13958–62.
[347] Wang Z, Wang D, Zhang F, Jin J. Tröger's base-based microporous polyimide membranes for high-performance gas separation. ACS Macro Lett 2014;3:597–601.
[348] Japip S, Wang H, Xiao Y, Chung TS. Highly permeable zeolitic imidazolate framework (ZIF)-71 nano-particles enhanced polyimide membranes for gas separation. J Membr Sci 2014;467:162–74.
[349] Wang Z, Wang D, Zhang S, Hu L, Jin J. Interfacial design of mixed matrix membranes for improved gas separation performance. Adv Mater. 2016;28:3399–405.
[350] Nafisi V, Hägg M-B. Gas separation properties of ZIF-8/6FDA-durene diamine mixed matrix membrane. Sep Purif Technol 2014;128:31–8.
[351] Nafisi V, Hägg M-B. Development of nanocomposite membranes containing modified Si nanoparticles in PEBAX-2533 as a block copolymer and 6FDA-durene diamine as a glassy polymer. ACS Appl Mater Interfaces 2014;6:15643–52.
[352] Zornoza B, Téllez C, Coronas J, Esekhile O, Koros WJ. Mixed matrix membranes based on 6FDA polyimide with silica and zeolite microsphere dispersed phases. AIChE J 2015;61:4481–90.
[353] Japip S, Xiao Y, Chung T-S. Particle size effects on gas transport properties of 6FDA-Durene/ZIF-71 mixed matrix membranes. Ind Eng Chem Res 2016;55:9507–17.
[354] Chen K, Xu K, Xiang L, Dong X, Han Y, Wang C, et al. Enhanced CO_2/CH_4 separation performance of mixed-matrix membranes through dispersion of sorption-selective MOF nanocrystals. J Membr Sci 2018;563:360–70.
[355] Zamidi Ahmad M, Navarro M, Lhotka M, Zornoza B, Téllez C, Fila V, et al. Enhancement of CO_2/CH_4 separation performances of 6FDA-based co-polyimides mixed matrix membranes embedded with UiO-66 nanoparticles. Sep Purif Technol 2018;192:465–74.
[356] Park HB, Jung CH, Lee YM, Hill AJ, Pas SJ, Mudie ST, et al. Polymers with cavities tuned for fast selective transport of small molecules and ions. Science 2007;318:254–8.
[357] Wang H, Chung T-S. The evolution of physicochemical and gas transport properties of thermally rearranged polyhydroxyamide (PHA). J Membr Sci 2011;385:86–95.
[358] Han SH, Kwon HJ, Kim KY, Seong JG, Park CH, Kim S, et al. Tuning microcavities in thermally rearranged polymer membranes for CO_2 capture. PCCP 2012;14:4365–73.
[359] Park HB, Han SH, Jung CH, Lee YM, Hill AJ. Thermally rearranged (TR) polymer membranes for CO_2 separation. J Membr Sci 2010;359:11–24.
[360] Liu Q, Paul DR, Freeman BD. Gas permeation and mechanical properties of thermally rearranged (TR) copolyimides. Polymer 2016;82:378–91.
[361] Jo HJ, Soo CY, Dong G, Do YS, Wang HH, Lee MJ, et al. Thermally rearranged poly (benzoxazole-co-imide) membranes with superior mechanical strength for gas separation obtained by tuning chain rigidity. Macromolecules 2015;48:2194–202.

[362] Brunetti A, Cersosimo M, Kim JS, Dong G, Fontananova E, Lee YM, et al. Thermally rearranged mixed matrix membranes for CO_2 separation: an aging study. Int J Greenhouse Gas Control 2017;61:16–26.
[363] Kim S, Hou J, Wang Y, Ou R, Simon GP, Seong JG, et al. Highly permeable thermally rearranged polymer composite membranes with a graphene oxide scaffold for gas separation. J Mater Chem A 2018;6:7668–74.
[364] Wolińska-Grabczyk A, Wójtowicz M, Jankowski A, Grabiec E, Kubica P, Musioł M, et al. Synthesis, characterization, and gas permeation properties of thermally rearranged poly(hydroxyimide)s filled with mesoporous MCM-41 silica. Polymer 2018;158:32–45.
[365] Estes G, Seymour R, Cooper SL. Infrared studies of segmented polyurethane elastomers. II. Infrared dichroism. Macromolecules 1971;4:452–7.
[366] Semsarzadeh MA, Ghalei B, Fardi M, Esmaeeli M, Vakili E. Structural and transport properties of polydimethylsiloxane based polyurethane/silica particles mixed matrix membranes for gas separation. Korean J Chem Eng 2014;31:841–8.
[367] Wang T, Zhao L, Shen J-N, Wu L-G, Van der Bruggen B. Enhanced performance of polyurethane hybrid membranes for CO_2 separation by incorporating graphene oxide: the relationship between membrane performance and morphology of graphene oxide. Environ Sci Technol 2015;49:8004–11.
[368] Knight P, Lyman D. Gas permeability of various block copolyether—urethanes. J Membr Sci 1984;17:245–54.
[369] Ruaan RC, Ma WC, Chen SH, Lai JY. Microstructure of HTPB-based polyurethane membranes and explanation of their low O_2/N_2 selectivity. J Appl Polym Sci 2001;82:1307–14.
[370] Huang S-L, Lai J-Y. On the gas permeability of hydroxyl terminated polybutadiene based polyurethane membranes. J Membr Sci 1995;105:137–45.
[371] Sadeghi M, Semsarzadeh MA, Barikani M, Ghalei B. Study on the morphology and gas permeation property of polyurethane membranes. J Membr Sci 2011;385:76–85.
[372] Semsarzadeh MA, Sadeghi M, Barikani M. Effect of chain extender length on gas permeation properties of polyurethane membranes. Iran Polym J 2008;17:431.
[373] Isfahani AP, Ghalei B, Bagheri R, Kinoshita Y, Kitagawa H, Sivaniah E, et al. Polyurethane gas separation membranes with ethereal bonds in the hard segments. J Membr Sci 2016;513:58–66.
[374] Li H, Freeman BD, Ekiner OM. Gas permeation properties of poly (urethane-urea) s containing different polyethers. J Membr Sci 2011;369:49–58.
[375] Galland G, Lam T. Permeability and diffusion of gases in segmented polyurethanes: structure–properties relations. J Appl Polym Sci 1993;50:1041–58.
[376] Sadeghi M, Semsarzadeh MA, Barikani M, Chenar MP. Gas separation properties of polyether-based polyurethane–silica nanocomposite membranes. J Membr Sci 2011;376:188–95.
[377] Sadeghi M, Arabi Shamsabadi A, Ronasi A, Isfahani AP, Dinari M, Soroush M. Engineering the dispersion of nanoparticles in polyurethane membranes to control membrane physical and transport properties. Chem Eng Sci 2018;192:688–98.
[378] Rodrigues MA, Ribeiro JDS, Costa EDS, Miranda JLD, Ferraz HC. Nanostructured membranes containing UiO-66 (Zr) and MIL-101 (Cr) for O_2/N_2 and CO_2/N_2 separation. Sep Purif Technol 2018;192:491–500.
[379] Dai Z, Noble RD, Gin DL, Zhang X, Deng L. Combination of ionic liquids with membrane technology: a new approach for CO_2 separation. J Membr Sci 2016;497:1–20.
[380] Petra C, Katalin B-B. Application of ionic liquids in membrane separation processes. INTECH: Open Access Publisher; 2011.
[381] Moghadam F, Kamio E, Matsuyama H. High CO_2 separation performance of amino acid ionic liquid-based double network ion gel membranes in low CO_2 concentration gas mixtures under humid conditions. J Membr Sci 2017;525:290–7.
[382] Tomé LC, Marrucho IM. Ionic liquid-based materials: a platform to design engineered CO_2 separation membranes. Chem Soc Rev 2016;45:2785–824.
[383] Park CH, Lee JH, Jang E, Lee KB, Kim JH. $MgCO_3$-crystal-containing mixed matrix membranes with enhanced CO_2 permselectivity. Chem Eng J 2017;307:503–12.
[384] Lu S-C, Khan AL, Vankelecom IF. Polysulfone-ionic liquid based membranes for CO_2/N_2 separation with tunable porous surface features. J Membr Sci 2016;518:10–20.
[385] He W, Zhang F, Wang Z, Sun W, Zhou Z, Ren Z. Facilitated separation of CO_2 by liquid membranes and composite membranes with task-specific ionic liquids. Ind Eng Chem Res 2016;55:12616–31.
[386] Zhang C, Zhang W, Gao H, Bai Y, Sun Y, Chen Y. Synthesis and gas transport properties of poly(ionic liquid) based semi-interpenetrating polymer network membranes for CO_2/N_2 separation. J Membr Sci 2017;528:72–81.
[387] Doyle KA, Murphy LJ, Paula ZA, Land MA, Robertson KN, Clyburne JA. Characterization of a new ionic liquid and its use for CO_2 capture from ambient air: studies on solutions of diethylenetriamine (DETA) and [DETAH] NO_3 in polyethylene glycol. Ind Eng Chem Res 2015;54:8829–41.
[388] Livi S, Duchet-Rumeau J, Gérard JF, Pham TN. Polymers and ionic liquids: a successful wedding. Macromol Chem Phys 2015;216:359–68.
[389] Deng J, Bai L, Zeng S, Zhang X, Nie Y, Deng L, et al. Ether-functionalized ionic liquid based composite membranes for carbon dioxide separation. RSC Adv 2016;6:45184–92.
[390] Casado-Coterillo C, Fernández-Barquín A, Zornoza B, Téllez C, Coronas J, Irabien Á. Synthesis and characterisation of MOF/ionic liquid/chitosan mixed matrix membranes for CO_2/N_2 separation. RSC Adv 2015;5:102350–61.
[391] Ahmad N, Leo C, Mohammad A, Ahmad A. Modification of gas selective SAPO zeolites using imidazolium ionic liquid to develop polysulfone mixed matrix membrane for CO_2 gas separation. Microporous Mesoporous Mater 2017;244:21–30.
[392] Karunakaran M, Villalobos L, Kumar M, Shevate R, Akhtar F, Peinemann K-V. Graphene oxide doped ionic liquid ultrathin composite membranes for efficient CO_2 capture. J Mater Chem A 2017;5:649–56.
[393] Ghasemi Estahbanati E, Omidkhah Nasrin M, Ebadi Amooghin A. Preparation and characterization of novel Ionic liquid/Pebax membranes for efficient CO_2/light gases separation. J Ind Eng Chem 2017;51:77–89.
[394] Li H, Tuo L, Yang K, Jeong H-K, Dai Y, He G, et al. Simultaneous enhancement of mechanical properties and CO_2 selectivity of ZIF-8 mixed matrix membranes: interfacial toughening effect of ionic liquid. J Membr Sci 2016;511:130–42.
[395] Ma J, Ying Y, Guo X, Huang H, Liu D, Zhong C. Fabrication of mixed-matrix membrane containing metal–organic framework composite with task-specific ionic liquid for efficient CO_2 separation. J Mater Chem A 2016;4:7281–8.
[396] Mohshim DF, Mukhtar H, Man Z. Composite blending of ionic liquid–poly (ether sulfone) polymeric membranes: green materials with potential for carbon dioxide/methane separation. J Appl Polym Sci 2016;133:43999.
[397] McDonald JL, MacFarlane DR, Forsyth M, Pringle JM. A novel class of gas separation membrane based on organic ionic plastic crystals. Chem Commun 2016;52:12940–3.
[398] Ghasemi Estahbanati E, Omidkhah Nasrin M, Ebadi Amooghin A. Interfacial design of ternary mixed matrix membranes containing Pebax 1657/silver-nanopowder/[BMIM][BF4] for improved CO_2 separation performance. ACS Appl Mater Interfaces 2017;9:10094–105.
[399] Ahmad NNR, Leo CP, Mohammad AW, Ahmad AL. Interfacial sealing and functionalization of polysulfone/SAPO-34 mixed matrix membrane using acetate-based ionic liquid in post-impregnation for CO_2 capture. Sep Purif Technol 2018;197:439–48.
[400] Zarca G, Horne WJ, Ortiz I, Urtiaga A, Bara JE. Synthesis and gas separation properties of poly (ionic liquid)-ionic liquid composite membranes containing a copper salt. J Membr Sci 2016;515:109–14.
[401] Singh ZV, Cowan MG, McDanel WM, Luo Y, Zhou R, Gin DL, et al. Determination and optimization of factors affecting CO_2/CH_4 separation performance in poly (ionic liquid)-ionic liquid-zeolite mixed-matrix membranes. J Membr Sci 2016;509:149–55.
[402] Cowan MG, Gin DL, Noble RD. Poly(ionic liquid)/ionic liquid ion-gels with high “Free” ionic liquid content: platform membrane materials for CO_2/light gas separations. Acc Chem Res 2016;49:724–32.
[403] Lau CH, Konstas K, Doherty CM, Kanehashi S, Ozcelik B, Kentish SE, et al. Tailoring physical aging in super glassy polymers with functionalized porous aromatic frameworks for CO_2 capture. Chem Mater 2015;27:4756–62.
[404] Fernández-Barquín A, Casado-Coterillo C, Palomino M, Valencia S, Irabien A. LTA/poly(1-trimethylsilyl-1-propyne) mixed-matrix membranes for high-temperature CO_2/N_2 separation. Chem Eng Technol 2015;38:658–66.
[405] Sanaeepur H, Ebadi Amooghin A, Moghadassi A, Kargari A, Moradi S, Ghanbari D. A novel acrylonitrile–butadiene–styrene/poly (ethylene glycol) membrane: preparation, characterization, and gas permeation study. Polym Adv Technol 2012;23:1207–18.

[406] Sanaeepur H, Ebadi Amooghin A, Moghadassi A, Kargari A. Preparation and characterization of acrylonitrile–butadiene–styrene/poly(vinyl acetate) membrane for CO_2 removal. Sep Purif Technol 2011;80:499–508.
[407] Olivieri L, Ligi S, De Angelis MG, Cucca G, Pettinau A. Effect of graphene and graphene oxide nanoplatelets on the gas permselectivity and aging behavior of poly(trimethylsilyl propyne) (PTMSP). Ind Eng Chem Res 2015;54:11199–211.
[408] Fernández-Barquín A, Rea R, Venturi D, Giacinti-Baschetti M, De Angelis MG, Casado-Coterillo C, et al. Effect of relative humidity on the gas transport properties of zeolite A/PTMSP mixed matrix membranes. RSC Adv 2018;8:3536–46.
[409] Yong WF, Kwek KHA, Liao K-S, Chung T-S. Suppression of aging and plasticization in highly permeable polymers. Polymer 2015;77:377–86.
[410] Tien-Binh N, Vinh-Thang H, Chen XY, Rodrigue D, Kaliaguine S. Crosslinked MOF-polymer to enhance gas separation of mixed matrix membranes. J Membr Sci 2016;520:941–50.
[411] Sekizkardes AK, Kusuma VA, Dahe G, Roth EA, Hill LJ, Marti A, et al. Separation of carbon dioxide from flue gas by mixed matrix membranes using dual phase microporous polymeric constituents. Chem Commun 2016;52:11768–71.
[412] Zhao H, Feng L, Ding X, Zhao Y, Tan X, Zhang Y. The nitrogen-doped porous carbons/PIM mixed-matrix membranes for CO_2 separation. J Membr Sci 2018;564:800–5.
[413] Tien-Binh N, Rodrigue D, Kaliaguine S. In-situ cross interface linking of PIM-1 polymer and UiO-66-NH_2 for outstanding gas separation and physical aging control. J Membr Sci 2018;548:429–38.
[414] Chen M, Soyekwo F, Zhang Q, Hu C, Zhu A, Liu Q. Graphene oxide nanosheets to improve permeability and selectivity of PIM-1 membrane for carbon dioxide separation. J Ind Eng Chem 2018;63:296–302.
[415] Alberto M, Bhavsar R, Luque-Alled JM, Vijayaraghavan A, Budd PM, Gorgojo P. Impeded physical aging in PIM-1 membranes containing graphene-like fillers. J Membr Sci 2018;563:513–20.
[416] Sabetghadam A, Liu X, Orsi AF, Lozinska MM, Johnson T, Jansen KMB, et al. Towards high performance metal-organic framework–microporous polymer mixed matrix membranes: addressing compatibility and limiting aging by polymer doping. Chem–Eur J 2018;24:12796–800.
[417] Ghalei B, Sakurai K, Kinoshita Y, Wakimoto K, Isfahani Ali P, Song Q, et al. Enhanced selectivity in mixed matrix membranes for CO_2 capture through efficient dispersion of amine-functionalized MOF nanoparticles. Nat Energy 2017;2:17086.
[418] Japip S, Liao K-S, Xiao Y, Chung T-S. Enhancement of molecular-sieving properties by constructing surface nano-metric layer via vapor cross-linking. J Membr Sci 2016;497:248–58.
[419] Jusoh N, Yeong YF, Cheong WL, Lau KK, Shariff AM. Facile fabrication of mixed matrix membranes containing 6FDA-durene polyimide and ZIF-8 nanofillers for CO_2 capture. J Ind Eng Chem 2016;44:164–73.
[420] Liu X, Wang X, Bavykina AV, Chu L, Shan M, Sabetghadam A, et al. Molecular-scale hybrid membranes derived from metal-organic polyhedra for gas separation. ACS Appl Mater Interfaces 2018;10:21381–9.
[421] Smith ZP, Bachman JE, Li T, Gludovatz B, Kusuma VA, Xu T, et al. Increasing M_2(dobdc) loading in selective mixed-matrix membranes: a rubber toughening approach. Chem Mater 2018;30:1484–95.
[422] Liu G, Labreche Y, Chernikova V, Shekhah O, Zhang C, Belmabkhout Y, et al. Zeolite-like MOF nanocrystals incorporated 6FDA-polyimide mixed-matrix membranes for CO_2/CH_4 separation. J Membr Sci 2018;565:186–93.
[423] Jacques NM, Rought PRE, Fritsch D, Savage M, Godfrey HGW, Li L, et al. Locating the binding domains in a highly selective mixed matrix membrane via synchrotron IR microspectroscopy. Chem Commun 2018;54:2866–9.
[424] Ahmad MZ, Martin-Gil V, Perfilov V, Sysel P, Fila V. Investigation of a new co-polyimide, 6FDA-bisP and its ZIF-8 mixed matrix membranes for CO_2/CH_4 separation. Sep Purif Technol 2018;207:523–34.
[425] Etxeberria-Benavides M, David O, Johnson T, Łozińska MM, Orsi A, Wright PA, et al. High performance mixed matrix membranes (MMMs) composed of ZIF-94 filler and 6FDA-DAM polymer. J Membr Sci 2018;550:198–207.
[426] Kim S, Shamsaei E, Lin X, Hu Y, Simon GP, Seong JG, et al. The enhanced hydrogen separation performance of mixed matrix membranes by incorporation of two-dimensional ZIF-L into polyimide containing hydroxyl group. J Membr Sci 2018;549:260–6.
[427] Sabetghadam A, Liu X, Benzaqui M, Gkaniatsou E, Orsi A, Lozinska MM, et al. Influence of filler pore structure and polymer on the performance of MOF-based mixed-matrix membranes for CO_2 capture. Chem–Eur J 2018;24:7949–56.
[428] Duan C, Jie X, Zhu H, Liu D, Peng W, Cao Y. Gas-permeation performance of metal organic framework/polyimide mixed-matrix membranes and additional explanation from the particle size angle. J Appl Polym Sci 2018;135:45728.
[429] Ameri E, Sadeghi M, Zarei N, Pournaghshband A. Enhancement of the gas separation properties of polyurethane membranes by alumina nanoparticles. J Membr Sci 2015;479:11–9.
[430] Isfahani AP, Sadeghi M, Dehaghani AHS, Aravand MA. Enhancement of the gas separation properties of polyurethane membrane by epoxy nanoparticles. J Ind Eng Chem 2016;44:67–72.
[431] Sadeghi M, Mehdi Talakesh M, Ghalei B, Shafiei M. Preparation, characterization and gas permeation properties of a polycaprolactone based polyurethane-silica nanocomposite membrane. J Membr Sci 2013;427:21–9.
[432] Molki B, Aframehr WM, Bagheri R, Salimi J. Mixed matrix membranes of polyurethane with nickel oxide nanoparticles for CO_2 gas separation. J Membr Sci 2018;549:588–601.
[433] Mohammad Gheimasi K, Bakhtiari O, Ahmadi M. Preparation and characterization of MWCNT-TEPA/polyurethane nanocomposite membranes for CO_2/CH_4 separation: experimental and modeling. Chem Eng Res Des 2018;133:222–34.
[434] Taheri Afarani H, Sadeghi M, Moheb A, Esfahani EN. Optimization of the gas separation performance of polyurethane–zeolite 3A and ZSM-5 mixed matrix membranes using response surface methodology. Chin J Chem Eng 2018.
[435] Ghalei B, Isfahani AP, Nilouyal S, Vakili E, Salooki MK. Effect of polyvinyl alcohol modified silica particles on the physical and gas separation properties of the polyurethane mixed matrix membranes. Silicon 2019.
[436] Sodeifian G, Raji M, Asghari M, Rezakazemi M, Dashti A. Polyurethane-SAPO-34 mixed matrix membrane for CO_2/CH_4 and CO_2/N_2 separation. Chin J Chem Eng 2019.
[437] Hudiono YC, Carlisle TK, Bara JE, Zhang Y, Gin DL, Noble RD. A three-component mixed-matrix membrane with enhanced CO_2 separation properties based on zeolites and ionic liquid materials. J Membr Sci 2010;350:117–23.
[438] Ban Y, Li Z, Li Y, Peng Y, Jin H, Jiao W, et al. Confinement of ionic liquids in nanocages: tailoring the molecular sieving properties of ZIF-8 for membrane-based CO_2 capture. Angew Chem 2015;127:15703–7.
[439] Hao L, Li P, Yang T, Chung T-S. Room temperature ionic liquid/ZIF-8 mixed-matrix membranes for natural gas sweetening and post-combustion CO_2 capture. J Membr Sci 2013;436:221–31.
[440] Fam W, Mansouri J, Li H, Hou J, Chen V. Gelled graphene oxide-ionic liquid composite membranes with enriched ionic liquid surfaces for improved CO_2 separation. ACS Appl Mater Interfaces 2018;10:7389–400.
[441] Nasir R, Ahmad NNR, Mukhtar H, Mohshim DF. Effect of ionic liquid inclusion and amino–functionalized SAPO-34 on the performance of mixed matrix membranes for CO_2/CH_4 separation. J Environ Chem Eng 2018;6:2363–8.
[442] Ilyas A, Muhammad N, Gilani MA, Vankelecom IFJ, Khan AL. Effect of zeolite surface modification with ionic liquid [APTMS][Ac] on gas separation performance of mixed matrix membranes. Sep Purif Technol 2018;205:176–83.
[443] Sekizkardes AK, Zhou X, Nulwala HB, Hopkinson D, Venna SR. Ionic cross-linked polyether and silica gel mixed matrix membranes for CO_2 separation from flue gas. Sep Purif Technol 2018;191:301–6.
[444] Ebadi Amooghin A, Sanaeepur H, Kargari A, Moghadassi A. Direct determination of concentration-dependent diffusion coefficient in polymeric membranes based on the Frisch method. Sep Purif Technol 2011;82:102–13.
[445] Zornoza B, Irusta S, Téllez C, Coronas J. Mesoporous silica sphere− polysulfone mixed matrix membranes for gas separation. Langmuir 2009;25:5903–9.
[446] Yong HH, Park HC, Kang YS, Won J, Kim WN. Zeolite-filled polyimide membrane containing 2,4,6-triaminopyrimidine. J Membr Sci 2001;188:151–63.

[447] Husain S, Koros WJ. Mixed matrix hollow fiber membranes made with modified HSSZ-13 zeolite in polyetherimide polymer matrix for gas separation. J Membr Sci 2007;288:195–207.
[448] Ordonez MJC, Balkus KJ, Ferraris JP, Musselman IH. Molecular sieving realized with ZIF-8/Matrimid® mixed-matrix membranes. J Membr Sci 2010;361:28–37.
[449] Won J, Seo J, Kim J, Kim H, Kang Y, Kim SJ, et al. Coordination compound molecular sieve membranes. Adv Mater 2005;17:80–4.
[450] Zornoza B, Martinez-Joaristi A, Serra-Crespo P, Tellez C, Coronas J, Gascon J, et al. Functionalized flexible MOFs as fillers in mixed matrix membranes for highly selective separation of CO_2 from CH_4 at elevated pressures. Chem Commun 2011;47:9522–4.
[451] Kim S, Chen L, Johnson JK, Marand E. Polysulfone and functionalized carbon nanotube mixed matrix membranes for gas separation: theory and experiment. J Membr Sci 2007;294:147–58.
[452] Sanip SM, Ismail AF, Goh PS, Soga T, Tanemura M, Yasuhiko H. Gas separation properties of functionalized carbon nanotubes mixed matrix membranes. Sep Purif Technol 2011;78:208–13.
[453] Hudiono YC, Carlisle TK, LaFrate AL, Gin DL, Noble RD. Novel mixed matrix membranes based on polymerizable room-temperature ionic liquids and SAPO-34 particles to improve CO_2 separation. J Membr Sci 2011;370:141–8.

Dr. Ebadi Amooghin received his Ph.D. from Tarbiat Modares University, Tehran, Iran, in 2015. He is currently with the Department of Chemical Engineering at Arak University, Arak, Iran. His expertise includes membrane separation technologies for CO_2 capture and design and synthesis of mixed matrix membranes (MMMs) for gas separation. He has published more than 40 papers in refereed journals and authored and co-authored several book chapters and books.

Samaneh Mashhadikhan received her M.Sc. in Chemical Engineering from Islamic Azad University, South Tehran branch, Tehran, Iran in 2011. She is pursuing toward her Ph.D. in Chemical Engineering at Arak University, Arak, Iran, since 2014. Her research interests include membrane science and technology for gas separation, mathematical modeling and super-critical extraction.

Dr. Sanaeepur received his Ph.D. in Petrochemical Engineering from Amirkabir University of Technology (Tehran Polytechnic), Mahshahr, Iran, in 2015. He is currently with the Department of Chemical Engineering at Arak University, Arak, Iran. His current research focuses on the design and synthesis of functional materials with specific properties for mixed matrix membranes. He has published several scientific papers in peer reviewed journals, book chapters, books, and conference articles. He is a member of the editorial board for the Journal of Membrane Science and Research (JMSR).

Dr. Moghadassi is an associate professor of Chemical Engineering at Department of Chemical Engineering, Arak University, Arak, Iran. He received his Ph.D. from Claude Bernard University Lyon 1, France, in 1996. He has been engaged in the fields of chemical engineering, membrane science and technology, simulation, modelling and optimization of industrial processes, and has published over 100 refereed journal papers and several book chapters and books.

Professor Matsuura studied at the University of Tokyo and the Institute of Chemical Technology of the Technical University of Berlin. He was appointed to Professor Emeritus of the University of Ottawa upon his retirement in 2002 after serving as professor of the Department of Chemical Engineering (currently Department of Chemical and Biological Engineering) and the director of the Industrial Membrane Research Institute (IMRI). He also served at the Advanced Membrane Technology Research Centre (AMTEC) of University Technology Malaysia (UTM), Skudai, Malaysia, as a distinguished visiting professor, in years 2007, 2009-2018. He delivered many lectures at the overseas research institutions and the international conferences. He has published about 600 papers in refereed journals, authored and co-authored 6 books and edited 8 books.

Professor Ramakrishna, FREng is the Chair of Circular Economy Taskforce at the National University of Singapore (NUS), which is ranked among the top 25 universities in the world. He is the Editor-in-Chief of Springer NATURE Journal Materials Circular Economy (https://www.springer.com/materials/journal/42824). He is an editorial board member of NATURE Scientific Reports. He is a member of World Economic Forum (WEF) Committee on Future of Production-Sustainability. He is an international advisor to the National Environmental Agency's Clean Enviro Summit Singapore (https://www.cleanenvirosummit.sg/programme/clean-environment-leaders-summit) His leadership roles includes NUS University Vice-President (Research Strategy); Dean of NUS Faculty of Engineering; Director of NUS Enterprise; Director of NUS Industry Liaison Office; Founding Co-Director of NUS Nanoscience & Nanotechnology Initiative, NUSNNI; and Founding Chairman of Solar Energy Research Institute of Singapore, SERIS. He founded a successful international organization – the Global Engineering Deans Council, GEDC (http://gedcouncil.org/ambassadors). He advices universities, corporations and governments around the world (http://www.universityworldnews.com/article.php?story=20181002111202821) He is an elected Fellow of UK Royal Academy of Engineering (FREng); Singapore Academy of Engineering; Indian National Academy of Engineering; and ASEAN Academy of Engineering & Technology. He is an elected Fellow of International Union of Societies of Biomaterials Science and Engineering (FBSE); Institution of Engineers Singapore; ISTE, India; Institution of Mechanical Engineers and Institute of Materials, Minerals & Mining, UK; and American Association of the Advancement of Science; ASM International; American Society for Mechanical Engineers; American Institute for Medical & Biological Engineering, USA. He received PhD from the University of Cambridge, UK; and The General Management Training from the Harvard University, USA. He is a Highly Cited Researcher in the world (Clarivate Analytics). Thomson Reuters recognized among the World's Most Influential Scientific Minds. A European study placed him among the only 1,000 researchers with H index over 130 in the history of science and technology (http://www.webometrics.info/en/node/58). Over the years, his peer reviewed papers received ~85,000 citations and 137 H-index. He received numerous recognitions which include CUT Honorary Engineering Doctorate; APA Distinguished Researcher Award, IFEES President award – Global Visionary; GEDC Ambassador; ASEAN Outstanding Engineer Award; IES Prestigious Engineering Achievement Award; IITM Distinguished Alumni Award; NUS Outstanding Researcher Award; CPS Biomaterials Award; Cambridge Nehru Fellowship, and Singapore LKY Fellowship.